

**Regulation of Renal Ion Channels by Serum and Glucocorticoid  
Inducible Kinase Isoforms, Ubiquitin Ligase Nedd4-2 and NHE3  
Regulating Factor 2 in the *Xenopus Laevis* Oocyte Expression  
System**

**INAUGURAL-DISSERTATION**

zur Erlangung des Grades eines Dr. med. vet.  
beim Fachbereich Veterinärmedizin  
der Justus-Liebig-Universität Gießen

**HAMDY M. EMBARK**

Aus dem Institut für Physiologie  
der Universität Tübingen  
Abteilung Physiologie I  
Betreuer: Prof. Dr. F. Lang

Eingereicht über das Institut für Veterinär-Physiologie der  
Justus-Liebig-Universität Gießen  
im Fachbereich vertreten durch: Prof. Dr. R. Gerstberger

**Regulation of Renal Ion Channels by Serum and Glucocorticoid  
Inducible Kinase Isoforms, Ubiquitin Ligase Nedd4-2 and NHE3  
Regulating Factor 2 in the *Xenopus Laevis* Oocyte Expression  
System**

**INAUGURAL-DISSERTATION**

zur Erlangung des Grades eines Dr. med. vet.  
beim Fachbereich Veterinärmedizin  
der Justus-Liebig-Universität Gießen

Eingereicht von

**HAMDY M. EMBARK**

Tierarzt aus  
Aswan (Ägypten)

Gießen 2004

Mit Genehmigung des Fachbereichs Veterinärmedizin  
der Justus-Liebig-Universität Gießen

Dekan:	Professor Dr. Dr. h. c. B. Hoffmann
Gutachter:	Professor Dr. F. Lang Professor Dr. R. Gerstberger
Tag der Disputation:	22. März 2004

*...to my family*

List of Abbreviations .....	i
<b>1 INTRODUCTION .....</b>	<b>1</b>
1.1 The renal ion channels .....	2
1.2 The renal epithelial K <sup>+</sup> channels ROMK (K <sub>ir</sub> 1.1).....	2
1.2.1 Physiological roles of ROMK channels in the kidney .....	2
1.2.2 Alternative splicing of the <i>romk</i> (K <sub>ir</sub> 1.1 or <i>KCNJ1</i> ) gene .....	4
1.2.3 Molecular structure.....	6
1.2.4 Physiological regulation of channel activity.....	7
1.2.5 The antenatal Bartter Syndrome (aBS) .....	8
1.3 The renal epithelial Ca <sup>2+</sup> channel ECaC1 (TRPV5).....	11
1.3.1 Physiological roles of ECaC1 in the kidney .....	11
1.3.2 Genomic structures of <i>ECAC1</i> and <i>ECAC2</i> genes.....	12
1.3.3 Molecular structure.....	13
1.3.4 Physiological regulation of channel activity.....	14
1.3.5 Clinical implications of ECaC1 channel regulation .....	15
1.4 The renal ClC-K/barttin chloride channels .....	16
1.4.1 Expression pattern and physiological functions .....	16
1.4.2 Genomic structures of <i>CLCNKA</i> and <i>CLCNKB</i> genes.....	18
1.4.3 Molecular structure.....	19
1.4.4 Physiological regulation of channel activity.....	20
1.4.5 Pathophysiological significance of ClC-K/barttin channels .....	21
1.5 Serum and glucocorticoid inducible kinase and protein kinase B .....	22
1.6 The Na <sup>+</sup> /H <sup>+</sup> exchanger regulating factor (NHERF) .....	24
1.7 The ubiquitin protein ligase Nedd4 .....	26
1.8 <i>Xenopus laevis</i> oocytes and electrophysiological recording .....	30
1.9 AIMS OF THE PRESENT STUDY .....	33
<b>2 MATERIALS AND METHODS .....</b>	<b>34</b>
2.1 Equipment and materials .....	35
2.1.1 Laboratory equipment.....	35
2.1.2 Materials .....	36
2.1.3 Chemicals and reagents .....	36
2.1.4 Solutions, medium and buffer.....	40
2.2 Heterologous expression in <i>Xenopus</i> oocytes .....	45
2.2.1 <i>In vitro</i> cRNA transcription .....	45
2.2.2 Preparation of oocytes.....	48

---

2.2.3	cRNA injection .....	48
2.3	Electrophysiological recording .....	50
2.3.1	Two-electrode voltage-clamp .....	50
2.3.2	Recording of intracellular pH (pH <sub>i</sub> ).....	51
2.4	Site-directed mutagenesis of ROMK1.....	54
2.5	Deletion of PDZ domains in NHERF2.....	57
2.6	Pull-down assays .....	57
2.7	Detection of cell surface expression by chemiluminescence .....	58
2.8	Cell surface biotinylation.....	59
2.9	Western blotting and immunohistochemistry for ROMK1 .....	60
2.10	Immunohistochemistry for CIC-Ka/barttin channels .....	60
2.11	Uptake measurements .....	61
2.12	Data evaluation.....	61
<b>3</b>	<b>RESULTS.....</b>	<b>63</b>
3.1	Regulation of the renal epithelial K <sup>+</sup> channel ROMK1 (K <sub>ir</sub> 1.1a).....	64
3.1.1	Up-regulation of ROMK1 by SGK1 and NHERF2.....	64
3.1.2	Current-Voltage relationship (I-V) of ROMK1 expressing oocytes.....	66
3.1.3	Inhibition of ROMK1 by cytosolic acidification.....	66
3.1.4	pH sensitivity of ROMK1 .....	68
3.1.5	SGK1 determines pH sensitivity of ROMK1.....	69
3.1.6	Increase of ROMK1 abundance in the cell membrane .....	74
3.1.7	Influence of SGK1 and NHERF2 coexpression on ROMK1 stability..	78
3.1.8	Stimulation of ROMK1 requires second PDZ domain of NHERF2.....	79
3.2	Regulation of the renal epithelial Ca <sup>2+</sup> channel ECaC1 (TRPV5) .....	85
3.2.1	Stimulation of tracer Ca <sup>2+</sup> entry via TRPV5.....	85
3.2.2	Inhibitory effect of chelerythrine on tracer Ca <sup>2+</sup> entry.....	88
3.2.3	Inhibition of tracer Ca <sup>2+</sup> uptake by ruthenium red .....	89
3.2.4	Ca <sup>2+</sup> currents via TRPV5 stimulated by SGK1 and NHERF2 .....	90
3.2.5	TRPV5 activate an endogenous chloride conductance (I <sub>Cl(Ca)</sub> ).....	92
3.2.6	Inhibition of the I <sub>Cl(Ca)</sub> by ruthenium red and NPPB.....	96
3.2.7	Interaction of TRPV5 and NHERF2 proteins .....	98
3.2.8	Stimulation of TRPV5 requires Second PDZ domain of NHERF2 ....	100
3.3	Regulation of the renal CIC-Ka/barttin chloride channels .....	102
3.3.1	CIC-Ka/barttin induced currents .....	102
3.3.2	Regulation of CIC-Ka/barttin channels by Nedd4-2 and SGK1 .....	103
3.3.3	Regulation of CIC-Ka/barttin channels by SGK1 mutants .....	105

---

3.3.4	Regulation of ClC-Ka/barttin induced currents by SGK3 .....	107
3.3.5	Abolished down-regulation of ClC-Ka/barttin channels by Nedd4-2 ..	109
3.3.6	Immunolocalization of ClC-Ka and barttin channels .....	111
<b>4</b>	<b>DISCUSSION .....</b>	<b>113</b>
4.1	Regulation of the renal epithelial K <sup>+</sup> channel ROMK1 .....	114
4.1.1	Up-regulation of K <sup>+</sup> transport via ROMK1 by SGK1 and NHERF2 ...	114
4.1.2	Determination of pH sensitivity of ROMK1 channel by SGK1 .....	117
4.1.3	Stimulation of ROMK1 requires PDZ domains of NHERF2 .....	119
4.2	Regulation of Ca <sup>2+</sup> entry via TRPV5 by SGKs and NHERF2 .....	122
4.3	Regulation of Cl <sup>-</sup> transport via ClC-Ka/barttin by SGKs and Nedd4-2...	125
	Summary .....	129
	Zusammenfassung .....	131
	References .....	133
	Acknowledgments .....	155
	Curriculum Vitae .....	157
	List of Publications .....	158

---

**List of Abbreviations**

AMP	adenosine monophosphate
ATP	adenosine triphosphate
ATPase	adenosine triphosphatase
Bq	Bequerel
B-RAF	protein kinase oncoprotein
BSND	Bartter syndrome with sensorineural deafness
cAMP	cyclic adenosine monophosphate
°C	degree(s) Celsius (centigrade)
cDNA	complementary deoxyribonucleic acid
ClC-K	kidney chloride channel
cRNA	complementary ribonucleic acid
DEPC	diethylpyrocarbonate
DMSO	dimethylsulfoxide
DNA	desoxyribonucleic acid
dNTP	desoxyribonucleotidetriphosphate
DTNB	5,5'-dithio-bis[-2-nitrobenzoic acid]
ECaC1	epithelial calcium channel type 1
EDTA	ethylene diamine tetra-acetate
EGTA	ethyleneglycol-bis ( $\beta$ -aminoethyl)-N, N, N', N'-tetraacetic acid
$E_K^+$	equilibrium potential for the ion $K^+$
ELISA	enzyme-linked immunoabsorbent assay
ENaC	epithelial $Na^+$ channel
FBA	feedback amplifier
FmocCl	9-fluorenyl-methoxycarbonyl chloride
GST	glutathione S-transferase
h	human
HEPES	N-(2-Hydroxyethyl) piperazine-N-(2-ethanesulfonic acid)
HEK293	human embryonic kidney cell line
HepG2	human hepatoma cell line
$IC_{50}$	concentration at which a 50% inhibition is reached
IGF-1	insulin-like growth factor 1
I-V	current-voltage relation
KCNE1	potassium channel, inwardly rectifying, subfamily E, member 1
KCNJ1	potassium channel, inwardly rectifying, subfamily J, member 1
KCNQ1	potassium channel, inwardly rectifying, subfamily Q, member 1
kDa	kilodalton
$K_{ir}$	inward-rectifier potassium channels
Kv	voltage-gated potassium channel
m	mouse
M1	membrane-spanning domain 1
M2	membrane-spanning domain 2
mM	millimolar
mRNA	messenger ribonucleic acid
mV	millivolt
$\mu A$	microampere
$\mu Ci$	microcurie (1 Ci = $37 \times 10^9$ Bq)



$\mu\text{M}$	micromolar
NaPi	sodium-dependent phosphate transporter
Nedd4	neuronal precursor cell-expressed developmentally down-regulated 4
NHE3	$\text{Na}^+/\text{H}^+$ exchanger type 3
NHERF	$\text{Na}^+/\text{H}^+$ exchanger type 3 regulating factor
NKCC	sodium potassium chloride cotransporter
NMDG	N-methyl-D-glucamine
NPPB	5-Nitro-2-(3-phenylpropylamino)benzoic acid
p53	53 kDa tumor suppressor protein
PAGE	polyacrylamide gelelectrophoresis
PBS	phosphate buffer saline
PCR	polymerase chain reaction
PD	potential difference across the cell membrane
PDZ	PSD 95/ <i>Drosophila</i> disk large/ZO-1 domain (PDZ domain)
$\text{pH}_i$	intracellular pH
$\text{pK}_{\text{app}}$	apparent pK
PKA	protein kinase A; cAMP-dependent protein kinase
PKB (Akt)	protein kinase B; oncogene from Akt mouse
PKC	protein kinase C
pmol	picomole
pS	picoSiemens
PT	proximal tubule
PTH	parathyroid hormone
r	rat
RNA	ribonucleic acid
ROMK	renal outer-medullary $\text{K}^+$ channel
rpm	revolutions (rounds) per minute
SDS	sodium dodecyl sulfate
SEM	standard error of the mean
SGK	serum and glucocorticoid inducible kinase
TEA	tetraethylammonium
TEVC	two-electrode voltage clamp
TRIS	Tris(hydroxymethyl)aminomethane
TRPV	transient receptor potential (vanilloid family)
U937	human macrophage cell line
$V_m$	membrane potential
v/v	volume/volume
w/v	weight/volume

# **1 INTRODUCTION**

## **1.1 The renal ion channels**

There are many proteins embedded in cell membranes. Ion channels are one class of such molecules and provide pores for the passive diffusion of ions across biological membranes. They are often highly selective for a particular ionic species, leading to a classification into sodium ( $\text{Na}^+$ ), potassium ( $\text{K}^+$ ), calcium ( $\text{Ca}^{2+}$ ), chloride ( $\text{Cl}^-$ ) and unspecific cation channels.

Epithelial cells in the kidney perform vectorial transport of  $\text{Na}^+$ ,  $\text{K}^+$ ,  $\text{Ca}^{2+}$ ,  $\text{Cl}^-$  and water. These processes are mediated by a number of channels and pumps, and play a vital role in the maintenance of the ionic composition of the extracellular fluid compartment. A variety of hormones, amongst these the adrenal mineralocorticoid aldosterone, regulate renal ion and water transport functions (Loffing et al., 2001b).

## **1.2 The renal epithelial $\text{K}^+$ channels ROMK ( $\text{K}_{\text{ir}}1.1$ )**

### **1.2.1 Physiological roles of ROMK channels in the kidney**

Intracellular  $\text{K}^+$  (approximately 145 mM) represents the major portion of total body  $\text{K}^+$ . The  $\text{K}^+$  concentration in the extracellular fluid ranges from 3.5-5 mM. To maintain a constant serum  $\text{K}^+$  level, 95% of dietary  $\text{K}^+$  absorbed from the intestine is excreted through the kidney and the remaining portion is eliminated via the colon (Thier, 1986; Stanton, 1989). Under pathophysiological conditions like chronic renal failure, colonic excretion is increased and can contribute significantly to  $\text{K}^+$  homeostasis (Martin et al., 1986).

$\text{K}^+$  secretion in the kidney is a very complex process depending on flow rate, luminal  $\text{K}^+$ ,  $\text{Na}^+$  and  $\text{Cl}^-$  concentrations, hormones and the acid-base status (Stanton, 1989; Wang, 1995; Giebisch, 1998).

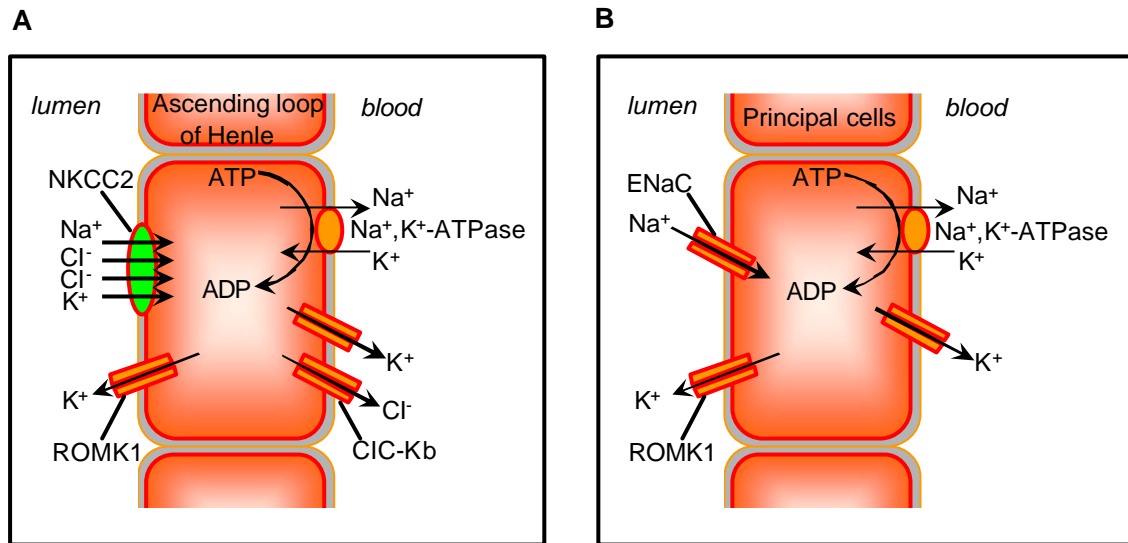


**Fig. 1. Apical ROMK channels mediate potassium secretion and regulate NaCl reabsorption in the kidney** (adapted from Hunter, 2001). **(A)** Salt reabsorption in tubular cells of the thick ascending limb of Henle (TALH); left (luminal side): apical membrane with NKCC2 cotransporter and ROMK1 channels; right: basolateral membrane with Na<sup>+</sup>,K<sup>+</sup>-ATPase and ClC-Kb channels. **(B)** K<sup>+</sup> secretion in principal cells of the distal convoluted tubule and cortical collecting duct; left (luminal side): apical membrane with ROMK1 channels and ENaC channels; right: basolateral membrane with Na<sup>+</sup>,K<sup>+</sup>-ATPase. Arrows indicate the direction of ion fluxes under physiological conditions.

In the thick ascending limb of Henle's loop, K<sup>+</sup> participates in the reabsorption of NaCl from the primary urine (Hebert and Andreoli, 1984; Bleich et al., 1990; Wang et al., 1990a, b) as illustrated in Fig. 1A. Luminal Na<sup>+</sup>, K<sup>+</sup> and Cl<sup>-</sup> enter the tubular cells via the furosemide-sensitive Na<sup>+</sup>-K<sup>+</sup>-2Cl<sup>-</sup> cotransporter (NKCC2). This process depends on K<sup>+</sup> efflux through apical K<sup>+</sup> channels ROMK (K<sub>ir</sub>1.1), which allow recycling of luminal K<sup>+</sup> (Hebert, 1998). Cl<sup>-</sup> and Na<sup>+</sup> are eliminated from the cells by cAMP-dependent Cl<sup>-</sup> channels (ClC-Kb) and Na<sup>+</sup>,K<sup>+</sup>-ATPase in the basolateral membrane, respectively (Giebisch, 1998; Köckerling et al., 1998).

K<sup>+</sup> secretion (Fig. 1B) is mediated by principal cells in the distal tubules and cortical collecting duct (Wang, 1995; Köckerling et al., 1998). Na<sup>+</sup> influx through amiloride-sensitive epithelial Na<sup>+</sup> channels (ENaC) in the apical membrane is

rate limiting for  $K^+$  excretion. The driving force for  $Na^+$  influx is generated by the action of basolateral  $Na^+,K^+$ -ATPase which also provides the necessary  $K^+$  gradient. Both  $Na^+$  reabsorption and  $K^+$  secretion are stimulated by aldosterone. This hormone was shown to increase the apical  $Na^+$  conductance within hours and to up-regulate expression of ENaC and  $Na^+,K^+$ -ATPase (O'Neil, 1990). Intercalated cells (not shown), which constitute the second type of epithelial cells in these nephron segments, partially reabsorb urinary  $K^+$  via  $H^+,K^+$ -ATPase (Graber and Pastoriza-Munoz, 1993; Giebisch, 1998).

$K^+$  secretion in the distal tubule is mediated by intermediate conductance (35-39 pS) weak inward-rectifier  $K^+$  channels (Wang et al., 1990a, b, 1992, 1994). Their activity has been shown to be linked to basolateral  $Na^+,K^+$ -ATPase by a pathway involving ion exchange,  $Ca^{2+}$  and protein kinase C (PKC) (Wang et al., 1993). In addition to regulation by protein kinases (Wang and Giebisch, 1991b), they have been shown to be particularly sensitive to changes in intracellular pH ( $pH_i$ ) (Wang et al., 1990a, b; Wang and Giebisch, 1991a). Intracellular acidification in the physiological range reversibly reduced channel open probability (Wang et al., 1990a, b). An inward-rectifier  $K^+$  channel (31 pS) with a similar sensitivity to  $pH_i$  has been characterized in luminal membranes of the thick ascending limb of Henle's loop (Bleich et al., 1990).

These functional properties together with immunocytochemical data (Xu et al., 1997) confirmed that ROMK ( $K_{ir}1.1$ ) channels underly the  $K^+$  conductance involved in renal salt reabsorption and  $K^+$  secretion.

### 1.2.2 Alternative splicing of the *romk* (*K<sub>ir</sub>1.1* or *KCNJ1*) gene

ROMK ( $K_{ir}1.1$ ) was originally cloned from a rat kidney cDNA library (Ho et al., 1993) as a member of the inward-rectifier ( $K_{ir}$ ) family of  $K^+$  channels (Nichola and Lopatin, 1997) encoded by the *romk* (*K<sub>ir</sub>1.1* or *KCNJ1*) gene (Lu et al., 2002). Genomic analysis revealed that rat and human *romk* genes contain 6 exons, which are spliced alternatively to yield various ROMK isoforms (Shuck et al., 1994; Yano et al., 1994; Boim et al., 1995; Kondo et al., 1996; Beesley et al., 1999) as indicated in Fig. 2. Since exon 6 (core) encodes the major part of

the channel protein, splicing results primarily in variable length of the NH<sub>2</sub>-terminus. ROMK2 (K<sub>ir</sub>1.1b) is shortened by 19 amino acids, and ROMK3 (K<sub>ir</sub>1.1c) is extended by 7 amino acids compared to ROMK1 (K<sub>ir</sub>1.1a).

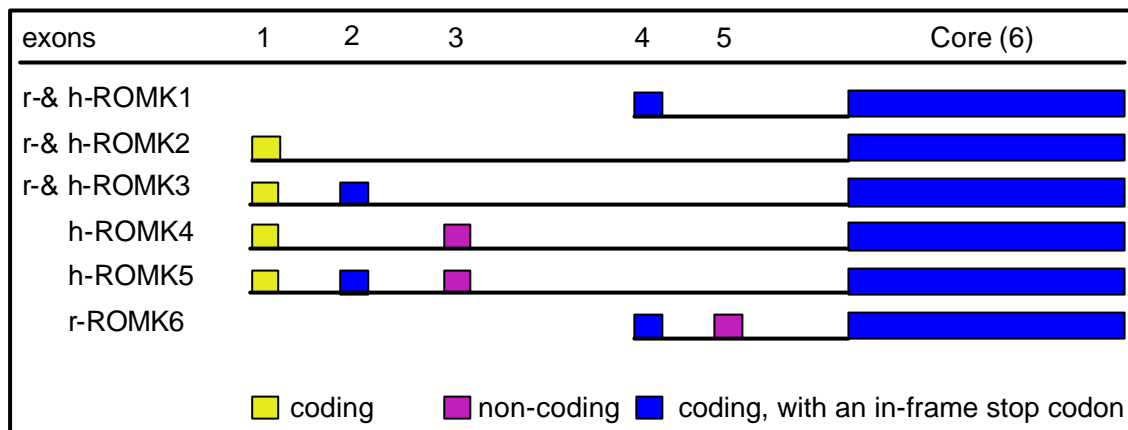


**Fig. 2. Structure of the rat and human *romk* genes encoding various ROMK isoforms** (adapted from Kondo et al., 1996). Alternative splicing of the *romk* gene yields 6 different ROMK mRNAs. Exons 2 and 4 code for different NH<sub>2</sub>-termini in ROMK3 (K<sub>ir</sub>1.1c) and ROMK1 (K<sub>ir</sub>1.1a), respectively. Exons 1, 3 and 5 do not contribute to the primary structure of ROMK subunits. Exon 6 (core) encodes ROMK2 (K<sub>ir</sub>1.1b) and the major part of the other K<sub>ir</sub>1.1 splice variants.

ROMK1 as well as the other splice variants are differentially expressed along the nephron in the kidney (Frindt and Palmer, 1989; Wang et al., 1990a, b; Zhou et al., 1994; Boim et al., 1995; Lee and Hebert, 1995), with the exception of ROMK6 (K<sub>ir</sub>1.1f), which is ubiquitously transcribed in various tissues including kidney, brain, heart, liver, pancreas and skeletal muscle (Kondo et al., 1996). Up to date, no functional differences could be observed between K<sub>ir</sub>1.1 isoforms when expressed in *Xenopus* oocytes. Thus, all K<sub>ir</sub>1.1 experiments in this study were carried out with the rROMK1 (K<sub>ir</sub>1.1a).

### 1.2.3 Molecular structure

ROMK belongs to a family of structurally and functionally related K<sup>+</sup> channels designated as K<sub>ir</sub> channels (Doupnik et al., 1995). The membrane topology and secondary structure of K<sub>ir</sub> channels has been predicted from hydropathy plots of their primary amino acid sequence and investigated by detailed mutagenesis (Ben-Efraim and Shai, 1996, 1997). Two hydrophobic segments, M1 and M2, form membrane spanning domains and flank a stretch of amino acids that is highly homologous to the H5 region of voltage-gated K<sup>+</sup> channels known as the P (pore) region which contains the putative channel pore (Fig. 3). NH<sub>2</sub>- and COOH-termini are thought to be located in the cytoplasm, although a partial association with the membrane can not be excluded. There is experimental evidence that parts of the COOH-terminus contribute to the intracellular vestibule of the pore (Taglialatela et al., 1994; Baukrowitz et al., 1999). The last three amino acids (389-391) (TQM, where T is threonine, Q is glutamine, and M is methionine) in the COOH-terminus form a type 1 PDZ binding motif (X-S/T-X-I/V/L/M, where X is any amino acid, S is serine, T is threonine, I is isoleucine, V is valine, L is leucine, and M is methionine) which is necessary for high affinity interaction with the PDZ domain of the NHERF proteins (Fanning and Anderson, 1996).

Several potential phosphorylation sites for both protein kinase A (PKA) and protein kinase C (PKC) are present on the predicated ROMK1 channel protein. All three protein kinase A (PKA) phospho-acceptor sites in ROMK1, embedded within the cytoplasmic NH<sub>2</sub>- (Ser-44) and COOH-termini (Ser-219 and Ser-313), must be phosphorylated for full channel function (MacGregor et al., 1998). Close inspection of the NH<sub>2</sub>-terminal PKA site in ROMK1 reveals that it also falls within a canonical serum and glucocorticoid inducible kinase (SGK1) phosphorylation sequence (recognized by a R-X-R-X-X-S/T, where R is arginine, X is any amino acid, S is serine, and T is threonine) (Kobayashi and Cohen, 1999b; Park et al., 1999), suggesting that the channel, and serine 44 in particular, might also be a target of SGK1 (Yoo et al., 2003).

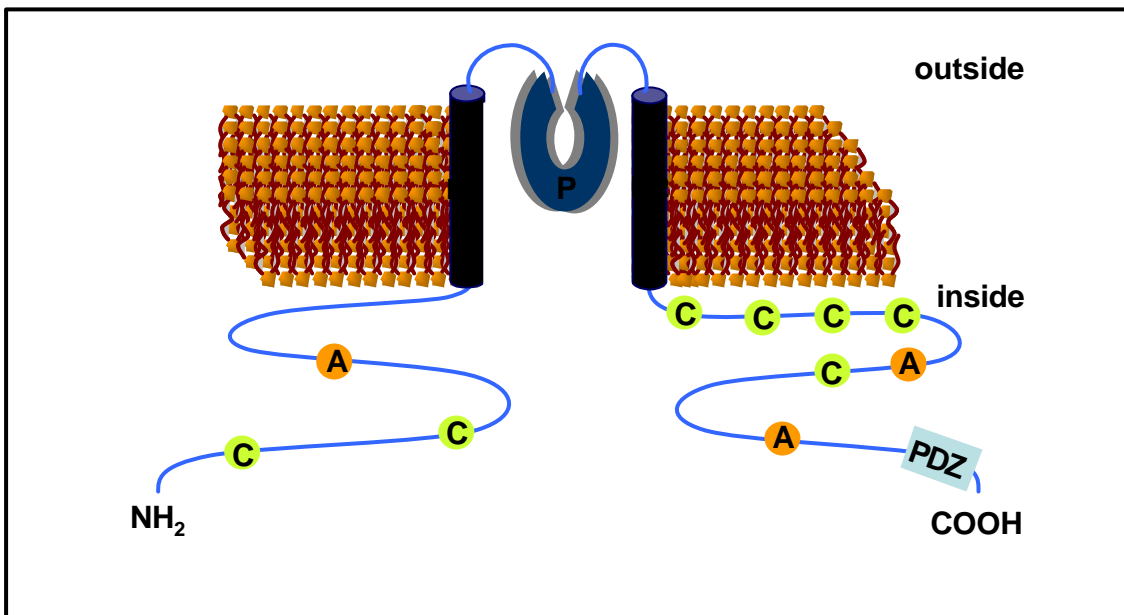


**Fig. 3. Structural model of the ROMK channel** (adapted from Wang et al., 1997). ROMK is formed by two transmembrane-spanning domains (M1 and M2) which flank a stretch of amino acids that is highly homologous to the H5 region of voltage-gated  $K^+$  channels known as the P-region. The intracytoplasmic amino- and carboxy-terminal tails contain several potential regulatory domains, including several potential protein kinase A (PKA) and protein kinase C (PKC) phosphorylation sites as well as putative PDZ binding motif.

#### 1.2.4 Physiological regulation of channel activity

Tsai and colleagues showed that  $K_{ir}1.1$  channels are particularly sensitive to changes in intracellular pH ( $pH_i$ ) (Tsai et al., 1995).  $pH_i$  did not affect the single channel current amplitude, but a decrease in channel open probability upon acidification (Fakler et al., 1996; Choe et al., 1997; McNicholas et al., 1998). The steady-state current- $pH_i$  relation showed a  $pH_i$  value for half maximal activation ( $pK_{app}$ ) of 6.9 and a Hill coefficient of around 3 indicating cooperativity of the gating process. Binding of  $K^+$  ions to an extracellular site has been shown to be essential for  $K_{ir}1.1$  channel activity but not for that of other  $K_{ir}$  channels (Doi et al., 1996). The halfmaximal  $K^+$  concentration determined in whole-cell experiments was around 4.5 mM but shifted to higher values when the intracellular pH was decreased.



Binding of the negatively charged phospholipid phosphatidylinositol 4,5-bisphosphate (PIP<sub>2</sub>) appears to be a general property of K<sub>ir</sub> channels (Hilgemann and Ball, 1996; Huang et al., 1998), and has also been reported for K<sub>ir</sub>1.1. Fusion proteins constructed from the K<sub>ir</sub>1.1 COOH-terminus bound PIP<sub>2</sub> *in vitro*, and the presence of PIP<sub>2</sub> was shown to be necessary for K<sub>ir</sub>1.1 channel activity (Huang et al., 1998).

Indeed, regulatory phosphorylation by PKA has been demonstrated for K<sub>ir</sub>1.1 channels in renal epithelial cells (McNicholas et al., 1994) and biochemically verified in detail (Xu et al., 1996). It is possibly facilitated by A-kinase-associated proteins (Ali et al., 1998). In fact, activation of ROMK by PKA is thought to underlie the regulation of renal potassium transport by vasopressin (Cassola et al., 1993). In addition, ROMK is a substrate of PKC and serine residues 4 and 201 are the two main PKC phosphorylation sites that are essential for the expression of ROMK in the cell surface (Lin et al., 2002).

Finally, aldosterone, vasopressin, and other factors precisely regulate ROMK activity, controlling potassium excretion in accord with the demands of potassium balance (Giebisch, 1998; Palmer, 1999; Gallazzini et al., 2003). Because ROMK channels normally exhibit a very high open probability near unity, physiologic augmentation of channel activity, as controlled by hormones and dietary potassium (Wang et al., 1992), is achieved largely by regulated changes in the number of active channels in the plasmalemma.

#### **1.2.5 The antenatal Bartter Syndrome (aBS)**

Hereditary renal tubular disorders leading to severe salt wasting and impaired urinary concentrating ability are rare diseases with an incidence of approximately 1: 50000 newborns. The first patients have been described by Bartter and colleagues with symptoms of excessive renal salt loss, hyperreninism, hyperaldosteronism with low or normal blood pressure, hypokalemic metabolic alkalosis, decreased pressor responsiveness to infused angiotensin II, and hyperplasia of the juxtaglomerular complex (Bartter et al., 1962, 1998).

In the following years, cases showing variants of this syndrome were reported by several groups (Gitelman et al., 1966; Fanconi et al., 1971; Seyberth et al., 1985; International collaborative study group for Bartter-like syndromes, 1997; Feldmann et al., 1998). Currently, at least three types with biochemical and physiological characteristics that are similar to those resulting from long-term application of certain diuretics can be distinguished (Seyberth et al., 1987, 1997; Köckerling et al., 1998):

- Bartter syndrome type I and II (antenatal (neonatal) Bartter Syndrome) (aBS), more correctly termed Hyperprostaglandin E-Syndrome (HPS; (Konrad et al., 1999)) or FSLT (furosemide-like salt-losing tubulopathy).
- Gitelman Syndrome; synonyms: Hypocalciuric Bartter Syndrome or TSLT (thiazide-like salt-losing tubulopathy).
- “Classic” Bartter syndrome or Bartter syndrome type III (Rodriguez-Soriano, 1998).

This classification was confirmed by identification of the genes underlying these defects. Five genes have been identified as causing Bartter syndrome, with the unifying pathophysiology being the loss of salt transport by the thick ascending limb. Phenotypic differences in Bartter types relate to the specific physiological roles of the individual genes in the kidney and other organ systems (Hebert, 2003). Mutations at the gene encoding for the thiazide-sensitive  $\text{Na}^+\text{-Cl}^-$  cotransporter (*NCCT* or *SLC12A3*) of the renal distal convoluted tubule were found in the majority of patients with Gitelman syndrome (Simon et al., 1996a). The most severe form, aBS, is genetically heterogeneous: Mutations either at the gene encoding the furosemide-sensitive  $\text{Na}^+\text{-K}^+\text{-2Cl}^-$  cotransporter (*NKCC2* or *SLC12A1*) or the gene encoding an ATP-sensitive inwardly rectifying potassium channel (*ROMK* or *KCNJ1*) of the medullary thick ascending limb (mTAL) of the Henle’s loop have been identified in aBS (type I and type II, respectively) patients (Simon et al., 1996b). Recently, either deletions or mutations at the gene encoding a renal chloride channel (*CLC-Kb*) have been identified in the majority of patients with “Classic” Bartter syndrome. Also loss-of-function mutations in the *BSND* gene, which encodes the integral membrane

protein barttin thus cause Bartter syndrome with sensorineural deafness and renal failure (Birkenhäger et al., 2001; Hebert, 2003).

Antenatal (neonatal) Bartter Syndrome (aBS) is inherited as an autosomal recessive entity. Mutations of *romk* gene appear to be rare, since the gene shows little allelic variation in the healthy population and most identified mutations are unique for single patients. Typically, affected children are compound heterozygous, i.e. they harbour a different mutation on either *romk* gene. Point mutations linked to aBS are apparently distributed over the whole coding region of the gene.

The molecular mechanisms leading to impairment or loss of  $K_{ir}1.1$  channel function are yet unknown. A major pathophysiological consequence seems to be the impairment of NaCl reabsorption in the ascending loop of Henle which depends on  $K^+$  recycling through  $K_{ir}1.1$  channels ((Hebert, 1998), see also Fig. 1A). The resulting loss of salt and fluid leads to polyhydramnios and premature delivery due to intrauterine polyuria (Seyberth et al., 1997). Polyuria remains life-threatening in young children if they are not treated by substitution with fluid, NaCl and KCl. Prostaglandin E2 (PGE2) is markedly elevated and plays an important role in the pathogenesis as it aggravates salt and fluid loss. Renin and aldosterone levels are also increased, but are insufficient to counteract the loss of NaCl, as  $Na^+$  reabsorption by principal cells in the distal tubulus depends on the presence of functional  $K_{ir}1.1$  channels in the apical membrane (Fig. 1B). Other secondary symptoms are hypercalciuria, which may lead to nephrocalcinosis, and alkalosis possibly resulting from excessive  $H^+/K^+$  exchange in the collecting duct to reduce  $K^+$  loss (Seyberth et al., 1985, 1997; Köckerling et al., 1998).

### 1.3 The renal epithelial $\text{Ca}^{2+}$ channel ECaC1 (TRPV5)

#### 1.3.1 Physiological roles of ECaC1 in the kidney

As depicted in Fig. 4, ECaC1 mediates the first step of  $\text{Ca}^{2+}$  reabsorption in the cortical collecting duct. The transported  $\text{Ca}^{2+}$  binds to calbindin- $\text{D}_{28\text{K}}$  (CaBP28K) and diffuses through the cytosol to the basolateral membrane, where  $\text{Ca}^{2+}$  is then extruded through the  $\text{Na}^+/\text{Ca}^{2+}$  exchanger (NCX1) and plasma membrane  $\text{Ca}^{2+}$ -ATPase (PMCA1b) (Hoenderop et al., 2002).

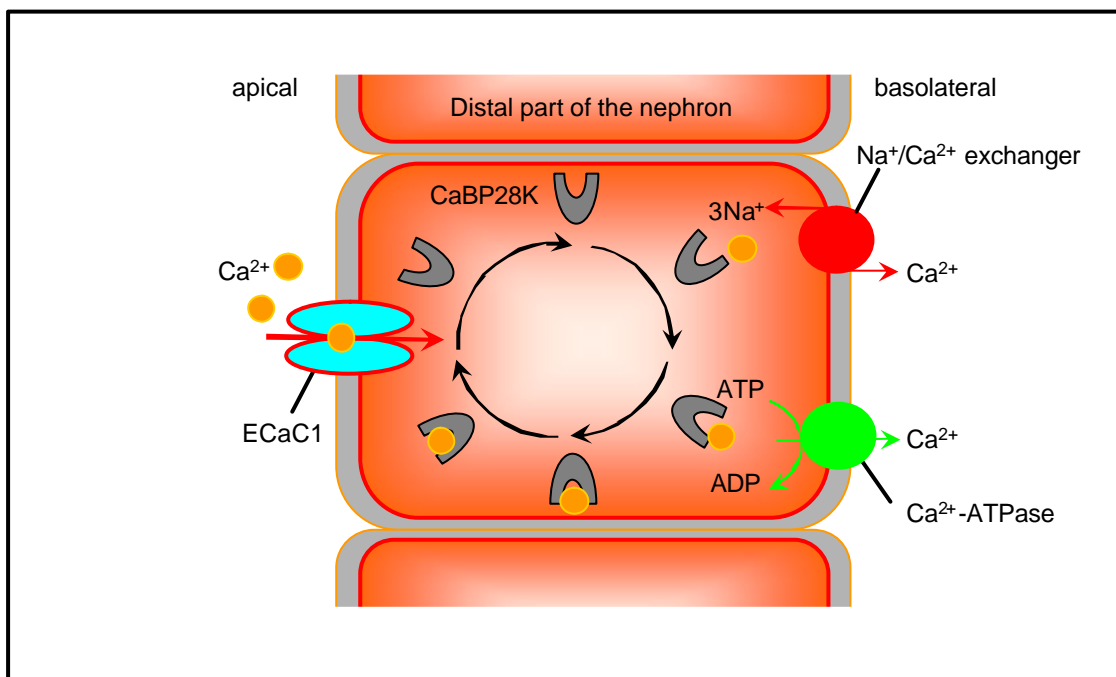


**Fig. 4.** Transcellular  $\text{Ca}^{2+}$  transport in cells lining the distal part of the nephron (adapted from Hoenderop et al., 2000a). Entry of  $\text{Ca}^{2+}$  is facilitated by the apical  $\text{Ca}^{2+}$  channel ECaC1 (TRPV5). Subsequently, the ion binds to calbindin- $\text{D}_{28\text{K}}$  (CaBP28K) and diffuses through the cytosol to the basolateral membrane. Here,  $\text{Ca}^{2+}$  ions are extruded by a  $\text{Na}^+/\text{Ca}^{2+}$  exchanger (NCX1) and a  $\text{Ca}^{2+}$ -ATPase (PMCA1b).

### 1.3.2 Genomic structures of *ECAC1* and *ECAC2* genes

The epithelial calcium channel ECaC has been cloned recently from rabbit kidney by Hoenderop and co-workers using functional expression cloning strategy based on cDNA library generated from a  $\text{Ca}^{2+}$  transporting primary culture of rabbit connecting tubules (Hoenderop et al., 1999a). Genomic analysis revealed that the *ECAC* gene contains 15 exons and 4 putative vitamin D-responsive elements (VDREs) (Müller et al., 2000) as depicted in Fig. 5. More recently, human (Müller et al., 2000) and rat ECaC1 (Peng et al., 2000; Hoenderop et al., 2000b) have been characterized.

Another type of ECaC, expressed in the intestine, has been cloned from rabbit (Hoenderop et al., 2000c), rat (CaT1) (Peng et al., 1999) and human (Barley et al., 2001) which has been designated to ECaC2. Wissenbach and co-workers (2001) have additionally cloned the human ECaC2 expressed in the placenta (CaT2).



**Fig. 5. Genomic structures of *ECAC1* and *ECAC2*** (adapted from Weber et al., 2001). Exons (dark blue boxes) and introns (black lines).

### 1.3.3 Molecular structure

The epithelial calcium channel ECaC1 is a member of the osmosensitive, transient receptor potential channel (OTRPC) family that comprises several types of  $\text{Ca}^{2+}$ -permeable cation channels (Harteneck et al., 2000), including the vanilloid receptor 1 (VR1) and the vanilloid receptor-like channel 1 (VRL1). ECaC1 shows similarity with all these channels (Birnbaumer et al., 1996; Caterina et al., 1999; Hoenderop et al., 2000a; Nilius et al., 2001a) according to the predicted topology showing six transmembrane domains with a putative loop pore between transmembrane segment 5 and 6 (Fig. 6). However, ECaC1 exhibits only 30% homology with those channels, indicating that ECaC1 is considered to be the first member of a new class of  $\text{Ca}^{2+}$  channels within this family (Hoenderop et al., 2000b).

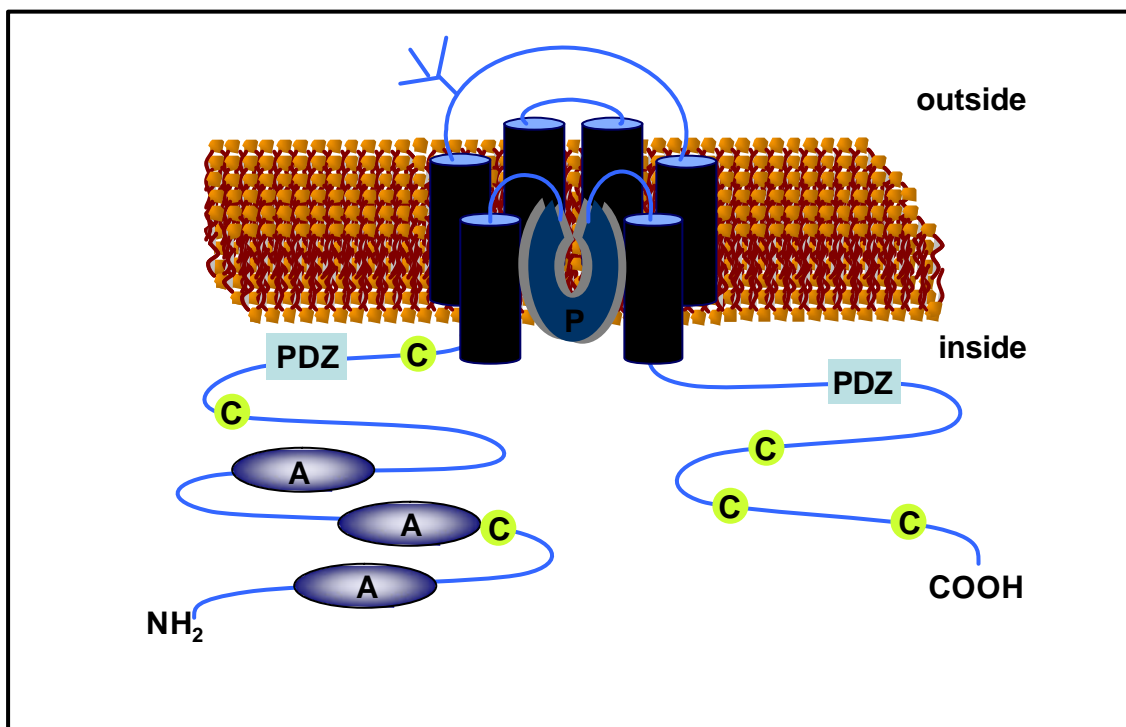


**Fig. 6. Proposed topology of the ECaC1 protein** (adapted from Hoenderop et al., 2002). Consisting of six transmembrane-spanning domains with a stretch of amino acids that is highly homologous to the H5- or P-region between transmembrane segment 5 and 6. Cytosolic  $\text{NH}_2$ - and  $\text{COOH}$ -terminal tails containing several potential regulatory domains, including ankyrin repeats, PDZ binding motifs, and sites for PKC phosphorylation.

### 1.3.4 Physiological regulation of channel activity

$\text{Ca}^{2+}$  transport in the distal nephron plays a key role in the fine regulation of extracellular  $\text{Ca}^{2+}$  concentration. It is therefore the target of environmental and hormonal regulation. For instance, ECaC1 is stimulated by extracellular pH and intracellular calcium (Vennekens et al., 2001; Nilius et al., 2001b). Moreover,  $1,25(\text{OH})_2\text{D}_3$ , an active metabolite of vitamin D, has been reported to stimulate  $\text{Ca}^{2+}$  reabsorption in the distal nephron (Bindels et al., 1991; Hoenderop et al., 2000a; Suki and Rose, 1996; van Baal et al., 1996). This stimulating effect is accomplished by up-regulation of calbindin- $\text{D}_{28\text{K}}$  (Christakos et al., 1989; Hunziker and Schrickel, 1988) and most recently by stimulation of ECaC (Hoenderop et al., 2001a). It has been revealed that the human ECaC promoter contains indeed four putative vitamin D-responsive elements (Hoenderop et al., 2001a; Müller et al., 2000).

In addition, parathyroid hormone (PTH) has been revealed to stimulate the active  $\text{Ca}^{2+}$  transport in the distal convoluted tubule (DCT) as well as in the connecting tubule (CNT) (Bindels et al., 1991; Friedman and Gesek, 1995; Hoenderop et al., 2000a). This stimulatory effect is mediated by coupling of the PTH receptor to both adenylyl cyclase and phospholipase C which in turn can activate cAMP and PKC signaling cascades (Friedman and Gesek, 1995; Hoenderop et al., 1999b). ECaC1 contains indeed several conserved sites for PKC phosphorylation suggesting that ECaC1 could be a target of PTH regulation (Hoenderop et al., 2002).

The natriuretic effect of thiazide, the inhibitor of the apical  $\text{Na}^+\text{-Cl}^-$  cotransporter (NCC) expressed in the distal convoluted tubule, has been shown to be accompanied by hypocalciuria (Sutton et al., 1979). Several findings have been gathered to elucidate such inverse relationships between  $\text{Na}^+$  and  $\text{Ca}^{2+}$  reabsorption. One hypothesis is that NCC inhibition results in hyperpolarization due to decrease of the intracellular  $\text{Cl}^-$  activity. Consequently, apical  $\text{Ca}^{2+}$  entry will be enhanced (Friedman, 1998). ECaC1 accordingly becomes a good candidate for regulation since its activity reaches a maximal value during hyperpolarization (Hoenderop et al., 1999c; Vennekens et al., 2000). However,

this notion is not convincingly supported by several experiments (Friedman, 1998). In theory, the basolateral  $\text{Na}^+/\text{Ca}^{2+}$  exchanger (NCX1) could be alternatively involved since thiazide induced natriuresis results in reduction of the intracellular  $\text{Na}^+$  concentration and thus to inhibition of  $\text{Ca}^{2+}$  efflux. However, several lines of evidence show only little overlap of NCX1 and NCC (Hoenderop et al., 2000c; Hoenderop et al., 2001a; Loffing et al., 2001a).

Finally, the identification of ECaC1 merits more interest, since it could underlie the idiopathic hypercalciuria (Müller et al., 2002).

### **1.3.5 Clinical implications of ECaC1 channel regulation**

The epithelial calcium channel ECaC1 represents the molecular basis of the apical  $\text{Ca}^{2+}$  entry step in transcellular  $\text{Ca}^{2+}$  reabsorption. Because this pathway allows the body to actively regulate the net amount of  $\text{Ca}^{2+}$  leaving the body, the delineation of the molecular mechanisms involved in its regulation could provide new insights in disturbances of  $\text{Ca}^{2+}$  homeostasis (Hoenderop et al., 2002).

The identification of ECaC1 shed new light on  $\text{Ca}^{2+}$  homeostasis-related disorders (Hoenderop et al., 2000b). The epithelial calcium channel involved in multifactorial pathogenesis of disorders such as idiopathic hypercalciuria, kidney stone disease, postmenopausal osteoporosis and the hypocalciuria in chronic thiazide treatment and Gitelman's syndrome (Nijenhuis et al., 2003).



## 1.4 The renal ClC-K/barttin chloride channels

### 1.4.1 Expression pattern and physiological functions

Within the kidney, ClC-K1 was located predominantly in the thin ascending limb of Henle's loop (Uchida et al., 1993), a nephron segment known for its high Cl<sup>-</sup> permeability. ClC-K1 appeared to be expressed in both apical and basolateral membranes (Uchida et al., 1995). In contrast, another study using an antibody that recognized both ClC-K1 and ClC-K2 (Vandewalle et al., 1997) found exclusive labeling of basolateral membranes in the late nephron segments. Proximal tubules and glomerula were not stained, but the thin ascending limb, the medullary and cortical thick ascending limb of Henle's loop, as well as the distal convoluted tubule and intercalated cells of the cortical collecting duct were labeled (Vandewalle et al., 1997; Estévez et al., 2001).

The assumption that the staining of the thin ascending loop is exclusively due to ClC-K1 (Uchida et al., 1995; Matsumura et al., 1999) indicated that ClC-K2 is present along the thick ascending limb, the distal convoluted tubule, and even in downstream segments of the nephron (Vandewalle et al., 1997). These results were largely confirmed by in situ hybridization (Yoshikawa et al., 1999). An antibody directed against a rabbit ClC-K isoform (rbClC-Ka) inhibited <sup>36</sup>Cl efflux from rabbit medullary thick ascending limbs in suspension (Winters et al., 1997). However, the significance of this finding is not clear, as the antibody, which was raised against an intracellular epitope, was added extracellularly.

Staining of the  $\beta$ -subunit barttin shows a complete overlap with ClC-K expression (Estévez et al., 2001), indicating that it forms heteromers with both ClC-K1 and ClC-K2. This applies also for the inner ear, where staining with ClC-K antibodies (Estévez et al., 2001; Sage and Marcus, 2001) and with barttin show complete overlap in basolateral membranes of the *Stria vascularis* and dark cells of the vestibular organ (Estévez et al., 2001). Both cell types are involved in K<sup>+</sup> secretion.

As CIC-K1 and CIC-K2 mRNA could both be detected in cochlear RNA (Estévez et al., 2001), it was concluded that both  $\alpha$ -subunits combine with barttin in marginal cells of the *Stria vascularis*. Patch-clamping of marginal cells revealed indeed  $\text{Cl}^-$  currents that resembled CIC-K currents in their voltage dependence, ion selectivity, and sensitivity to extracellular pH and  $\text{Ca}^{2+}$  concentration (Ando and Takeuchi, 2000). As depicted in Fig. 7, CIC-K chloride channels participate in transepithelial  $\text{Cl}^-$  transport in the kidney and inner ear (Estévez et al., 2001).

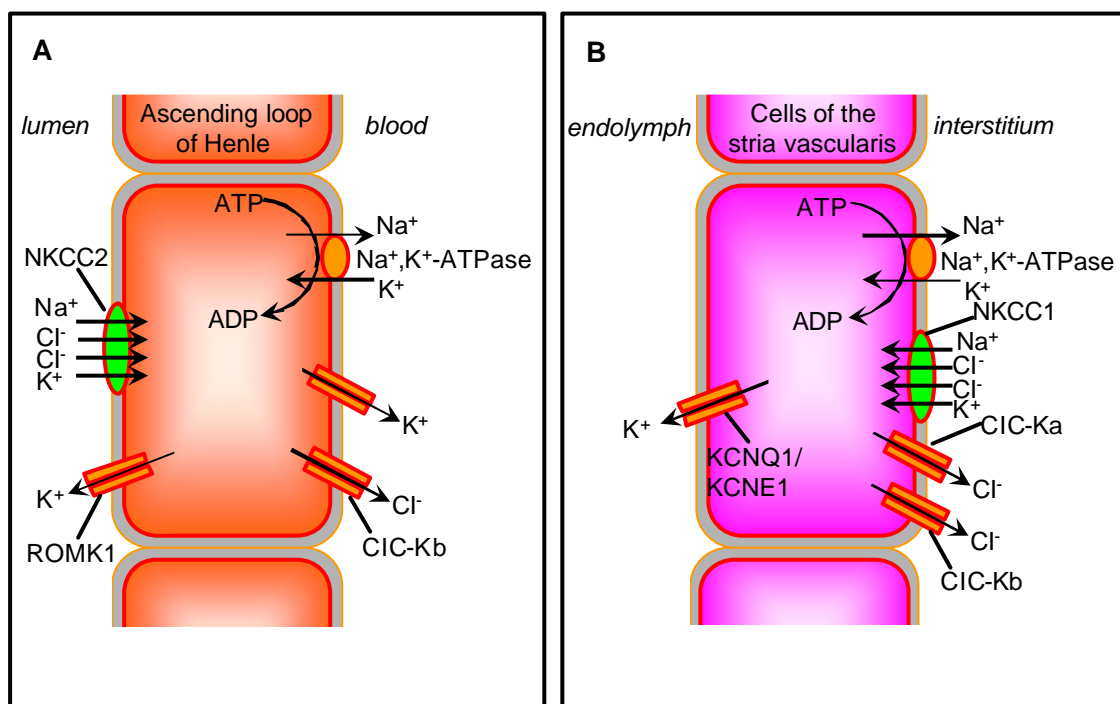


**Fig. 7. CIC-K/barttin heteromers function in transepithelial transport in kidney (A) and the inner ear (B)** (adapted from Estévez et al., 2001). **(A)** In cells of the renal thick ascending limb, apical NKCC2 cotransporters driving  $\text{Cl}^-$  uptake require ROMK1 to recycle  $\text{K}^+$ .  $\text{Cl}^-$  exits basolaterally through channels containing CIC-Kb  $\alpha$ -subunits and barttin  $\beta$ -subunits. Mutations in all four genes cause Bartter's syndrome. **(B)** In strial marginal cells, basolateral NKCC1 raises intracellular  $\text{K}^+$  concentration. In parallel, basolateral CIC-Ka/barttin and CIC-Kb/barttin channels recycle  $\text{Cl}^-$ .  $\text{K}^+$  exits apically through channels containing KCNQ1  $\alpha$ -subunits and KCNE1  $\beta$ -subunits. Loss of KCNQ1, KCNE1, NKCC1 or barttin causes deafness. Neither loss of CIC-K1 (the orthologue of CIC-Ka) nor of CIC-Kb alone entails deafness.

### 1.4.2 Genomic structures of *CLCNKA* and *CLCNKB* genes

Two members of the chloride channel gene family are predominantly expressed in the kidney. In the rat, these two isoforms were called *ClC-K1* and *ClC-K2* (Uchida et al., 1993; Kieferle et al., 1994; Adachi et al., 1994), whereas they are called *CLCNKA* and *CLCNKB* in humans (Kieferle et al., 1994; Saito-Ohara et al., 1996). Physiological (Matsumura et al., 1999; Simon et al., 1997) and morphological (Kieferle et al., 1994; Uchida et al., 1995; Vandewalle et al., 1997; Yoshikawa et al., 1999) evidence now suggests that *ClC-K1* corresponds to *CLCNKA*, and *ClC-K2* to *CLCNKB*. The gene structure analysis revealed that the two-chloride channel genes have identical organization, with each channel encoded by 19 exons as depicted in Fig. 8. The lengths of the introns of each gene are generally similar. Overall, the genes show 94% DNA sequence identity in exons (Simon et al., 1997).

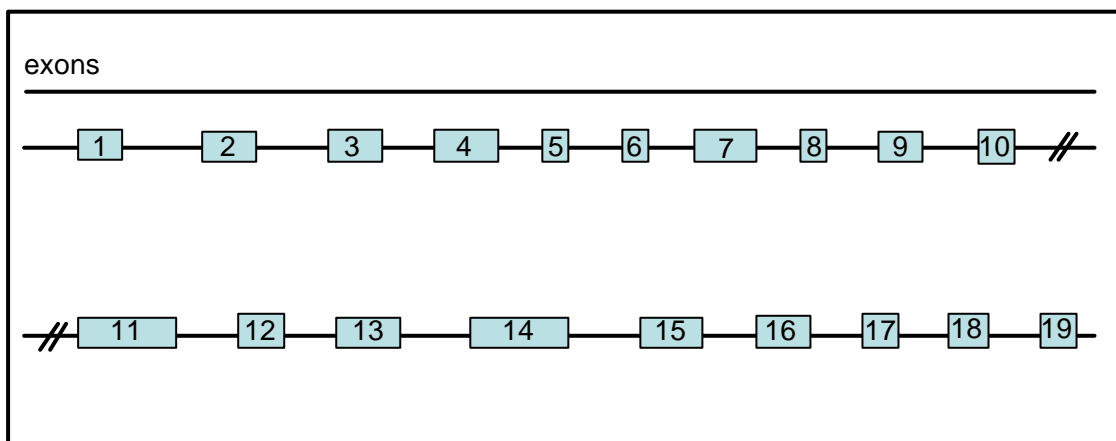


**Fig. 8. Organization of *CLCNKA* and *CLCNKB* genes** (adapted from Simon et al., 1997). *CLCNKA* and *CLCNKB* have identical organization, with each channel encoded by nineteen exons. The lengths of the introns of each gene are similar.

### 1.4.3 Molecular structure

The initial hydropathy analysis of the *Torpedo* channel CIC-0 indicated the presence of up to 13 transmembrane domains that were dubbed D1-D13 (Jentsch et al., 1990). Domain D13 does not cross the cell membrane and both its carboxy- and amino-termini are located intracellularly (Gründer et al., 1992). Some of the domains are extracellularly located (D4) and others seem to be missing from certain CIC channels, based on their low hydropathy index and low degree of sequence conservation (Brandt and Jentsch, 1995) as indicated in Fig. 9. It is now clear that all CIC-K isoforms need barttin (Birkenhäger et al., 2001), a relatively small protein (320 amino acid) with two transmembrane spans next to the amino-terminus, as a  $\beta$ -subunit *in vitro* and *in vivo* (Estévez et al., 2001). Interestingly, its COOH-terminus contains a PY motif (PXPPY, where P is proline, X is any amino acid, and Y is tyrosine). This PY motif mediates binding to the WW domains of Nedd4 (Chen and Sudol, 1995).

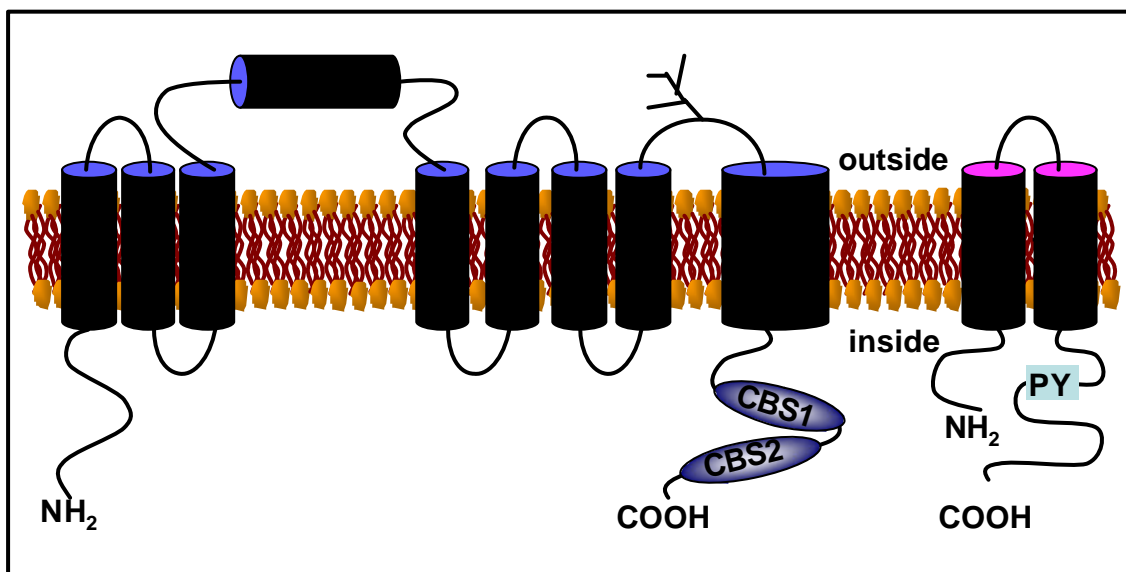


**Fig. 9. Transmembrane topology of CIC-K/barttin channels** (adapted from Jentsch et al., 2002). The CIC-K protein contains 12 transmembrane domains that were dubbed D1-D12. NH<sub>2</sub>- and COOH-termini are located intracellularly. The COOH-terminus has two CBS (cystathionine  $\beta$ -synthase) domains that have a so far unspecified role in protein-protein interaction (shown at left). CIC-K proteins associate with the  $\beta$ -subunit barttin, which spans the membrane twice (shown at right).

#### 1.4.4 Physiological regulation of channel activity

Renal CIC-K expression is influenced by changes in water and salt load. Dehydration increased transcription of CIC-K1 (Uchida et al., 1993; Vandewalle et al., 1997), compatible with its role in antidiuresis.

CIC-K2 was reported to be overexpressed in the renal medulla of Dahl salt-sensitive rats (Castrop et al., 2000). It was down-regulated by high-salt diet. To understand this regulation, promoters of both isoforms were isolated and subjected to an initial characterization (Uchida et al., 1998, 2000; Rai et al., 1999).

When expressed in *Xenopus* oocytes, rat CIC-K1 yielded anion currents with a moderate outward rectification that showed only little time-dependent relaxations. Their halide selectivity was  $\text{Br}^- > \text{Cl}^- > \text{I}^-$  (Uchida et al., 1998). Currents were decreased by extracellular acidification and by removing extracellular  $\text{Ca}^{2+}$  (Uchida et al., 1995). Increasing extracellular  $\text{Ca}^{2+}$  concentration led to further enhancement of currents, and no saturation was reached even at 5 mM  $\text{Ca}^{2+}$ .

$\text{Mg}^{2+}$  and  $\text{Ba}^{2+}$  lacked such an effect. To obtain definitive evidence that these currents are mediated by CIC-K1, a valine in a highly conserved domain at the end of D3 was replaced by glutamate, which is found in nearly all other CIC channels at that position. This drastically changed gating, which now slowly opened the channel upon hyperpolarization. Moreover, the halide selectivity was changed to  $\text{Cl}^- > \text{Br}^- > \text{I}^-$  (Waldegger and Jentsch, 2000).

CIC-K2 expression was reported to yield similar, outwardly rectified currents, which, however, lacked the initial gating component and displayed a  $\text{Br}^- > \text{I}^- > \text{Cl}^-$  selectivity (Adachi et al., 1994). Disconcertingly, a splice variant lacking transmembrane domain D2 gave currents with indistinguishable properties, suggesting that endogenous oocyte currents have been reported.

Two groups (Kieferle et al., 1994; Zimniak et al., 1996) were initially unable to get currents from any CIC-K channel, including both human isoforms. While the expression of CIC-K1 by Uchida and colleagues (1993, 1998) could later be reproduced by Waldegger and Jentsch (Waldegger and Jentsch, 2000), they

remained unable to observe currents with ClC-K2, ClC-Kb, and surprisingly also with ClC-Ka. To get as close to ClC-Kb currents as possible, a series of rat ClC-K1/human ClC-Kb chimeras was constructed. The currents from a chimera containing large parts of ClC-Kb differed markedly from ClC-K1. In particular, the  $\text{Cl}^- > \text{Br}^- > \text{I}^-$  selectivity differed from ClC-K1. In contrast to experiments reported for ClC-1/ClC-3 chimeric channels (Fahlke et al., 1997), the transplantation of a ClC-Kb stretch between D3 and D5 did not suffice to impose "ClC-Kb-like" features on ClC-K1. However, a stretch from D1 to D5 was sufficient (Waldegger and Jentsch, 2000), suggesting that pore properties are not "encoded" by a single small part of the protein.

It was recently shown (Estévez et al., 2001) that both isoforms of ClC-K need the  $\beta$ -subunit barttin for proper function. Barttin strongly enhanced ClC-K1 currents and led for the first time to measurable currents from ClC-Ka and ClC-Kb. In combination with barttin, both ClC-Ka and -Kb currents were enhanced by extracellular  $\text{Ca}^{2+}$  and inhibited by low extracellular pH (Estévez et al., 2001). The stimulation of ClC-Ka currents by barttin was due to an increased expression at the cell surface (Waldegger et al., 2002). Mutation in a putative PY motif in barttin's carboxy-terminus increased currents, possibly indicating a regulation of surface expression (Estévez et al., 2001) similar to that described for ClC-5 (Schwake et al., 2001).

#### 1.4.5 Pathophysiological significance of ClC-K/barttin channels

Mutations in *CLCNKB* underlie Classic Bartter syndrome or Bartter's syndrome type III (Simon et al., 1997), strongly suggesting that ClC-Kb (and ClC-K2 in rodents) mediates basolateral  $\text{Cl}^-$  efflux in the thick ascending limb of Henle's loop. The disruption of *Clcnk1* (the mouse orthologue of ClC-Ka) in mice led to nephrogenic diabetes insipidus (Matsumura et al., 1999), probably because it mediates  $\text{Cl}^-$  flux across cells of the thin ascending limb of Henle's loop (Uchida et al., 1995; Matsumura et al., 1999; Akizuki et al., 2001). Mutations in the common  $\beta$ -subunit barttin result in Bartter's syndrome with sensorineural deafness (BSND) and kidney failure (Birkenhäger et al., 2001).

### **1.5 Serum and glucocorticoid inducible kinase and protein kinase B**

Webster and co-workers (1993) were the first to observe an increase in mRNA encoding a kinase in a rat mammary tumor cell line after 30 min serum and glucocorticoid treatment. This kinase was then named serum and glucocorticoid induced kinase (SGK). SGK belongs to the serine/threonine kinase gene family. Its catalytic domain has significant sequence homology (45-55% identity) with rac protein kinase, the PKC family, ribosomal protein S6 kinase, cyclic AMP-dependent protein kinase A (PKA) (Webster et al., 1993) as well as protein kinase B (Kobayashi et al., 1999a).

Human SGK was subsequently identified in a human hepatoma cell line which is regulated by cell shrinkage (Waldegger et al., 1997) through p38/mitogen-activated protein kinase (MAP) kinase (Waldegger et al., 2000b). More recently, two additional human SGK have been cloned, termed SGK2 and SGK3, whose catalytic domains share 80% identity (Kobayashi et al., 1999a). SGK3 is also known as cytokine-independent survival kinase (CISK) since it is involved in cell survival through its Phox homology (PX) domain (Xu et al., 2001). Despite the high sequence similarity between all types of SGK, several differences are apparently present. SGK2 is only present at significant levels in liver, kidney and pancreas and only at lower levels in the brain, whereas SGK1 and SGK3 are ubiquitously expressed in all tissues examined. Furthermore, SGK1 is to a greater extent regulated by insulin-like growth factor 1 (IGF-1) whereas activation of SGK2 and SGK3 by H<sub>2</sub>O<sub>2</sub> are only partially inhibited by inhibitors of phosphatidylinositol 3-kinase (PI3-kinase) (Kobayashi et al., 1999a).

SGK1 expression is regulated by aldosterone (Brennan and Fuller, 2000; Chen et al., 1999; Cowling and Birnboim, 2000; Náray-Fejes-Tóth et al., 1999; Shigaev et al., 2000), transforming growth factor beta (Waldegger et al., 1999) and a wide variety of additional factors (Lang and Cohen, 2001). The activation of SGK1, SGK2 and SGK3 is mediated through PI3-kinase and 3-phosphoinositide-dependent protein kinase 1 (PDK1) and PDK2 (Kobayashi and Cohen, 1999b; Park et al., 1999). SGK1 is involved in many physiological and pathological processes such as membrane transport (Wagner et al., 2001;

Wang et al., 2001; Gamper et al., 2002a, b), cell growth and survival (Xu et al., 2001), fibrosis (Wärntges et al., 2002), chronic inflammation (Fillon et al., 2002) and probably hypertension (Busjahn et al., 2002). In addition, SGK has been shown to facilitate memory consolidation of spatial learning in rat (Tsai et al., 2002).

Protein kinase B was firstly discovered as a kinase with a catalytic domain homolog to PKA and PKC (Jones et al., 1991; Coffey and Woodgett, 1991). In contrast to SGK, PKB has a pleckstrin homology (PH) domain. SGK1 is phosphorylated at Thr-256 and Ser-422 by PDK1/2 (Kobayashi and Cohen, 1999b), PKB must be phosphorylated at two residues, Thr-308 and Ser-473 (Alessi et al., 1996) to be active. Phosphorylation of Thr-308 is mediated by PDK1, whereas the mechanism of Ser-473 phosphorylation is less clear. In addition to PDK1, kinases potentially involved in Ser-473 phosphorylation include integrin-linked kinase (ILK) or an ILK associated kinase (Delcommenne et al., 1998; Lynch et al., 1999) and PKB itself (Toker and Newton, 2000).

Similar to SGK, PKB is capable of phosphorylating several proteins containing certain sequence motifs, for instance glycogen synthase kinase 3 beta (GSK3 $\beta$ ), B-Raf and the fork head transcription factor 1 (FKHR1). PKB has been known to be a key mediator of the insulin signaling pathway. Overexpression of PKB not only leads to an increased glycogen and protein synthesis but also to an enhancement of glucose and amino acids uptake (Barthel et al., 1997; Hajdich et al., 1998). Moreover, certain changes in gene expression induced by insulin are stimulated by PKB (Barthel et al., 1997, 1999).



## 1.6 The Na<sup>+</sup>/H<sup>+</sup> exchanger regulating factor (NHERF)

The Na<sup>+</sup>/H<sup>+</sup> exchanger regulating factor, NHERF (also known as NHERF1 and ERM-binding phosphoprotein 50 (EBP50)), was firstly identified in kidney as a protein cofactor essential for cAMP regulation of the activity of NHE3 (Weinman et al., 1995). Shortly thereafter, a second member of this family was isolated from small intestine and renal brush border and characterized (NHERF2, also called NHE3 kinase A-regulated protein (E3KARP) and TKA1) as an activator of the platelet-derived growth factor receptor tyrosine kinase (Yun et al., 1997, 1998).

NHERF and NHERF2 contain two tandem protein-protein interactive PDZ (PSD-95/*Drosophila* disk large/ZO-1) domains (Weinman et al., 1995) and a carboxy-terminal ezrin-radixin-moesin-merlin-binding domain interacting with the amino-terminal domain of merlin and the ERM proteins known as ezrin-radixin-moesin-association domain (ERMAD) (Murthy et al., 1998; Reczek and Bretscher, 1998). Following the demonstration that these proteins bind ezrin (Reczek et al., 1997), a new model was developed for regulation of target proteins, in which NHERF (or NHERF2), ezrin, and protein kinase form a multiprotein signal complex linking target protein to the actin cytoskeleton. The formation of this complex is proposed to facilitate the phosphorylation and regulation of target protein (Fig. 10).

NHERF interacts, via its PDZ domains, with a variety of membrane receptors such as  $\beta_2$ -adrenergic receptor ( $\beta_2$ -AR), platelet-derived growth factor receptor (PDGFR), the P2Y1 purinergic receptor (Hall et al., 1998a, b), as well as with ion transport proteins such as cystic fibrosis transmembrane regulator (CFTR) (Hall et al., 1998b), the G protein-coupled receptor kinase (GRK6A) (Hall et al., 1999), the  $\beta_1$ -subunit of the H<sup>+</sup>-ATPase (Breton et al., 2000), c-yes tyrosine kinase-associated protein (YAP65) (Mohler et al., 1999) and NHE3 (Weinman et al., 1998).

A previous study has shown, that the potassium channel, Kv1.3, which contains PDZ binding motifs at the carboxy-terminal was targeted apically in polarized cells, whereas its splice variant devoid of PDZ motifs was localized at the

basolateral membrane (Ponce et al., 1997). NHERF and NHERF2 are predominantly found in the apical membrane indicating their involvement in directing target proteins to the apical membrane. Moreover, ezrin, an anchoring protein interacting with NHERF, is exclusively associated with apical membranes (Shenolikar et al., 1988). However, NHERF can also be found basolaterally thus permitting NHERF to target certain proteins to the basolateral membrane such as the  $\text{Na}^+\text{-HCO}_3^-$  cotransporter (Bernardo et al., 1999).

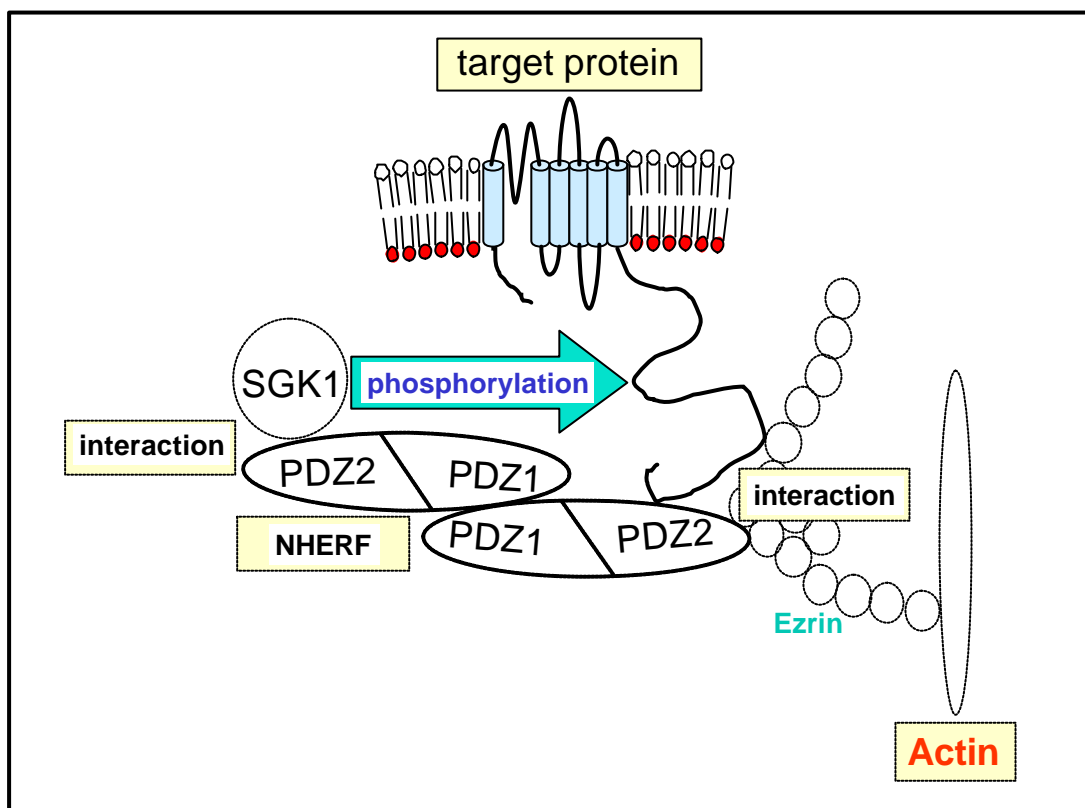


**Fig. 10. NHERF, a membrane-cytoskeletal adapter.** The interaction between NHERF and target protein occurs via the second PDZ domain (PDZ2) of NHERF and an internal region (PDZ binding motifs) located within the cytoplasmic domain of target protein. The second PDZ domain (PDZ2) of NHERF also binds SGK1. This is probably achieved by dimerization of NHERF. A homodimer of NHERF should be able to bind target protein on one end and SGK1 on the other end rendering phosphorylation and stabilization of target protein by mediating interaction with actin cytoskeleton via ezrin.

### 1.7 The ubiquitin protein ligase Nedd4

Nedd4 (neuronal precursor cell-expressed, developmentally down-regulated 4) was identified originally as a developmentally regulated mouse gene highly expressed in early embryonic central nervous system (Kumar et al., 1992). Further analysis revealed that the expression of Nedd4 is not restricted to the embryonic central nervous system and that it is expressed at varying levels in different tissues including lung, kidney, and colon (Staub et al., 1996, 1997; Kumar et al., 1997).

At the time that Nedd4 was first cloned in 1992, the only identifiable structure in the protein was a  $\text{Ca}^{2+}$ /lipid-binding (CaLB) domain (C2 domain) and three to four repeats of approximately 40 amino acids. These repeats are now known as WW domains (Sudol, 1996). In 1993, the COOH-terminal region of Nedd4 was discovered to be similar to human papilloma virus (HPV) oncoprotein E6-associated protein (E6-AP). E6-AP is a ubiquitin-protein ligase involved in the E6-mediated ubiquitination of p53 (Scheffner et al., 1993, 1995).

The  $\text{Ca}^{2+}$ /lipid-binding (CaLB) domain (C2 domain) is located towards the amino-terminus of Nedd4. The C2 domain was first identified in protein kinase C and is responsible for  $\text{Ca}^{2+}$ -dependent binding of membrane phospholipids (Knopf et al., 1986). The function of the C2 domain in the Nedd4 protein is not well understood, but it might mediate the redistribution of Nedd4 from the cytosol to the plasma membrane in response to fluctuations in intracellular  $\text{Ca}^{2+}$  concentration (Plant et al., 1997).

The WW domains are located between the C2 and ubiquitin-protein ligase domains in the middle of the Nedd4 protein. WW domains (also known as WWP or rsp5 domains) derive their name from the presence of two highly conserved tryptophan residues and a conserved proline residue in a sequence of ~35 amino acids (Sudol, 1996). Functionally, WW domains have been proposed to operate in a manner similar to the SH3 domains in that they bind polyproline ligands (Sudol, 1996).

The ubiquitin-protein ligase domain is situated at the COOH-termini of the Nedd4 protein. It is a large domain (approximately 350 residues) and was first

characterized in the human ubiquitin-protein ligase E6-AP, and hence is often referred to as the HECT (homologous to E6-AP COOH-terminus) domain (Scheffner et al., 1993, 1995).

The presence of these three domains in Nedd4 suggested that Nedd4 could be involved in  $\text{Ca}^{2+}$ -mediated ubiquitination of membrane protein(s). Recently, a number of proteins have been discovered that share the same modular structure as Nedd4 and appear to be part of a family of ubiquitin-protein ligases. Some of these proteins have been implicated in a variety of cellular functions.

The characteristic feature of the Nedd4 family of proteins is the organization of the C2, WW and ubiquitin-protein ligase domains. Two closely related Nedd4 isoforms (or paralogues) exist: Nedd4-1 (also named Nedd4, KIAA0093, or RPF1) and Nedd4-2 (also known as KIAA0439, LdI-1, Nedd4La, Nedd18, or Nedd4-L) (Kamynina et al., 2001).

Nedd4-1 is composed of one C2 domain, a HECT domain, and three to four WW domains. The rat and mouse species contain three WW domains, whereas in humans there are four WW domains. The difference in the number of WW domains may be due to alternative splicing, as there is evidence for multiple transcripts in human Nedd4-1 (Kamynina et al., 2001).

Nedd4-2 contains four WW domains and a HECT domain (Fig. 11). Only human and *Xenopus laevis* Nedd4-2 comprise a C2 domain, whereas such a domain appears to be lacking in mouse Nedd4-2. Again, there is evidence for alternative splicing of this isoform as well (Chen et al., 2001; Kamynina et al., 2001), and there may be isoforms that contain, and others that do not contain, a C2 domain.

It has been proposed that the WW domains of Nedd4 bind to the proline-rich motifs (XPPXY) present in the carboxy-termini of the three subunits of ENaC (Staub et al., 1996) and that binding to the channel allows subsequent ubiquitination of several lysine residues in the amino-termini of the  $\alpha$ - and  $\gamma$ -subunits but not in the  $\beta$  subunit. Although  $\alpha$ - and  $\gamma$ -subunits are ubiquitinated by Nedd4, only ubiquitination of  $\alpha$ -subunit is functionally important (Staub et al., 1997). By analogy to certain membrane proteins with rapid turnover,

ubiquitination of ENaC could serve as a signal for retrieval of channels from the plasma membrane and their subsequent degradation in lysosomes. In fact, coinjection of Nedd4 and ENaC in *Xenopus* oocytes decreases the amiloride-sensitive current of wild-type ENaC channels but not channels lacking the proline-rich motifs (Goulet et al., 1998; Abriel et al., 1999).

If Nedd4 were to decrease the number of channels at the cell surface, it would be an attractive candidate as a mediator of inhibitory processes such as the effects of increasing intracellular  $\text{Na}^+$ . The rate of  $\text{Na}^+$  entry across the apical membrane is regulated to match the basolateral extrusion rate and thereby to maintain cell volume and intracellular  $\text{Na}^+$  concentration  $[\text{Na}^+]_i$ . In salivary glands, increased  $[\text{Na}^+]_i$  inhibits ENaC by a mechanism that involves subunits of the guanine nucleotide-binding  $G_o$  protein (Komwatana et al., 1996). The intermediate steps of the pathway are not known. Dinudom et al., 1998, seeking evidence linking Nedd4 to this pathway, showed that the inhibitory effect of increasing  $[\text{Na}^+]_i$  in salivary cells could be abolished by blocking the activity of Nedd4 either with anti-Nedd4 antibodies or by injecting fusion proteins containing WW domains (Dinudom et al., 1998; Harvey et al., 1999). Similar results were obtained in oocytes where increasing concentrations of  $[\text{Na}^+]_i$  produced a reduction of the amiloride-sensitive current in oocytes expressing wild-type ENaC but not in oocytes expressing the carboxy-terminal truncated channels (Kellenberger et al., 1998).

Recently, Lu et al., 1999, showed that the WW domains of Nedd4 bind with high affinity to peptides containing serines or threonines, but only when the peptides are phosphorylated at the serine or threonine residues (Lu et al., 1999). The amino acid sequences of the peptides recognized by the WW domains of Nedd4 were different from the previously reported proline-rich peptides, which also can interact with Nedd4 *in vitro* but with low affinity. Some of the known substrates for Nedd4 are proteins such as uracil permease and Cdc25C that do not contain the typical proline-rich motifs but have serine and threonine residues that undergo phosphorylation. The findings of Lu are consistent with Nedd4 mediating the ubiquitination of proteins by binding to sequences containing

phosphoserine or phosphothreonine different from the bona fide proline-rich motifs, and thus raise questions about ENaC being a substrate for Nedd4.

Even if Nedd4 turns out not to bind ENaC, all the currently available data can still be explained because the proline-rich domains of ENaC also contain endocytic signals for removal of channels from the plasma membrane (Shimkets et al., 1997). Therefore, deletions or disruptions of these sequences would retain channels in the plasma membrane explaining all the mutagenesis performed *in vitro* and also the phenotype of the mutations found in patients with hypertension.

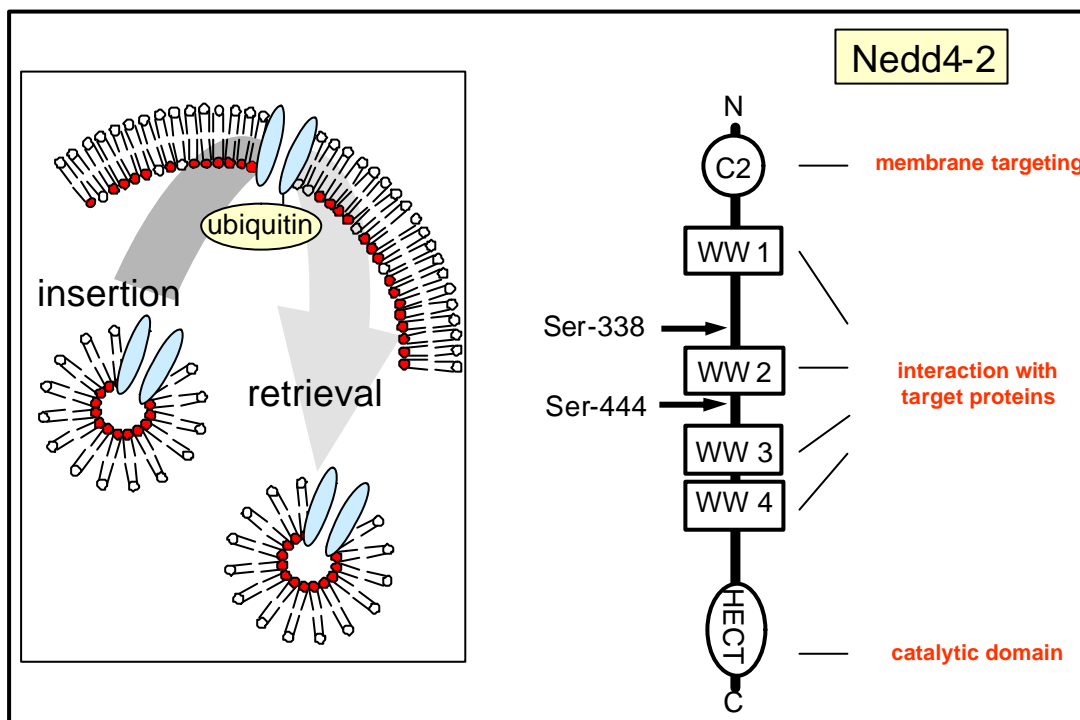


**Fig. 11. Domain organization of Nedd4-2 with the consensus phosphorylation sites of SGK1**, depicting the C2 domain, four WW domains and the ubiquitin protein ligase HECT domain (right panel). The binding of Nedd4-2 to targets proteins (proline-rich proteins) is shown, resulting in ubiquitination, internalization, and subsequent degradation of these proteins (left panel). Abbreviations are: C2,  $\text{Ca}^{2+}$ -dependent lipid binding; WW domains, named after a pair of conserved tryptophans, are highly compact (35-45 residues) modular domains and serve protein-protein interaction; HECT, a domain homologous to the E6-AP-COOH-terminal domain is the catalytic portion of this protein.

### **1.8 *Xenopus laevis* oocytes and electrophysiological recording**

One of the first and still most widely used assay system for quantifying an authentic protein biosynthetic process is the fully grown oocyte of the South African clawed frog, *Xenopus laevis*. The value of *Xenopus laevis* first became apparent in 1971, when Gurdon and co-workers discovered that the oocyte constitutes an efficient system for translating foreign messenger RNA (Gurdon et al., 1971).

The *Xenopus* oocyte is a cell specialized for the production and storage of proteins for later use during embryogenesis and developmentally divided into 6 stages (Dumont, 1972). In addition, the complex architecture of the frog oocyte includes the subcellular systems involved in the export and import of proteins. Therefore, the mRNA-microinjected oocyte is an appropriate system in which to study the synthesis of specific polypeptides, as well as the storage of particular proteins in various subcellular organelles and the export of others into the extracellular space. Moreover, the subcellular compartmentalization, as well as the structure and biochemical, physiological, and biological properties of the synthesized protein, may be examined from exogenous proteins in the injected oocyte (reviewed in Wagner et al., 2000).

For experimental studies oocytes of stages V-VI are used with a diameter of some 1.3 mm allowing easy preparation. The developmental stages V-VI are characterized by the occurrence of 2 poles i.e. the vegetable (light) and the animal (dark) poles. While the nucleus resides in the animal pole (Nieuwkoop, 1977), more mRNA is present in the vegetable pole (Capco and Jeffery, 1982). The main ion conductance in *Xenopus* oocytes is a  $\text{Ca}^{2+}$ -dependent  $\text{Cl}^-$  conductance governing the resting membrane potential close to the  $\text{Cl}^-$  reversal potential of -40 mV, (Dascal, 1987).

The primary advantage of using *Xenopus* oocytes for the expression of transporters is the ability to perform detailed electrophysiological recording using an *in vivo* system. In the simplest arrangement, the membrane is penetrated with a single microelectrode and the membrane potential is measured. The oocyte can easily be penetrated with two microelectrodes. This

arrangement allows the use of one of the two classical methods: current clamp or voltage clamp. Most electrophysiological studies on oocytes were performed using the two-electrode voltage-clamp. The large size of the oocytes also permits extracellular recording of currents flowing through the cell membrane at various locations using a vibrating probe. The patch clamp method has been successfully applied in devitellinized oocytes for the study of single channels (Hamill et al., 1981).

Whole-cell voltage clamping of oocytes involves two electrodes inserted into the oocyte. The large size of the oocyte (about 1 mm in diameter and 0.5 to 1  $\mu$ l in volume for stage V-VI oocytes) make this feasible, and is both the major advantage and disadvantage of the system. The advantage is that it is possible to insert multiple electrodes and injection needles into the same oocyte. Therefore, modulators of channel function can be injected inside the cell while recording, so that a rapid and direct response to an intracellular signal can be observed. The disadvantage is that the large size results in an extremely large membrane capacitance (about 150-200 nF), which causes a slow clamp setting time following voltage shifts. This makes it difficult to obtain any data during the first 1 to 2 msec of a hyper- or depolarization, the time during which rapidly activating voltage sensitive channels such as the cardiac sodium channel open. The large capacitance is not a serious problem in examining slow responses or ligand-gated responses in the absence of voltage shifts (Stuhmer, 1992).

Despite their advantages, several precautions should be taken into consideration. First, the expression of endogenous carriers may interfere with the exogenously expressed proteins in various ways. For instance, it has been observed that injection of heterologous membrane proteins at high levels can induce endogenous channels (Tzounopoulos et al., 1995). Second, due to the fact that *Xenopus laevis* is a poikilothermic animal, its oocytes are best kept at lower temperature and most experiments are carried out at room temperature. Hence, temperature sensitive processes i.e. protein trafficking or kinetics may be altered (Wagner et al., 2000).



Finally, since *Xenopus* oocytes may have different signaling pathways, precaution should be taken when studying the regulation of expressed proteins. It has been revealed that the PTH receptor regulates the internalization of NaPi, mediated by the PKA and PKC pathway. However, in NaPi-3 expressing *Xenopus* oocytes PKC-mediated PTH regulation can not be observed (Wagner et al., 1996). Instead, coupling to the PKA pathway leads to the alteration of PKA-regulated ion channels (Waldegger et al., 1996). Exposing the *Xenopus* oocytes to the regulators of intracellular signaling such as PKC activator phorbol esters may unspecifically lead to internalization of the plasma membrane and the expressed proteins (Vasilets and Schwarz, 1992; Loo et al., 1996).

In summary, the *Xenopus* oocyte system has the advantage that channels, receptors and transporters can rapidly be expressed and analyzed both biochemically and electrophysiologically in an *in vivo* situation. The system can be used quite effectively as an assay for the functional cloning of channels that have only been identified by their electrophysiological properties. Once cDNA clones have been isolated, oocytes are an excellent system for correlating structure with function using a combination of molecular biological and electrophysiological techniques.

## 1.9 AIMS OF THE PRESENT STUDY

The motivation of this study was to resolve the role of Serum and Glucocorticoid Inducible Kinase isoforms, ubiquitin protein ligase Nedd4-2 and NHERF3 regulating factor 2 in the regulation of renal tubular transport. To this end the major channels mediating transport of potassium, calcium and chloride which are expressed in the renal tubules have been investigated. It included:

(1) ROMK1 channel:

- Identification of a mutual interaction of SGK1 and NHERF2 in the regulation of ROMK1 channel activity.
- Exploration whether alterations of the charge at phosphorylation site of SGK1 on the ROMK1 indeed modify the pH sensitivity of ROMK1.
- Definition of the molecular requirements for the interaction of ROMK1 with SGK1/NHERF2.

(2) ECaC1 (TRPV5) channel:

- Investigation of the role of SGK isoforms, protein kinase B and NHERF2 in the regulation of ECaC1 (TRPV5) activity.
- Definition of the molecular requirements for the interaction of ECaC1 (TRPV5) with SGK1/NHERF2.

(3) CIC-Ka/barttin channels:

- Verification of general implications for the regulation of CIC-Ka/barttin chloride channels by the ubiquitin protein ligase Nedd4-2 and the SGK isoforms SGK1, SGK2 and SGK3.

## **2 Materials and Methods**

## 2.1 Equipment and materials

### 2.1.1 Laboratory equipment

Acquisition software	ADInstruments, Castle Hill, Australia
Autoclave	Technoklav 50, Tecnomara, Fernwald
Balance	Mettler AE 163, Mettler Waagen, Gießen
Digitization board	ITC16, HEKA electronics, Lamprecht
Digital-pH-Meter 646	Knick, Freiburg
Electrode puller	DMZ-Universal Puller, Zeitz-Instrumente, Augsburg
Gel electrophoresis	Horizon 58, Life Technologies, Gaithersburg MD, USA; power supply EPS 600, Pharmacia Biotech, Uppsala, Sweden
Incubator	WTB Binder, Tuttlingen
Incubator Type B 5070	Heraeus, Hanau
Liquid scintillator	Wallac, Freiburg
Microcentrifuge MC13	Amicon, Austin, Texas, USA
Microcentrifuge Micro12-24	Bachofer, Reutlingen
Microinjector	World Precision Instruments, Sarasota, Florida, USA
Minifuge RF	Heraeus, Hanau
Oscilloscope	HM 1007, Hameg, Frankfurt
Precision forceps (size 3 & 5)	Dumont, Basel, Switzerland
Pump	WISA, Wuppertal
PCR-Mastercycle gradient	Eppendorf, Hamburg
Photometer	Eppendorf, Hamburg
Pipettes	Pipetman P2/P20/P200/P1000, Gilson Medical Electronics, Villiers-le-Bel, France

---

Refrigerator UF 85-300S	Colora Messtechnik, Lorch
Shakers	MS1 IKA Works Inc., Wilmington NC, USA, and Thermomixer 5436 Eppendorf, Hamburg
Speed Vac (Vacuum conc.)	Bachofer, Reutlingen
Temperature-controlled bath	GFL 1003, Gesellschaft für Labortechnik mbH, Burgwedel
TEVC Amplifier	Axon Instruments, Inc., USA
Ultrasonic bath	Transsonic T420, Elma, Singen
UV-Spectrometer	GeneQuant Amersham-Pharmacia, Freiburg
Vortex Genie 2	Bender & Hobein AG, Zürich, Switzerland
Water Filter Seralpur UP 50	Seral, Ransbach-Baumbach

### 2.1.2 Materials

Embedding polymer	Technovit 7100, Heraeus Kulzer, Wehrheim
Filter tips	SafeSeal Tips, Biozym Diagnostic, Oldendorf
Glass slides	Superior, sealed with Entellan, E. Merck, Darmstadt
Microloaders	Eppendorf, Hamburg
Petri dishes (sterile)	Greiner, Frickenhausen
X-ray films	Biomax MR, Eastman Kodak Company, Rochester NY, USA

### 2.1.3 Chemicals and reagents

Agar Agar	Roth, Karlsruhe
Agarose	electrophoresis grade, Life Technologies, Paisley, Scotland

---

Antibiotics I	stock solution (10.000 U Ampicillin and 10 mg streptomycin per ml), Sigma, St. Louis, Missouri, USA
Antibiotics II	stock solution (50 mg Gentamycin per ml), Sigma, St. Louis, Missouri, USA
Bovine serum albumin	Sigma-Aldrich, Deisenhofen
Bromphenol blue	Sigma-Aldrich Chemie, Steinheim
Cap-Analog m <sup>7</sup> G(5')ppp(5')G	Roche, Mannheim
Carbontetrachloride	Fluka Chemicals, Deisenhofen
Chemoluminescence ECL kit	Amersham, Freiburg
Collagenase D	Roche, Mannheim
cRNA synthesis and DNase I	mMessage-mMachine kit, Ambion, Austin, USA
Cu-phenanthroline	Sigma-Aldrich Chemie, Steinheim
Developer and replenisher	Biomax MR, Eastman Kodak Company, Rochester NY, USA
Diethylpyrocarbonat (DEPC)	Sigma-Aldrich, Deisenhofen
Dimethylsulfoxid (DMSO)	Sigma-Aldrich, Deisenhofen
DNA-Ladder, 1 kb and 100bp	Life Technologies, Eggenstein
DNA sequencing kit	DNA Sequencing Kit, Amersham, Cleveland, USA
DNAase (RNAase free)	Roche, Mannheim
dNTPs, 100 mM	Life Technologies, Eggenstein
DTT, DTNB	Sigma, St. Louis, Missouri, USA
EDTA	Sigma-Aldrich Chemie, Steinheim
EGTA	Sigma-Aldrich Chemie, Steinheim
Ethidium bromide	Sigma-Aldrich Chemie, Steinheim
Ficoll	Sigma-Aldrich Chemie, Steinheim
Fixer and replenisher	Biomax MR, Eastman Kodak Company, Rochester NY, USA

---

FmocCl	Sigma, St. Louis, Missouri, USA
Formamid	Roth, Karlsruhe
Glutathione-sepharose 4B beads	Pierce Biotechnology Inc., Rockford, IL; USA
Glycerol-gelatin	Sigma-Aldrich, Deisenhofen
GSH	Sigma, St. Louis, Missouri, USA
H <sup>+</sup> -cocktail	proton ionophore II-cocktail A, Fluka Chemicals, Deisenhofen
ImmunoPure immobilized Streptavidin beads	Pierce Biotechnology Inc., Rockford, IL; USA
Isopropanol	Sigma-Aldrich Chemie, Steinheim
LB medium	Luria Broth base, Gibco BRL, Life Technologies, Paisley, Scotland
[ <sup>35</sup> S]methionine	NEN life science products Inc., Boston, MA; USA
Mercaptoethanol	Sigma-Aldrich Chemie, Steinheim
Methoxyverapamil	Sigma-Aldrich Chemie, Steinheim
Normal Goat serum	Sigma, St. Louis, Missouri, USA
Paraformaldehyde	Sigma-Aldrich Chemie, Steinheim
PCR buffer	Gibco BRL, Life Technologies, Karlsruhe
pGEX-4T	Amersham Pharmacia Biotech AB, Uppsala, Sweden
pGEX6p-2	Amersham Pharmacia Biotech AB, Uppsala, Sweden
Plasmid preparation kit	Midi Prep Kit, Qiagen, Hilden
Poly-Acrylamide	Applichem, Darmstadt
Primary antibodies	rat monoclonal anti-HA, Roche, Mannheim, mouse monoclonal anti-V5, Invitrogen, Karlsruhe
Primary rabbit anti-ROMK1 antibody	Chemicon, Temecula, USA
QIAfilter Plasmid Midi Kit	Qiagen, Hilden

---

QuickChange™ Site-directed Mutagenesis kit	Stratagene, Heidelberg
Restriction enzymes	Boehringer, Mannheim
RNAase inhibitor	Promega, Mannheim
RNA ladder	0.24-9.5 kb RNA Ladder, Life Technologies, Karlsruhe
Scintillation fluid	Ultima Gold, Packard, Groningen, the Netherlands
SDS	Roth, Karlsruhe
Secondary antibodies	Cy-2- or Cy-3-coupled antibodies, Amersham Pharmacia Biotech, Freiburg
Secondary Alexa 488 goat anti-rabbit antibody	Molecular Probes, Leiden, The Netherlands
Sulfo-NHS-LC-Biotin	Pierce Biotechnology Inc., Rockford, IL; USA
Taq polymerase	Gibco BRL, Life Technologies, Karlsruhe
T7 (or Sp6) RNA Polymerase	Roche, Mannheim
Tributylchlorosilane	Fluka Chemicals, Deisenhofen
Tris-HCl	Sigma-Aldrich Chemie, Steinheim
Tween 20	Roth, Karlsruhe
X-ray films	Biomax MR, Eastman Kodak Company, Rochester NY, USA
5'-Cy5 labelled primers	Gibco BRL, Life Technologies, Karlsruhe
$^{45}\text{Ca}^{2+}$	ICN Biomedicals, GmbH, Eschwege

Other chemicals are of high chemical grade and purchased from Sigma (Deisenhofen), Fluka (Deisenhofen) or Roche (Mannheim).



#### 2.1.4 Solutions, medium and buffer

**Table 1: Solutions related to *E. coli* Bacteria**

	LB-Medium	LB- Selection- Medium	LB-Agar	SOB- Medium	SOC- Medium
Ampicillin (µg/ml)	-	100	-	-	-
Bactoagar % (w/v)	-	-	1.5	-	-
Bactotrypton % (w/v)	1	1	1	2	2
Glucose (mmol/l)	-	-	-	-	20
Yeast extract % (w/v)	0.5	0.5	0.5	0.5	0.5
KCl (mmol/l)	-	-	-	2.5	2.5
MgCl <sub>2</sub> (mmol/l)	-	-	-	10	10
NaCl % (w/v)	1	1	1	0.05	0.05
pH	7.4	7.4	7.4	7.0	7.0

**Table 2: Solutions used for enzymatic defolliculation and storage of *Xenopus* oocytes**

	ND96	ND96 Storage Solution	OR-2 (Oocytes-Ringer)
NaCl (mmol/l)	96	96	82.5
KCl (mmol/l)	2	2	2
CaCl <sub>2</sub> (mmol/l)	1.8	1.8	-
MgCl <sub>2</sub> (mmol/l)	1	1	1
Tris-HEPES (mmol/l)	5	5	5
Na-Pyruvate (mmol/l)	-	2.5	-
Theophylline (mmol/l)	-	0.5	-
Gentamycin (µg/ml)	-	50	-
pH	7.4	7.4	7.4

**Table 3: Solutions used for ROMK1 and ClC-Ka/barttin measurements**

	ND96
NaCl (mmol/l)	96
KCl (mmol/l)	2
CaCl <sub>2</sub> (mmol/l)	1.8
MgCl <sub>2</sub> (mmol/l)	1
Tris-HEPES (mmol/l)	5
pH	7.4

The final solutions were titrated to the pH indicated using HCl or NaOH. The flow rate of the superfusion was 20 ml/min and a complete exchange of the bath solution was reached within about 10 s.

**Table 4: Solutions used for ECaC1 measurements**

	Storage solution	Bath solution	Wash solution	Uptake solution	Stop solution
NaCl (mmol/l)	88	96	96	96	96
KCl (mmol/l)	1	2	2	2	-
CaCl <sub>2</sub> (mmol/l)	0.4	-	-	0.1	0.5
MgCl <sub>2</sub> (mmol/l)	-	1	1	1	1
MgSO <sub>4</sub> (mmol/l)	0.8	-	-	-	-
BaCl <sub>2</sub> (mmol/l)	-	1	1	1	-
<sup>45</sup> Ca <sup>2+</sup> (μCi/ml)	-	-	-	7	-
Ca(NO <sub>3</sub> ) <sub>2</sub> (mmol/l)	0.3	-	-	-	-
LaCl <sub>3</sub> (mmol/l)	-	-	-	-	1.5
NaHCO <sub>3</sub> (mmol/l)	2.4	-	-	-	-
EGTA (mmol/l)	-	1	1	-	-
HEPES (mmol/l)	5	5	5	5	5
Gentamycin (μg/ml)	25	-	-	-	-
Methoxyverapamil (μmol/l)	-	10	10	10	-
pH	7.4	7.4	7.4	7.4	7.4

**Table 5: Buffers used for Molecular Biology**

	PBS-Buffer	TAE-Buffer	TBE-Buffer	TE <sup>-4</sup> -Buffer	Oocytes lysis Buffer
Boric acid (mmol/l)	-	-	8.9	-	-
EDTA (mmol/l)	-	1	1	-	0.5
EGTA (mmol/l)	-	-	-	-	0.5
Acetic acid (mmol/l)	-	20	-	-	-
KH <sub>2</sub> PO <sub>4</sub> (mmol/l)	10	-	-	-	-
NaCl % (w/v)	0.9	-	-	-	0.6
Na <sub>2</sub> -EDTA (mmol/l)	-	-	0.1	-	-
Na <sub>2</sub> PO <sub>4</sub> (mmol/l)	10	-	-	-	-
Tris-HCl (mmol/l)	-	40	8.9	10	50
Triton X-100%	-	-	-	-	1
Aprotinine µg/ml	-	-	-	-	25
Leupeptin µg/ml	-	-	-	-	25
pH	7.4	8	9	8	8

- **PBS-Buffer:** phosphate-buffered saline.
- **TAE-Buffer:** Tris-acetate/EDTA electrophoresis buffer.
- **TBE-Buffer:** Tris-borate/EDTA electrophoresis buffer.
- **TE<sup>-4</sup>-Buffer:** Tris-EDTA.
- **Aprotinine and Leupeptin:** protease inhibitors only added in oocytes lysis buffer.

**Table 6: Buffers used for DNA Gel Electrophoresis**

	Agarose-Simple Buffer	6 x Sample Buffer	4 x SDS-PAGE Loading Buffer
2-Mercaptoethanol (ml)	-	-	0.4
Bromphenol blue % (w/v)	0.01	0.25	0.4 ml 1% (w/v)
Ficoll 400% (w/v)	20	-	-
Glycerol % (v/v)	-	30	40
H <sub>2</sub> O <sub>dest.</sub> (ml)	-	-	1.9
SDS (ml)	-	-	1.6 ml 10%
TBE	1 x	-	-
Tris-HCl (ml)	-	-	1 ml 0,5 M
Xylenxyanol % (w/v)	-	0.25	-
pH	-	-	6.8

## 2.2 Heterologous expression in *Xenopus* oocytes

### 2.2.1 *In vitro* cRNA transcription

As illustrated in Fig. 12, *in vitro* cRNA transcription involves 2 consecutive steps i.e. linearisation of the plasmid DNA containing the inserted cDNA of interest by the corresponding restriction enzyme and the synthesis of RNA.

- a. The inserted DNA should be cut at the 3' end yielding a 5' protruding or a blunt end by restriction enzyme. Plasmid DNA (10 µg) was incubated with 20 U restriction enzyme and an 10x buffer (5 µl) in a final volume of 50 µl at 37°C for 2 h or overnight.
- b. To ascertain the linearization process, a 5 µl aliquot was taken out and analysed on a 1% agarose.
- c. 1 volume isopropanol (50 µl) and 1/10 volume 3 M sodium acetate (5 µl) pH 5.2 was then added and incubated at room temperature for 10 min to precipitate the DNA.
- d. The precipitated DNA was recovered by centrifugation at 17,000 rpm for 15 min at 4°C. The DNA pellet was washed by adding 100 µl of cold 70% ethanol to the pellet followed by centrifugation at 17,000 rpm for 5 min at 4°C. This washing stage was repeated. The DNA pellet was air dried and then resuspended in 10 µl of DNase free H<sub>2</sub>O. The concentration of DNA was determined spectrophotometrically by measuring the absorbance at 260 nm.
- e. 1 µg of linearised DNA was added to 1 µl rNTPS (20 nM), 2.5 µl Cap analogue (to prevent the degradation of the 5' end of the synthesized RNA), 1 µl RNAase inhibitor (to protect the RNA from degradation by RNAase) and 2.4 µl 10 x transcription buffer(s).
- f. After mixing, 1 µl of T7 polymerase was added and then incubated at 37°C for 1 h.
- g. 1 µl DNase was added and the mixture was subsequently shaken for 15 min at 37°C.
- h. After addition of 100 µl DEPC-water and 125 µl phenolchloroform, the mixture was centrifuged at 13,000 rpm for 2 min.

- i. The upper part, inorganic phase, was then removed and placed into a new Eppendorf tube.
- j. The inorganic phase was frozen at  $-70^{\circ}\text{C}$  for a minimum of 15 min after addition of  $12.5\ \mu\text{l}$  of 3 M sodium acetate at pH 5.2 and  $375\ \mu\text{l}$  100% ethanol.
- k. After centrifugation at 17000 rpm for 15 min at  $4^{\circ}\text{C}$ , the supernatant was removed and the pellet was washed 2 times with  $200\ \mu\text{l}$  of 70% ethanol.
- l. The washed pellet was dried at room temperature and reconstituted in  $25\ \mu\text{l}$  of DEPC water.
- m. The RNA was quantified by measuring the absorbance at 260 nm.

To increase the translation of the cloned cRNA in *Xenopus* oocytes, the plasmid vectors also contained 5' and 3' untranslated regions of cDNA such as the one coding for  $\beta$ -globin.

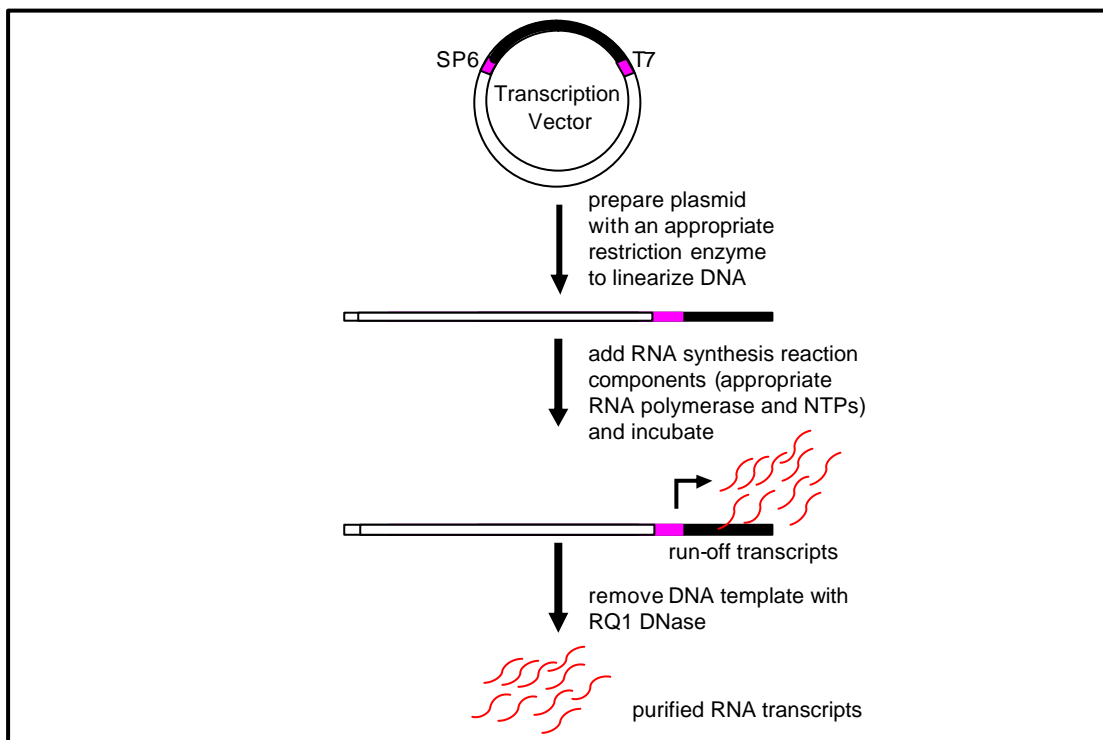


**Fig. 12. Steps of *in vitro* cRNA transcription** (adapted from Swanson and Folander, 1992). The common RNA polymerases used for *in vitro* transcription are SP6, T7 and T3 polymerases, named for the bacteriophages from which they were isolated or cloned. These RNA phage polymerases are DNA template-dependent and have distinct, highly specific promoter sequence requirements. Depending on the orientation of the DNA sequence relative to the promoter, the template may be designed to generate a sense or antisense strand RNA.

**Table 7: List of plasmids used with additional informations for *in vitro* transcription**

	Plasmid Vector	Resistance	Restriction Enzyme	Polymerase	Provided by
ROMK1	pSport	Ampicillin	Not I	T7	Cecilia Canessa
<sup>S44D</sup> ROMK1	pSport	Ampicillin	Not I	T7	Monica Palmada
<sup>S44A</sup> ROMK1	pSport	Ampicillin	Not I	T7	
ROMKHA	PBF	Carbenicillin	Mlu I	Sp6	
ROMK $\Delta$ 4	pSport	Ampicillin	Not I	T7	
ECaC1 (TRPV5)	pSport	Ampicillin	Not I	T7	Rene Bindels
CIC-Ka	PTLN	Ampicillin	Mlu I	Sp6	Siegfried Waldegger
Barttin	POG	Ampicillin	Ksp I	T7	
<sup>Y98A</sup> Barttin	POG	Ampicillin	Ksp I	T7	Monica Palmada
Nedd4-2	PSPeasy SB	Ampicillin	ClaI	Sp6	Olivier Straub
SGK1	pOG	Ampicillin	Not I	T7	Siegfried Waldegger
SGK2-3	pGEMHJ	Ampicillin	StuI/NotI	T7	Yuxi Feng
<sup>S422D</sup> SGK1	pGHJ	Ampicillin	SaII/StuI	T7	Philip Cohen
<sup>K127N</sup> SGK1	pGHJ	Ampicillin	Stu I	T7	
<sup>T308D, S473D</sup> PKB	pGHJ	Ampicillin	Sal I	T7	
NHERF2	PET30a	Kanamycin	Sal I	T7	Chris Yun
NHERF2 $\Delta$ P1	PET30a	Kanamycin	Xho I	T7	
NHERF2 $\Delta$ P2	PET30a	Kanamycin	Sal I	T7	

The present table indicates the restriction enzymes and RNA polymerases needed for linearization and transcription for every plasmid used in this work.



### 2.2.2 Preparation of oocytes

An adult female *Xenopus laevis* frog was submersed in one liter of 3-aminobenzoic acid ethyl ester (0.1%) for about 15-30 min (Fig. 13A). After the frog was fully anesthetized it was placed on ice for surgery. A small abdominal incision (1 cm) was carried out and a segment of ovary was removed (Fig. 13B, C). Subsequently the wound was closed with a reabsorbable suture (Fig. 13D). The frog was then kept wet and warm by placing it in a cavity filled by a small amount of warm water to avoid drowning and hypothermia.

The ovarian sacs were manually separated into groups of 10-20 oocytes, put into a 15 ml tube and then enzymatically defolliculated by treatment with an OR-2 (Oocytes-Ringer) solution containing 1-2 mg/ml collagenase A for 2-2.5 h at room temperature (Fig. 13E) with gentle agitation.

Defolliculation of the oocytes was stopped by washing several times with ND96. This step also removes all detritus permitting oocyte sorting. Oocytes were then sorted using a self-made apparatus (Fig. 13F). Only large oocytes (stage V or VI) were selected and stored overnight in a ND96 storage solution at 16°C.

### 2.2.3 cRNA injection

After storing overnight, oocytes were injected using glass microcapillaries (filled with the required cRNA) mounted in a micromanipulator-controlled microinjector (Fig. 13G). Precaution should be taken that cRNA was not contaminated with RNAases and that the injection capillary was not clogged with small particles. To avoid those problems several procedures were carried out such as using only sterile pipettes, gloves and DEPC treated water for dilution of cRNA.

Glass capillaries were pulled using a normal puller. The tip was manually broken under the microscope (diameter of about 10-20  $\mu$ m), backfilled with paraffin oil to seal the pipette from air and loaded with cRNA by suction (usually 1-2  $\mu$ l).

Oocytes were then placed into a 35 mm petri dish with a polypropylene mesh glued to the bottom to fix the oocytes and injected with a given volume of cRNA (usually 25 nl).

After injection, oocytes were kept in storage solution at 15°C. To avoid sticking of oocytes to the petri dish or to other oocytes, the dish was gently shaken. At least every two days the storage solution was exchanged and damaged oocytes were removed to maximise the survival of the oocytes.

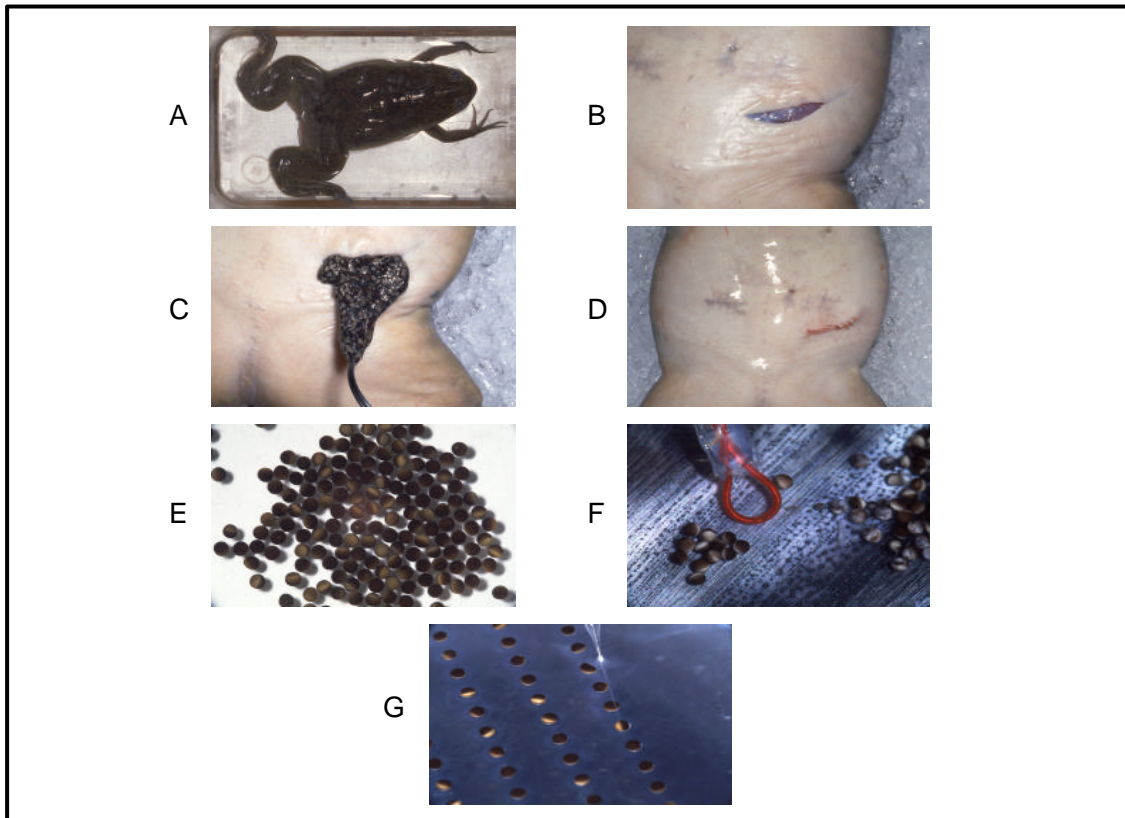


**Fig. 13. Steps of the oocytes preparation and injection.** (A) The frog is anesthetized in 1 liter of 3-aminobenzoic acid ethyl ester (1%) in tap water at near room temperature. (B) The frog is placed on its back during operation. An incision about 1 cm long is made in the skin. (C) A small portion of the ovary is pulled out with forceps and removed with a pair of scissors. (D) The peritoneum and the muscle tissue are sewn up and then the skin closed off using cat gut. (E) The clump of oocytes is immediately transferred to a petri dish containing modified Barth medium with antibiotic. (F) Oocytes of stage V and VI are separated with a platinum wire loop. (G) For injection, the oocytes are aligned relative to the tip of the needle.

## 2.3 Electrophysiological recording

### 2.3.1 Two-electrode voltage-clamp

Two-electrode voltage-clamp (TEVC) was used to measure whole cell currents in *Xenopus laevis* oocytes expressing ion transport or channels. As shown in Fig. 14, oocytes were impaled by two glass electrodes. One was to record membrane potential while the other was to deliver currents. Both were made from pulled glass capillaries with a thin filament which were filled with 3 mM KCl and subsequently inserted with an Ag/AgCl<sub>2</sub> electrode. The bath-grounding electrode was made of 3% agar and 3 M KCl.

The membrane potential electrode was connected to a feedback amplifier comparing the signal with the voltage clamp command. The difference of these signals, which was highly amplified, was applied as a current through the other electrode across the cell membrane and to the bath-grounding electrode. The whole set up was grounded and shielded with a Faraday cage (Ohlemeyer and Meyer, 1992).

In two-electrode voltage-clamp experiments of ROMK1, currents were recorded following a step change of the holding potential from -80 mV to -20 mV. For electrophysiological measurements of ECaC1, currents were recorded during a 4s linear voltage ramp from -150 mV to +50 mV or 2.5 s voltage step from -50 mV to -110 mV. The intermediate holding potential between the voltage ramps was -50 mV. But, in case of ClC-Ka/barttin, currents were determined in two-electrode voltage-clamp experiments utilizing a pulse protocol of 1 s pulses from -140 mV to +40 mV. The intermediate holding-voltage was -60 mV. Steady-state current at the end of each voltage step was taken for data analysis. Data were filtered at 10 Hz, and recorded with MacLab digital to analog converter and software for data acquisition and analysis (ADInstruments, Castle Hill, Australia). The flow rate of the superfusion was 20 ml/min and a complete exchange of the bath solution was reached within about 10 s.

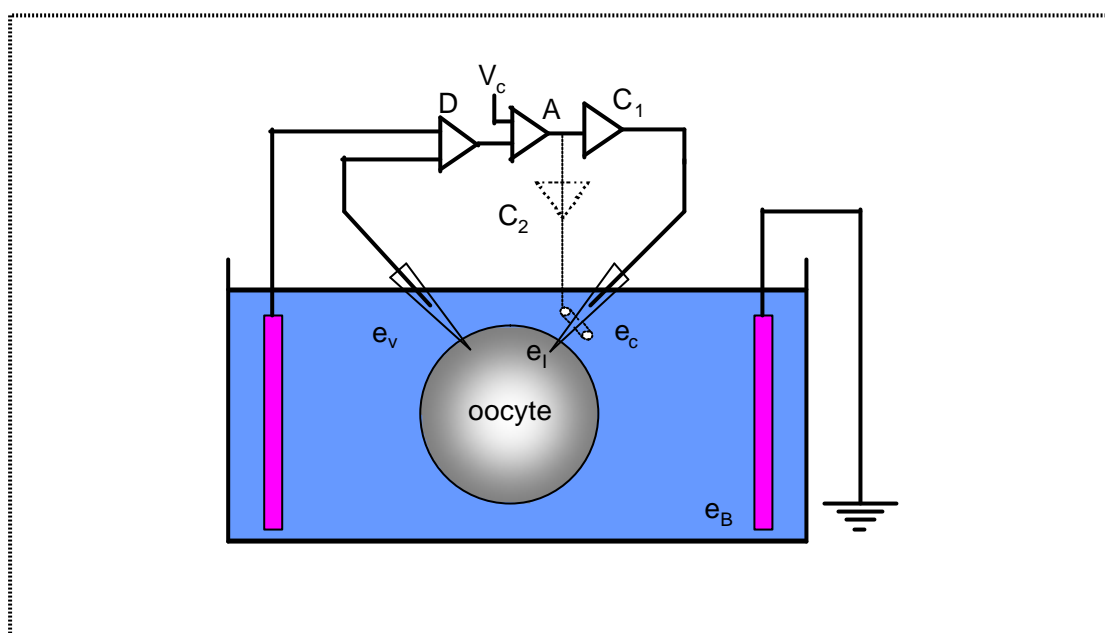


**Fig. 14. The two-electrode voltage-clamp** (adapted from Baumgartner et al., 1999). The voltage recording electrode  $e_v$  monitors the membrane potential; this is compared with a command voltage  $V_c$ , and the magnified difference is applied to a current injection electrode,  $e_i$ . A bath electrode  $e_B$  serves as the return path for the injected current.

### 2.3.2 Recording of intracellular pH (pH<sub>i</sub>)

Intracellular pH measurements were performed using ion-selective microelectrodes prepared from pulled borosilicate electrodes, which were silanized and filled with H<sup>+</sup>-ionophore and backfilled solution. Silanization changes the lipophobicity of the capillary and it was important to allow the ionophore to reach the tip of the electrodes (Thomas, 1978). Silanization was carried out by backfilling the prospective ion-selective electrode with 5% tributylchlorosilane in 99.9% pure carbon tetrachloride (Fig. 15A). To ensure a smooth coating and to remove the solvent, the electrodes were baked at 400-450°C for 5 min (Fig. 15B). A column of H<sup>+</sup> cocktail (proton ionophore II-cocktail A, Fluka Chemicals, Deisenhofen) was filled into the tip of the silanized electrode. The silanized electrode was then backfilled with a solution of 100 mM Na-citrate, pH 6.0, whereas the shank of the reference electrode was filled with 3 M KCl (Fig. 15C). The electrodes were calibrated using solutions with pH 6.0,

7.0 and 8.0. Only electrodes with a linear slope > 50 mV/pH unit and stable calibration were used. Signals were recorded with an electrometer (WPI model FD223, Sarasota, FL, USA).

On the basis of the calibration curve for the pH-sensitive electrode, the chemical potentials for  $H^+$  ( $E_{H^+}$ ) of oocytes were calculated as the difference between the membrane potential measured simultaneously with a 3 M KCl microelectrode and the electrochemical potential of the pH-sensitive electrode ( $V_{H^+}$ ). Where applicable, intracellular pH has been adjusted by variations of extracellular pH in the presence and absence of 3 mM butyrate.

As shown in Fig. 16, oocytes were impaled by two electrodes i.e reference and ion-selective electrodes, respectively, which were placed on a three-dimensional micromanipulator and connected via Ag/AgCl<sub>2</sub> electrodes to the input of an ultra-high-impedance electrometer (FD 223, WPI, New Haven, Conn, USA). The electrical circuit was then closed via bath electrode (3 M KCl agarose Ag/AgCl<sub>2</sub>). Whereas the reference electrode was used to measure the transmembrane potential ( $V_m$ ), the pH electrode was employed to measure the proton electrochemical potential across the membrane ( $V_H$ ).  $pH_i$  was then obtained by the following equation

$$pH_i = pH_{ref} - (V_H - V_m)/S$$

where  $pH_{ref}$  is the pH of the calibration solution and S is the slope of calibration curve of pH electrode. Only the pH electrode having at least 50 mV/ pH unit was used in the studies.

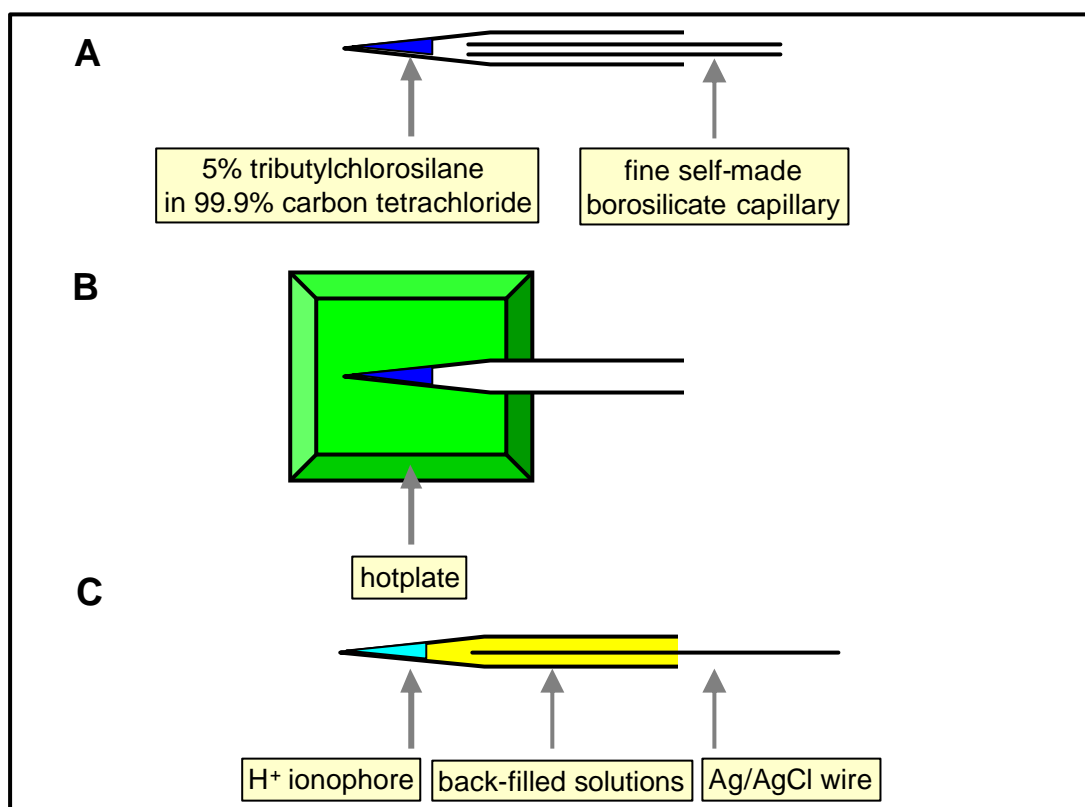


**Fig. 15. Construction of ion-selective microelectrode.** Ion-selective electrode is prepared from pulled borosilicate electrodes, which is backfilled with 5% tributylchlorosilane in 99.9% carbon tetrachloride (A). To ensure a smooth coating and to remove the solvent the electrode is baked at 400-450°C for 5 min (B). A column of  $H^+$  cocktail (proton ionophore II-cocktail A) of ~300  $\mu m$  in length, is established at the tip of the electrode (C). The electrode is then backfilled with a solution of 100 mM Na-citrate, pH 6.0.

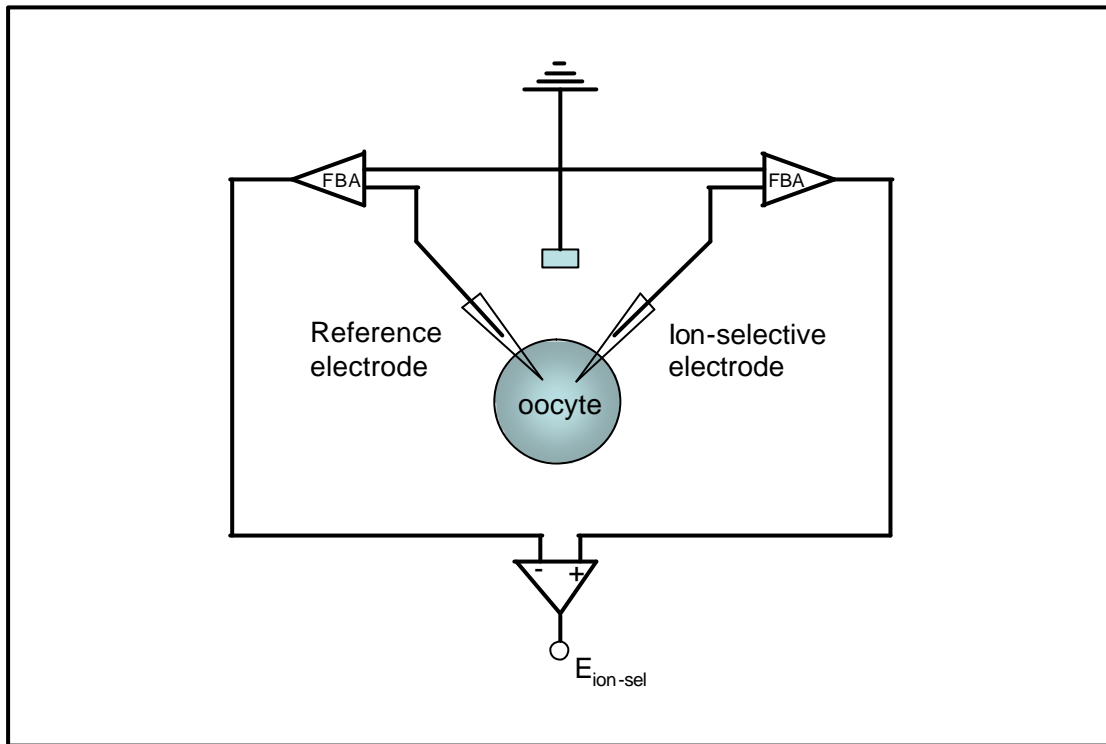


**Fig. 16.** Set-up for recording from ion-selective microelectrodes and their application for *xenopus* oocytes (adapted from Schwarz and Rettinger, 2000).

## 2.4 Site-directed mutagenesis of ROMK1

Site directed mutagenesis and subsequent functional studies were performed to elucidate the structural-functional role of the mutated sequence. For that purpose, site directed mutagenesis was carried out using the QuickChange<sup>TM</sup> site-directed mutagenesis kit (Stratagene, Heidelberg). This kit is used to make point mutations, switch amino acids, and delete or insert single or multiple amino acids.

The basic procedure utilizes a supercoiled double-stranded DNA (dsDNA) vector with an insert of interest and two synthetic oligonucleotide primers containing the desired mutation (Fig. 17). All sequences used for the design of the oligonucleotide primers were obtained from the PubMed database. The primers, each complementary to opposite strands of the vector, are extended during temperature cycling by *PfuTurbo* DNA polymerase. Incorporation of the

oligonucleotide primers generates a mutated plasmid. Following temperature cycling, the product is treated with *DpnI* endonuclease. This endonuclease (target sequence: 5'-GmATC-3') is specific for methylated and hemimethylated DNA and is used to digest the parental DNA.

The DNA isolated from almost all *E. coli* strains is methylated and therefore susceptible to *DpnI* digestion. In contrast, the mutation-containing synthesized DNA is not methylated and is not going to be digested by *DpnI*, remaining in a circular state. Since circular DNA incorporates into bacteria much easier than linear DNA, only the mutated DNA is going to be inserted and replicate by the bacteria. After isolating the plasmid DNA, the vector is resequenced to check for the desired mutation and then cRNA is synthesized as depicted in Fig. 12.

The following primers were used to generate ROMK1 $\Delta$ 4 (ROMK1 lacking the last 4 COOH-terminal amino acids) and ROMK1 $\Delta$ 4-HA (ROMK1 lacking the last 4 COOH-terminal amino acids containing hemagglutinin (HA) tag): ROMK1 $\Delta$ 4, sense (s): 5' GTTGATGAAACGGACTAGCAGTGGCTTTTC 3'; ROMK1 $\Delta$ 4, antisense (as): 5' GAAAAGCCACTGCTAGTCCGTTTCATCAAC 3'. Thereafter ROMK1 $\Delta$ 4 and ROMK1 $\Delta$ 4-HA were sequenced to verify the presence of the desired mutation.

The only SGK1 phosphorylation site in ROMK1, serine44, was also mutated into alanine (<sup>S44A</sup>ROMK1) or into aspartate (<sup>S44D</sup>ROMK1). The mutation of serine44 into alanine avoids phosphorylation of ROMK1 by SGK1. In contrast, mutation of serine44 into aspartate mimicks the phosphorylation state of ROMK1. The following primers were used to generate <sup>S44A</sup>ROMK1 and <sup>S44D</sup>ROMK1:

- |   |           |       |
|---|-----------|-------|
| (1) S44A  | sense     | (s):  |
| 5' GGCAACGGGCAAGGCTGGTCGCTAAAGAAGGAAGATGTAAC 3' |           |       |
| (2) S44A  | antisense | (as): |
| 5' GTTACATCTTCCTTCTTTAGCGACCAGCCTTGCCCGTTGCC 3' |           |       |
| (3) S44D  | sense     | (s):  |
| 5' GCAACGGGCAAGGCTGGTCGATAAAGAAGGAAGATGTAAC 3'  |           |       |



(4) S44D

antisense

(as):

5' GTTACATCTTCCTTCTTTATCGACCAGCCTTGCCCGTTGC 3'.

Thereafter both mutants were sequenced to verify the presence of the desired mutation.

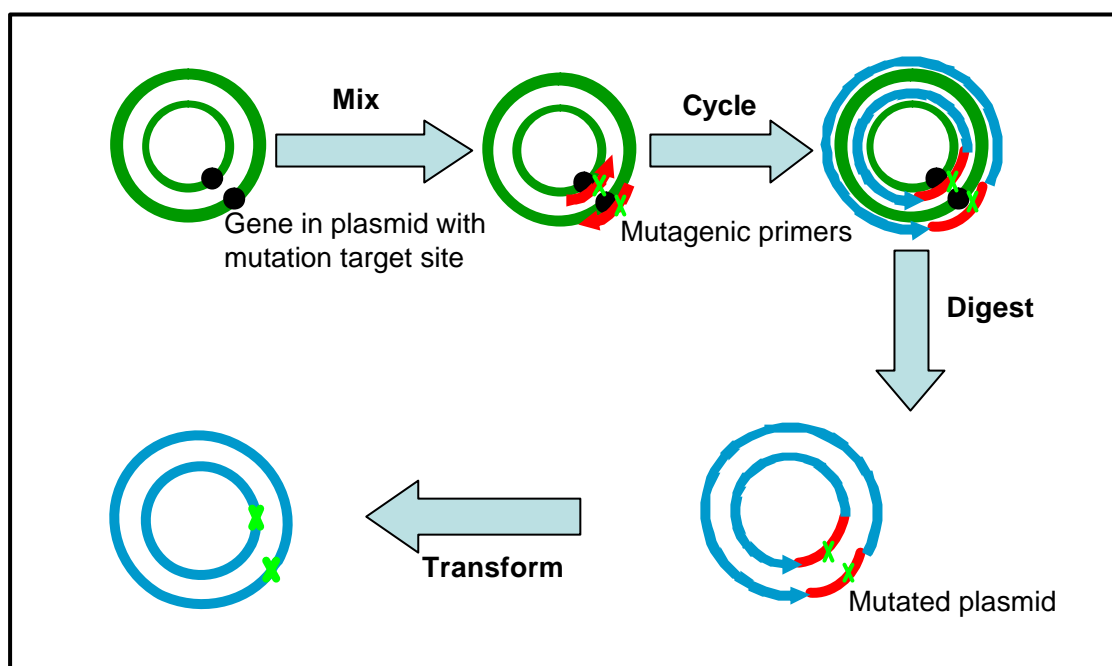


**Fig. 17. A Schematic representation of site-directed mutagenesis using the QuickChange mutagenesis kit.** A plasmid (green circles) containing the gene of interest with site targeted for mutation (closed circles), is extended (arrows) from complementary primers (red bold arcs) containing the desired mutation (x). The extension process continues until the site of primer annealing is reached, yielding an *in vitro* generated copy of the plasmid with staggered nicks (blue circles). The parent plasmid template, originally isolated from a methylation-competent bacterial host, is methylated; the *in vitro*-extended copy is not. The addition of *DpnI* leads to the digestion of the parent plasmid leaving the nicked copy, which is repaired in the bacterium (XL 1-Blue *E.coli*) following transformation.

## 2.5 Deletion of PDZ domains in NHERF2

The NHERF2 $\Delta$ P1 and NHERF2 $\Delta$ P2 constructs were prepared via PCR from a human NHERF2 cDNA. The NHERF2 $\Delta$ P1 (corresponding to amino acids 149-337 of human NHERF2) and NHERF2 $\Delta$ P2 (corresponding to amino acids 9-128) were inserted into the pET-30a (Novagen) vector using EcoRI and XhoI sites for NHERF2 $\Delta$ P1 and EcoRI and Sall sites for NHERF2 $\Delta$ P2. The sequences of the PCR products were confirmed by nucleotide sequencing.

## 2.6 Pull-down assays

In order to ascertain whether ECaC1 (TRPV5) and NHERF2 interact with one another, pull-down assays were performed. The amino- and carboxy-tails of mouse TRPV5 were amplified by PCR using mouse kidney cDNA

(NH<sub>2</sub>-tail forward:

- 5' CCGAATTCGGATGGGGGCTAAACTCCTTGGATC 3';
- reverse 5' CGCGCTCGAGCTCAAGGCTGTCCATATTTCTTCCACTT 3';

COOH-tail forward:

- 5' CCCCTGGGATCCGGCGACACTCACTGGCGAGTGGCC 3';
- reverse: 5' ACAGAAGTCGACTCAGAAATGGTAGATCTCCTC 3'),

digested with EcoRI and XhoI (NH<sub>2</sub>-tail) or BamHI and Sall (COOH-tail) and cloned into pGEX6p-2 vector (Amersham Pharmacia Biotech AB, Uppsala, Sweden). pGEX6p-2 constructs were transformed in *Escherichia coli* BL21 and glutathione S-transferase (GST) fusion proteins were expressed and purified according to the manufacturer's protocol (Amersham Pharmacia Biotech AB). [<sup>35</sup>S]methionine labeled full-length TRPV5 and NHERF2 were prepared using a reticulocyte lysate system in the presence of canine microsomal membranes (Promega Madison, WI) and added to GST or GST-fusion proteins immobilized on glutathione-sepharose 4B beads. The binding buffer contained 20 mM Tris-HCl, pH 7.4, 140 mM NaCl, 0.2% (w/v) Triton-X-100 and 0.2% (v/v) NP-40, supplemented with 1 mM CaCl<sub>2</sub> or 2 mM EDTA. After 2 h incubation at room

temperature, the beads were washed extensively with binding buffer. Bound proteins were eluted with SDS-PAGE loading buffer, separated on SDS-PAGE gels and visualized by autoradiography.

The NHERF2 $\Delta$ P1 and NHERF2 $\Delta$ P2 constructs prepared by PCR were cloned into pGEX-4T (Amersham Pharmacia Biotech AB) and also expressed as GST fusion proteins in *Escherichia coli*. [<sup>35</sup>S]methionine labeled SGK1 was prepared using the TNT *in vitro* transcription-translation system (Promega Madison, WI). 4  $\mu$ g of GST fusion proteins immobilized on glutathione-agarose beads were incubated with 5  $\mu$ l of <sup>35</sup>S-labeled SGK1 for 4 h at 4°C in binding buffer containing 10 mM Tris pH 7.2, 150 mM NaCl, 0.2% Tween 20. After the incubation time, the beads were washed extensively with binding buffer. Bound proteins were eluted with SDS-PAGE loading buffer, separated on SDS-PAGE gels and visualized by autoradiography.

## 2.7 Detection of cell surface expression by chemiluminescence

Defolliculated oocytes were first injected with NHERF2 cRNA (5 ng/oocyte) and/or <sup>S422D</sup>SGK1 cRNA (12 ng/oocyte), and two days later with ROMK1-HA cRNA (90 pg/oocyte). Oocytes were prepared for the surface labeling assay as recently described (Zerangue et al., 1999, Konstas et al., 2001), with 1  $\mu$ g/ml primary, rat monoclonal anti-HA (hemagglutinin) antibody (clone 3F10, Boehringer), and 2  $\mu$ g/ml secondary, peroxidase-conjugated affinity-purified F(ab')<sub>2</sub> goat anti-rat IgG antibody (Jackson ImmunoResearch). Oocytes were incubated in primary antibody for 180 min and in secondary antibody for 90 min at room temperature. Individual oocytes were placed in 50  $\mu$ l of SuperSignal ELISA Femto Maximum Sensitivity Substrate (Pierce), and chemiluminescence was quantified in a Turner TD-20/20 luminometer (Sunnyvale, CA) by integrating the signal over a period of 15 s. Results are given in relative light units (RLU/s/oocyte). Nonexpressing oocytes were not included in the analysis and were defined as those with a surface expression value within one standard deviation (SD) of the mean of water-injected oocytes from the same batch.

For parallel electrophysiological, analysis injected oocytes were kept in modified Barth's solution and were studied approximately 16 h after injection with ROMK1-HA cRNA. Oocytes were routinely clamped at a holding potential of -80 mV. The barium-sensitive current ( $\Delta I_{Ba^{2+}}$ ) was determined as the difference in current between the presence and absence of 10 mM barium in a KCl solution (in mM: 95 KCl, 1 CaCl<sub>2</sub>, 1 MgCl<sub>2</sub>, 10 HEPES, adjusted to pH 7.4 with TRIS).

## **2.8 Cell surface biotinylation**

For cell surface biotinylation, 55-75 oocytes of each group were rinsed three times with ice-cold PBS buffer (pH 8.0). The oocytes were then incubated 30 min at room temperature in 0.5 mg/ml Sulfo-NHS-LC-Biotin (Pierce, Rockford, IL, USA) diluted in PBS buffer. After washing 4 times with ice-cold PBS, the cells were dissolved in lysis buffer containing 50 mM Tris (pH 7.5), 0.5 mM EDTA (pH 8.0), 0.5 mM EGTA, 100 mM NaCl, 1% Triton X-100, 25 µg/ml aprotinin and 25 µg/ml leupeptin for 30 min on ice. The solubilized oocytes were centrifuged for 15 min at 14000 rpm, and then the supernatant was incubated with 50 µl of ImmunoPure immobilized streptavidin beads at 4°C overnight. The biotin-streptavidin-agarose bead complexes were then washed 4 times with lysis buffer. The final pellets were dissolved in 20 µl sample buffer and boiled for 5 min for SDS-PAGE.

The biotinylated membrane proteins were separated by 8% SDS-PAGE and transferred electrophoretically to nitrocellulose membranes. After blocking with 5% non-fat dry milk in PBS (pH 7.4)/0.15% Tween 20 for 1h at room temperature, the blots were incubated with the primary rabbit anti-ROMK1 antibody (Chemicon, USA) at 4°C overnight (dilution 1:250 in PBS/0.15% Tween 20/2.5% non-fat dry milk). After washing, the first antibody was detected by secondary sheep anti-rabbit IgG antibody conjugated with horseradish peroxidase for 1 h at room temperature. Antibody binding was detected with the enhanced chemoluminescence ECL kit (Amersham, Freiburg) and exposure to X-ray film.

## **2.9 Western blotting and immunohistochemistry for ROMK1**

For determination of ROMK1 expression in whole cell lysates, 30 cells of each group were homogenized in lysis buffer containing 50 mM Tris (pH 7.5), 0.5 mM EDTA (pH 8.0), 0.5 mM EGTA, 100 mM NaCl, 1% Triton X-100 and protein inhibitor cocktail (Roche) at the recommended concentrations. Proteins were transferred to nitrocellulose membranes at 100 V for 90 min. For immunoblotting, rabbit anti-ROMK1 antibody (diluted 1:250 in PBS/0.15% Tween 20/5% non-fat dry milk) was used to detect ROMK1. After blocking with 5% non-fat dry milk in PBS/ 0.15% Tween 20/for 1 h at room temperature, blots were incubated with the primary antibody at 4°C overnight. Secondary peroxidase-conjugated sheep anti-rabbit IgG (diluted 1:1000 in PBS/0.15% Tween 20/5% non-fat dry milk) was used for luminescent detection with an enhanced chemoluminescence (ECL) kit (Amersham, Freiburg).

Oocytes for immunohistochemistry were devitellinized and fixed in Dent's solution (80% Methanol, 20% DMSO) overnight at -20°C. After washing with PBS, permeabilization and blocking were performed at room temperature for 30 min by incubation in PBS containing 0.2% Triton-100 and 10% normal goat serum. Then oocytes were incubated with rabbit anti-ROMK1 antibody (dilution 1:250) at 4°C for 12 h. The secondary Alexa-488 coupled goat anti-rabbit antibody (Molecular Probes, The Netherlands, dilution 1:200) was added at 4°C for 12 h. The embedding procedure in acrylamide (Technovit 7100) was carried out according to the manufacturer's instructions (Heraeus Kulzer, Wehrheim). Embedded oocytes were cut into 5 µm sections and analysed with a fluorescence microscope (Optiphot, Düsseldorf).

## **2.10 Immunohistochemistry for CIC-Ka/barttin channels**

Prior to embedding (Tissue-Tek, Miles Inc., Elkhardt, USA) and cutting, *Xenopus* oocytes expressing the indicated epitope-tagged constructs (HA-epitope for CIC-Ka and V5 epitope for barttin) were fixed in 4% paraformaldehyde in PBS at 4°C overnight. 5 µm cryosections were blocked for 30 min in PBS containing 10% (v/v) normal goat serum (Sigma-Aldrich,

Deisenhofen), 0.2% (w/v) bovine serum albumin (Sigma-Aldrich, Deisenhofen), and 0.3% (v/v) Triton X-100. The primary antibodies (rat monoclonal anti-HA, Roche, Mannheim; mouse monoclonal anti-V5, Invitrogen, Karlsruhe) were diluted in the blocking solution (anti-HA 1/400, anti-V5 1/2000) and added to the slices for two hours at room temperature. After the slices were washed with PBS, secondary Cy-2- or Cy-3-coupled antibodies (Amersham Pharmacia Biotech, Freiburg) were added at the recommended dilutions for two hours at room temperature. Afterwards the slices were again washed with PBS and mounted with glycerol-gelatin (Sigma, Deisenhofen). Epifluorescence microscopy was used to detect antibody localization.

### **2.11 Uptake measurements**

Calcium uptake was measured similar to what has been described earlier (Peng et al., 1999, 2000; Hoenderop et al., 2001b) with slight modifications. In detail, uptake of  $^{45}\text{Ca}^{2+}$  (ICN Biomedicals GmbH, Eschwege), delivered as  $\text{CaCl}_2$  in aqueous solution (specific activity: 0.185-1.11 TBq/g  $\text{Ca}^{2+}$ ) was determined 3 days after injection of oocytes with the respective cRNAs by incubating 10-15 oocytes at 20°C in uptake solution containing 96 mM NaCl, 2 mM KCl, 1 mM  $\text{MgCl}_2$ , 0.1 mM  $\text{CaCl}_2$ , 1 mM  $\text{BaCl}_2$ , 10  $\mu\text{M}$  methoxyverapamil, 5 mM HEPES-Tris, pH 7.4. Radioactive  $^{45}\text{Ca}^{2+}$  was added to give a final concentration of 7  $\mu\text{Ci}$  per ml. After different incubation times, the oocytes were washed three times in stop buffer containing 96 mM NaCl, 1 mM  $\text{MgCl}_2$ , 0.5 mM  $\text{CaCl}_2$ , 1.5  $\text{LaCl}_3$ , 5 mM HEPES-Tris, pH 7.4. Single oocytes were then placed separately in scintillation vials and solubilized in 200  $\mu\text{l}$  10% (w/v) sodium dodecyl sulfate. After addition of 3 ml scintillation fluid (Ultima Gold, Packard, Groningen, The Netherlands), radioactivity in the samples was measured in a liquid scintillation counter (Wallac, Freiburg).

### **2.12 Data evaluation**

Data are expressed as means  $\pm$  SEM, n represents the number of oocytes and N represents the number of batches investigated. All experiments were

repeated with at least 3 batches of oocytes from different frogs; in all repetitions, qualitatively similar data were obtained. All data were tested for significance using the Student t-test, and only results with  $P < 0.05$  were considered statistically significant.

## **3 RESULTS**



### 3.1 Regulation of the renal epithelial K<sup>+</sup> channel ROMK1 (K<sub>ir</sub>1.1a)

#### 3.1.1 Up-regulation of ROMK1 by SGK1 and NHERF2

As shown in Fig. 18, the injection of cRNA encoding ROMK1 led to the expression of a K<sup>+</sup> current of  $7.3 \pm 0.4 \mu\text{A}$  ( $n = 35$ ). The current was almost completely inhibited by addition of 10 mM K<sup>+</sup> channel blocker Ba<sup>2+</sup>. No significant increase of the K<sup>+</sup> current was observed after coinjection of the constitutively active kinase <sup>S422D</sup>SGK1 together with ROMK1 ( $7.0 \pm 0.4 \mu\text{A}$ ,  $n = 35$ ) under conditions where ENaC-mediated Na<sup>+</sup> currents were stimulated five-fold (Wagner et al., 2001). Similarly, the coexpression of NHERF2 together with ROMK1 did not significantly enhance the current ( $8.2 \pm 0.3 \mu\text{A}$ ,  $n = 35$ ). In contrast, the coexpression of <sup>S422D</sup>SGK1 together with NHERF2 and ROMK1 led to a statistically significant increase of the current ( $17.5 \pm 1.3 \mu\text{A}$ ,  $n = 35$ ). In oocytes not injected with ROMK1 (not shown), the K<sup>+</sup>-current was negligible ( $0.05 \pm 0.01 \mu\text{A}$ ,  $n = 6$ ) and not significantly increased by injection of <sup>S422D</sup>SGK1 ( $0.06 \pm 0.01 \mu\text{A}$ ,  $n = 6$ ), NHERF2 ( $0.05 \pm 0.01 \mu\text{A}$ ,  $n = 6$ ) or both, <sup>S422D</sup>SGK1 and NHERF2 ( $0.06 \pm 0.01 \mu\text{A}$ ,  $n = 6$ ).

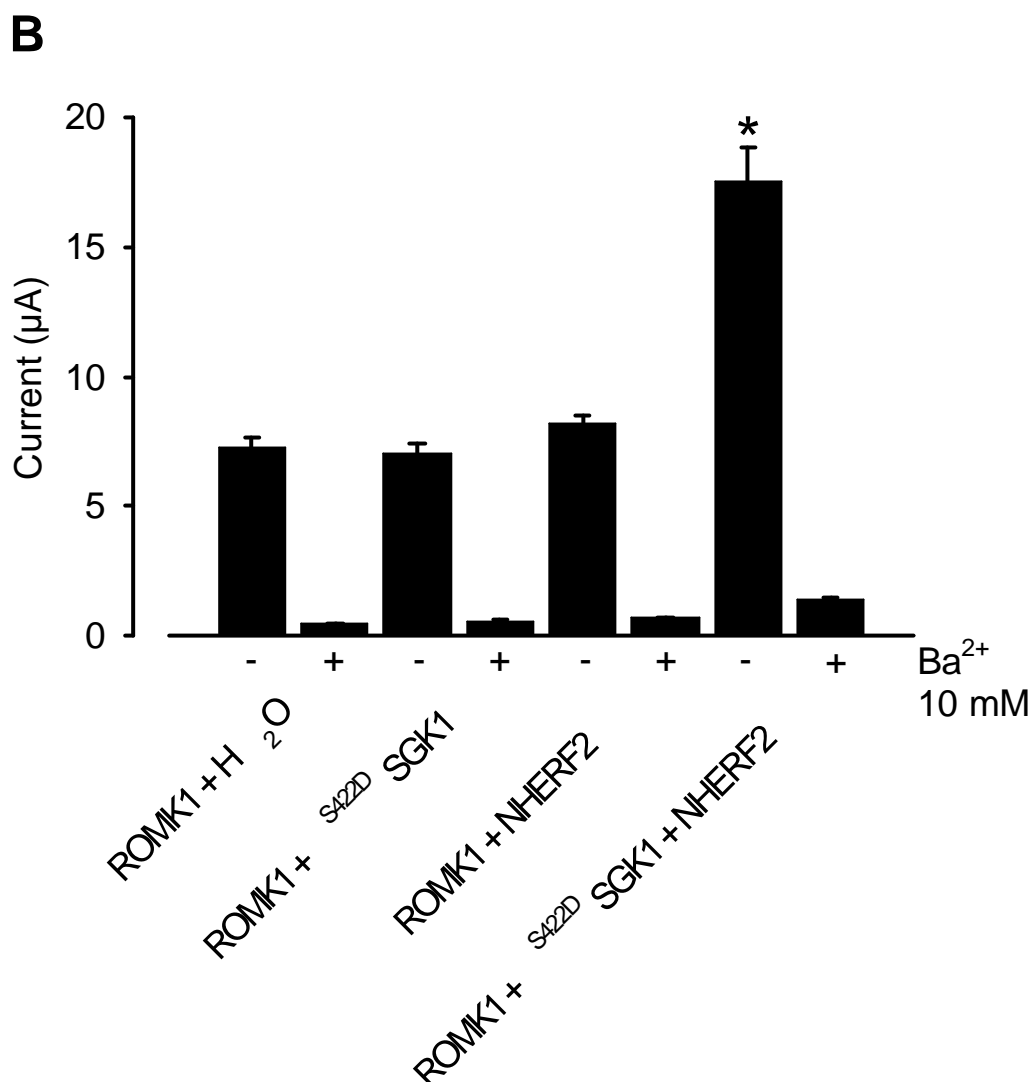


**Fig. 18. Up-regulation of the renal epithelial K<sup>+</sup> channel ROMK1 by SGK1 and NHERF2.** *Xenopus laevis* oocytes were injected with cRNA of ROMK1 alone or with S<sup>422D</sup>SGK1 (SGK1) and/or NHERF2. Addition of 10 mM Ba<sup>2+</sup> nearly completely inhibited outward K<sup>+</sup> current. Only the combined coexpression of S<sup>422D</sup>SGK1 (SGK1) and NHERF2 increases ROMK1 channel activity. Arithmetic means  $\pm$  SEM (n = 35). \* indicates significant difference between expression of ROMK1 alone and coexpression of ROMK1 together with S<sup>422D</sup>SGK1 (SGK1) and NHERF2.

### 3.1.2 Current-Voltage relationship (I-V) of ROMK1 expressing oocytes

The stimulation of ROMK1 channel activity was not paralleled by profound alterations of voltage dependence. As shown in Fig. 19, the relative I-V relation was not significantly affected by the combined coexpression of <sup>S422D</sup>SGK1 and NHERF2.

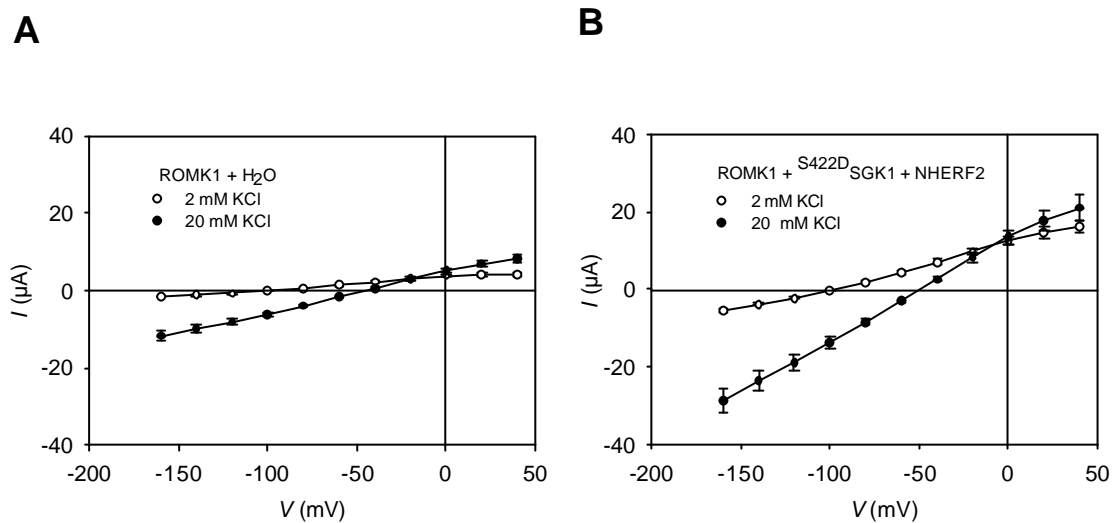


**Fig. 19. I-V relationship of ROMK1 expressing oocytes.** The current (I) as a function of the potential difference across the cell membrane (V) in oocytes injected with ROMK1 alone (left) and in oocytes injected with ROMK1 together with NHERF2 and <sup>S422D</sup>SGK1 (right) at both, 2 mM K<sup>+</sup> (open symbols) and 20 mM K<sup>+</sup> (closed symbols). Arithmetic means  $\pm$  SEM (n = 6).

### 3.1.3 Inhibition of ROMK1 by cytosolic acidification

Given the exquisite pH sensitivity of ROMK1, the stimulating effect of SGK1 and NHERF2 could in theory have been due to cytosolic alkalinization or due to alteration of pH sensitivity of the channel. According to ion-selective microelectrodes, the cytosolic pH values approached  $7.11 \pm 0.02$  (n = 5) in oocytes expressing ROMK1 alone and  $7.11 \pm 0.04$  (n = 5) in oocytes expressing ROMK1 together with SGK1 and NHERF2. Moreover, ROMK1 retained its pH

sensitivity after coexpression of SGK1 and NHERF2. ROMK1 channel activity was almost abolished by cytosolic acidification with butyrate in both oocytes expressing ROMK1 alone and in oocytes coexpressing ROMK1 together with SGK1 and NHERF2 (Fig. 20).

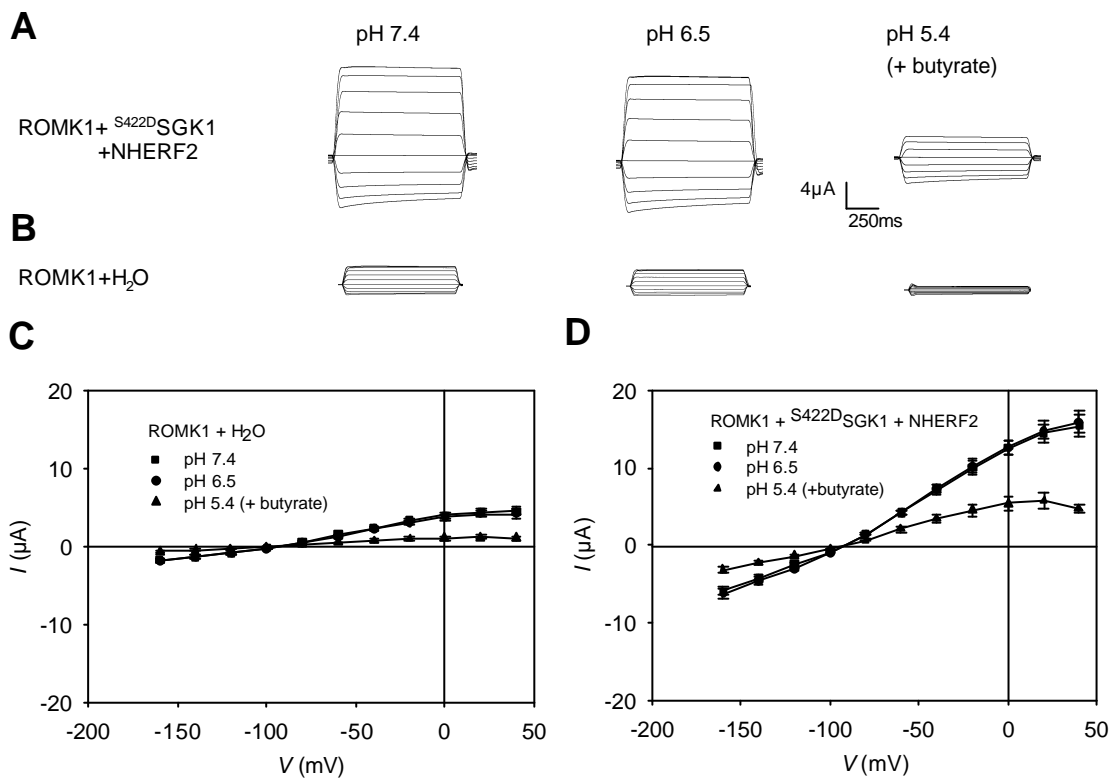


**Fig. 20. Inhibition of ROMK1 activity by cytosolic acidification.** Influence of extracellular pH (pH 7.4 or 6.5) and of intracellular acidification by addition of 3 mM butyrate on ROMK1-induced current in oocytes expressing ROMK1 alone (B, C) or together with <sup>S422D</sup>SGK1 and NHERF2 (A, D). Upper panels, original tracings; lower panels, I-V curves. Arithmetic means  $\pm$  SEM (n = 5-9).

### 3.1.4 pH sensitivity of ROMK1

However, a detailed analysis of pH dependence revealed a small, but significant shift of  $pK_a$  of ROMK1 towards more acidic values upon coexpression of <sup>S422D</sup>SGK1 (SGK1) and NHERF2 (Fig. 21). To explore whether this shift was secondary to the enhanced  $K^+$  channel activity, an additional series was performed on oocytes injected with 20 ng ROMK1 alone. As illustrated in Fig. 21 and Tab. 8, the  $pK_a$  values were not significantly modified by higher ROMK1 channel expression. Even though statistically significant, the small shift of ROMK1-pH sensitivity upon coexpression of <sup>S422D</sup>SGK1 (SGK1) and NHERF2 was not sufficient to explain the strong activation of the channel.

**Table 8: pH sensitivity of ROMK1 in the absence or presence of <sup>S422D</sup>SGK1 (SGK1) plus NHERF2**

Clone	$pK_a$	$I_{max}$	No. of oocytes
ROMK1 (5 ng)	$6.95 \pm 0.04$	$3845 \pm 362$	9
ROMK1 (5 ng) + SGK1 + NHERF2	$6.87 \pm 0.04^*$	$9331 \pm 1500$	9
ROMK1 (20 ng)	$6.96 \pm 0.02$	$6635 \pm 1596$	3

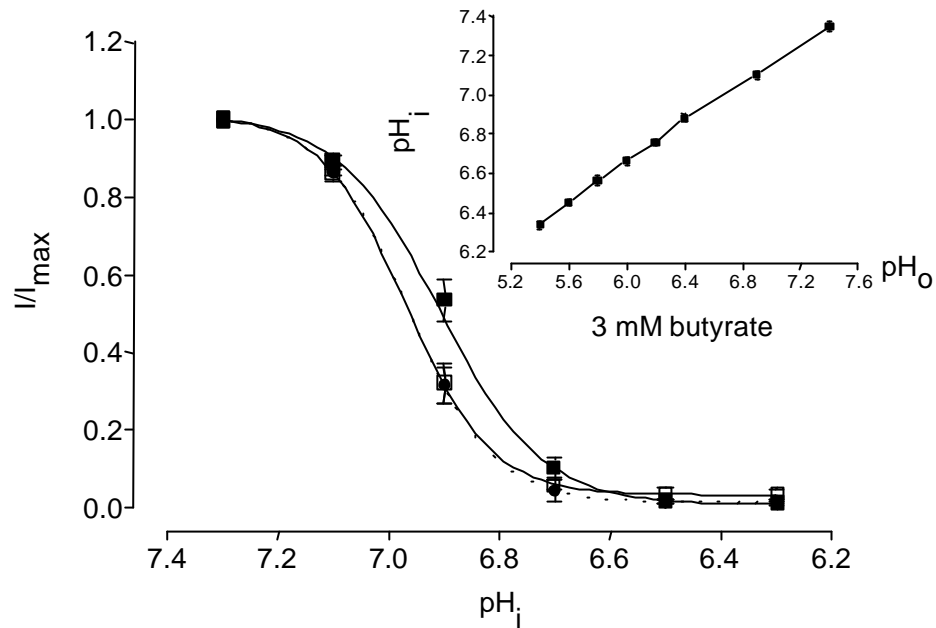
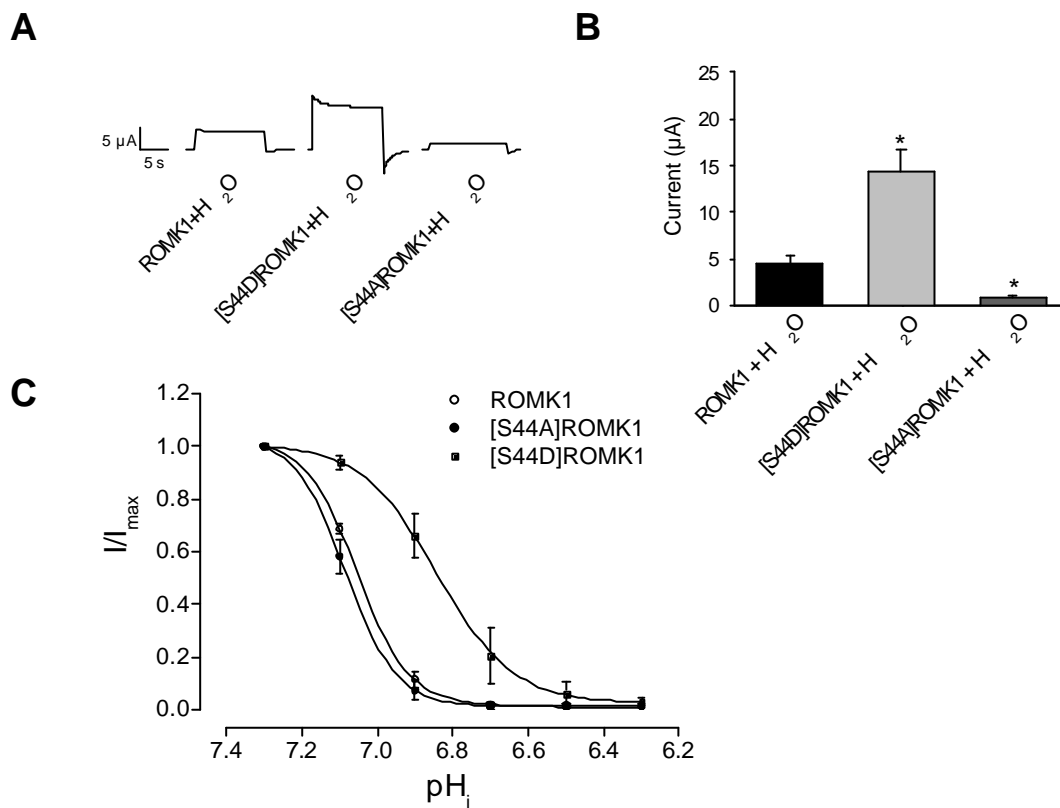


**Fig. 21. Proton sensitivity of ROMK1 is shifted upon coexpression with <sup>S422D</sup>SGK1 (SGK1) and NHERF2.** Ordinate: normalized inward current of oocytes expressing either ROMK1 alone (5 ng, ?; 20 ng, ?) or ROMK1 together with NHERF2 and <sup>S422D</sup>SGK1 (i). Arithmetic means  $\pm$  SEM (n = 3-9). Currents at different values of internal pH (pH<sub>i</sub>) were normalized to the maximum inward conductance for that oocyte. Abscissa: intracellular pH (pH<sub>i</sub>), as controlled by variation of extracellular pH (pH<sub>o</sub>) in the presence of 3 mM butyrate (see insert).

### 3.1.5 SGK1 determines pH sensitivity of ROMK1

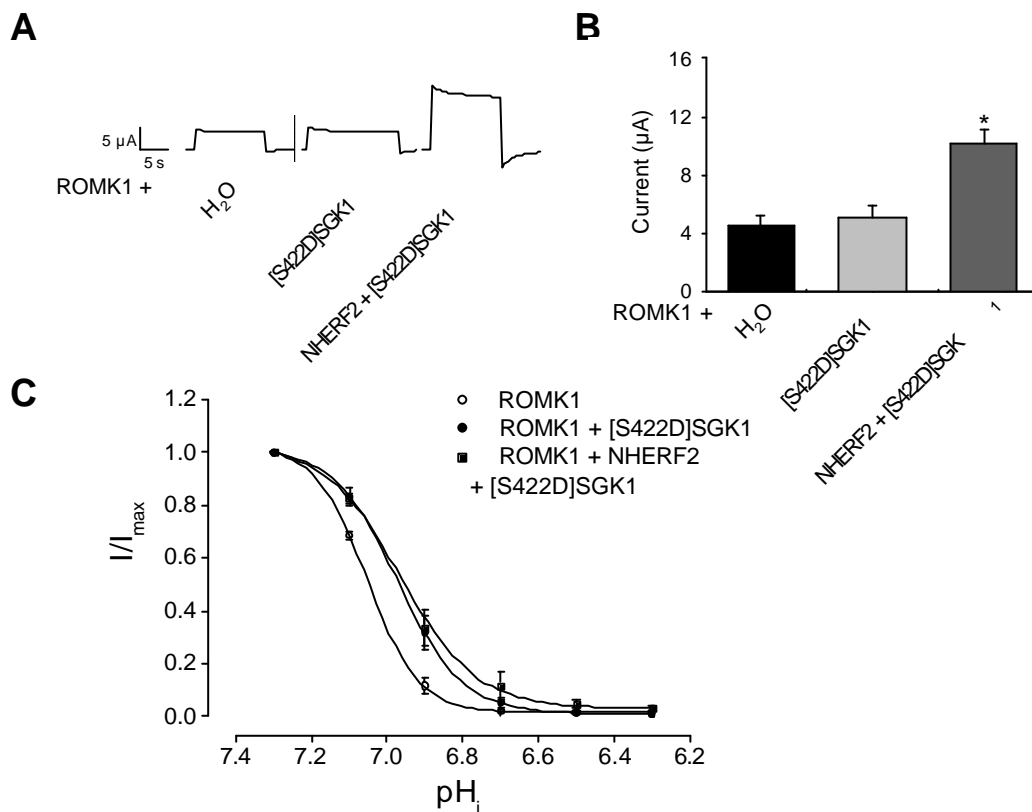
As illustrated in Fig. 22, the expression of wild type ROMK1, <sup>S44A</sup>ROMK1 and <sup>S44D</sup>ROMK1 induced a K<sup>+</sup> current in *Xenopus* oocytes ( $I_{KR}$ ) which was highly sensitive to the cytosolic pH (pH<sub>i</sub>). The maximal  $I_{KR}$  obtained at pH<sub>i</sub> 7.3 ( $I_{max}$ ) was significantly larger in <sup>S44D</sup>ROMK1 expressing oocytes ( $14.3 \pm 2.5 \mu A$ , n = 5) than in oocytes expressing wild type ROMK1 ( $4.5 \pm 0.7 \mu A$ , n = 9).  $I_{max}$  was significantly lower in oocytes injected with <sup>S44A</sup>ROMK1 ( $0.9 \pm 0.2 \mu A$ , n = 9) than in oocytes expressing wild type ROMK1. The cytosolic pH required for

halfmaximal  $k_R$  ( $pK_a$ ) amounted to  $7.05 \pm 0.01$  for wild type ROMK1.  $pK_a$  was shifted to slightly more alkaline values ( $7.07 \pm 0.02$ ,  $n = 9$ ) following replacement of the serine by alanine ( $S^{44A}$ ROMK1) and to more acidic values ( $6.83 \pm 0.05$ ,  $n = 5$ ) following replacement of the serine by aspartate ( $S^{44D}$ ROMK1). The mutations did not only modify pH sensitivity but as well the maximal activity of the channels. The activity at pH 7.3 was  $S^{44D}$ ROMK1 > wild type ROMK1 >  $S^{44A}$ ROMK1 (Fig. 22).



**Fig. 22.  $K^+$  currents ( $I_{KR}$ ) in *Xenopus* oocytes injected with wild type ROMK1,  $S^{44A}$ ROMK1 or  $S^{44D}$ ROMK1. (A)** Original recordings from oocytes expressing wild type ROMK1,  $S^{44A}$ ROMK1 or  $S^{44D}$ ROMK1; **(B)** Arithmetic means  $\pm$  SEM ( $n = 5-9$ ) of the maximal current ( $I_{max}$ ) at  $pH_i$  of 7.3; **(C)** Arithmetic means  $\pm$  SEM ( $n = 5-9$ ) of  $k_R$  (in fractions of  $I_{max}$ ) as a function of  $pH_i$ .

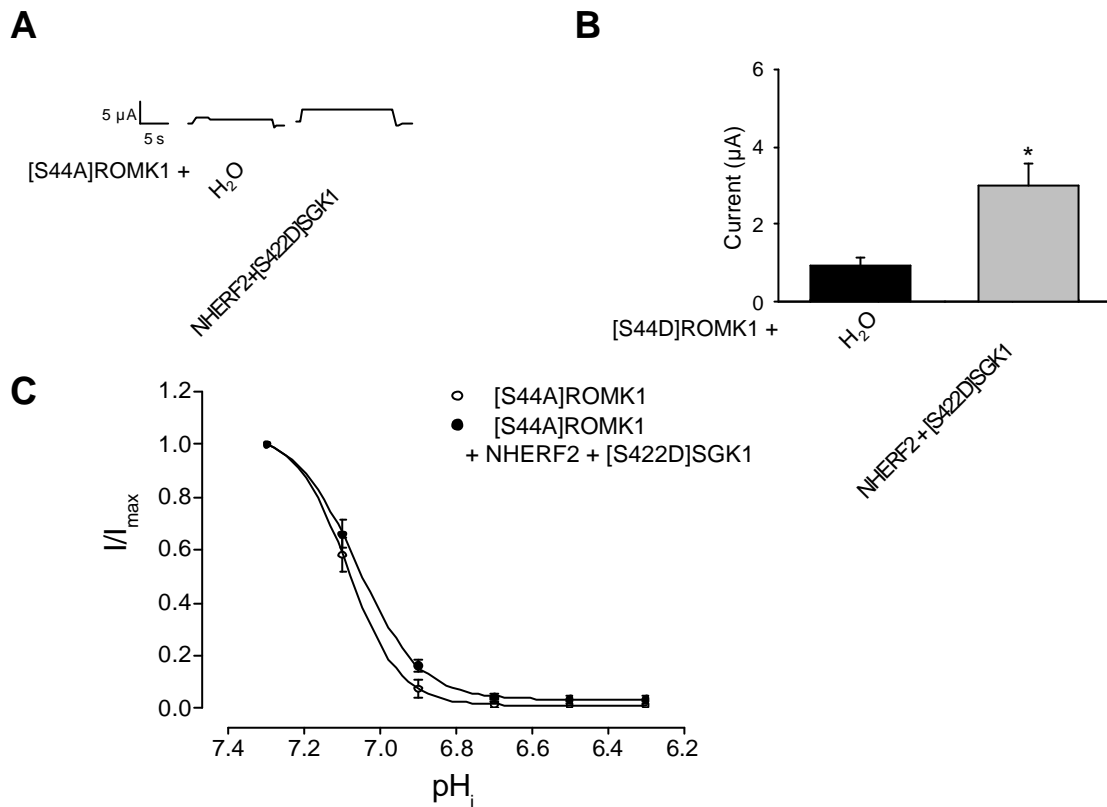
The coexpression of  $S^{422D}$ SGK1 and NHERF2 enhanced the activity ( $I_{\max}$ ) of wild type ROMK1 (Fig. 23), of  $S^{44A}$ ROMK1 (Fig. 24) and of  $S^{44D}$ ROMK1 (Fig. 25). Thus, an intact SGK1 phosphorylation consensus sequence was not required for increase of  $I_{\max}$  by SGK1 and NHERF2. At high  $S^{44D}$ ROMK1 expression rates (injection of 5 ng  $S^{44D}$ ROMK1 cRNA) the current could not be further stimulated by  $S^{422D}$ SGK1 and NHERF2. The injection of lower channel cRNA levels (0.5 ng), however, disclosed the ability of  $S^{422D}$ SGK1 and NHERF2 coexpression to enhance  $S^{44D}$ ROMK1 activity (Fig. 25).



**Fig. 23. Effect of  $S^{422D}$ SGK1 with or without NHERF2 coexpression on ROMK1 mediated  $K^+$  currents.** (A) Original recordings from oocytes expressing wild type ROMK1 with or without  $S^{422D}$ SGK1 with or without NHERF2; (B) Arithmetic means  $\pm$  SEM (n = 9) of the maximal current ( $I_{\max}$ ) at  $pH_i$  of 7.3 in oocytes expressing wild type ROMK1 with or without  $S^{422D}$ SGK1 and with or without NHERF2; (C) Arithmetic means  $\pm$  SEM (n = 9) of  $I_{KR}$  (in fractions of  $I_{\max}$ ) as a function of cytosolic pH ( $pH_i$ ) in oocytes expressing wild type ROMK1 with or without  $S^{422D}$ SGK1 and with or without NHERF2.

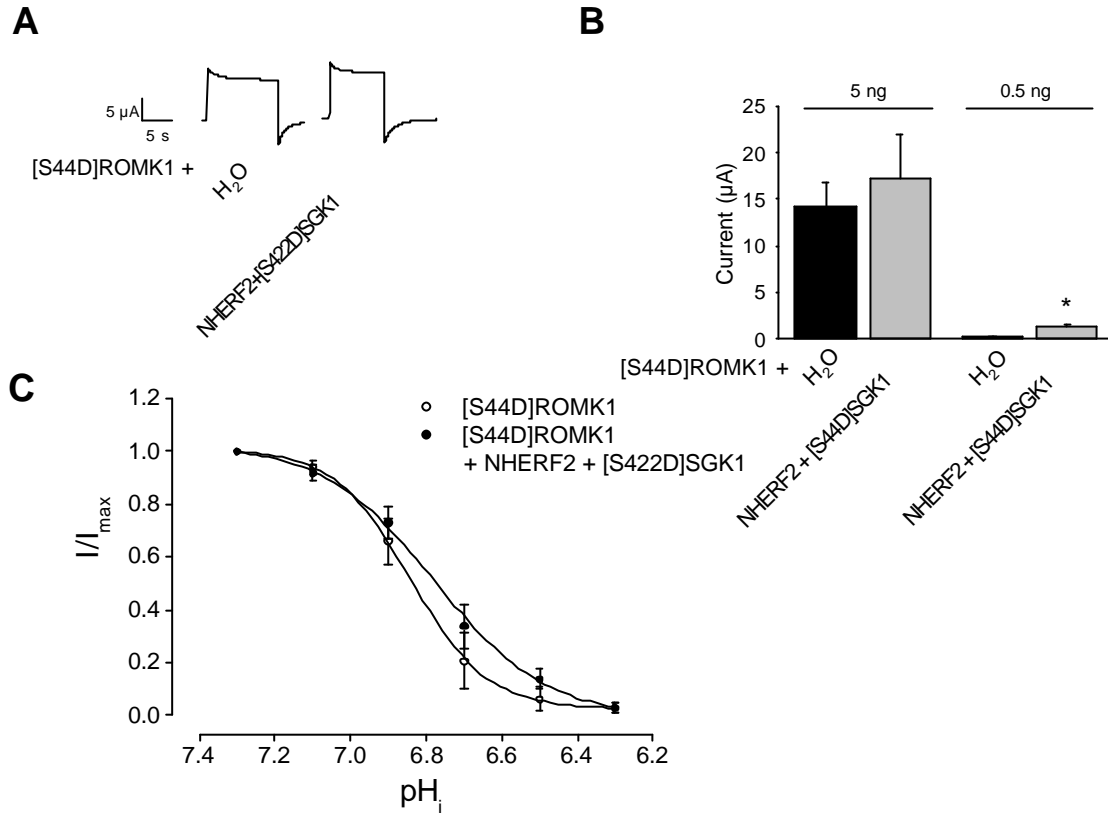


In contrast to regulation of  $I_{\max}$  by  $S^{422D}$ SGK1 and NHERF2, the regulation of pH sensitivity was dependent on an intact SGK1 phosphorylation consensus sequence.  $S^{422D}$ SGK1 and NHERF2 led to a significant shift of  $pK_a$  only in wild type ROMK1 (to  $6.95 \pm 0.03$ ,  $n = 9$ , Fig. 23), but neither in  $S^{44A}$ ROMK1 (Fig. 24) and  $S^{44D}$ ROMK1 (Fig. 25). Wild type ROMK1  $pK_a$  was shifted by  $S^{422D}$ SGK1 even in the absence of NHERF2 (to  $6.97 \pm 0.02$ ,  $n = 9$ , Fig. 23).



**Fig. 24. Effect of coexpression of  $S^{422D}$ SGK1 and NHERF2 on  $S^{44A}$ ROMK1 mediated  $K^+$  currents.** (A) Original recordings from oocytes expressing  $S^{44A}$ ROMK1 with or without  $S^{422D}$ SGK1 and NHERF2; (B) Arithmetic means  $\pm$  SEM ( $n = 9$ ) of the maximal current ( $I_{\max}$ ) at  $pH_i$  of 7.3 in oocytes expressing  $S^{44A}$ ROMK1 with or without  $S^{422D}$ SGK1 and NHERF2; (C) Arithmetic means  $\pm$  SEM ( $n = 9$ ) of  $k_R$  (in fractions of  $I_{\max}$ ) as a function of cytosolic pH ( $pH_i$ ) in oocytes expressing  $S^{44A}$ ROMK1 with or without  $S^{422D}$ SGK1 and NHERF2.

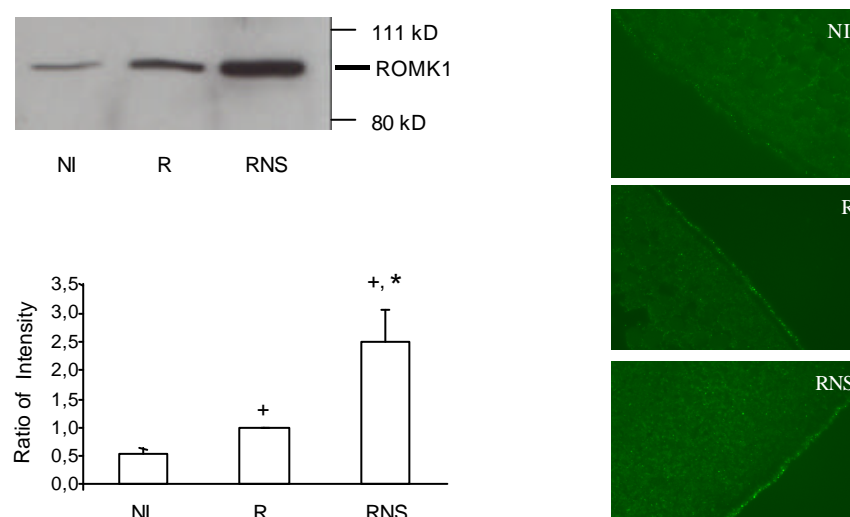
The shifts of  $pK_a$  in wild type ROMK1 following coexpression of  $S^{422D}$ SGK1 and NHERF2 or  $S^{422D}$ SGK1 alone were both significantly different from the respective shifts in  $S^{44A}$ ROMK1 and  $S^{44D}$ ROMK1.

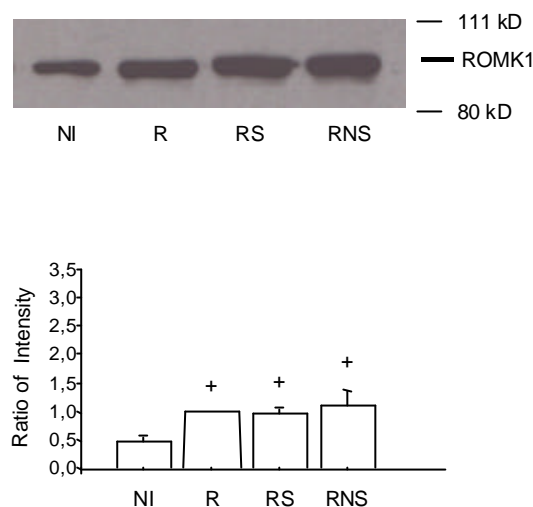


**Fig. 25. Effect of coexpression of  $S^{422D}$ SGK1 and NHERF2 on  $S^{44D}$ ROMK1 mediated  $K^+$  currents.** (A) Original recordings from oocytes expressing  $S^{44D}$ ROMK1 with or without  $S^{422D}$ SGK1 and NHERF2; (B) Arithmetic means  $\pm$  SEM ( $n = 9$ ) of the maximal current ( $I_{max}$ ) at  $pH_i$  of 7.3 in oocytes injected with 5 or 0.5 ng  $S^{44D}$ ROMK1 with or without  $S^{422D}$ SGK1 and NHERF2; (C) Arithmetic means  $\pm$  SEM ( $n = 9$ ) of  $I_{KR}$  (in fractions of  $I_{max}$ ) as a function of cytosolic pH ( $pH_i$ ) in oocytes expressing  $S^{44D}$ ROMK1 with or without  $S^{422D}$ SGK1 and NHERF2.

### 3.1.6 Increase of ROMK1 abundance in the cell membrane

Data from a number of reports have suggested that SGK1 stimulates ENaC-mediated  $\text{Na}^+$  current by augmenting channel abundance in the plasma membrane (Alvarez de la Rosa et al., 1999; Loffing et al., 2001b; Wagner et al., 2001). To determine the effect of SGK1 and NHERF2 on ROMK1 abundance in the plasma membrane, western blot and immunohistochemistry were performed on cell membranes from oocytes expressing ROMK1 together with SGK1 and NHERF2 and in oocytes expressing ROMK1 alone. As shown in Fig. 26A, SGK1 and NHERF2 did indeed stimulate ROMK1 plasma membrane abundance as determined by densitometry of western blots of biotinylated membranes. Moreover, determination of cell surface expression by chemiluminescence again disclosed the stimulating effect of SGK1/NHERF2 on ROMK1 cell surface expression (Fig. 27). Increased expression of ROMK1 in the plasma membrane was not due to *de novo* protein synthesis because western blots from whole cell lysates did not show any difference in ROMK1 expression in oocytes injected with ROMK1, SGK1 and NHERF2 as compared to those injected with ROMK1 alone (Fig. 26B).

**A**

**B**

**Fig. 26. Increase of ROMK1 abundance in the cell membrane by coexpression of SGK1 and NHERF2.** (A) Expression of ROMK1 in the cell membrane. In oocytes expressing S<sup>422D</sup>SGK1 and NHERF2, the abundance of ROMK1 channel protein at the surface of the oocyte membrane is significantly increased. ROMK1 abundance in oocytes expressing ROMK1 alone (R) and expressing ROMK1 together with S<sup>422D</sup>SGK1 and NHERF2 (RNS). Left: Western blot of ROMK1 in biotinylated membrane. Ratio of intensity is compared to the intensity obtained in oocytes expressing ROMK1 alone (R). N.I., for not injected oocytes; + denotes significant difference between oocytes injected with ROMK1 and those injected with water; \* indicates significant difference between expression of ROMK1 alone and coexpression of ROMK1 together with S<sup>422D</sup>SGK1 and NHERF2 (RNS). Arithmetic means  $\pm$  SEM (n = 30). Right: Immunohistochemistry. ROMK1 staining in the cell membrane of oocytes expressing S<sup>422D</sup>SGK1 and NHERF2 (RNS) is higher than in oocytes expressing ROMK1 alone (R). (B) Expression of ROMK1 in whole cell lysates. In oocytes expressing S<sup>422D</sup>SGK1 and NHERF2, the abundance of ROMK1 channel protein in whole cell lysates is not modified significantly as compared to those expressing ROMK1 alone. RS, for oocytes injected with ROMK1 together with S<sup>422D</sup>SGK1. Ratio of intensity is compared to the intensity obtained in oocytes expressing ROMK1 alone (R). + denotes significant difference between oocytes injected with ROMK1 and those injected with water. Arithmetic means  $\pm$  SEM (n = 6).

---

In an additional series of experiments were performed to examine whether ROMK1-HA surface expression was stimulated using a chemiluminescence assay in parallel with  $\Delta I_{Ba}^{2+}$  measurements. Fig. 27 summarises results from one of three similar experiments. These results demonstrate that both surface expression and  $\Delta I_{Ba}^{2+}$  are increased in oocytes expressing SGK1/NHERF2/ROMK1-HA oocytes as compared with SGK1/ROMK1-HA control oocytes. Coexpression of NHERF2 increased  $\Delta I_{Ba}^{2+}$  by 232% and ROMK1-HA surface labelling by 227%. Increasing the surface expression of ROMK1-HA is sufficient to explain the stimulation of  $\Delta I_{Ba}^{2+}$  in oocytes coexpressing SGK1/NHERF2 and ROMK1-HA.

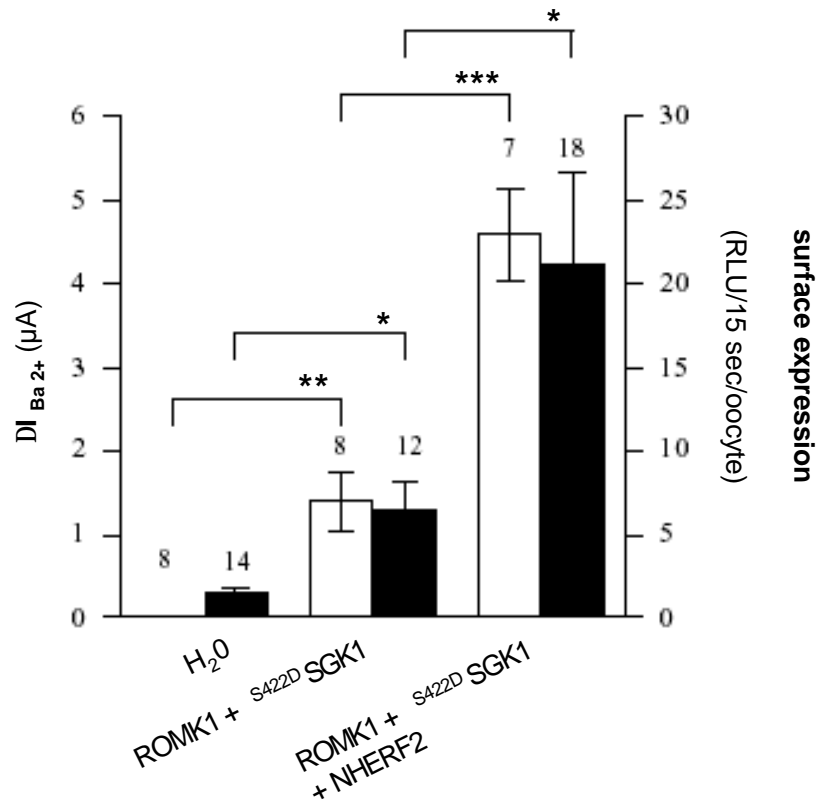
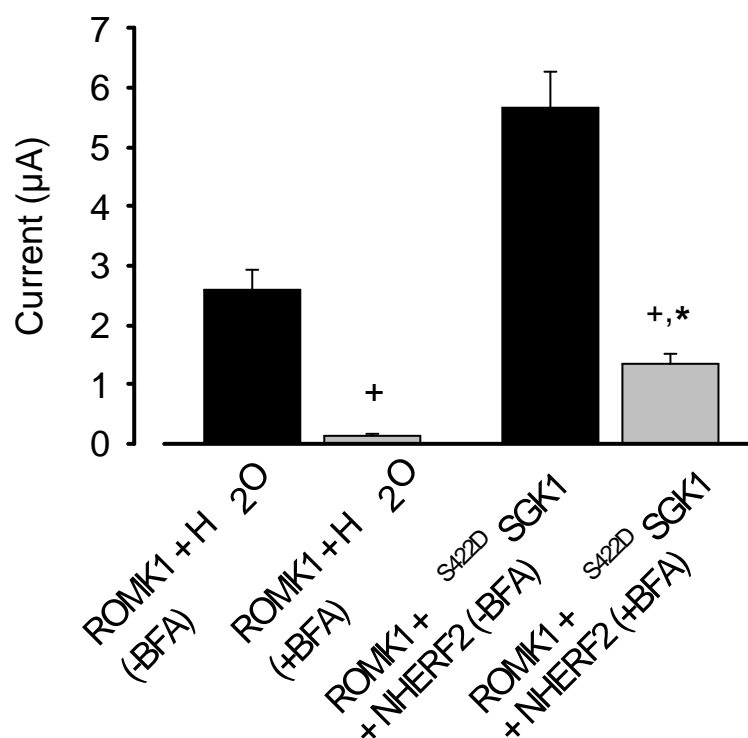


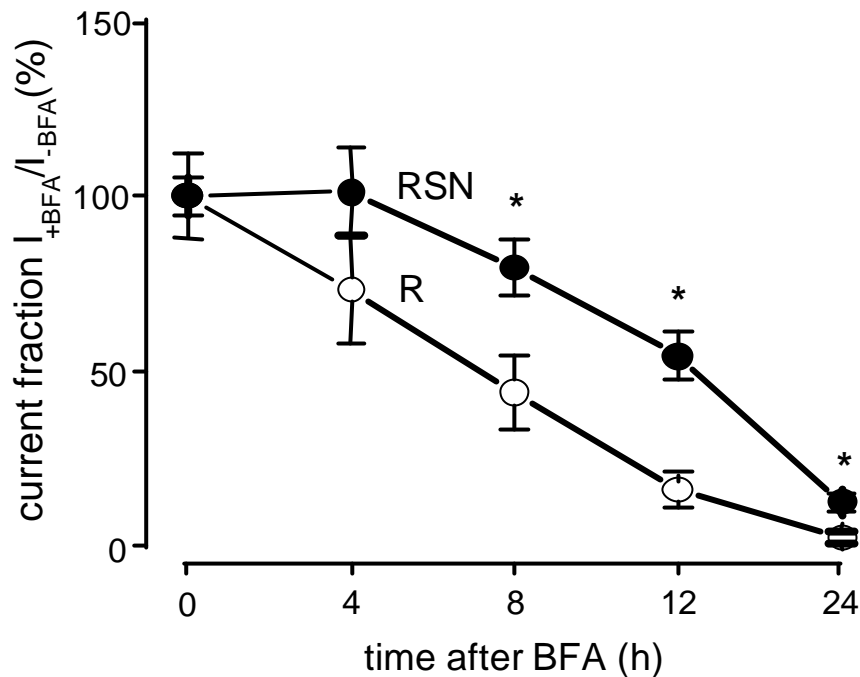
**Fig. 27. Determination of ROMK1 surface expression by chemiluminescence.** Surface expression of extracellularly HA-tagged ROMK1 and  $\Delta I_{Ba^{2+}}$  were assessed in parallel in oocytes coexpressing <sup>S422D</sup>SGK1 + ROMK1-HA and in oocytes from the same batch coexpressing <sup>S422D</sup>SGK1 + NHERF2 + ROMK1-HA. Water-injected control oocytes were used to determine nonspecific chemiluminescence and endogenous  $\Delta I_{Ba^{2+}}$ . Both  $\Delta I_{Ba^{2+}}$  (open bars) and surface expression of ROMK1-HA (filled bars) were significantly increased in <sup>S422D</sup>SGK1 + NHERF2 + ROMK1-HA oocytes compared with <sup>S422D</sup>SGK1 + ROMK1-HA control oocytes (\*,  $p < 0.05$ ; \*\*,  $p < 0.01$ ; \*\*\*,  $p < 0.001$ ). Numbers above bars represent the number of oocytes studied. Chemiluminescence as a measure of surface expression is given in relative light units per 15 sec per oocyte (RLU/15 s per oocyte).

### 3.1.7 Influence of SGK1 and NHERF2 coexpression on ROMK1 stability

In principle, SGK1 and NHERF2 could increase plasma membrane ROMK1 expression by increasing channel insertion, decreasing removal, or a combination of the two. To distinguish these possibilities, K<sup>+</sup> currents were monitored in oocytes exposed to brefeldin A (5  $\mu$ M), which blocks cellular secretory mechanisms by inhibiting vesicle formation at the Golgi apparatus, during different time points (0, 4, 8, 12, and 24 h). The treatment did not affect viability of the oocytes, and the cell membrane potential of noninjected oocytes approached  $-40 \pm 7$  mV ( $n = 24$ ) before and  $-41 \pm 6$  mV ( $n = 24$ ) following a 24 h exposure to brefeldin A. The respective values for nontreated oocytes were  $-40 \pm 4$  mV ( $n = 24$ ) and  $-42 \pm 4$  mV ( $n = 24$ ) before and after 24 h incubation in brefeldin-free buffer. Incubation of oocytes expressing ROMK1 in brefeldin A (5  $\mu$ M)-containing solution led to a gradual decrease of channel activity, which was significantly and rapidly decreased after 24 h incubation in oocytes expressing ROMK1 alone as compared with oocytes expressing ROMK1 together with SGK1 and NHERF2 (Fig. 28). This finding points to a stabilizing effect of SGK1 plus NHERF2 coexpression on ROMK1 channel protein in the plasma membrane.

**A**



**B**

**Fig. 28. Influence of SGK1 and NHERF2 coexpression on ROMK1 stability.**

Influence of 5  $\mu$ M brefeldin A (BFA) on ROMK1 channel activity with or without coexpression of NHERF2 plus <sup>S422D</sup>SGK1 (SGK1). Coexpression of <sup>S422D</sup>SGK1 (SGK1) plus NHERF2 blunts the decrease of channel activity in brefeldin treated oocytes, determined after 24 h incubation (in A) and at the indicated time points (in B). Arithmetic means  $\pm$  SEM (n = 6). \* indicates significant difference between expression of ROMK1 (R) alone and coexpression of ROMK1 together with <sup>S422D</sup>SGK1 (SGK1) and NHERF2 (RSN).

### 3.1.8 Stimulation of ROMK1 requires second PDZ domain of NHERF2

As shown in Fig. 29, SGK1 is able to bind GST-tagged NHERF2. SGK1 does not only bind to the full length NHERF2 (GST-NHERF2) but as well to the isolated second PDZ domain (GST-P2) of NHERF2. In contrast, the isolated first PDZ domain (GST-P1) and GST alone do not bind SGK1.



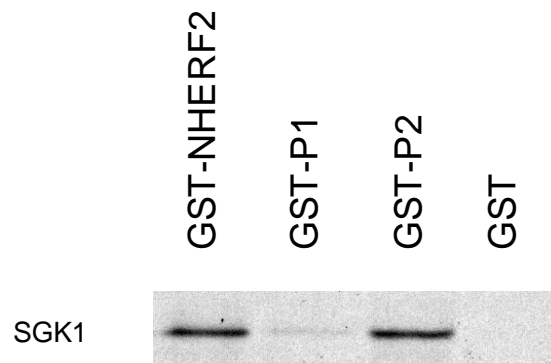


**Fig. 29. Binding of SGK1 to NHERF2. Dependence on the second PDZ domain.** 4  $\mu$ g of GST fusion proteins encoding full length NHERF2, the first or second PDZ domain of NHERF2 immobilized on glutathione-agarose beads (GST-P1, GST-P2) were incubated with 5  $\mu$ l of  $^{35}$ S-labeled SGK1 for 4 h at 4°C in binding buffer. After the incubation time, the beads were washed extensively and bound proteins were eluted with SDS-PAGE loading buffer, separated on SDS-PAGE gels and visualized by autoradiography. Note that SGK1 interacts with the second PDZ (P2) domain of NHERF2 and with the first PDZ (P1) domain only very weakly.

The second PDZ domain of NHERF2 is further required for the stimulating effect of NHERF2 and  $^{S422D}$ SGK1 (SGK1) on the ROMK1 induced  $K^+$  current  $I_{KR}$  (Fig. 30).  $I_{KR}$  is markedly enhanced by coexpression of ROMK1 together with both, constitutively active  $^{S422D}$ SGK1 and wild type NHERF2 (from  $5.1 \pm 0.5 \mu A$  in ROMK1 expressing oocytes ( $n = 16$ ) to  $13.8 \pm 0.8 \mu A$  in oocytes expressing  $^{S422D}$ SGK1/NHERF2/ROMK1,  $n = 23$ ). Coexpression of  $^{S422D}$ SGK1 together with NHERF2 deficient of the first PDZ domain (NHERF2 $\Delta$ P1) similarly increases  $I_{KR}$  ( $12.3 \pm 1.4 \mu A$ ,  $n = 15$ ). In contrast, coexpression of ROMK1 with  $^{S422D}$ SGK1 and NHERF2 lacking the second PDZ domain (NHERF2 $\Delta$ P2) does not yield an  $I_{KR}$  exceeding that after expression of ROMK1 alone ( $4.7 \pm 0.8 \mu A$ ,  $n = 15$ ).

Thus, the second PDZ domain is required for the stimulating effect of  $S^{422D}$ SGK1/NHERF2 on ROMK1.

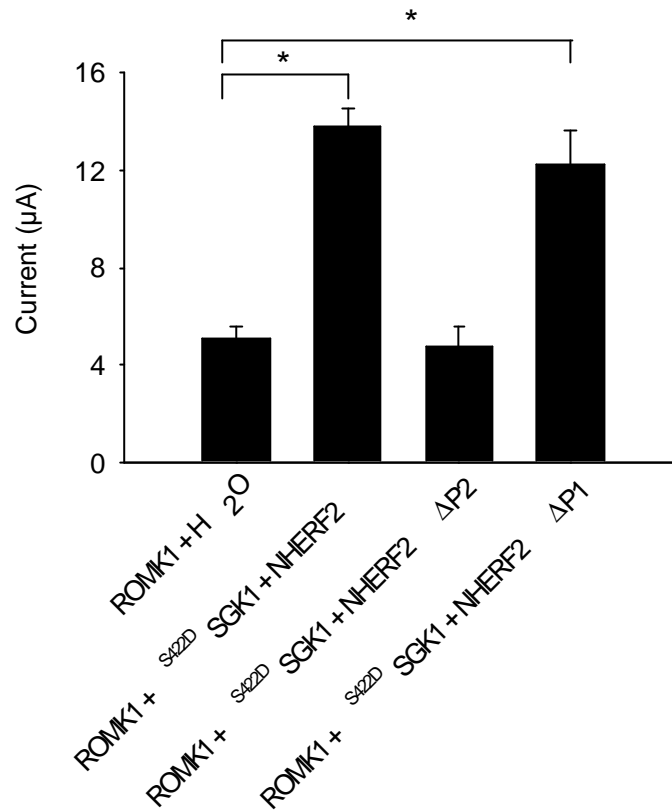


**Fig. 30. Requirement of the second PDZ domain of NHERF2 for the stimulation of K<sup>+</sup> channel activity by constitutively active  $S^{422D}$ SGK1.** *Xenopus laevis* oocytes were injected with cRNA encoding ROMK1,  $S^{422D}$ SGK1 (SGK1) and either water, wildtype NHERF2, NHERF2 lacking the first PDZ domain (NHERF2 $\Delta$ P1) or NHERF2 lacking the second PDZ domain (NHERF2 $\Delta$ P2). Only the combined coexpression of  $S^{422D}$ SGK1 and wild type NHERF2 or NHERF2 $\Delta$ P1 increases ROMK1 channel activity. Arithmetic means  $\pm$  SEM (n = 15-23). \* indicates significant difference between expression of ROMK1 alone and coexpression of ROMK1 together with  $S^{422D}$ SGK1 (SGK1) and NHERF2 or its analogus.

Further studies were performed to identify the requirement for the putative PDZ binding motif in the ROMK1 channel protein. As illustrated in Fig. 31, expression of a ROMK1 mutant lacking the putative PDZ-binding motif (ROMK1 $\Delta$ 4) yields a

$I_{KR}$  similar to the  $I_K$  observed following expression of wild type ROMK1 alone ( $3.5 \pm 0.6 \mu A$  in ROMK $\Delta 4$  expressing oocytes ( $n = 27$ ) and  $3.2 \pm 0.3 \mu A$  in ROMK1 expressing oocytes ( $n = 25$ ). However, the additional coexpression of  $S^{422D}$ SGK1/NHERF2 increases  $I_{KR}$  only in *Xenopus* oocytes expressing wild type ROMK1. Thus, the putative PDZ binding motif in the ROMK1 channel protein is required for the interaction with  $S^{422D}$ SGK1/NHERF2.

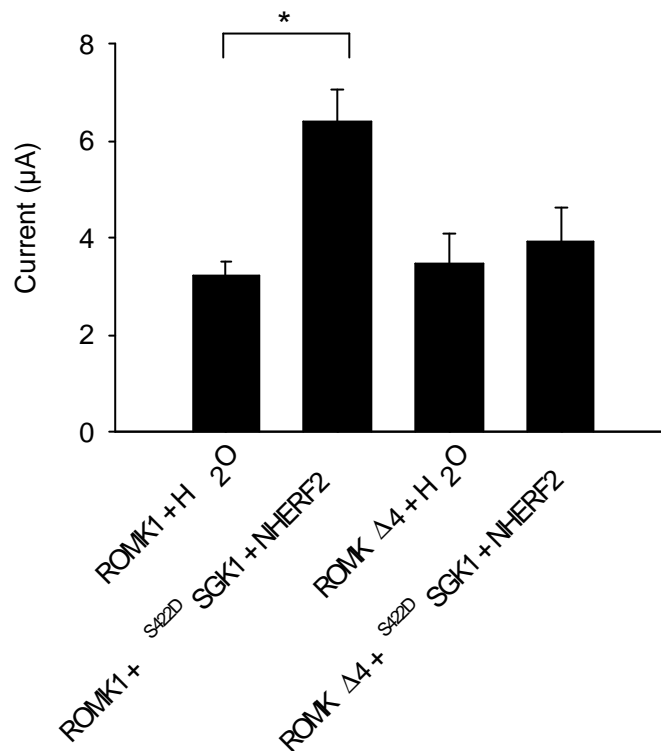


**Fig. 31. Requirement of the COOH-terminal PDZ binding motif in ROMK1 for the stimulation by  $S^{422D}$ SGK1/NHERF2.** *Xenopus laevis* oocytes were injected with cRNA encoding either wild type ROMK1 or ROMK1 lacking the PDZ binding motif present at the COOH-terminal end (ROMK $\Delta 4$ ) with or without additional injection with constitutively active  $S^{422D}$ SGK1 (SGK1) and wildtype NHERF2. Wild type ROMK1 but not ROMK1 lacking the PDZ binding motif is up-regulated by the additional expression of  $S^{422D}$ SGK1/NHERF2. Arithmetic means  $\pm$  SEM ( $n = 25-27$ ). \* indicates significant difference between expression of ROMK1 alone and coexpression of ROMK1 together with  $S^{422D}$ SGK1 (SGK1) and NHERF2.

The PDZ domains of NHERF2 are thought to link NHERF2 and associated proteins to the cytoskeleton and thus to accomplish the targeting to or stabilization of transport proteins in the cell membrane (Yun et al., 1998; Shenolikar and Weinmann, 2001; Biber, 2001; Yun, 2003). Therefore the ROMK1 surface expression was examined, using a chemiluminescence assay in parallel with electrophysiological measurements, upon coexpression of NHERF2 and ROMK1 mutants. Fig. 32 demonstrates that both surface expression (in A) and current (in B) are increased in oocytes expressing <sup>S422D</sup>SGK1/NHERF2/ROMK1 compared with ROMK control oocytes. Coexpression of <sup>S422D</sup>SGK1/NHERF2 increased ROMK1-HA surface labeling 4-fold and ROMK1-mediated currents from  $0.6 \pm 0.2 \mu\text{A}$  in ROMK1 expressing oocytes ( $n = 12$ ) to  $5.6 \pm 1.4 \mu\text{A}$  in oocytes expressing <sup>S422D</sup>SGK1/NHERF2/ROMK1 ( $n = 12$ ). ROMK1-HA surface expression was also enhanced up to 3.8-fold upon coexpression of <sup>S422D</sup>SGK1 and NHERF2 lacking the first PDZ domain (NHERF2 $\Delta$ P1). However, coexpression of NHERF2 lacking the second PDZ domain failed to increase ROMK1 expression and ROMK1-mediated currents ( $0.6 \pm 0.2 \mu\text{A}$  in ROMK1 expressing oocytes ( $n = 12$ ) vs.  $1.2 \pm 0.3 \mu\text{A}$  in oocytes expressing <sup>S422D</sup>SGK1/NHERF2 $\Delta$ P2/ROMK1,  $n = 12$ ). No changes in ROMK1 expression or activity by <sup>S422D</sup>SGK1/NHERF2 was observed when the PDZ binding motif at the COOH-terminal end of ROMK1 was deleted ( $3.2 \pm 0.4 \mu\text{A}$  in ROMK1 $\Delta$ 4 expressing oocytes ( $n = 12$ ) compared to  $3.4 \pm 0.8 \mu\text{A}$  in oocytes expressing <sup>S422D</sup>SGK1/NHERF2/ROMK1 $\Delta$ 4,  $n = 12$ ).

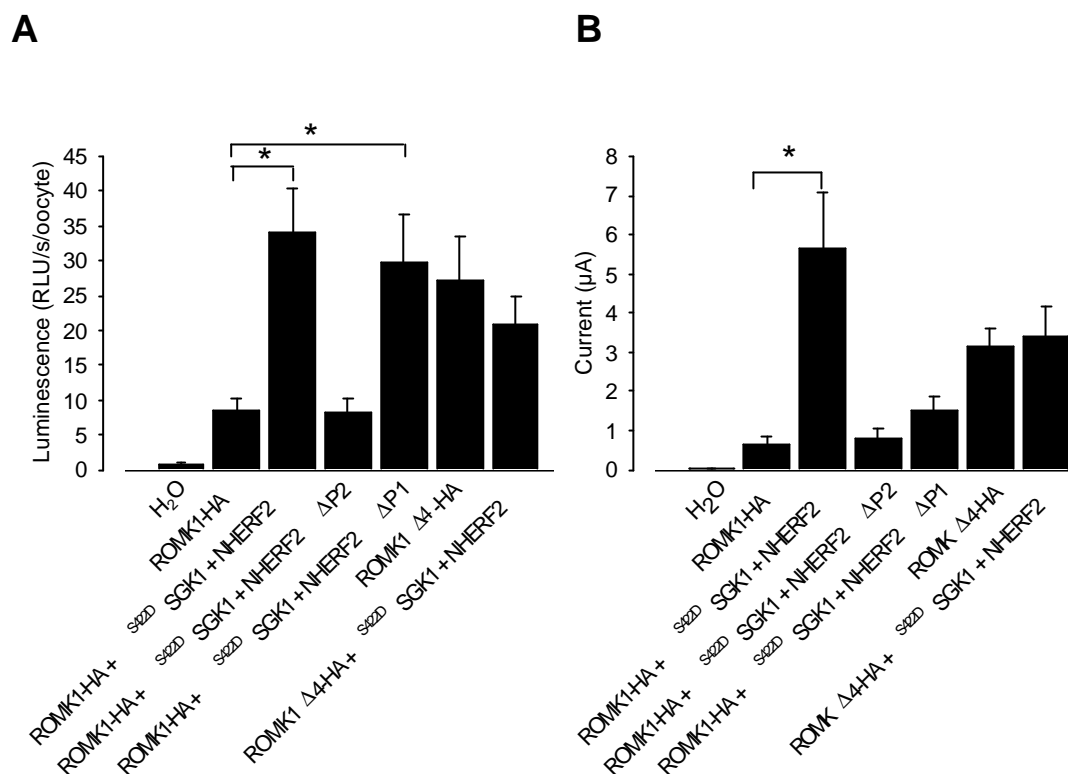


**Fig. 32. Determination of ROMK1 surface expression by chemiluminescence.** Surface expression of extracellularly HA-tagged ROMK1 and  $I_{KR}$  were assessed in parallel in oocytes expressing ROMK1-HA alone and in oocytes coexpressing ROMK1-HA together with <sup>S422D</sup>SGK1, full-length NHERF2 or NHERF2 lacking the first (NHERF2ΔP1) or second (NHERF2ΔP2) PDZ domain. Water injected control oocytes were used to determine nonspecific chemiluminescence and endogenous  $I_{KR}$ . Both ROMK1-HA expression and  $I_{KR}$  were significantly increased upon <sup>S422D</sup>SGK1/NHERF2 expression. Coexpression of <sup>S422D</sup>SGK1 with NHERF2ΔP2 failed to stimulate ROMK1-HA expression and activity. Similarly, <sup>S422D</sup>SGK1/NHERF2 did not affect ROMK1Δ4-HA expression and activity. Arithmetic means  $\pm$  SEM (n = 12-20). Chemiluminescence as a measure of surface expression is given in relative light units per sec per oocyte (RLU/s/oocyte).

## 3.2 Regulation of the renal epithelial $\text{Ca}^{2+}$ channel ECaC1 (TRPV5)

### 3.2.1 Stimulation of tracer $\text{Ca}^{2+}$ entry via TRPV5

As evident from Fig.33A, uptake of radioisotope of  $\text{Ca}^{2+}$  ( $^{45}\text{Ca}^{2+}$ ) into *Xenopus* oocytes was increased some 7-fold by expression of TRPV5. The increase of  $\text{Ca}^{2+}$  uptake reflects the  $\text{Ca}^{2+}$  transporting capacity of TRPV5. Additional expression of either NHERF2, SGK1, SGK2, SGK3 or constitutively active  $\text{T308D,S473D}$ PKB alone did not further stimulate  $^{45}\text{Ca}^{2+}$  entry. However, expression of TRPV5 together with both, SGK1 and NHERF2 resulted in significant further stimulation of  $\text{Ca}^{2+}$  uptake. In the absence of TRPV5, expression of SGK1 and NHERF2 did not increase  $\text{Ca}^{2+}$  uptake (not shown). Thus, coexpression of SGK1 and NHERF2 increase  $\text{Ca}^{2+}$  uptake by stimulation of TRPV5. Similarly, the coexpression of TRPV5 together with SGK3 and NHERF2 increased  $\text{Ca}^{2+}$  uptake. Both kinases stimulate TRPV5, an effect requiring the presence of NHERF2. In contrast, the coexpression of neither SGK2 nor  $\text{T308D,S473D}$ PKB significantly modified the  $\text{Ca}^{2+}$  uptake into oocytes expressing TRPV5 and NHERF2.

Thus, SGK1 and SGK3, but not SGK2 or  $\text{T308D,S473D}$ PKB stimulate TRPV5 in the presence of NHERF2. As illustrated in Fig. 33B, constitutively active  $\text{S422D}$ SGK1 coexpressed with TRPV5 and NHERF2 similarly stimulated  $\text{Ca}^{2+}$  entry. Up to 60 min,  $\text{Ca}^{2+}$  entry was linear in oocytes expressing TRPV5 alone or together with  $\text{S422D}$ SGK1 and NHERF2.

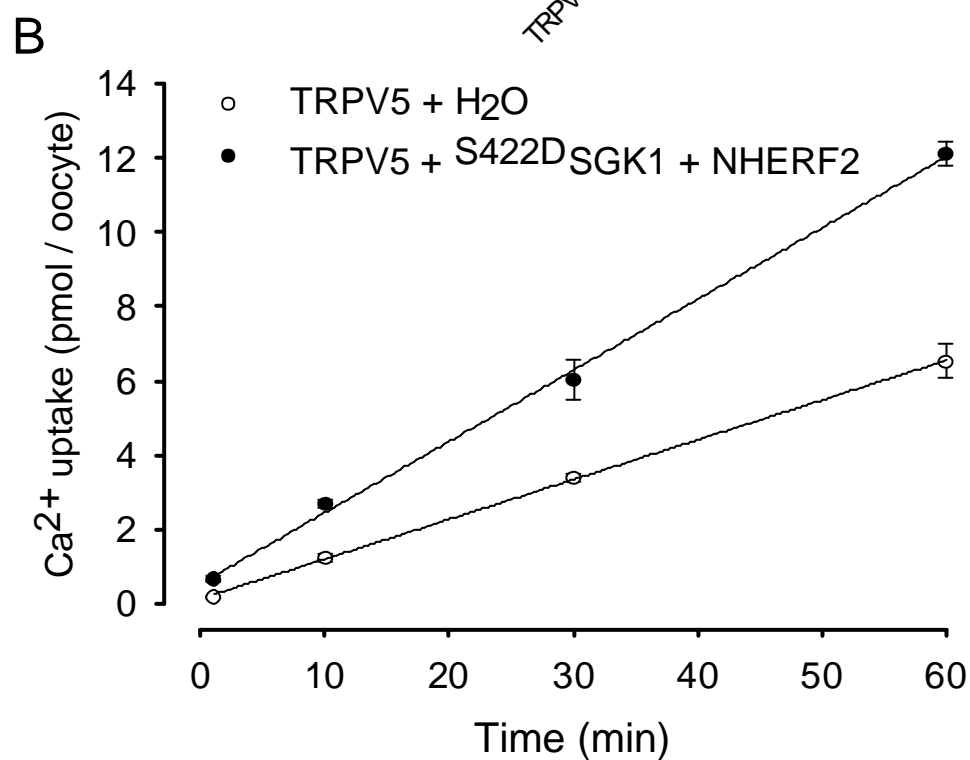
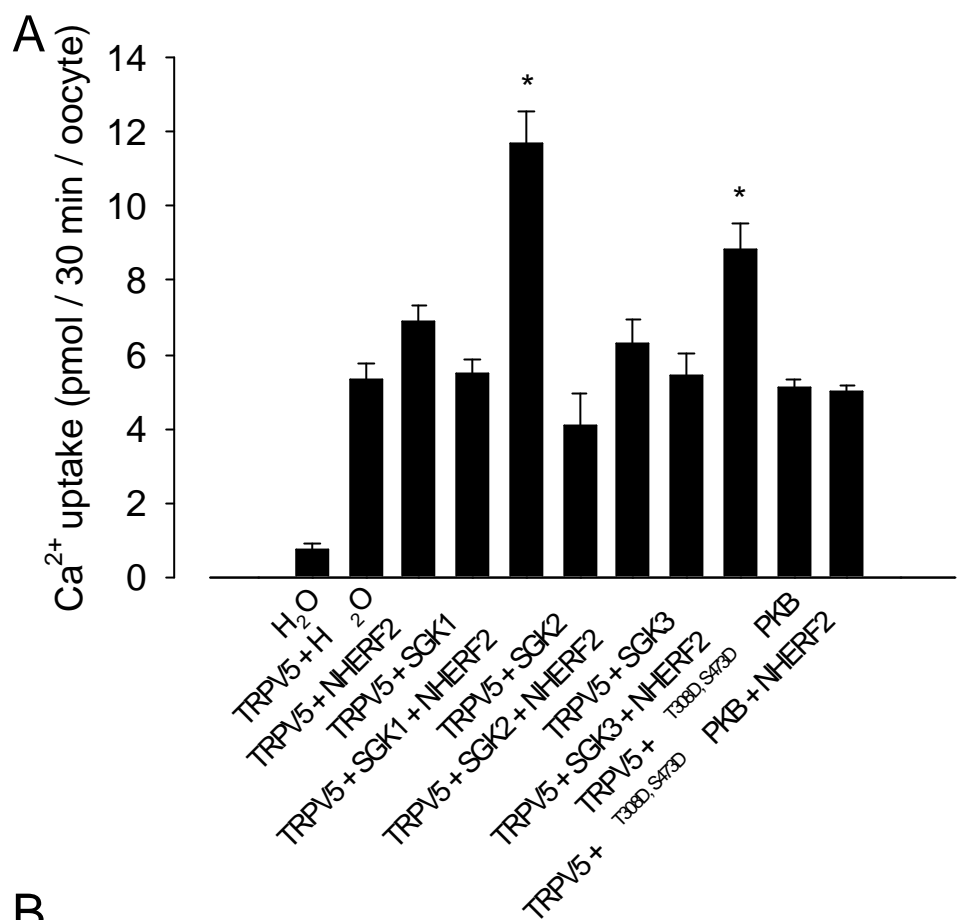


**Fig. 33. Stimulation of tracer  $\text{Ca}^{2+}$  entry by the combined expression of TRPV5, NHERF2 and SGK1 or SGK3 but not SGK2 or protein kinase B.**

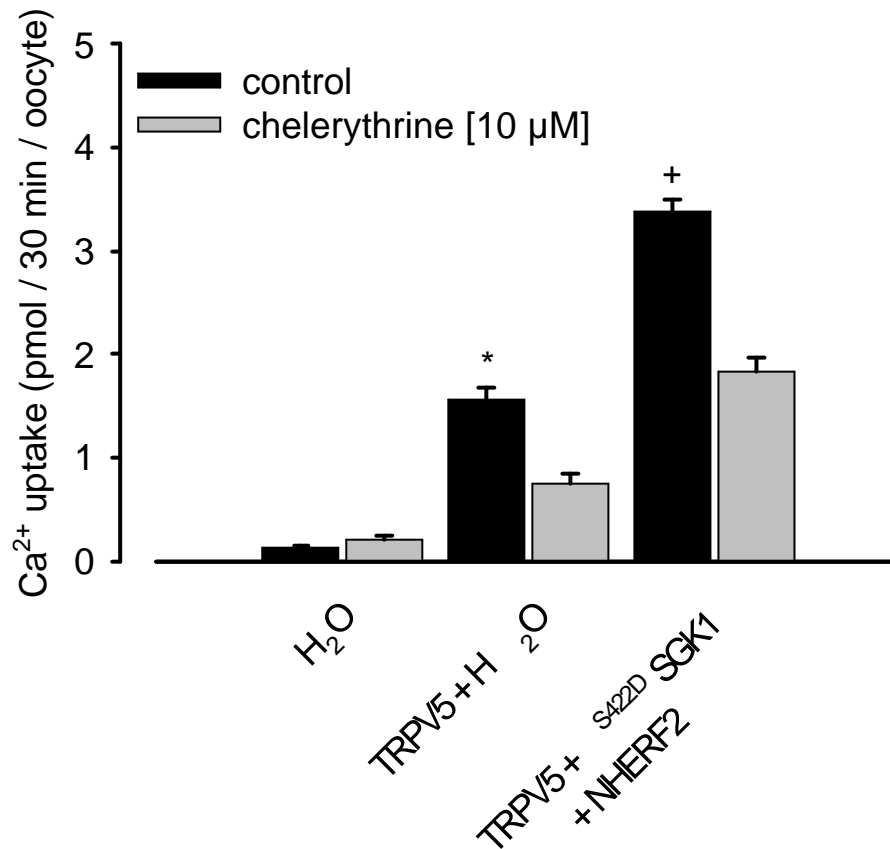
**(A)** *Xenopus laevis* oocytes were injected with either water or cRNA encoding TRPV5 and NHERF2 with or without coinjection of cRNA encoding wild type NHERF2, SGK1, SGK2, SGK3 or constitutively active <sup>T308D,S473D</sup>PKB.  $^{45}\text{Ca}^{2+}$  uptake was measured after 30 min of incubation. Arithmetic means  $\pm$  SEM (n = 8-10). \* denotes significant difference (p < 0.05) between *Xenopus* oocytes expressing TRPV5 alone and oocytes expressing TRPV5 together with NHERF2 and the respective kinase.

**(B)**  $^{45}\text{Ca}^{2+}$  uptake after 1, 10, 30 and 60 min in oocytes expressing TRPV5 and oocytes expressing TRPV5 together with <sup>S422D</sup>SGK1 and NHERF2. Arithmetic means  $\pm$  SEM (n = 6-10).



### 3.2.2 Inhibitory effect of chelerythrine on tracer $\text{Ca}^{2+}$ entry

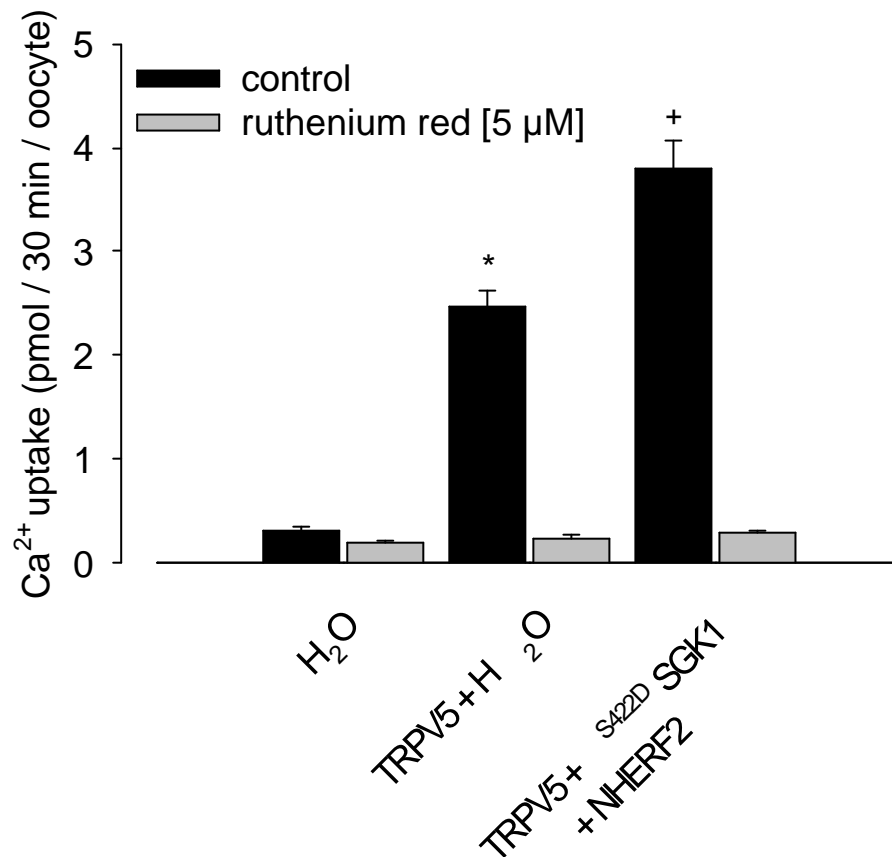
In earlier studies, the stimulation of ENaC by SGK1 was shown to be reversed by the kinase inhibitor chelerythrine (Lang et al., 2000). As illustrated in Fig. 34, 10  $\mu\text{M}$  chelerythrine indeed decreased  $\text{Ca}^{2+}$  uptake into TRPV5 expressing oocytes.



**Fig. 34. Inhibitory effect of chelerythrine on tracer  $\text{Ca}^{2+}$  entry.** *Xenopus laevis* oocytes were injected with water alone or TRPV5 with or without cRNA encoding <sup>S422D</sup>SGK1 and NHERF2.  $\text{Ca}^{2+}$  entry via TRPV5 with or without <sup>S422D</sup>SGK1 and NHERF2 was partially inhibited by addition of 10  $\mu\text{M}$  chelerythrine. Arithmetic means  $\pm$  SEM (n = 6-8). \* denotes significant difference ( $p < 0.05$ ) between *Xenopus* oocytes expressing TRPV5 and oocytes injected with water. + denotes significant difference ( $p < 0.05$ ) between *Xenopus* oocytes expressing TRPV5 together with <sup>S422D</sup>SGK1 and NHERF2 and oocytes expressing TRPV5 alone.

### 3.2.3 Inhibition of tracer $\text{Ca}^{2+}$ uptake by ruthenium red

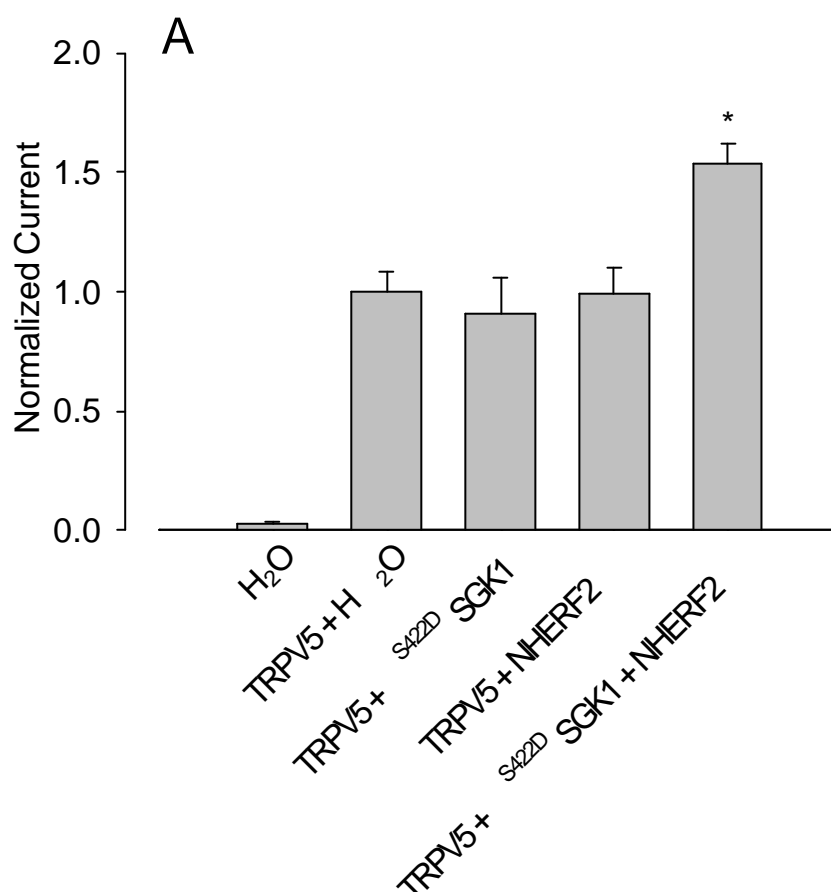
Previously, TRPV5 has been shown to be inhibited by ruthenium red (Hoenderop et al., 2001b), a polycationic dye. Thus, the effect of ruthenium red on  $\text{Ca}^{2+}$  uptake has been tested. As shown in Fig. 35, 5  $\mu\text{M}$  ruthenium red completely abolished the increase of  $\text{Ca}^{2+}$  uptake in TRPV5 expressing oocytes with or without additional expression of  $\text{S}^{422\text{D}}$ SGK1 and NHERF2.



**Fig. 35. Inhibition of tracer  $\text{Ca}^{2+}$  uptake by ruthenium red.** *Xenopus laevis* oocytes were injected with water alone or TRPV5 with or without cRNA encoding  $\text{S}^{422\text{D}}$ SGK1 and NHERF2. Application of 5  $\mu\text{M}$  ruthenium red completely inhibits TRPV5 mediated  $\text{Ca}^{2+}$  entry. Arithmetic means  $\pm$  SEM (n = 6-8). \* denotes significant difference ( $p < 0.05$ ) between oocytes expressing TRPV5 and oocytes injected with water. + denotes significant difference ( $p < 0.05$ ) between oocytes expressing TRPV5 together with  $\text{S}^{422\text{D}}$ SGK1 and NHERF2 and oocytes expressing TRPV5 alone.

### 3.2.4 $\text{Ca}^{2+}$ currents via TRPV5 stimulated by SGK1 and NHERF2

Further studies have been performed to determine the influence of  $\text{S}^{422\text{D}}$ SGK1 on TRPV5 induced currents. As reported earlier, the entry of  $\text{Ca}^{2+}$  triggers  $\text{Ca}^{2+}$  sensitive  $\text{Cl}^-$  channels (Hoenderop et al., 1999a). To determine the  $\text{Ca}^{2+}$  current directly, the  $\text{Cl}^-$  channels had to be suppressed. Therefore, the oocytes were bathed in  $\text{Cl}^-$  free extracellular fluid for 24 hours. As shown in Fig. 36, the addition of 10 mM  $\text{CaCl}_2$  induced an inward current which was 4.5 fold larger in TRPV5 expressing oocytes as compared to water injected oocytes. Coexpression of TRPV5 together with  $\text{S}^{422\text{D}}$ SGK1 and NHERF led to a further significant increase of the current. In contrast, the current was not increased by coexpression of TRPV5 with either NHERF2 or SGK1 alone (Fig. 36A).  $I_{\text{Ca}}$  was insensitive to the  $\text{Cl}^-$  channel inhibitor NPPB (Fig. 36B).



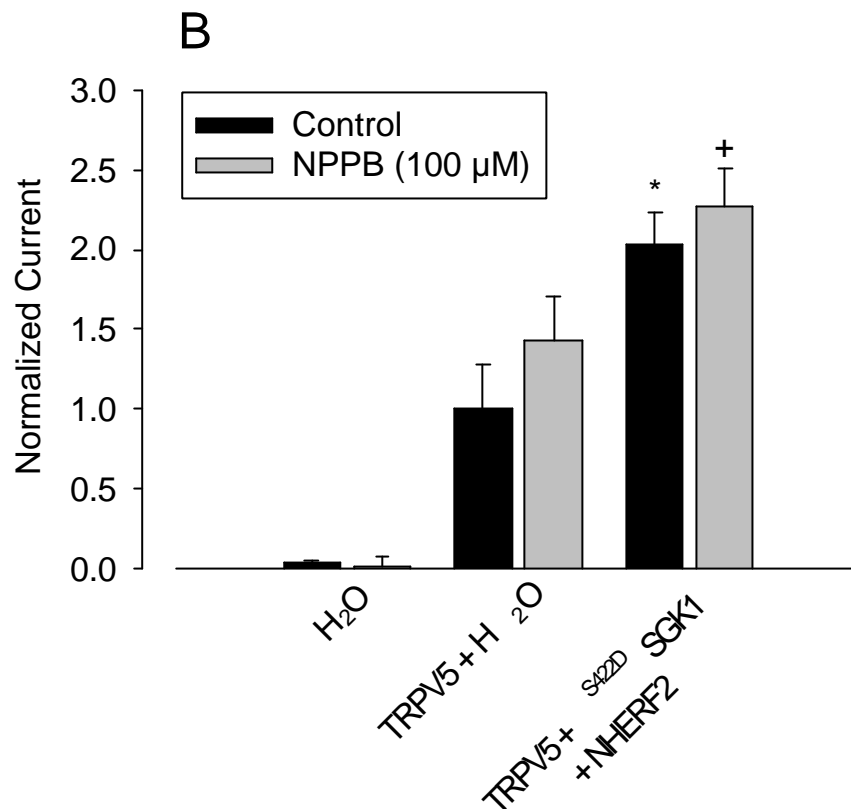


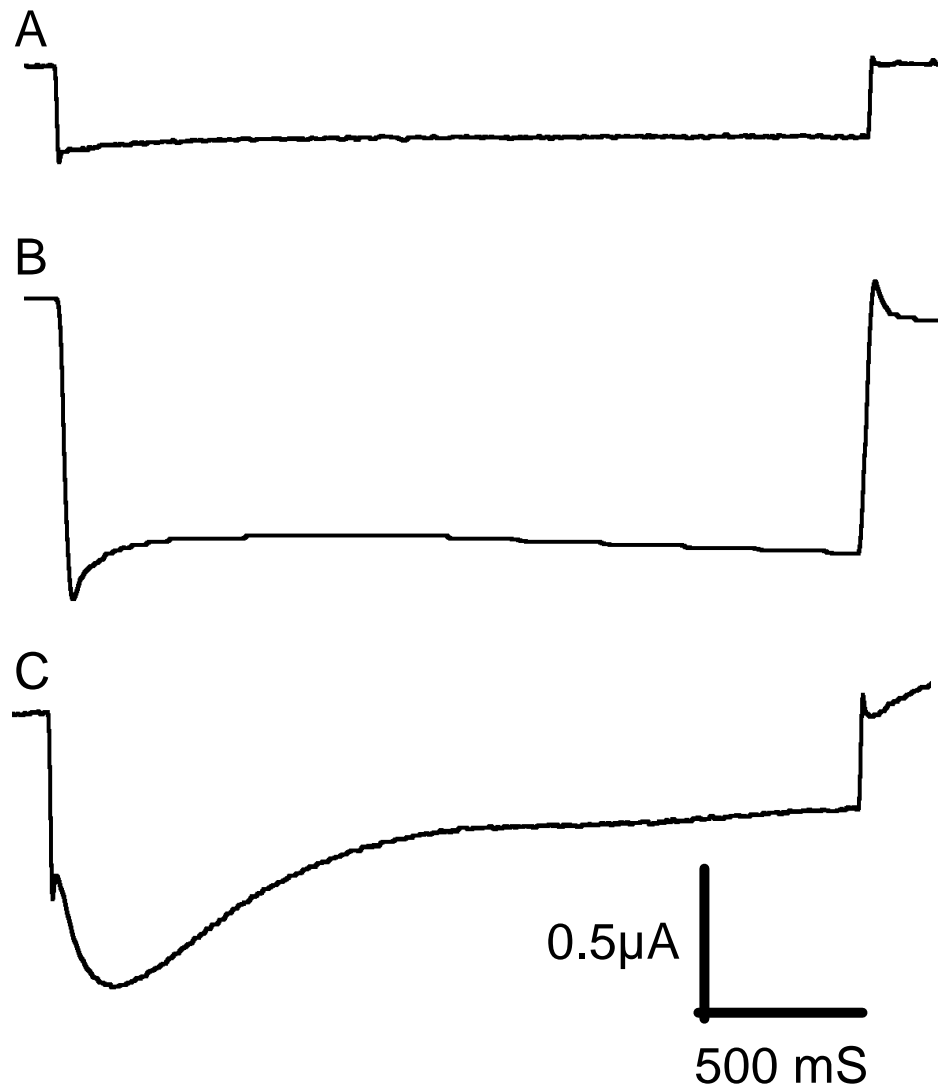
**Fig. 36. Stimulation of  $\text{Ca}^{2+}$  currents by the combined expression of TRPV5, NHERF2 and the  $\text{S}^{422\text{D}}$ SGK1.**

**(A)** TRPV5 expressing oocytes but not water injected oocytes show an inward current upon addition of 10 mM  $\text{Ca}^{2+}$  to the bath. Coexpression of TRPV5 together with  $\text{S}^{422\text{D}}$ SGK1 and NHERF2 leads to a significant increase of the current compared to oocytes expressing TRPV5 alone.  $\text{S}^{422\text{D}}$ SGK1 and NHERF2 alone do not alter TRPV5 channel activity significantly. Arithmetic means  $\pm$  SEM ( $n = 8-26$ ). \* denotes significant difference ( $p < 0.05$ ) between oocytes expressing TRPV5 and oocytes injected with water. + denotes significant difference ( $p < 0.05$ ) between oocytes expressing TRPV5,  $\text{S}^{422\text{D}}$ SGK1 together with NHERF2 and oocytes expressing TRPV5 alone.

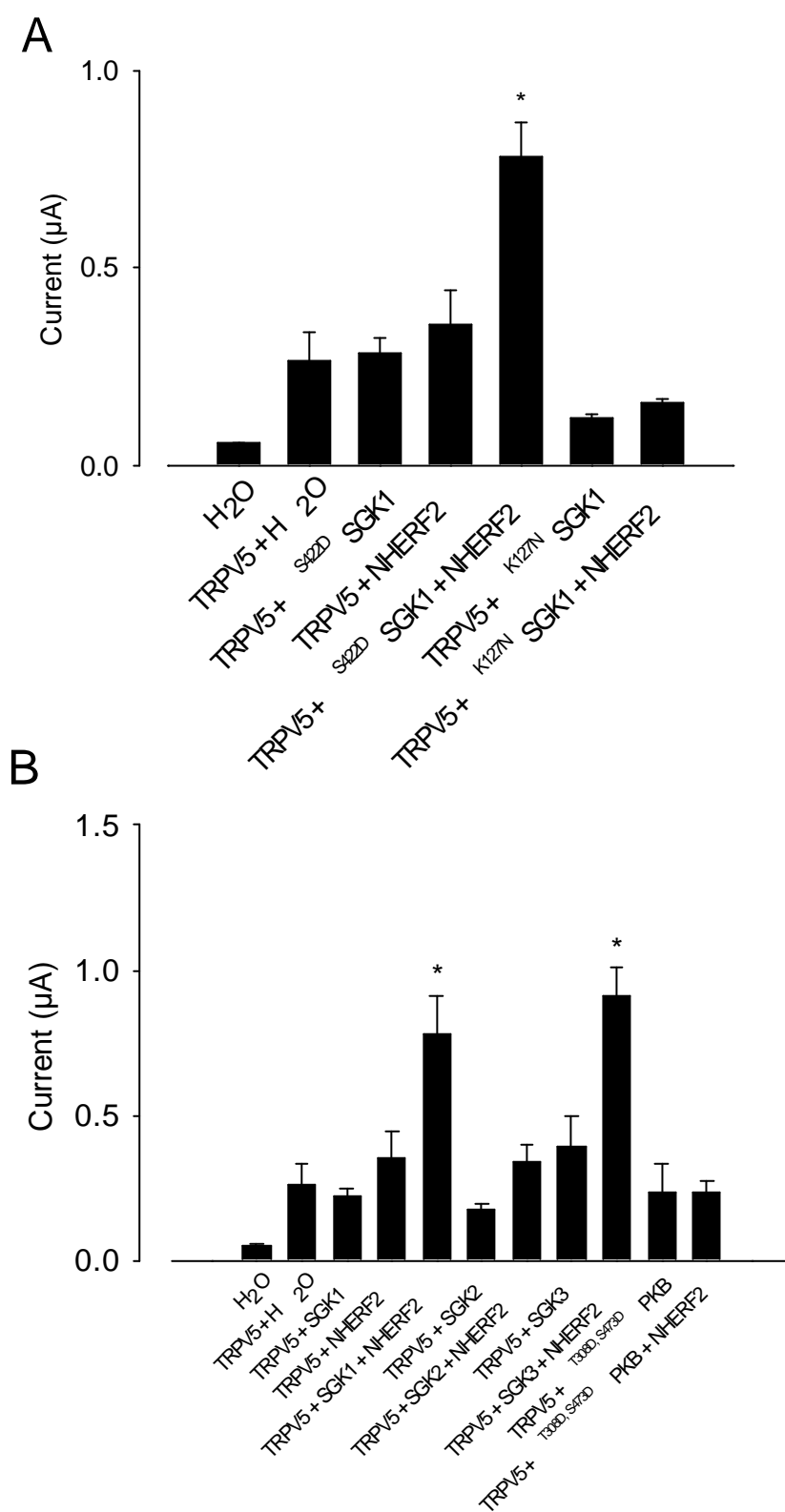
**(B)** The inward current into TRPV5 expressing oocytes in the absence of  $\text{Cl}^-$  induced by high extracellular  $\text{Ca}^{2+}$  is not sensitive to the chloride channel blocker NPPB. Arithmetic means  $\pm$  SEM ( $n = 5-12$ ). \* denotes significant difference ( $p < 0.05$ ) between oocytes expressing TRPV5,  $\text{S}^{422\text{D}}$ SGK1 together with NHERF2 and oocytes expressing TRPV5 alone. + denotes significant difference between oocytes expressing TRPV5,  $\text{S}^{422\text{D}}$ SGK1 together with NHERF2 and oocytes expressing TRPV5 alone under continuous presence of 100  $\mu\text{M}$  NPPB.

### 3.2.5 TRPV5 activate an endogenous chloride conductance ( $I_{Cl(Ca)}$ )

In the presence of  $Cl^-$ , the  $Ca^{2+}$  entry through TRPV5 stimulated  $Ca^{2+}$  sensitive  $Cl^-$  channels led to the appearance of a large  $Cl^-$  current ( $I_{Cl(Ca)}$ ). In TRPV5 expressing oocytes, hyperpolarization from -50 mV to -110 mV in the presence of 10 mM  $Ca^{2+}$  triggered a rapidly activating, slowly and partially inactivating inward current (Fig. 37C). The transiently activating current was only present in *Xenopus* oocytes expressing TRPV5. In water injected oocytes increase of cytosolic  $Ca^{2+}$  activity by addition of  $Ca^{2+}$  ionophore ionomycin (10  $\mu$ M) led to the stimulation of a non inactivating current (Fig. 37B). Fig. 37A depicts a recording from a water injected oocyte. Similar to tracer  $Ca^{2+}$  uptake and  $I_a$ ,  $I_{Cl(Ca)}$  was stimulated by coexpression of TRPV5 together with NHERF2 and either,  $S^{422D}$ SGK1 (Fig. 38A), SGK1 (Fig. 38B) or SGK3 (Fig. 38B). Coexpression of TRPV5 with either NHERF2,  $S^{422D}$ SGK1, SGK1 or SGK3 alone did not significantly enhance  $I_{Cl(Ca)}$ . Moreover, neither SGK2 nor  $T^{308D,S473D}$ PKB stimulated  $I_{Cl(Ca)}$ , even when NHERF2 was coexpressed (Fig. 38B). Thus,  $I_{Cl(Ca)}$  was enhanced by SGK1 and SGK3 but not by SGK2 or  $T^{308D,S473D}$ PKB and the effect of SGK1 and SGK3 required the presence of NHERF2. In oocytes not expressing TRPV5, the  $Ca^{2+}$  sensitive  $Cl^-$  current could be activated by  $Ca^{2+}$  ionophore ionomycin (10  $\mu$ M). As shown in Fig. 38C, the ionomycin induced  $Cl^-$  current was not significantly enhanced by expression of  $S^{422D}$ SGK1, NHERF2 or both.



**Fig. 37. Current response to a hyperpolarizing pulse. (A)** In water injected oocytes, hyperpolarization does not increase any voltage-dependent current. **(B)** Elevation of cytosolic  $\text{Ca}^{2+}$  by addition of the  $\text{Ca}^{2+}$  ionophore ionomycin (10  $\mu\text{M}$ ) led to the stimulation of a non inactivating current. **(C)** In TRPV5 expressing *Xenopus laevis* oocytes, hyperpolarization from -50 mV to -110 mV in the presence of 10 mM  $\text{Ca}^{2+}$  triggered a rapidly activating, slowly and partially inactivating inward current.



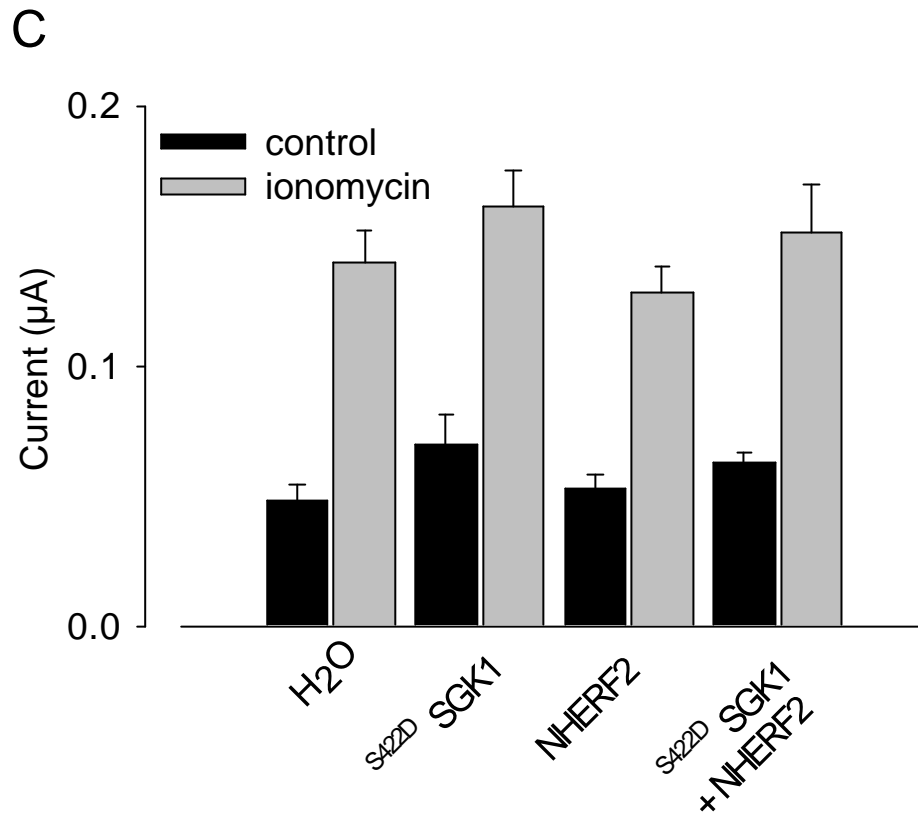
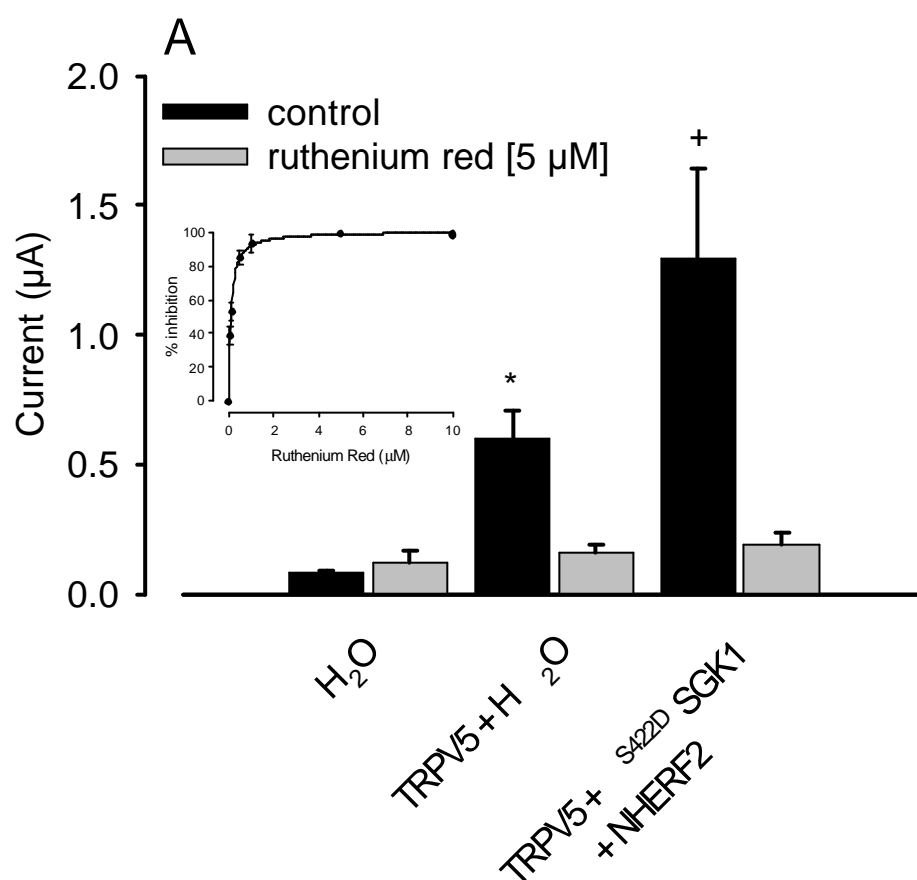


**Fig. 38. TRPV5 mediated calcium currents indirectly activate an endogenous chloride conductance ( $I_{Cl(Ca)}$ ).** (A) The endogenous chloride conductance ( $I_{Cl(Ca)}$ ) was stimulated by coexpression of TRPV5 together with NHERF2 and constitutively active SGK1 (<sup>S422D</sup>SGK1) but not with constitutively inactive SGK1 (<sup>K127N</sup>SGK1). (B)  $I_{Cl(Ca)}$  was enhanced by coexpression of TRPV5 together with NHERF2 and either, wild type SGK1 or SGK3 but not with SGK2 and constitutively active <sup>T308D,S473D</sup>PKB. Coexpression of TRPV5 with either NHERF2, <sup>S422D</sup>SGK1, SGK1 or SGK3 alone did not significantly enhance  $I_{Cl(Ca)}$ . Arithmetic means  $\pm$  SEM (n = 19-26). (C) The ionomycin induced endogenous  $Cl^-$  current was not significantly enhanced by expression of <sup>S422D</sup>SGK1, NHERF2 or both. Arithmetic means  $\pm$  SEM (n = 6).



### 3.2.6 Inhibition of the $I_{Cl(Ca)}$ by ruthenium red and NPPB

Thus, the increase of  $I_{Cl(Ca)}$  following coexpression of  $S^{422D}$ SGK1 and NHERF2 was not due to up-regulation of the  $Cl^-$  channel but due to up-regulation of TRPV5. As illustrated in Fig. 39,  $I_{Cl(Ca)}$  was abolished by ruthenium red (Fig. 39A) and by  $Cl^-$  channel blocker NPPB (Fig. 39B).



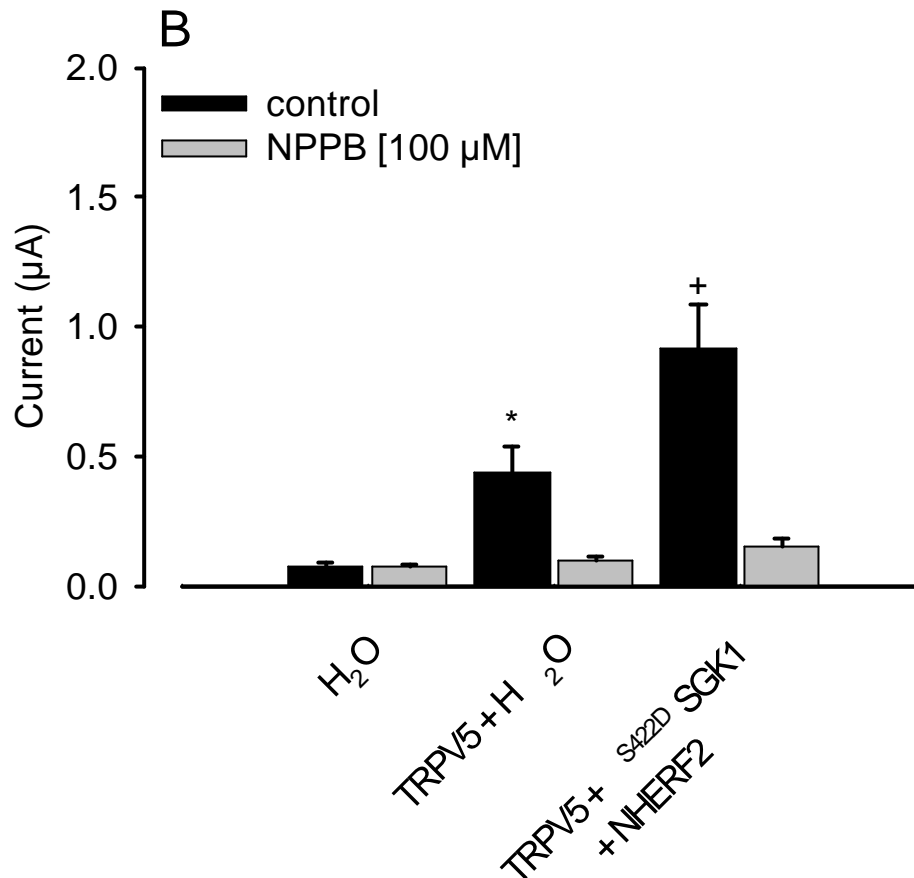


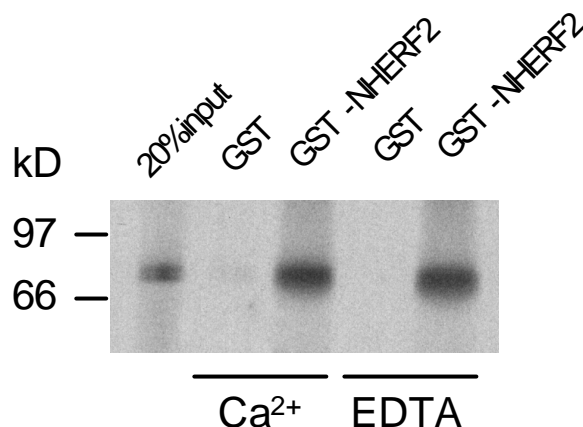
**Fig. 39. Inhibition of the TRPV5 induced current  $I_{Cl(Ca)}$  by ruthenium red and NPPB.** *Xenopus laevis* oocytes were injected with water alone or TRPV5 with or without cRNA encoding <sup>S422D</sup>SGK1 and NHERF2. **(A)** Inhibition of  $I_{Cl(Ca)}$  by application of 5  $\mu$ M ruthenium red. Arithmetic means  $\pm$  SEM (n = 7). **(B)** Inhibition of  $I_{Cl(Ca)}$  by application of 100  $\mu$ M NPPB. Arithmetic means  $\pm$  SEM (n = 5-8). Insert in A depicts dose-dependent inhibition of TRPV5 activity. \* denotes significant difference ( $p < 0.05$ ) between *Xenopus* oocytes expressing TRPV5 and oocytes injected with water. + denotes significant difference ( $p < 0.05$ ) between *Xenopus* oocytes expressing TRPV5 together with <sup>S422D</sup>SGK1 and NHERF2 and oocytes expressing TRPV5 alone.

---

### 3.2.7 Interaction of TRPV5 and NHERF2 proteins

To investigate if the regulatory effect of SGK1 and NHERF2 on TRPV5 activity is mediated by protein-protein interaction of NHERF2 and TRPV5, binding assays were performed. To this end, full-length [<sup>35</sup>S]methionine labeled TRPV5 protein was incubated with GST-NHERF2 fusion protein. TRPV5 interacted with GST-NHERF2, whereas no binding to GST alone was observed, indicating the specificity of the interaction (Fig. 40A). The binding was identical in the presence or absence (2 mM EDTA) of Ca<sup>2+</sup> (1 mM). Similarly, GST fusion proteins encompassing either the amino- or carboxy-tail of TRPV5 were incubated with [<sup>35</sup>S]methionine labeled NHERF2. NHERF2 interacted specifically with the carboxy-tail, while the amino-tail of TRPV5 was unable to bind NHERF2 (Fig. 40B). The binding was again Ca<sup>2+</sup>-independent.

A



B

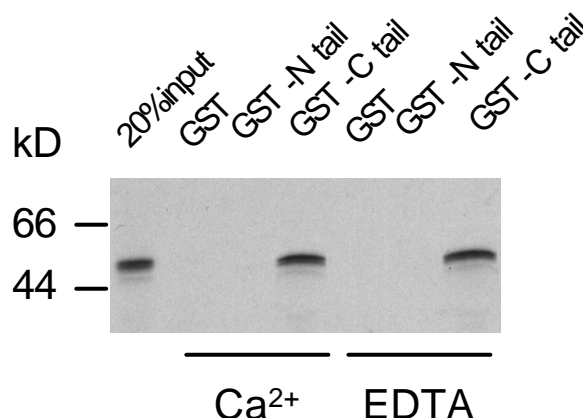


**Fig. 40. Interaction of TRPV5 and NHERF2 proteins. (A)** Full-length [ $^{35}\text{S}$ ]methionine labeled TRPV5 protein was incubated with GST-NHERF2 fusion protein in the presence and absence of 1 mM extracellular  $\text{Ca}^{2+}$ . TRPV5 interacted with GST-NHERF2, whereas no binding to GST alone was observed. The binding was identical in the presence of 1 mM or absence (2 mM EDTA) of  $\text{Ca}^{2+}$ . **(B)** GST fusion proteins encompassing either the amino- or carboxy-tail of TRPV5 were incubated with [ $^{35}\text{S}$ ]methionine labeled NHERF2. NHERF2 interacted specifically with the carboxy-tail, since the amino-tail of TRPV5 and GST alone were unable to bind NHERF2. The binding was identical in the presence of 1 mM or absence (2 mM EDTA) of  $\text{Ca}^{2+}$ .

### 3.2.8 Stimulation of TRPV5 requires Second PDZ domain of NHERF2

Further studies were performed to identify the PDZ binding domain of NHERF2 required for the stimulating effect of <sup>S422D</sup>SGK1 and NHERF2 on TRPV5 activity. As shown in Fig. 41,  $I_{Cl(Ca)}$  was markedly enhanced by coexpression of TRPV5 with both, <sup>S422D</sup>SGK1 and wild-type NHERF2, but not by coexpression of TRPV5 together with <sup>S422D</sup>SGK1 and NHERF2 lacking the second PDZ domain (NHERF2 $\Delta$ P2). In contrast, coexpression of <sup>S422D</sup>SGK1 together with a NHERF2 mutant deficient of the first PDZ domain (NHERF2 $\Delta$ P1) increased  $I_{Cl(Ca)}$  similar to coexpression of <sup>S422D</sup>SGK1 together with wild type NHERF2. Thus, the second but not the first PDZ domain is essential for up-regulation of TRPV5 activity. This requirement for the second PDZ domain is consistent with the interaction of SGK1 with the second but not first PDZ domain of NHERF2 (Yun et al., 1998).

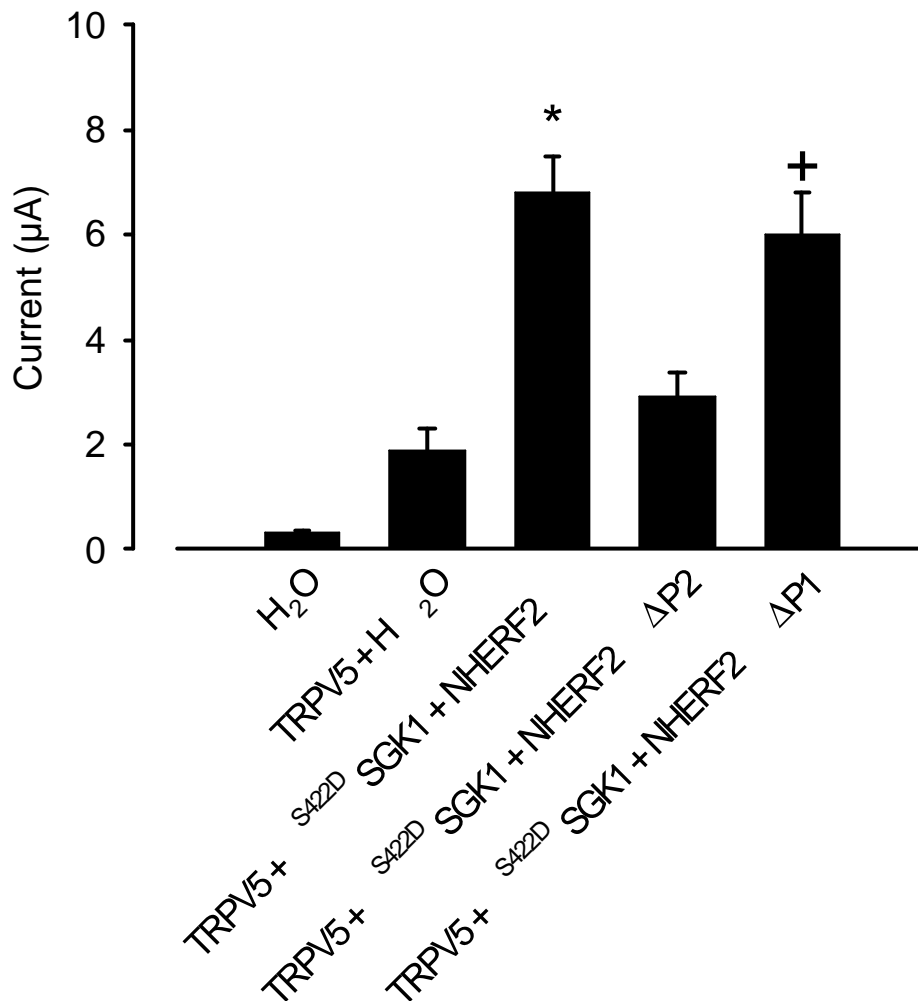


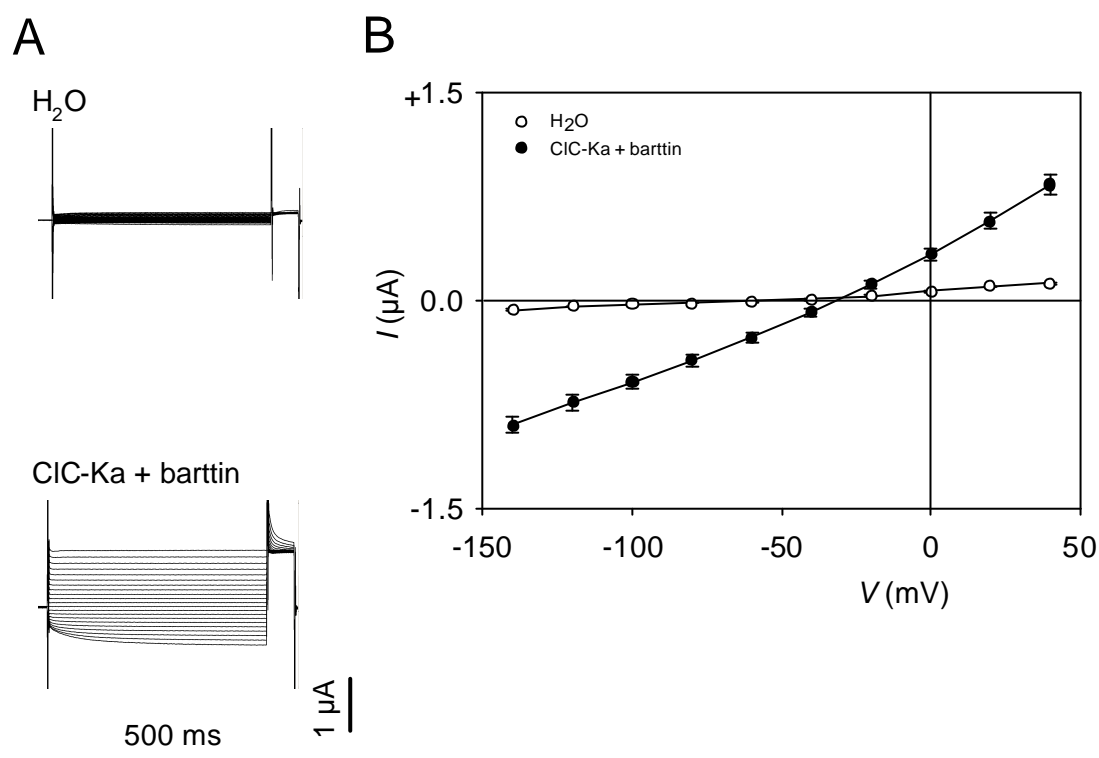
**Fig. 41. Requirement of the second PDZ domain of NHERF2 for the stimulation of TRPV5 activity by constitutively active <sup>S422D</sup>SGK1.**

*Xenopus laevis* oocytes were injected with water or cRNA encoding TRPV5 alone or with <sup>S422D</sup>SGK1 and either wild-type NHERF2, NHERF2 lacking the second PDZ domain (NHERF2ΔP2) or NHERF2 lacking the first PDZ domain (NHERF2ΔP1). Only the combined coexpression of <sup>S422D</sup>SGK1 and wild-type NHERF2 or NHERF2ΔP1 increases TRPV5 channel activity. Arithmetic means ± SEM (n = 14-22) of currents taken at -135 mV. \* indicates significant difference between expression of TRPV5 alone and of TRPV5 coexpressed with <sup>S422D</sup>SGK1 and NHERF2. + denotes significant difference (p < 0.05) between *Xenopus* oocytes expressing TRPV5 together with <sup>S422D</sup>SGK1 and NHERF2? 2 and oocytes expressing TRPV5 alone.

### 3.3 Regulation of the renal ClC-Ka/barttin chloride channels

#### 3.3.1 ClC-Ka/barttin induced currents

*Xenopus* oocytes expressing ClC-Ka together with barttin created a slightly inwardly rectifying current ( $I_{Cl}$ ) of  $-0.69 \pm 0.06 \mu\text{A}$  ( $n = 17-20$ ) at  $-140 \text{ mV}$ . The respective current  $I_{Cl}$  in water injected *Xenopus* oocytes amounted to  $-0.06 \pm 0.01 \mu\text{A}$  ( $n = 17-20$ ) (Fig. 42).



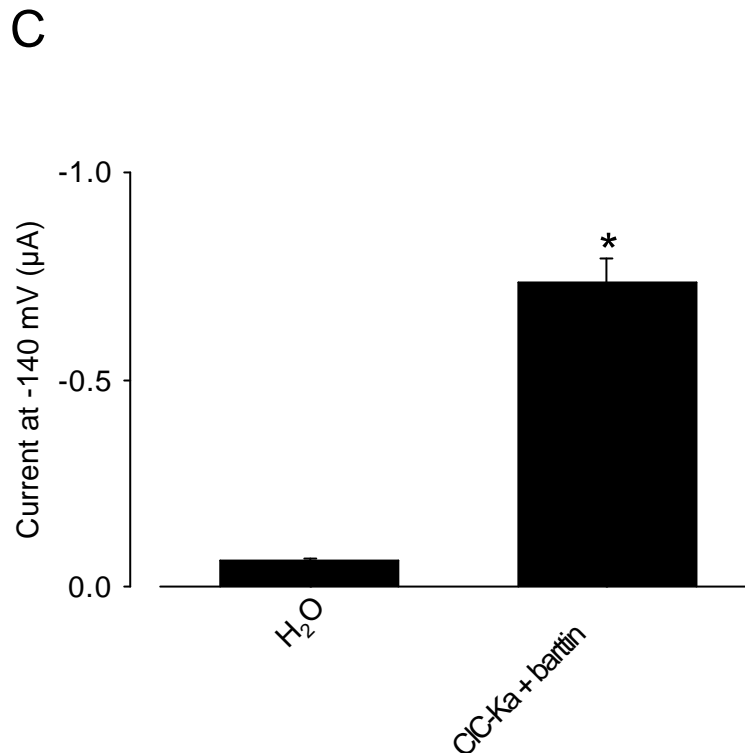


**Fig. 42. ClC-Ka/barttin induced currents.** *Xenopus laevis* oocytes were injected with water or with cRNA encoding ClC-Ka together with barttin. Slightly inwardly rectifying currents are observed in *Xenopus* oocytes expressing ClC-Ka/barttin but not in water injected oocytes. **(A)** Original tracings. **(B)** Current-voltage relations. **(C)** Absolute current values at a holding voltage of -140 mV. Arithmetic means  $\pm$  SEM (n = 17-20). \* indicates significant difference between currents in oocytes expressing ClC-Ka/barttin as compared to oocytes injected with water.

### 3.3.2 Regulation of ClC-Ka/barttin channels by Nedd4-2 and SGK1

As shown in Fig. 43, the coexpression of Nedd4-2 together with ClC-Ka/barttin decreased  $I_{Cl}$  significantly to  $-0.35 \pm 0.03 \mu A$  (n = 17). In contrast, coexpression of SGK1 with ClC-Ka/barttin significantly enhanced  $I_{Cl}$  to  $-0.93 \pm 0.07 \mu A$  (n = 18). Moreover, SGK1 reversed the effect of Nedd4-2. In *Xenopus* oocytes coexpressing ClC-Ka/barttin together with both, Nedd4-2 and SGK1,  $I_{Cl}$  approached  $-1.06 \pm 0.07 \mu A$  (n = 20).



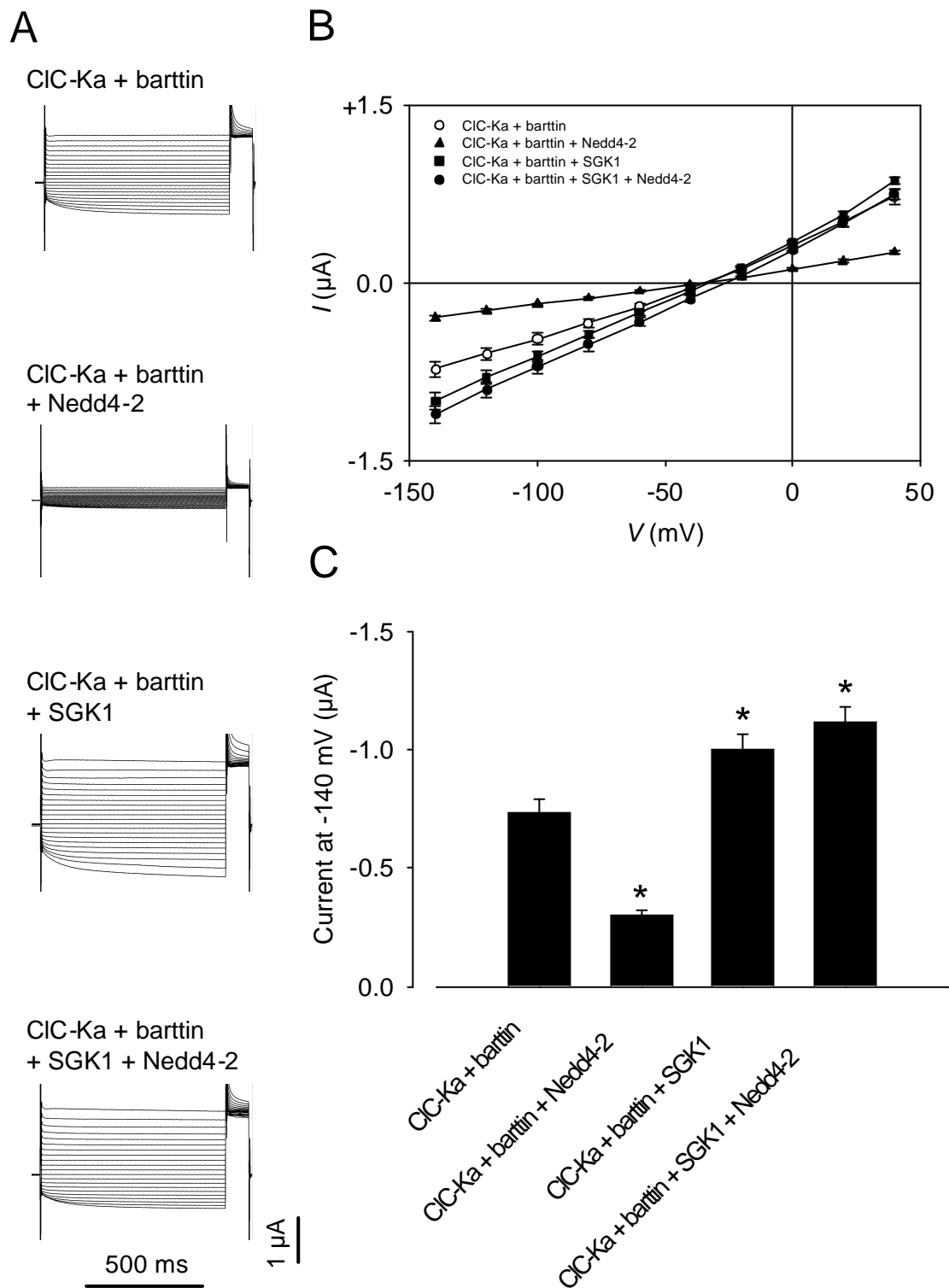


**Fig. 43. Regulation of ClC-Ka/barttin induced currents by Nedd4-2 and SGK1.** *Xenopus laevis* oocytes were injected with cRNA encoding ClC-Ka/barttin with or without cRNA encoding Nedd4-2 and/or SGK1. The ClC-Ka/barttin induced currents are down-regulated by coexpression of Nedd4-2 and up-regulated by SGK1. **(A)** Original tracings. **(B)** Current-voltage relations. **(C)** Absolute current values at a holding voltage of -140 mV. Arithmetic means  $\pm$  SEM (n = 17-20). \* indicates significant difference between the respective currents and the currents in oocytes expressing ClC-Ka/barttin alone.

### 3.3.3 Regulation of ClC-Ka/barttin channels by SGK1 mutants

The effect of SGK1 on  $I_{Cl}$  was mimicked by the constitutively active  $S^{422D}$ SGK1 but not by the inactive mutant  $K^{127N}$ SGK1 (Fig. 44). In *Xenopus* oocytes expressing ClC-Ka/barttin together with  $S^{422D}$ SGK1,  $I_{Cl}$  reached  $-1.06 \pm 0.08 \mu A$  (n = 20), whereas in oocytes expressing ClC-Ka/barttin together with  $K^{127N}$ SGK1,  $I_{Cl}$  was  $-0.56 \pm 0.06 \mu A$  (n = 17). While coexpression of  $S^{422D}$ SGK1 reversed the effect of Nedd4-2 ( $I_{Cl} = -0.97 \pm 0.07 \mu A$ , n = 20), the coexpression of the inactive mutant  $K^{127N}$ SGK1 did not reverse the inhibitory effect of Nedd4-2 ( $I_{Cl} = -0.48 \pm 0.04 \mu A$ , n = 18).

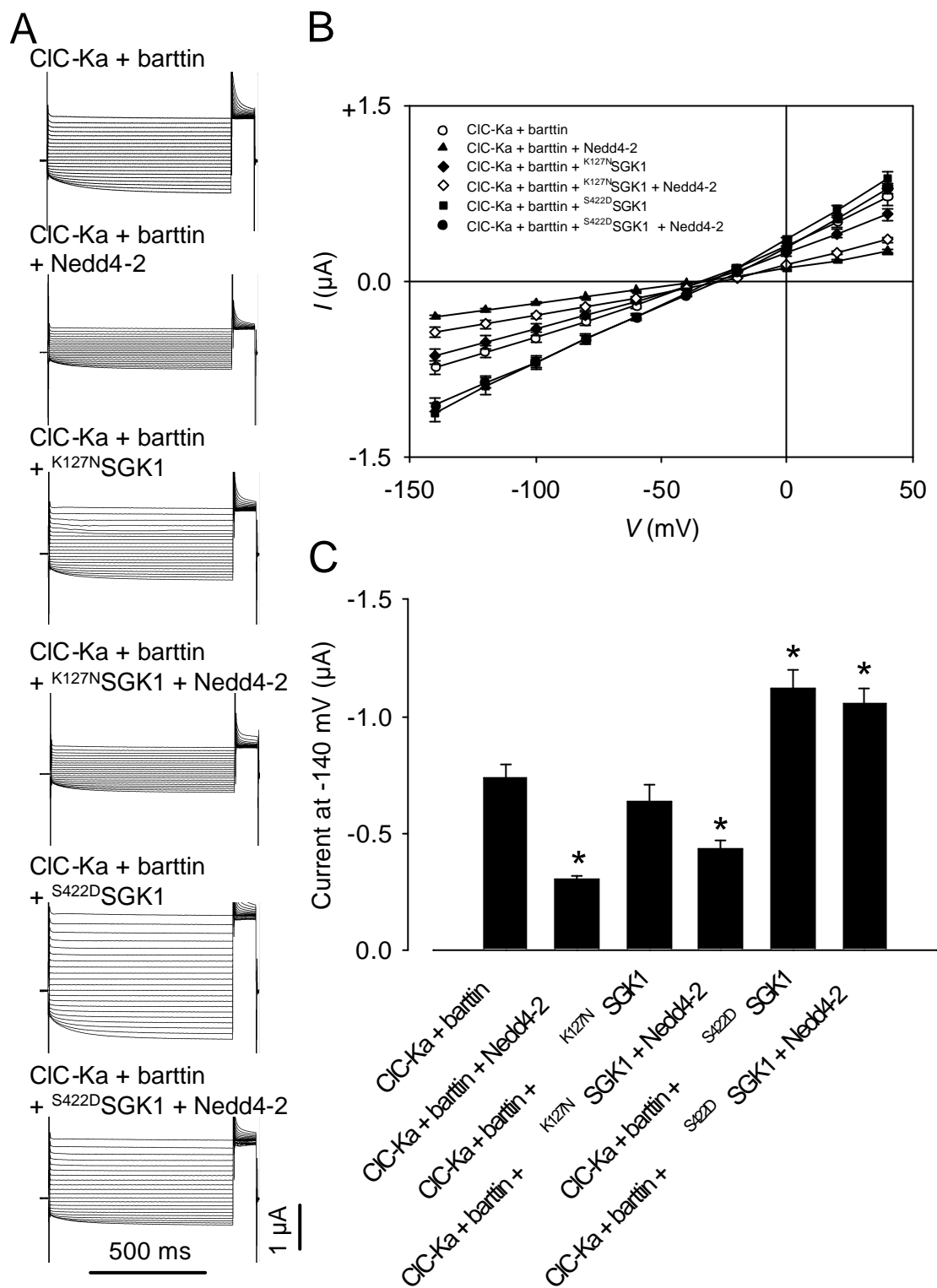


**Fig. 44. Regulation of ClC-Ka/barttin induced currents by constitutively active SGK1 but not inactive mutant kinase.** *Xenopus laevis* oocytes were injected with cRNA encoding ClC-Ka/barttin with or without cRNA encoding Nedd4-2 and/or either constitutively active <sup>S422D</sup>SGK1 or inactive <sup>K127N</sup>SGK1. <sup>S422D</sup>SGK1 but not <sup>K127N</sup>SGK1 enhances the ClC-Ka/barttin induced currents and reverses the down-regulation of those currents by Nedd4-2. **(A)** Original tracings. **(B)** Current-voltage relations. **(C)** Absolute current values at a holding voltage of -140 mV. Arithmetic means  $\pm$  SEM (n = 17-20). \* indicates significant difference between the respective currents and the currents in oocytes expressing ClC-Ka/barttin alone.

### 3.3.4 Regulation of ClC-Ka/barttin induced currents by SGK3

SGK3 but not SGK2 activated  $I_{Cl}$  similar to SGK1 (Fig. 45). In *Xenopus* oocytes expressing ClC-Ka/barttin together with SGK3  $I_{Cl}$  amounted  $-1.10 \pm 0.10 \mu A$  (n = 18), whereas in oocytes expressing ClC-Ka/barttin together with SGK2  $I_{Cl}$  was only  $-0.75 \pm 0.07 \mu A$  (n = 17). While coexpression of SGK3 reversed the effect of Nedd4-2 ( $I_{Cl} = -1.31 \pm 0.11 \mu A$ , n = 20), the coexpression of SGK2 did not reverse the inhibitory effect of Nedd4-2 ( $I_{Cl} = -0.47 \pm 0.05 \mu A$ , n = 18).

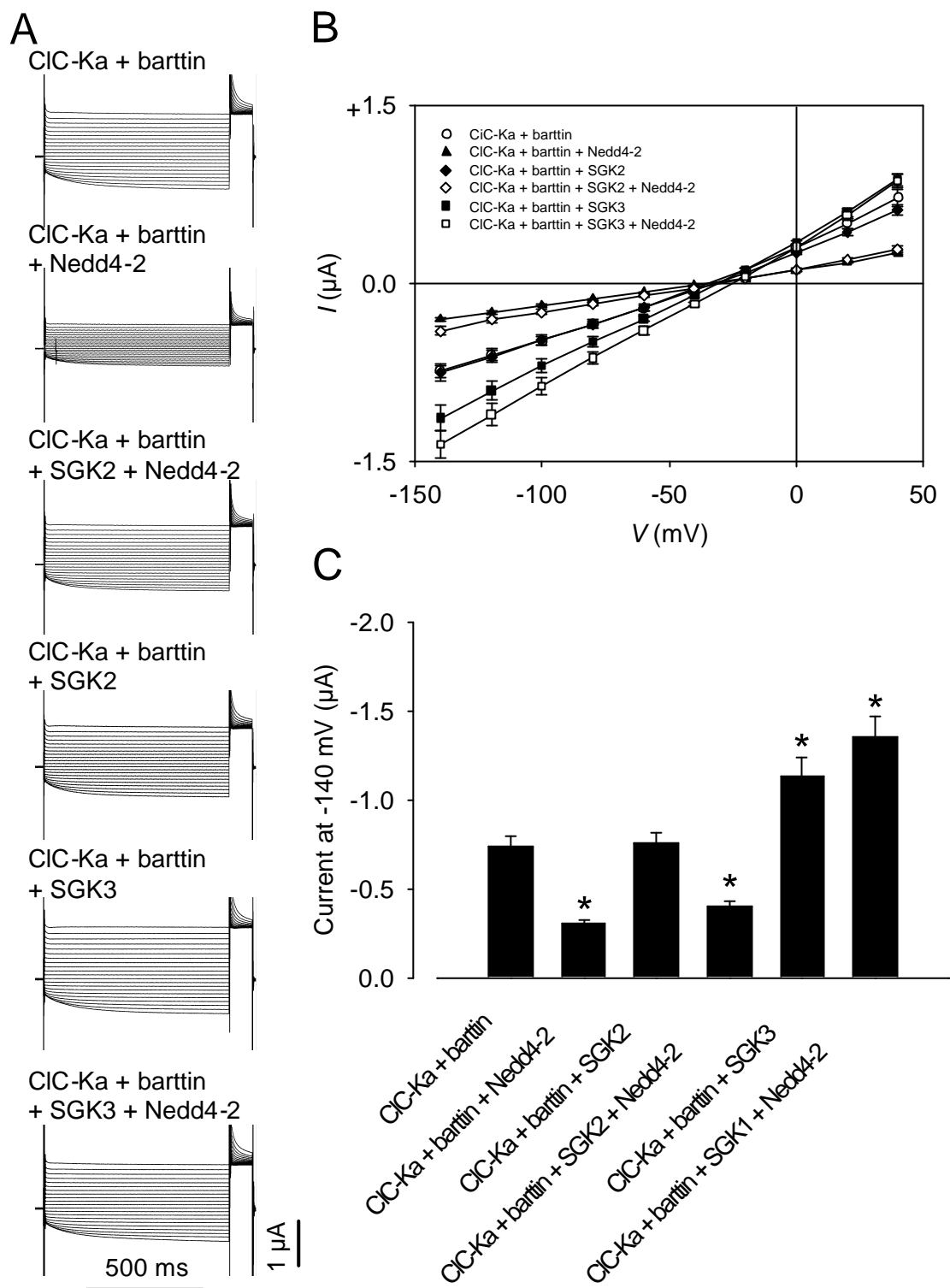


**Fig. 45. Regulation of ClC-Ka/barttin induced currents by SGK3 but not by SGK2.** *Xenopus laevis* oocytes were injected with cRNA encoding ClC-Ka/barttin with or without cRNA encoding Nedd4-2 and/or either SGK2 or SGK3. SGK3 but not SGK2 enhances the ClC-Ka/barttin induced currents and reverses the down-regulation of those currents by Nedd4-2. **(A)** Original tracings. **(B)** Current-voltage relations. **(C)** Absolute current values at a holding voltage of -140 mV. Arithmetic means  $\pm$  SEM (n = 17-20). \* indicates significant difference between the respective currents and the currents in oocytes expressing ClC-Ka/barttin alone.

### 3.3.5 Abolished down-regulation of ClCKa/barttin channels by Nedd4-2

Replacement of the tyrosine in the PY motif of barttin by alanine abolished the down-regulation of the ClC-Ka/barttin channels by Nedd4-2. Coexpression of Nedd4-2 with the mutant <sup>Y98A</sup>barttin does not lead to significant reduction of channel activity ( $I_{Cl} = -0.91 \pm 0.10 \mu A$ , n = 12) (Fig. 46) compared to expression of mutant <sup>Y98A</sup>barttin alone ( $I_{Cl} = -1.08 \pm 0.10 \mu A$ , n = 11).

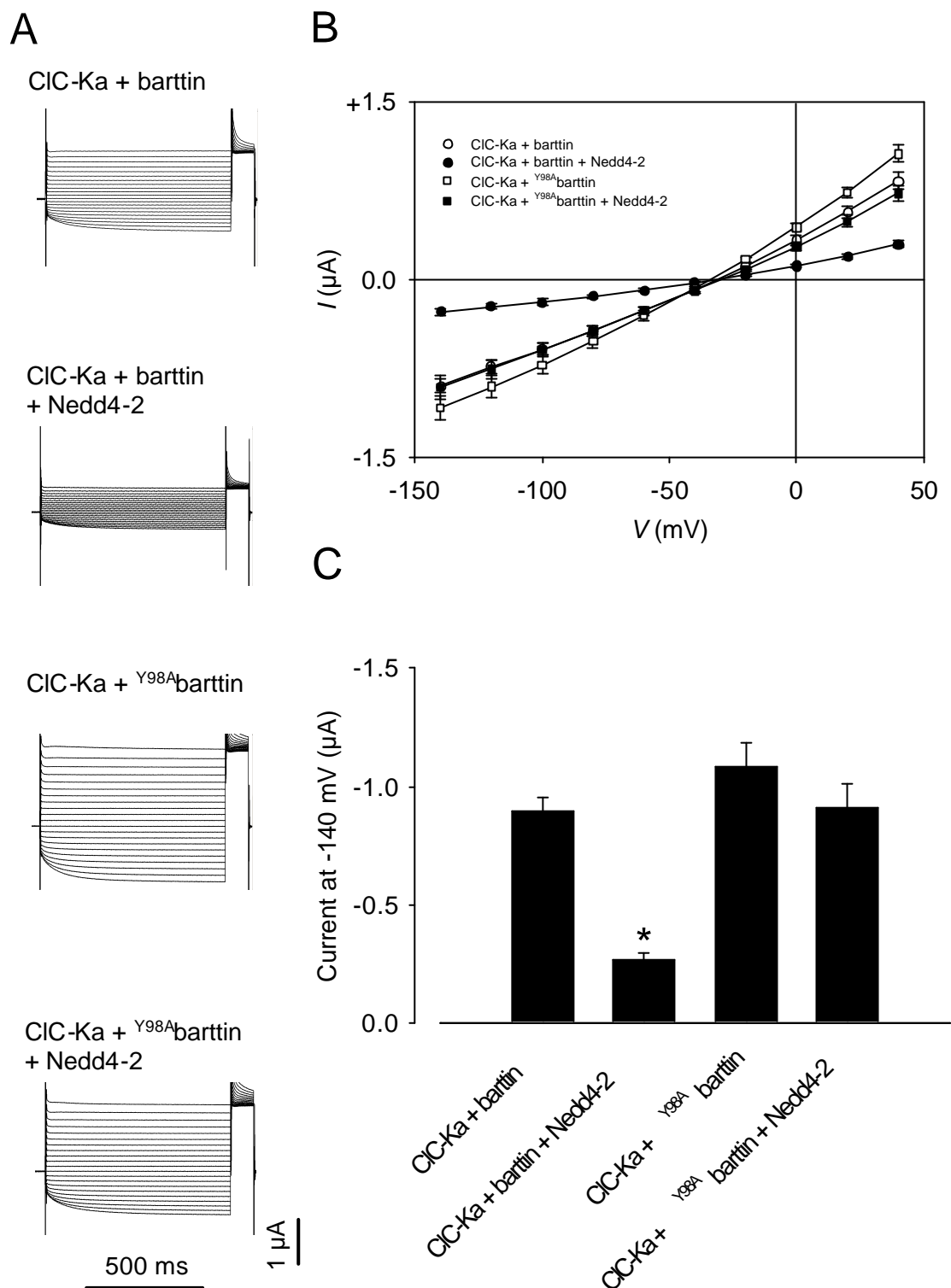


**Fig. 46. Nedd4-2 mediated down-regulation of ClCKa/barttin is abolished by elimination of the PY motif in <sup>Y98A</sup>barttin.** *Xenopus laevis* oocytes were injected with cRNA encoding ClC-Ka/barttin or ClC-Ka/<sup>Y98A</sup>barttin with or without Nedd4-2. While the wild-type ClC-Ka/barttin is down-regulated by Nedd4-2, the ClC-Ka/<sup>Y98A</sup>barttin remains unaffected. **(A)** Original tracings. **(B)** Current-voltage relations. **(C)** Absolute current values at a holding voltage of -140 mV. Arithmetic means  $\pm$  SEM (n = 11-12). \* indicates significant difference between the respective currents and the currents in oocytes expressing ClC-Ka/barttin alone.

### 3.3.6 Immunolocalization of ClC-Ka and barttin channels

Fig. 47 depicts the membrane expression of the ClC-Ka/barttin heterodimer. Fluorescence intensity is increased upon coexpression of SGK1 while Nedd4-2 reduces the signal. The effect of Nedd4-2 is partially reversed by additional coexpression of SGK1.



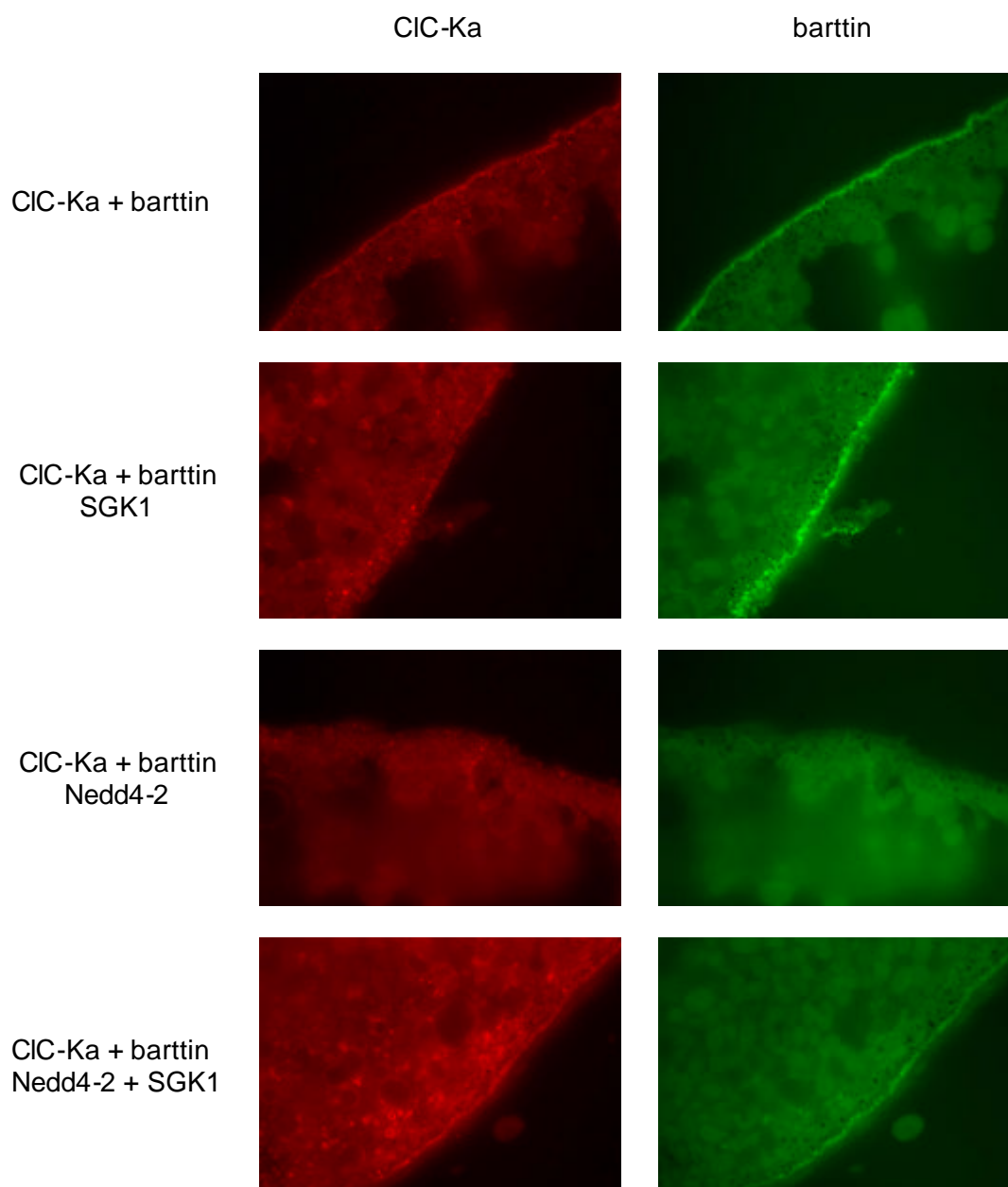


**Fig. 47. Immunolocalization of CIC-Ka and barttin in *Xenopus* oocyte membrane preparations.** Membrane staining for CIC-Ka (red) and barttin (green) is detected in absence and presence of SGK1 but not in presence of Nedd4-2. Additional expression of SGK1 in oocytes injected with CIC-Ka, barttin and Nedd4-2 reconstitutes the membrane localization of CIC-Ka and barttin.

## **4 DISCUSSION**

## 4.1 Regulation of the renal epithelial K<sup>+</sup> channel ROMK1

### 4.1.1 Up-regulation of K<sup>+</sup> transport via ROMK1 by SGK1 and NHERF2

The present experiments indicate that SGK1 alone is unable to up-regulate the ROMK1-mediated K<sup>+</sup> current in *Xenopus* oocytes, consistent with earlier experiments performed on the closely related ROMK2 channel (Chen et al., 1999). Interestingly, it appears that this lack of ROMK1 regulation is due to the requirement of NHERF2 expression for the SGK1 effect to be manifested. SGK1 has been shown to regulate the epithelial sodium channel (ENaC) in the absence of NHERF2 (Wagner et al., 2001). In fact, SGK1 stimulates ENaC by phosphorylating and thereby inhibiting the ubiquitin protein ligase Nedd4-2 in a PY motif-dependent manner (Debonneville et al., 2001). The ROMK1 sequence does not include a PY motif. On the other hand, ROMK1 has a PDZ binding motif at the COOH-terminus (Welling et al., 2001; Flagg et al., 2002), which is thought to be required for binding to NHERF2 (Yun et al., 2002a). The ENaC sequence does not include a PDZ binding motif, indicating that NHERF2 can not directly interact with ENaC.

The stimulatory effect is not due to changes in ROMK1 channel I-V relation and gating properties (Fig. 19). In theory, SGK1/NHERF2 could have been effective through alterations of cytosolic pH, as coexpression of SGK1 with NHERF2 was shown to modulate the activity of the Na<sup>+</sup>/H<sup>+</sup> exchanger 3 (NHE3) (Yun et al., 2002a). NHE3 is expressed in *Xenopus laevis* oocytes intrinsically. However, the data showed that the intracellular pH was not significantly altered by the expression of SGK1 and NHERF2 ruling out this possibility.

Instead, the combined action of SGK1 with NHERF2 enhances the abundance of ROMK1 in the plasma membrane, pointing to a stimulating effect on insertion or an inhibitory effect on the retrieval of the channel protein from the plasma membrane. These two possibilities could be discriminated by brefeldin A, a drug interfering with the insertion of membrane proteins (Pelham, 1991; Alvarez de la Rosa et al., 1999) as indicated in Fig. 48. In the presence of this drug, no further proteins can be inserted into the plasma membrane and the decay of channel

activity reflects solely the retrieval of channel proteins. The results demonstrate that the decay is significantly blunted by the combined expression of SGK1 and NHERF2 indicating that SGK1 and NHERF2 might affect ROMK1 at least in part by inhibition of protein retrieval. NHERF2 has previously been shown to link membrane proteins to cytoskeletal proteins such as ezrin and actin (Yun et al., 1998; Takeda et al., 2001). It is hence plausible that the membrane expression of ROMK1 is stabilized by its linkage to the cytoskeleton via NHERF2. This may in part decrease the retrieval of ROMK1 or prolong the retention time at the cell membrane surface.

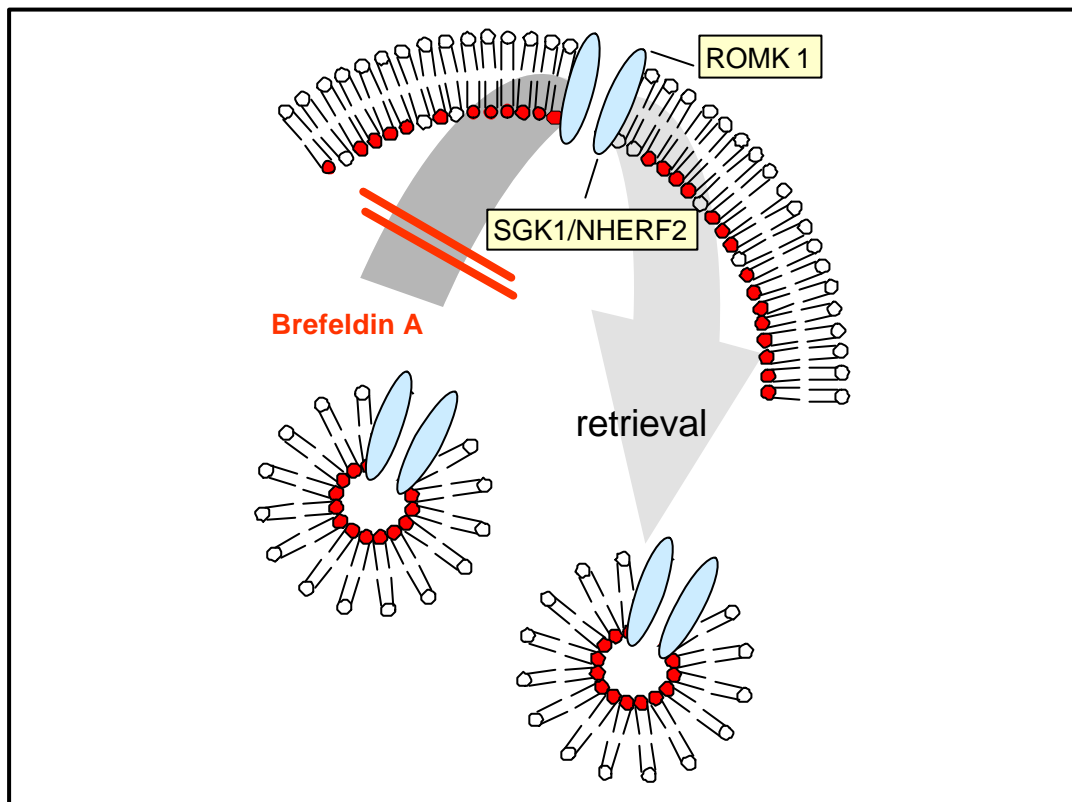


**Fig.48.** Brefeldin A inhibits the insertion of new ROMK1 channels into the plasma membrane and SGK1/NHERF2 delay the endocytotic retrieval of ROMK1 channels.

Even though the small shift of pH sensitivity cannot account for the marked enhancement of channel activity, it indicates that coexpression of NHERF2 or SGK1 does not only enhance channel abundance within the cell membrane but has a subtle but significant effect on channel properties. This effect is not due to enhanced protein abundance or channel activity, as the pH sensitivity was identical in oocytes injected with 5 ng or 20 ng of ROMK1 RNA despite the observed large differences in currents. Rather, SGK1 modifies the channel protein itself. In this respect, it may be of interest that the ROMK1 channel protein contains a consensus sequence for SGK1.

The involvement of different proteins in the regulation of ROMK1 increases the plasticity of  $K^+$  channel regulation. One requirement for the up-regulation of ROMK1 by the SGK1/NHERF2 mechanism is the genomic up-regulation of SGK1. This up-regulation is accomplished by aldosterone (Chen et al., 1999; Cowling and Birnboim, 2000), cell shrinkage (Waldegger et al., 1997) and a wide variety of additional factors (Lang and Cohen, 2001). Expressed SGK1 requires activation, which can be accomplished by insulin and IGF-1 through PI3-kinase and PDK1 (Kobayashi and Cohen, 1999b; Park et al., 1999). Thus, SGK1 integrates the signals coming from aldosterone on the one hand and insulin or IGF-1 on the other (Wang et al., 2001). The involvement of NHERF2 adds to the complexity of this system. In particular, observed variability in  $K^+$  excretion in response to mineralocorticoids could be influenced by NHERF2 activity or expression levels, hence accounting for the variability in hypokalemia seen in patients with primary aldosteronism (Gordon et al., 1994). A well described function of NHERF2 has been the regulation of the  $Na^+/H^+$  exchanger NHE3, pointing to a role of this molecule in the regulation of the acid-base balance (Yun et al., 1997; Zerangue et al., 1999). Renal  $K^+$  excretion is a function of acid-base balance (Giebisch, 1998), a correlation attributed to the exquisite sensitivity of ROMK1 to cytosolic pH (Tsai et al., 1995; Fakler et al., 1996; Kunzelmann et al., 2000; Leipziger et al., 2000). In face of the present observations, it is appealing to speculate that NHERF2 participates in the regulation of  $K^+$  excretion by acid-base balance. In any case, the effects of NHERF2 are not limited to the regulation of NHE3. Most recently, NHERF2 has

been shown to direct the signaling of the PTH receptor (Mahon et al., 2002), an observation further illustrating the diversity of NHERF2 functions.

#### **4.1.2 Determination of pH sensitivity of ROMK1 channel by SGK1**

As shown previously, the coexpression of the serum and glucocorticoid inducible kinase SGK1 and the Na<sup>+</sup>/H<sup>+</sup> exchanger regulating factor NHERF2 markedly increases the activity of the renal outer medullary K<sup>+</sup> channel ROMK1. In the absence of NHERF2, SGK1 is unable to stimulate ROMK1 or ROMK2. The present observations further confirm the significant shift of the pH sensitivity of ROMK1 upon stimulation with SGK1.

According to the present results, the shift of the ROMK1 pH sensitivity following coexpression of SGK1 is dependent on the intact consensus sequence in the ROMK1 channel protein and does not require the presence of NHERF2. Introduction of a negative charge in form of aspartate mimicking the negative charge of phosphoserine leads to a similar shift of pH sensitivity of the ROMK1 channel. This observation is highly suggestive of the involvement of phosphorylation at serine44 in the shift of pH sensitivity. Earlier studies have identified several amino acid residues involved in the tuning of ROMK1 pH sensitivity (Fakler et al., 1996; Choe et al., 1997; McNicholas et al., 1998; Schulte et al., 1999). Lysine80 was first identified as the structural element necessary for pH-dependent gating. pH gating of ROMK1 is driven by titration of the lysine residue, i.e. protonation of the εNH<sub>2</sub> group is a prerequisite for channel inactivation. Later studies (Schulte et al., 1999) demonstrated that an Arg41-Lys80-Arg311 triad controls ROMK1 pH sensitivity. The positively charged arginines establish a local field repelling hydrogen ions from the amino group of the Lys residue. Thus, the introduction of a negative charge at the Ser44 neighboring the Arg41-Lys80-Arg311 triad may modulate pH gating.

Interestingly, the effect of SGK1 on pH sensitivity does not require the presence of NHERF2. Thus, it appears that NHERF2 is not required for phosphorylation of ROMK1 by SGK1. It should further be noted that introduction of aspartate

leads to a much more profound shift of the pH sensitivity than coexpression of SGK1 with or without NHERF2.

The present observations further indicate that replacement of serine44 by either alanine or aspartate has profound effects on the maximal activity. Serine44 is one of the three PKA phosphorylation sites present in ROMK1 (Yoo et al., 2003). All three sites must be phosphorylated for full channel function. While phosphorylation of the two COOH-terminal sites (serine219 and serine313) is required to maintain the channel in a high open probability state, serine44 seems to control ROMK1 channel abundance in the plasma membrane. The markedly different maximal activity of the three ROMK1 mutants ( $S^{44D}$ ROMK1 > wild type ROMK1 >  $S^{44A}$ ROMK1) supports the hypothesis that serine44 is important for the trafficking of ROMK1 to the cell membrane.

However, the effects of phosphorylation at serine44 on pH sensitivity and maximal current are not intimately linked but can be dissociated, pointing to additional factors in their regulation. Coexpression of  $S^{422D}$ SGK1 without NHERF2 does not significantly increase maximal channel activity even though it leads to a shift of pH sensitivity. Thus, under these experimental conditions, phosphorylation of serine44 is apparently not sufficient to enhance ROMK1 activity. Similarly, no (Chen et al., 1999; Yun et al., 2002b) or only moderate (Yoo et al., 2003) stimulation of ROMK1 has been observed earlier in the absence of NHERF2. In contrast, the maximal current of  $S^{44D}$ ROMK1 is markedly enhanced even in the absence of NHERF2. It should be kept in mind that the shift of pH sensitivity is significantly larger for  $S^{44D}$ ROMK1 than for coexpression of wild type ROMK1 with  $S^{422D}$ SGK1. Thus, the impact of aspartate appears to be larger than the impact of serine-phosphorylation, explaining why the mutation of serine44 has a significantly larger effect on maximal current than phosphorylation. The presence of NHERF2 appears to enhance the trafficking without influencing the phosphorylation. Moreover, the effect of NHERF2 does not require phosphorylation of ROMK1. On the other hand, it requires the presence of SGK1, since coexpression of NHERF2 alone does not significantly up-regulate ROMK1. Thus, the effect of SGK1 is not exclusively due to phosphorylation of ROMK1. In any case, SGK1 modifies

ROMK1 activity by at least two distinct mechanisms: a shift of the pH sensitivity dependent on the negative charge at serine44 and a stimulation of maximal current favoured by but not dependent on the negative charge at serine44.

The stimulating effect of SGK1 on the activity of the epithelial Na<sup>+</sup> channel ENaC (Chen et al., 1999; Wagner et al., 2001) is not sensitive to site directed modification of the SGK1 consensus sequence in the ENaC channel protein. Instead, it is mediated by phosphorylation and inhibition of the ubiquitin protein ligase Nedd4-2 (Debonneville et al., 2001; Snyder et al., 2002). Besides ENaC and ROMK1, several transporters and channels have been shown to be regulated by SGK1, including the K<sup>+</sup> channels KCNE1/KCNQ1 (Embark et al., 2002) and Kv1.3 (Gamper et al., 2002a, b; Wärntges et al., 2002), the voltage gated Na<sup>+</sup> channel SCN5A (Boehmer et al., 2003b), the Na<sup>+</sup>/H<sup>+</sup> exchanger NHE3 (Yun et al., 2002a), the glutamine transporter SN1 (Boehmer et al., 2003a) and the Na<sup>+</sup>,K<sup>+</sup>-ATPase (Henke et al., 2002; Setiawan et al., 2002). There is little doubt that additional transport proteins will be added in near future. For none of these channels or carriers, phosphorylation of the channel protein by SGK1 has been shown. The requirement for NHERF2 has hitherto only been shown for ROMK1 (Yun et al., 2002b) and NHE3 (Yun et al., 2002a). The present observations demonstrate that at least two distinct molecular mechanisms may participate in the SGK1 dependent regulation of one channel protein, i.e. alteration of the channel properties by direct phosphorylation of the channel protein and increase of channel protein abundance in the cell membrane facilitated by but not dependent on channel phosphorylation.

#### **4.1.3 Stimulation of ROMK1 requires PDZ domains of NHERF2**

The present experiments confirm the previous observations disclosing a stimulating effect of the serum and glucocorticoid inducible kinase SGK1 and the Na<sup>+</sup>/H<sup>+</sup> exchanger regulating factor NHERF2 on the renal outer medullary K<sup>+</sup> channel ROMK1. While SGK1 alone is unable to stimulate ROMK1 (Yun et al., 2002b) or ROMK2 (Chen et al., 1999), the kinase is a potent stimulator of ROMK1 in the presence of NHERF2.



As shown in this study, to be effective NHERF2 requires an intact second PDZ domain. NHERF2 is thought to link membrane proteins to cytoskeletal proteins such as ezrin and actin, an effect accomplished by PDZ domains (Yun et al., 1998; Takeda et al., 2001). The binding to the cytoskeleton may serve to target or stabilize the protein in the cell membrane. It further show the requirement for the PDZ binding motif at the COOH-terminus of ROMK1.

In contrast to regulation of ROMK1 by SGK1, the well described stimulating effect of SGK1 on the activity of the epithelial Na<sup>+</sup> channel ENaC (Chen et al., 1999; Náray-Fejes-Tóth et al., 1999; Shigaev et al., 2000; Alvarez de la Rosa et al., 1999; Boehmer et al., 2000; Lang et al., 2000; Wagner et al., 2001; Loffing et al., 2001b) does not require the presence of NHERF2 but is mediated by inhibition of the ubiquitin protein ligase Nedd4-2 (Debonneville et al., 2001; Snyder et al., 2002). The involvement of Nedd4-2 in the SGK1 dependent regulation of ENaC and of NHERF2 in the SGK1 dependent regulation of ROMK1 allow some dissociation of renal tubular Na<sup>+</sup> reabsorption and K<sup>+</sup> secretion. In principal cells, ROMK1 maintains the electrical driving force for apical Na<sup>+</sup> entry through ENaC and the depolarization of the apical membrane by Na<sup>+</sup> entry through ENaC drives K<sup>+</sup> secretion (Giebisch, 1998; Wang, 1999). Thus, mineralocorticoid stimulation of Na<sup>+</sup> reabsorption is in general paralleled by stimulation of K<sup>+</sup> secretion (Wright and Giebisch, 1992). However, maintenance of both, adequate extracellular fluid volume and equilibrated K<sup>+</sup> balance, can be achieved only, if the relation of Na<sup>+</sup> reabsorption and K<sup>+</sup> secretion is not fixed.

Finally, despite the fact that SGK1 is able to directly stimulate ROMK1 activity, it is safe to suggest that ROMK1 is stimulated by the concerted action of SGK1 and NHERF2 (Fig. 49). The stimulatory effect requires the second PDZ domain of NHERF2 and the PDZ binding motif of ROMK1.

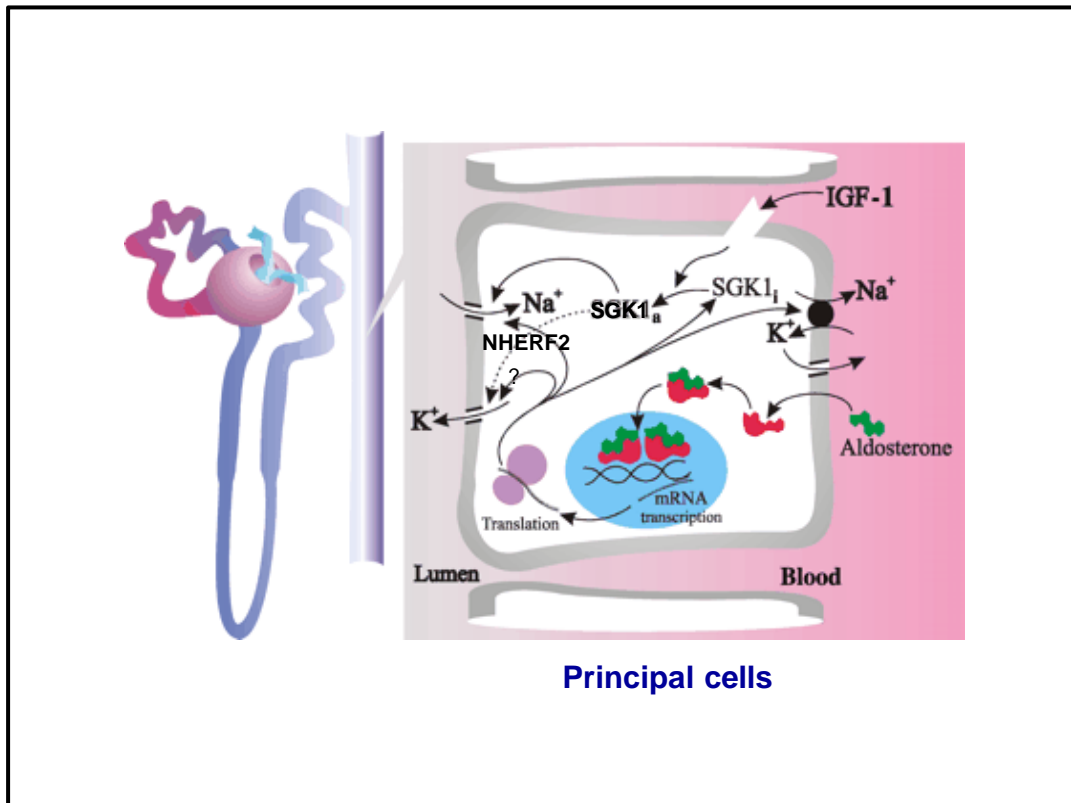


**Fig.49.** Role of SGK1 in the regulation of Na<sup>+</sup> reabsorption and K<sup>+</sup> secretion in principal cells of the collecting duct. Aldosterone stimulates the transcription and expression of SGK1. The inactive SGK1<sub>i</sub> requires activation to SGK1<sub>a</sub>, e.g. by insulin-like growth factor 1 (IGF-1). SGK1<sub>a</sub> then enhances the activity of the Na<sup>+</sup> channel ENaC and K<sup>+</sup> channel ROMK1 in the luminal cell membrane and of the Na<sup>+</sup>,K<sup>+</sup>-ATPase in the basolateral cell membrane. The regulation of ENaC is accomplished by inhibition of the ubiquitin ligase Nedd4-2, the regulation of ROMK1 requires the cooperation with the Na<sup>+</sup>/H<sup>+</sup> exchanger regulating factor NHERF2.

## 4.2 Regulation of $\text{Ca}^{2+}$ entry via TRPV5 by SGKs and NHERF2

The present observations clearly demonstrate that expression of TRPV5 induces  $\text{Ca}^{2+}$  influx allowing the cellular accumulation of  $\text{Ca}^{2+}$  and generating a  $\text{Ca}^{2+}$  current. In the presence of  $\text{Cl}^-$ ,  $\text{Ca}^{2+}$  entry through TRPV5 generates further currents (Hoenderop et al., 1999c) by activation of endogenous  $\text{Ca}^{2+}$  sensitive  $\text{Cl}^-$  channels (Callamaras and Parker, 2000). More importantly, the present observations disclose a completely novel mechanism regulating TRPV5 activity, i.e. the regulation by two members of the serum and glucocorticoid inducible kinase family and the NHE regulating factor NHERF2. The effect of SGK1 depends on an intact catalytic subunit as the inactive mutant  $\text{K127N}$ -SGK1 does not influence TRPV5 even in the presence of NHERF2. Thus, the kinases are obviously effective through phosphorylation of target proteins. The stimulating effect is shared by SGK1 and SGK3, but not by SGK2 or PKB. The TRPV5 stimulating capacity correlates with the ability of the two kinases to bind NHERF2 (Yun et al., 2002a). In contrast to SGK1 and SGK3, SGK2 does not bind NHERF2 (Yun et al., 2002a) and is, according to the present study, not able to stimulate TRPV5. PKB is similarly not able to stimulate TRPV5. A well known function of SGK1 is its participation in the regulation of the epithelial  $\text{Na}^+$  channel ENaC (Chen et al., 1999; Náray-Fejes-Tóth et al., 1999; Alvarez de la Rosa et al., 1999; Shigaev et al., 2000; Lang et al., 2000; Wagner et al., 2001). SGK1 is effective by increasing the abundance of the ENaC protein within the cell membrane (Alvarez de la Rosa et al., 1999; Loffing et al., 2001; Wagner et al., 2001). Most recently, SGK1 has been shown to up-regulate the voltage gated  $\text{K}^+$  channel Kv1.3 (Gamper et al., 2002a, b; Wärntges et al., 2002), the epithelial  $\text{Na}^+/\text{H}^+$  exchanger NHE3 (Yun et al., 2002) and the renal epithelial  $\text{K}^+$  channel ROMK1 (Yun et al., 2002b). Similar to SGK-dependent regulation of TRPV5, the regulation of ROMK1 by SGK1 has been shown to depend on NHERF2 (Yun et al., 2002b). The present study shows that the TRPV5 carboxy-tail interacts with NHERF2 and, to be effective, NHERF2 requires an intact second PDZ domain. Similar to ROMK1, the sequence of TRPV5 has a PDZ binding motif. In contrast to the regulation of TRPV5 and NHE3 and ROMK1, the regulation of ENaC or Kv1.3 does not require the participation of NHERF2.

SGK1 stimulates ENaC by phosphorylating the ubiquitin protein ligase Nedd4-2 in a PY motif-dependent manner (Debonneville et al., 2001; Snyder et al., 2002). The phosphorylation impedes the binding of Nedd4-2 to ENaC (Debonneville et al., 2001). The ENaC sequence does not include a PDZ binding motif, suggesting that NHERF2 can not directly interact with ENaC. As NHERF2 regulates both, TRPV5 and NHE3, it may participate in the link of TRPV5 activity and acid-base balance. TRPV5 displays an exquisite H<sup>+</sup> sensitivity (Hoenderop et al., 1999c; Akutsu et al., 2001; Hoenderop et al., 2002). Its activity is markedly reduced by lowering of the ambient pH. The sensitivity of renal tubular Ca<sup>2+</sup> transport to H<sup>+</sup> is of physiological significance, as on the one hand mineralization of bone depends on the deposition of Ca<sup>2+</sup> salts (Bushinsky and Krieger, 1992) and on the other precipitation of Ca<sup>2+</sup> phosphate salts is favoured by alkalinization of urine (Pak, 1992). Most recently, NHERF2 has been shown to direct the signaling of the PTH receptor (Mahon et al., 2002). Since PTH is a key regulator of TRPV5 (Hoenderop et al., 2002), this effect may similarly contribute to the regulation of TRPV5. However, according to the present observations, NHERF2 alone is unable to activate TRPV5 but requires the additional action of SGK1 or of one of its isoforms. SGK1 expression is highly variable, as it is up-regulated by glucocorticoids (Webster et al., 1993), aldosterone (Chen et al., 1999; Náray-Fejes-Tóth et al., 1999; Brennan and Fuller, 2000; Cowling and Birnboim, 2000; Shigaev et al., 2000), cell shrinkage (Waldegger et al., 1997) and a wide variety of additional factors (Lang and Cohen, 2001). Notably, SGK1 is under transcriptional control of 1,25(OH)2D3 (Akutsu et al., 2001). It is thus tempting to speculate that SGK1 participates in the regulation of TRPV5 by 1,25(OH)2D3 and PTH. Activation of SGK1 can be accomplished by insulin and IGF-1 through PI3-kinase and PDK1 (Kobayashi and Cohen, 1999b; Park et al., 1999). SGK1 integrates the signals coming from genomic regulators on the one hand and insulin or IGF-1 on the other (Wang et al., 2001). Thus, activation of SGK1 may contribute to the stimulating effect of both, 1,25(OH)2D3 and IGF-1 on intestinal Ca<sup>2+</sup> absorption (Bouillon, 1991).

Finally, TRPV5 is the target of a complex regulating mechanism involving both, the NHE regulating factor NHERF2 and the serum and glucocorticoid inducible kinase isoforms SGK1 and SGK3 (Fig. 50). The concerted action of NHERF2 and the kinases markedly up-regulates the activity of this key channel in the regulation of  $\text{Ca}^{2+}$  homeostasis.

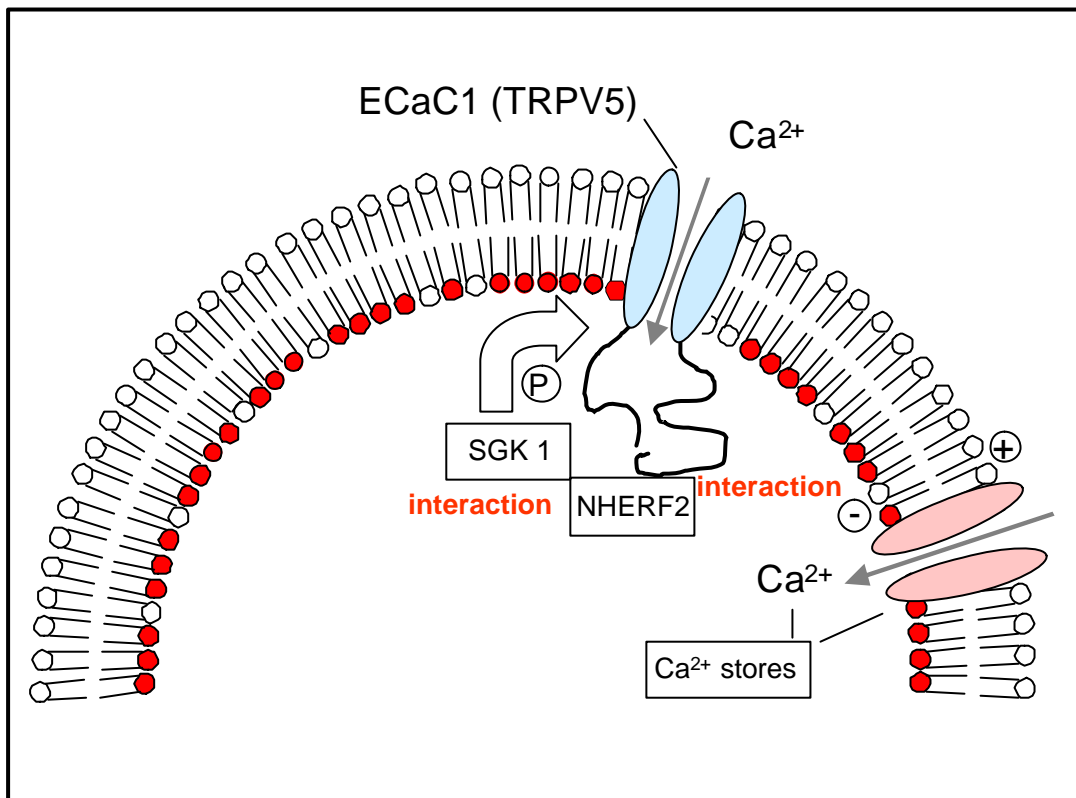


**Fig.50. Proposed transport model of ECaC1 (TRPV5) regulated by SGK1 and NHERF2.** The PDZ domains of NHERF2 interact with the carboxy-terminal of ECaC1 (TRPV5) as well as with the carboxy-terminal of SGK1. NHERF2 brings SGK1 into close proximity of ECaC1 (TRPV5) for phosphorylation and activation of channel activity.

### 4.3 Regulation of Cl<sup>-</sup> transport via CIC-Ka/barttin by SGKs and Nedd4-2

The present observations disclose a novel mechanism in the regulation of the renal epithelial Cl<sup>-</sup> channel composed of CIC-Ka and barttin. Similar to what has been shown for the epithelial Na<sup>+</sup> channel ENaC (Debonneville et al., 2001; Snyder et al., 2002), Nedd4-2 down-regulates CIC-Ka/barttin, an effect reversed by SGK1 and SGK3. Similar to ENaC (Debonneville et al., 2001; Snyder et al., 2002), barttin carries a PY motif (Estévez et al., 2001) which is important for its interaction with the ubiquitin ligase. As a matter of fact, elimination of the PY motif abolishes the down-regulation of CIC-Ka by Nedd4-2. The stimulatory effect of SGK1 and SGK3 on the CIC-Ka/barttin channel complex in the absence of coinjected Nedd4-2 cRNA could be explained by inhibition of an endogenous Nedd4-2. *Xenopus* oocytes do express low levels of both Nedd4-2 and SGK1 (Boehmer et al., 2003b) which presumably participate in the regulation not only of endogenous cell membrane proteins but as well of heterologously expressed channels and carriers.

An obvious requirement for the physiological significance of the observed regulation is the coexpression of the channels with Nedd4-2 and the kinases. SGK1 is expressed mainly in the collecting duct system (Loffing et al., 2001b) but may under pathophysiological conditions be expressed in further nephron segments such as thick ascending limb (Lang et al., 2000). Barttin is expressed throughout the distal nephron, i.e. medullary and cortical thick ascending limb, distal convoluted tubule, connecting tubule, cortical and medullary collecting duct (Waldegger et al., 2002). CIC-K1 and CIC-K2, the rat homologues of human CIC-Ka and CIC-Kb are similarly localized in all distal nephron segments (Waldegger et al., 2002).

As SGK1 is under transcriptional control of glucocorticoids (Webster et al., 1993; Brennan and Fuller, 2000) and mineralocorticoids (Chen et al., 1999; Náray-Fejes-Tóth et al., 1999; Cowling and Birnboim, 2000; Shigaev et al., 2000) and is activated by insulin and IGF-1 (Kobayashi and Cohen, 1999b), the present mechanism may well participate in the regulation of renal tubular Cl<sup>-</sup> transport by those hormones.

---

The functional significance of the regulation by SGK1 is reflected by the SGK1 knockout mouse (SGK1<sup>-/-</sup>). NaCl excretion by this mouse is normal under salt repletion and is decreased during salt deficient diet (Wulff et al., 2002). However, the adaptation following salt free diet is insufficient, i.e. the Na<sup>+</sup> and Cl<sup>-</sup> excretion remains significantly higher in the SGK1<sup>-/-</sup> mouse as compared to its wild-type littermate (SGK1<sup>+/+</sup>). As a result, in contrast to the SGK1<sup>+/+</sup> mouse, the SGK1<sup>-/-</sup> mouse suffers from weight loss, decline in blood pressure and decrease of renal glomerular filtration rate at low salt diet (Wulff et al., 2002). Those changes do occur despite a larger increase of plasma aldosterone concentration in the SGK1<sup>-/-</sup> mouse as compared to the SGK1<sup>+/+</sup> mouse (Wulff et al., 2002). The renal NaCl loss is at least partially due to insufficient up-regulation of ENaC in the cell membrane but according to the results of the present study may be paralleled by defective regulation of Cl<sup>-</sup> channels.

Finally, the present observations disclose a novel mechanism of Cl<sup>-</sup> channel regulation and a novel target for regulation by the ubiquitin ligase Nedd4-2 (Fig. 51) and the serum and glucocorticoid inducible kinase isoforms SGK1 and SGK3 (Fig. 52).

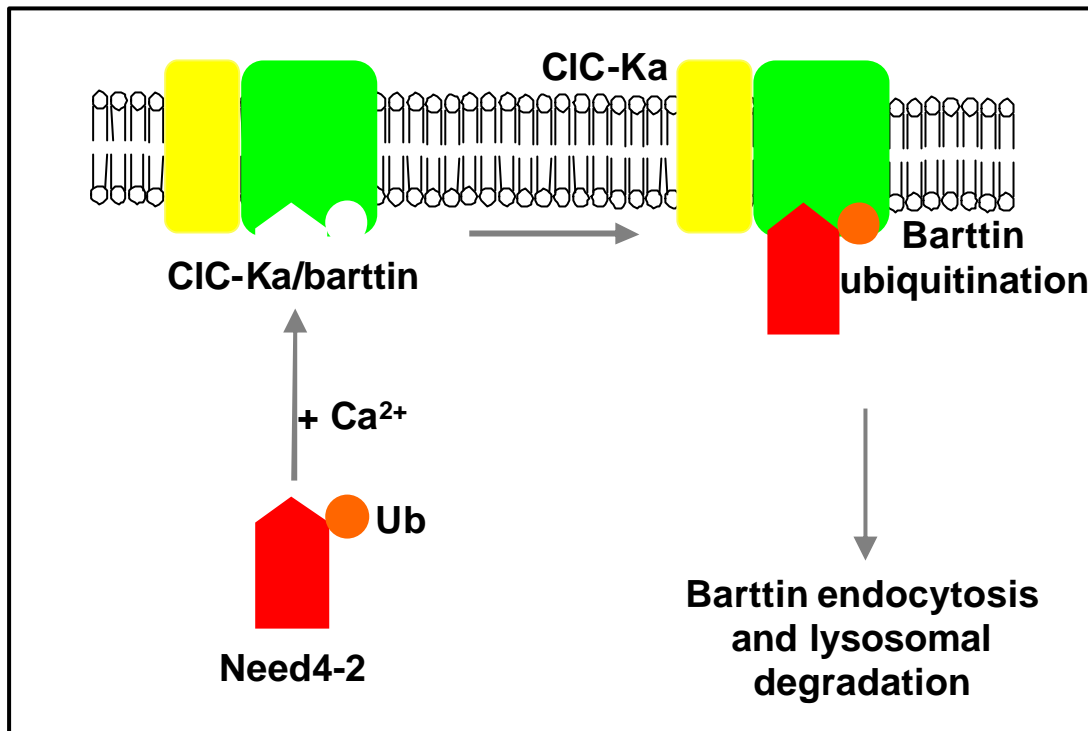


**Fig.51.** Proposed organization of proteins involved in the Nedd4-2-dependent regulation of CIC-Ka/barttin channels. Nedd4-2 is a cytosolic protein. Upon a rise in cytosolic  $[Ca^{2+}]$ , Nedd4-2 is mobilized to the apical membrane via its C2 domain. Once there, it binds the barttin-PY motif via its WW domains, allowing ubiquitination of the channel by Hect domain, which facilitates channel endocytosis and lysosomal degradation. Thus, Nedd4-2 is involved in regulating CIC-Ka/barttin stability at the cell surface.



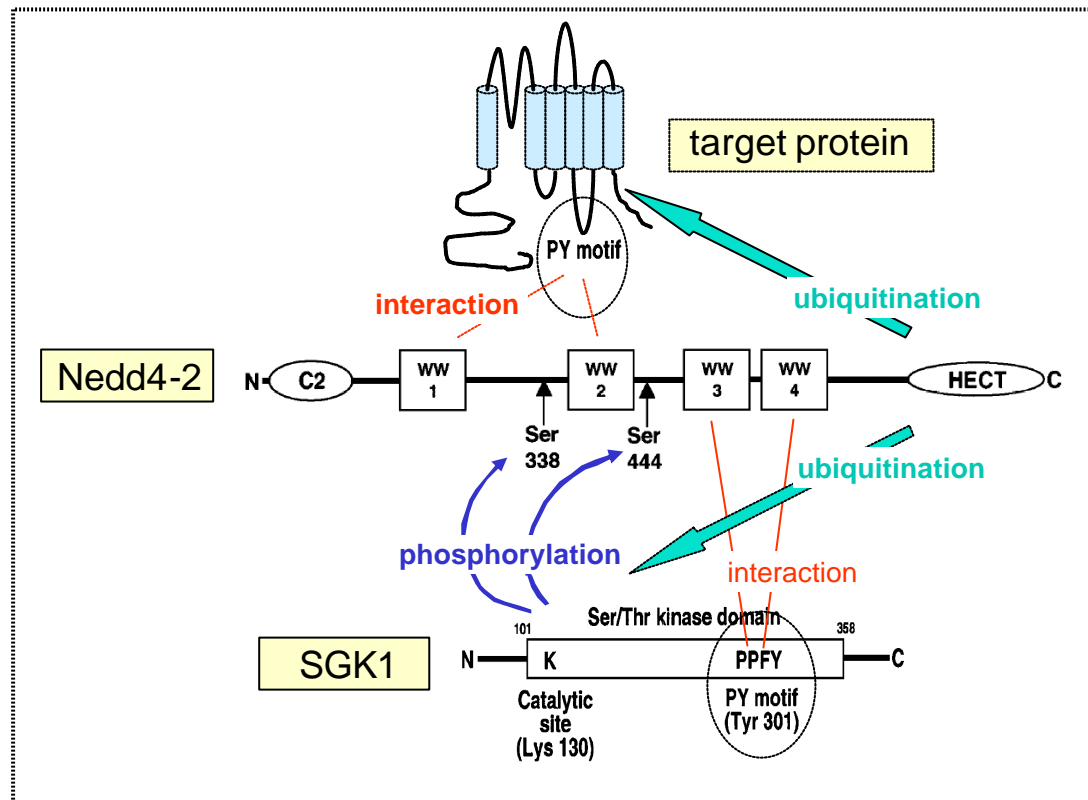


**Fig.52. SGK1 regulates Nedd4-2.** SGK1 binds via its PY motif to the WW domains of Nedd4-2. This interaction leads to the phosphorylation of serine444 and, to a lesser extent, serine338, which in turn reduces the affinity of Nedd4-2 towards target protein. Consequently, target protein becomes less ubiquitinated, leading to accumulation of target protein at the cell surface. This accumulation may be due to either increased insertion of protein at the cell surface or reduced internalization, or both.

### Summary

The Serum and Glucocorticoid induced protein Kinase (SGK) is a member of the serine/threonine protein kinase gene family and is activated by phosphorylation in response to signals that stimulate phosphatidylinositol 3-kinase (PI3-kinase). This process is mediated by 3-phosphoinositide-dependent protein kinase 1 (PDK1). Two additional isoforms of SGK have been identified, termed SGK2 and SGK3. SGK (1-3) are all strongly activated by phosphorylation in response to oxidative stress (e.g. H<sub>2</sub>O<sub>2</sub>) and insulin-like growth factor 1 (IGF-1). SGK1 RNA is induced in response to serum and/or glucocorticoids, aldosterone, high extracellular osmolarity and transforming growth factor beta (TGF-β).

The putative role of SGK1 and its isoforms in the regulation of renal ion channels implicated for potassium, calcium and chloride transport has been examined. In kidney, SGK1 transcript levels were excessively high in the distal tubule and collecting duct epithelial cells. SGK1 transcripts were also detected in thick ascending limb epithelial cells, when glucose concentrations are high.

NHERF2 and SGK1 interact to enhance ROMK1 activity in large part by enhancing the abundance of channel protein within the cell membrane. SGK1 interacts with NHERF2 through the second PDZ domain of NHERF2. Deletion of the second PDZ domain or of the putative PDZ binding motif on ROMK1 abolishes channel stimulation. This interaction allows the integration of genomic regulation and activation of SGK1 and NHERF2 in the control of ROMK1 activity and renal K<sup>+</sup> excretion. Phosphorylation by SGK1 or introduction of negative charge at serine44 shifts the pH sensitivity of the channel and contributes to the stimulation of maximal channel activity by the kinase.

Furthermore, the effect of serum and glucocorticoid induced kinase (SGK) isoforms and NHE3 regulating factor 2 (NHERF2) on epithelial calcium channel ECaC1 (TRPV5) has also been examined. Since coexpression of SGK1 or SGK3 and NHERF2 leads to stimulation of ECaC1 determined by measurement of Ca<sup>2+</sup> dependent chloride current as well as radioactively labelled Ca<sup>2+</sup> uptake, SGK2 and protein kinase B (PKB) failed to enhance ECaC1 irrespective of

NHERF2. Since the stimulating effect of SGK1 and NHERF2 on ECaC1 is abolished by ruthenium red and absent in the presence of ionomycin, it can be concluded that ECaC1 is stimulated in a direct way. Interaction of SGK1 and NHERF2 is then extensively studied by generating constitutively active <sup>S422D</sup>SGK1, and the inactive form <sup>K127N</sup>SGK1. <sup>S422D</sup>SGK1 but not <sup>K127N</sup>SGK1 can mimic the stimulating effect of wild type SGK1 co-injected with NHERF2. The kinase inhibitor chelerythrine (10  $\mu$ M) inhibits ECaC1 activity.

Moreover, pull-down assay shows the interaction of the carboxy-tail of ECaC1 and NHERF2 whereas functional experiments show the abolishment of the stimulatory effect of SGK1 and NHERF2 whose second PSD 95/*Drosophila* disk large/ZO-1 (PDZ) domain has been deleted. It is thus concluded, that SGK1 stimulates ECaC1 by interaction with the second PDZ domain of NHERF2. NHERF2 then binds to the carboxy-tail of ECaC1 rendering a stabilization of ECaC1 by mediating interaction with actin cytoskeleton via ezrin.

Finally, the effect of serum and glucocorticoid induced kinase (SGK) isoforms and ubiquitin ligase Nedd4-2 on renal epithelial Cl<sup>-</sup> channel (ClC-Ka/barttin) has also been studied. Expression of ClC-Ka/barttin induces a slightly inwardly rectifying current which is significantly decreased upon coexpression of Nedd4-2. The coexpression of <sup>S422D</sup>SGK1, SGK1 or SGK3, but not of SGK2 or <sup>K127N</sup>SGK1 significantly stimulated the current and reversed the effect of Nedd4-2. The down-regulation of ClC-Ka/barttin is abolished by elimination of the PY motif in ClC-Ka/<sup>Y98A</sup>barttin. The present observations disclose a novel mechanism regulating ClC-Ka which presumably participates in the regulation of transport in kidney and inner ear.

### **Zusammenfassung**

Die Serum und Glucocorticoid-abhängige Protein-Kinase (SGK) ist eine Serin/Threonin-Proteinkinase, die über eine Signalkaskade via Phosphatidylinositide 3-Kinase (PI3-kinase) und 3-Phosphoinositid-abhängige Proteinkinase 1 (PDK1) phosphoryliert und damit aktiviert wird. Auf gleichem Wege werden die später entdeckten Isoformen der SGK, die SGK2 und SGK3 aktiviert. Über den genannten Signalweg stimuliert insulin-like growth factor 1 (IGF-1) die drei Kinasen. Darüberhinaus werden sie durch oxidativen Stress aktiviert. Die Transkription der SGK1, nicht aber der SGK2 und SGK3, wird durch Serum, Glucocorticoide, Aldosteron, hohe extrazelluläre Osmolarität und transforming growth factor beta (TGF- $\beta$ ) gesteigert.

Die mutmaßliche Rolle der SGK1 und seiner Isoformen SGK2 und SGK3 in der Regulation renaler Ionenkanäle, die für Kalium-, Kalzium- und Chloridtransport verantwortlich sind, ist untersucht worden. In der Niere ist das SGK1 Expressionsniveau in Epithelzellen des distalen Tubulus und des Sammelrohrs sehr hoch. Bei hohen Glukosekonzentrationen werden SGK1 Transkripte auch im aufsteigenden Ast der Henle-Schleife nachgewiesen.

NHERF2 und SGK1 interagieren miteinander und steigern damit die ROMK1 Aktivität, indem sie vor allem die Anzahl der Ionenkanäle in der Zellmembran erhöhen. Dabei interagiert SGK1 mit NHERF2 über dessen zweite PDZ Domäne. Eine Deletion der zweiten PDZ Domäne oder der vermeintlichen PDZ Bindungsstelle im ROMK1 Protein verhindert die Kanalstimulation. Diese Interaktion erlaubt die Integration genomischer Regulation und Aktivierung durch SGK1 und NHERF bei der Kontrolle der ROMK1 Aktivität und der renalen Kaliumausscheidung.

Ferner wurde die Wirkung von Serum und Glucocorticoid induzierten Kinase (SGK) Isoformen und NHE3 Regulating Factor 2 (NHERF2) auf den epithelialen Kalcium Kanal (ECaC1) untersucht. Während SGK1 und SGK3 und NHERF2 eine ECaC1 Stimulierung, die durch den  $\text{Ca}^{2+}$ -abhängigen Chloridstrom sowie die radioaktiv markiertes  $\text{Ca}^{2+}$  Aufnahme bestimmt wird, zeigen, haben SGK2 und Protein kinase B (PKB) unabhängig von NHERF2 keinen solchen Effekt.

Die konstitutiv aktive Form <sup>S422D</sup>SGK1 und die inaktive <sup>K127N</sup>SGK1 wurden hergestellt. <sup>S422D</sup>SGK1 aber nicht <sup>K127N</sup>SGK1 zusammen mit NHERF2 verfügt immer noch über die Stimulationswirkung auf ECaC1. Der Kinase-hemmer Chelerythrin (10 µM) inhibiert die Aktivität von ECaC1.

Pull-down Assays zeigen die Interaktion vom Carboxy-Ende des ECaC1 mit NHERF2, während funktionelle Experimente die Herabsetzung der Stimulationswirkung von SGK1 und einer NHERF2 mit deletierter zweiter PDZ Domäne zeigen. Die Schlussfolgerung ist, dass SGK1 ECaC1 durch Interaktion mit dem zweiten PDZ Domain von NHERF2 stimuliert. NHERF2 bindet an das Carboxy-Ende Tail von ECaC1, welches ECaC1 dadurch mit dem Aktin Zytoskellet stabilisiert.

Letztendlich wurde zudem der Effekt der SGK Isoformen und der Ubiquitin Ligase Nedd4-2 auf den renalen, epithelialen Chloridkanal (ClC-Ka/barttin) untersucht. Expression von ClC-Ka/barttin verursacht einen schwach einwärts gleichrichtenden Strom, der signifikant durch die Koexpression von Nedd4-2 herabgesetzt wird. Die Koexpression von <sup>S422D</sup>SGK1, SGK1 oder SGK3, aber nicht die Koexpression von SGK2 oder <sup>K127N</sup>SGK1, stimulierte den Strom signifikant beziehungsweise hob teilweise den Effekt von Nedd4-2 auf. Die Herunterregulation von ClC-Ka/<sup>Y98A</sup>barttin wird durch die Elimination des PY Motifs im ClC-Ka/<sup>Y98A</sup>barttin aufgehoben. Die vorliegenden Beobachtungen legen einen neuen Regulationsmechanismus für ClC-Ka offen, der höchstwahrscheinlich in der Transportregulation in der Niere und im Innenohr beteiligt ist.

---

## References

- Abriel, H.**, Loffing, J., Rebhun, J. F., Pratt, J. H., Schild, L., Horisberger, J. D., Rotin, D. and Staub, O. (1999)  
Defective regulation of the epithelial Na<sup>+</sup> channel by Nedd4 in Liddle's syndrome. *J. Clin. Invest.* 103, 667-673
- Adachi, S.**, Uchida, S., Ito, H., Hata, M., Hiroe, M., Marumo, F. and Sasaki, S. (1994)  
Two isoforms of a chloride channel predominantly expressed in thick ascending limb of Henle's loop and collecting ducts of rat kidney. *J. Biol. Chem.* 269, 17677-17683
- Akizuki, N.**, Uchida, S., Sasaki, S. and Marumo, F. (2001)  
Impaired solute accumulation in inner medulla of *Clcnk1*<sup>-/-</sup> mice kidney. *Am. J. Physiol.* 280, F79-F87
- Akutsu, N.**, Lin, R., Bastien, Y., Bestawros, A., Enepekides, D. J., Black, M. J. and White, J. H. (2001)  
Regulation of gene expression by 1 $\alpha$ ,25-dihydroxyvitamin D3 and its analogue EB1089 under growth-inhibitory conditions in squamous carcinoma cells. *Mol. Endocrinol.* 15, 1127-1139
- Alessi, D. R.**, Andjelkovic, M., Caudwell, B., Cron, P., Morrice, N., Cohen, P. and Hemmings, B. A. (1996)  
Mechanism of activation of protein kinase B by insulin and IGF-1. *EMBO J.* 15, 6541-6551
- Ali, S.**, Chen, X., Lu, M., Xu, J. Z., Lerea, K. M., Hebert, S. C. and Wang, W. H. (1998)  
The A kinase anchoring protein is required for mediating the effect of protein kinase A on ROMK1 channels. *Proc. Natl. Acad. Sci. USA* 95, 10274-10278
- Alvarez de la Rosa, D. A.**, Zhang, P., Náray-Fejes-Tóth, A., Fejes-Tóth, G. and Canessa, C. M. (1999)  
The serum and glucocorticoid kinase *sgk* increases the abundance of epithelial sodium channels in the plasma membrane of *Xenopus* oocytes. *J. Biol. Chem.* 274, 37834-37839
- Ando, M.** and Takeuchi, S. (2000)  
mRNA encoding CIC-K1, a kidney Cl<sup>-</sup> channel is expressed in marginal cells of the *stria vascularis* of rat cochlea: its possible contribution to Cl<sup>-</sup> currents. *Neurosci. Lett.* 284, 171-174
- Barley, N. F.**, Howard, A., O'Callaghan, D., Legon, S. and Walters, J. R. (2001)  
Epithelial calcium transporter expression in human duodenum. *Am. J. Physiol.* 280, G285-G290
- Barthel, A.**, Kohn, A. D., Luo, Y. and Roth, R. A. (1997)  
A constitutively active version of the Ser/Thr kinase Akt induces production of the *ob* gene product, leptin, in 3T3-L1 adipocytes. *Endocrinology* 138, 3559-3562

- Barthel, A.**, Okino, S. T., Liao, J., Nakatani, K., Li, J., Whitlock, J. P., Jr. and Roth, R. A. (1999)  
Regulation of GLUT1 gene transcription by the serine/threonine kinase Akt1. *J. Biol. Chem.* 274, 20281-20286
- Bartter, F. C.**, Pronove, P., Gill, J. R., Jr. and MacCardle, R. C. (1962)  
Hyperplasia of the juxtaglomerular complex with hyperaldosteronism and hypokalemic alkalosis. *Am. J. Med.* 33, 811-828
- Bartter, F. C.**, Pronove, P., Gill, J. R., Jr. and MacCardle, R. C. (1968)  
Hyperplasia of the juxtaglomerular complex with hyperaldosteronism and hypokalemic alkalosis. A new syndrome. 1962. *J. Am. Soc. Nephrol.* 9, 516-528
- Baukowitz, T.**, Tucker, S. J., Schulte, U., Benndorf, K., Ruppersberg, J. P. and Fakler, B. (1999)  
Inward rectification in  $K_{ATP}$  channels: a pH switch in the pore. *EMBO J.* 18, 847-853
- Baumgartner, W.**, Islas, L. and Sigworth, F. J. (1999)  
Two-microelectrode voltage clamp of *Xenopus* oocytes: voltage errors and compensation for local current flow. *Biophys. J.* 77, 1980-1991
- Beesley, A. H.**, Ortega, B. and White, S. J. (1999)  
Splicing of a retained intron within ROMK  $K^+$  channel RNA generates a novel set of isoforms in rat kidney. *Am. J. Physiol.* 276, C585-C592
- Ben Efraim, I.** and Shai, Y. (1996)  
Secondary structure, membrane localization, and coassembly within phospholipid membranes of synthetic segments derived from the N- and C-termini regions of the ROMK1  $K^+$  channel. *Protein Sci.* 5, 2287-2297
- Ben Efraim, I.** and Shai, Y. (1997)  
The structure and organization of synthetic putative membranous segments of ROMK1 channel in phospholipid membranes. *Biophys. J.* 72, 85-96
- Bernardo, A. A.**, Kear, F. T., Santos, A. V. P., Ma, J., Steplock, D., Robey, R. B. and Weinman, E. J. (1999)  
Basolateral  $Na^+/HCO_3^-$  cotransport activity is regulated by the dissociable  $Na^+/H^+$  exchanger regulatory factor. *J. Clin. Invest.* 104, 195-201
- Biber, J.** (2001)  
Emerging roles of transporter-PDZ complexes in renal proximal tubular reabsorption. *Pflügers Arch.* 443, 3-5
- Bindels, R. J. M.**, Hartog, A., Timmermans, J. A. H. and van Os, C. H. (1991)  
Active  $Ca^{2+}$  transport in primary cultures of rabbit kidney CCD: stimulation by 1, 25-dihydroxyvitamin  $D_3$  and PTH. *Am. J. Physiol.* 261, F799-F807
- Birkenhäger, R.**, Otto, E., Schurmann, M. J., Vollmer, M., Ruf, E. M., Maier-Lutz, I., Beekmann, F., Fekete, A., Omran, H., Feldmann, D., Milford, D. V., Jeck, N., Konrad, M., Landau, D., Knoers, N. V., Antignac, C., Sudbrak, R., Kispert, A. and Hildebrandt, F. (2001)  
Mutation of BSND causes Bartter syndrome with sensorineural deafness and kidney failure. *Nat. Genet.* 29, 310-314

- Birnbaumer, L.**, Zhu, X., Jiang, M., Boulay, G., Peyton, M., Vannier, B., Brown, D., Platano, D., Sadeghi, H., Stefani, E. and Birnbaumer, M. (1996)  
On the molecular basis and regulation of cellular capacitative calcium entry: roles of Trp proteins. *Proc. Natl. Acad. Sci. USA* 93, 15195-15202
- Bleich, M.**, Schlatter, E. and Greger, R. (1990)  
The luminal K<sup>+</sup> channel of the thick ascending limb of Henle's loop. *Pflügers Arch.* 415, 449-460
- Boehmer, C.**, Wagner, C. A., Beck, S., Moschen, I., Melzig, J., Werner, A., Lin, J. T., Lang, F. and Wehner, F. (2000)  
The shrinkage-activated Na<sup>+</sup> conductance of rat hepatocytes and its possible correlation to rENaC. *Cell. Physiol. Biochem.* 10, 187-194
- Boehmer, C.**, Okur, F., Setiawan, I., Broer, S. and Lang, F. (2003a)  
Properties and regulation of glutamine transporter SN1 by protein kinases SGK and PKB. *Biochem. Biophys. Res. Commun.* 306, 156-162
- Boehmer, C.**, Wilhelm, V., Palmada, M., Wallisch, S., Henke, G., Brinkmeier, H., Cohen, P., Pieske, B. and Lang, F. (2003b)  
Serum and glucocorticoid inducible kinases in the regulation of the cardiac sodium channel SCN5A. *Cardiovasc. Res.* 57, 1079-1084
- Boim, M. A.**, Ho, K., Shuck, M. E., Bienkowski, M. J., Block, J. H., Slightom, J. L., Yang, Y., Brenner, B. M. and Hebert, S. C. (1995)  
ROMK inwardly rectifying ATP-sensitive K<sup>+</sup> channel. II. Cloning and distribution of alternative forms. *Am. J. Physiol.* 268, F1132-F1140
- Bouillon, R.** (1991)  
Growth hormone and bone. *Horm. Res.* 36, 49-55
- Brandt, S.** and Jentsch, T. J. (1995)  
ClC-6 and ClC-7 are two novel broadly expressed members of the ClC chloride channel family. *FEBS Lett.* 377, 15-20
- Brennan, F. E.** and Fuller, P. J. (2000)  
Rapid up-regulation of serum and glucocorticoid regulated kinase (sgk) gene expression by corticosteroids *in vivo*. *Mol. Cell. Endocrinol.* 166, 129-136
- Breton, S.**, Wiederhold, T., Marshansky, V., Nsumu, N. N., Ramesh, V. and Brown, D. (2000)  
The B1 subunit of the H<sup>+</sup>-ATPase is a PDZ-domain binding protein: colocalization with NHE-RF in renal Bintercalated cells. *J. Biol. Chem.* 275, 18219-18224
- Bushinsky, D. A.** and Krieger, N. S. (1992)  
Role of the skeleton in calcium homeostasis, In: Seldin, W., Giebisch, G.: *The Kidney*; Raven Press, New York, pp. 2395-2430
- Busjahn, A.**, Aydin, A., Uhlman, R., Krasko, C., Bähring, S., Szelestei, T., Feng, Y., Dahm, S., Sharma, A. M., Luft, F. C. and Lang, F. (2002)  
Serum and glucocorticoid regulated kinase (SGK1) gene and blood pressure. *Hypertension.* 40, 256-260



- Callamaras, N.** and Parker, I. (2000)  
Ca<sup>2+</sup>-dependent activation of Cl<sup>-</sup> currents in *Xenopus* oocytes is modulated by voltage. *Am. J. Physiol.* 278, C667-C675
- Capco, D. G.** and Jeffery, W. R. (1982)  
Transient localizations of messenger RNA in *Xenopus laevis* oocytes. *Dev. Biol.* 89, 1-12
- Cassola, A. C.,** Giebisch, G. and Wang, W. (1993)  
Vasopressin increases density of apical low-conductance K<sup>+</sup> channels in rat CCD. *Am. J. Physiol.* 264, F502-F509
- Castrop, H.,** Kramer, B. K., Riegger, G. A., Kurtz, A. and Wolf, K. (2000)  
Overexpression of chloride channel ClC-K2 mRNA in the renal medulla of Dahl salt-sensitive rats. *J. Hypertens.* 18, 1289-1295
- Caterina, M. J.,** Rosen, T. A., Tominaga, M., Brake, A. J. and Julius, D. (1999)  
A capsaicin receptor homologue with a high threshold for noxious heat. *Nature* 398, 436-441
- Chen, H.,** Ross, C. A., Wang, N., Huo, Y., Mackinnon, D. F., Potash, J. B., Simpson, S. G., McMahon, F. J., DePaulo, J. R., Jr. and McInnis, M. G. (2001)  
NEDD4L on human chromosome 18q21 has multiple forms of transcripts and is a homologue of the mouse Nedd4-2 gene. *Eur. J. Hum. Genet.* 9, 922-930
- Chen, H. I.** and Sudol, M. (1995)  
The WW domain of Yes-associated protein binds a proline-rich ligand that differs from the consensus established for Src homology 3-binding modules. *Proc. Natl. Acad. Sci. USA* 92, 7819-7823
- Chen, S. Y.,** Bhargava, A., Mastroberardino, L., Meijer, O. C., Wang, J., Buse, P., Firestone, G. L., Verrey, F. and Pearce, D. (1999)  
Epithelial sodium channel regulated by aldosterone-induced protein SGK. *Proc. Natl. Acad. Sci. USA* 96, 2514-2519
- Christakos, S.,** Gabrielides, C. and Rhoton, W. B. (1989)  
Vitamin D-dependent calcium binding proteins: chemistry, distribution, functional considerations, and molecular biology. *Endocr. Rev.* 10, 3-26
- Choe, H.,** Zhou, H., Palmer, L. G. and Sackin, H. (1997)  
A conserved cytoplasmic region of ROMK modulates pH sensitivity, conductance, and gating. *Am. J. Physiol.* 273, F516-F529
- Coffer, P. J.** and Woodgett, J. R. (1991)  
Molecular cloning and characterization of a novel putative protein serine kinase related to the cAMP-dependent and protein kinase C families. *Eur. J. Biochem.* 201, 475-481
- Cowling, R. T.** and Birnboim, H. C. (2000)  
Expression of serum and glucocorticoid regulated kinase (SGK) mRNA is up-regulated by GM-CSF and other proinflammatory mediators in human granulocytes. *J. Leucoc. Biol.* 67, 240-248

**Dascal, N.** (1987)

The use of *Xenopus* oocytes for the study of ion channels. CRC Crit. Rev. Biochem. 22, 317-386

**Debonneville, C.**, Flores, S. Y., Kamynina, E., Plant, P. J., Tauxe, C., Thomas, M. A., Munster, C., Chraïbi, A., Pratt, J. H., Horisberger, J. D., Pearce, D., Loffing, J. and Staub, O. (2001)

Phosphorylation of Nedd4-2 by SGK1 regulates epithelial Na<sup>+</sup> channel cell surface expression. EMBO J. 20, 7052-7059

**Delcommenne, M.**, Tan, C., Gray, V., Rue, L., Woodgett, J. and Dedhar, S. (1998)

Phosphoinositide-3-OH kinase-dependent regulation of glycogen synthase kinase 3 and protein kinase B/AKT by the integrin-linked kinase. Proc. Natl. Acad. Sci. USA 95, 11211-11216

**Dinudom, A.**, Harvey, K. F., Komwatana, P., Young, J. A., Kumar, S. and Cook, D. I. (1998)

Nedd4 mediates control of an epithelial Na<sup>+</sup> channel in salivary duct cells by cytosolic Na<sup>+</sup>. Proc. Natl. Acad. Sci. USA 95, 7169-7173

**Doi, T.**, Fakler, B., Schultz, J. H., Schulte, U., Brandle, U., Weidemann, S., Zenner, H. P., Lang, F. and Ruppertsberg, J. P. (1996)

Extracellular K<sup>+</sup> and intracellular pH allosterically regulate renal K<sub>ir</sub>1.1 channels. J. Biol. Chem. 271, 17261-17266

**Doupnik, C. A.**, Davidson, N. and Lester, H. A. (1995)

The inward rectifier potassium channel family. Curr. Opin. Neurobiol. 5, 268-277

**Dumont, J. N.** (1972)

Oogenesis in *Xenopus laevis* (Daudin). I. Stages of oocytes development in laboratory maintained animals. J. Morphol. 136, 153-157

**Embark, H. M.**, Boehmer, C., Vallon, V., Luft, F. and Lang, F. (2003)

Regulation of KCNE1-dependent K<sup>+</sup> current by the serum and glucocorticoid inducible kinase (SGK) isoforms. Pflügers Arch. 445, 601-606

**Estévez, R.**, Boettger, T., Stein, V., Birkenhager, R., Otto, E., Hildebrandt, F. and Jentsch, T. J. (2001)

Barttin is a Cl<sup>-</sup> channel beta-subunit crucial for renal Cl<sup>-</sup> reabsorption and inner ear K<sup>+</sup> secretion. Nature 414, 558-561

**Fahlke, C.**, Yu, H. T., Beck, C. L., Rhodes, T. H. and George, A. L., Jr. (1997)

Pore-forming segments in voltage-gated chloride channels. Nature 390, 529-532

**Fakler, B.**, Schultz, J. H., Yang, J., Schulte, U., Brandle, U., Zenner, H. P., Jan, L. Y. and Ruppertsberg, J. P. (1996)

Identification of a titratable lysine residue that determines sensitivity of kidney potassium channels (ROMK) to intracellular pH. EMBO J. 15, 4093-4099

- Fanconi, A.**, Schachenmann, G., Nüssli, R. and Prader, A. (1971)  
Chronic hypokalaemia with growth retardation, normotensive hyperrenin-hyperaldosteronism ("Bartter's syndrome"), and hypercalciuria. Report of two cases with emphasis on natural history and on catch-up growth during treatment. *Helv. Paed. Acta* 2, 144-163
- Fanning, A. S.** and Anderson, J. M. (1996)  
Protein-protein interactions: PDZ domain networks. *Curr. Biol.* 6, 1385-1388
- Fanning, A. S.** and Anderson, J. M. (1998)  
PDZ domains and the formation of protein networks at the plasma membrane. *Curr. Top. Microbiol. Immunol.* 228, 209-233
- Feldmann, D.**, Alessandri, J. L. and Deschenes, G. (1998)  
Large deletion of the 5' end of the ROMK1 gene causes antenatal Bartter syndrome. *J. Am. Soc. Nephrol.* 9, 2357-2359
- Fillon, S.**, Klingel, K., Warntges, S., Sauter, M., Gabrysch, S., Pestel, S., Tanneur, V., Waldegger, S., Zipfel, A., Viebahn, R., Haussinger, D., Broer, S., Kandolf, R. and Lang, F. (2002)  
Expression of the serine/threonine kinase hSGK1 in chronic viral hepatitis. *Cell. Physiol. Biochem.* 12, 47-54
- Flagg, T. P.**, Yoo, D., Sciortino, C. M., Tate, M., Romero, M. F. and Welling, P. A. (2002)  
Molecular mechanism of a COOH-terminal gating determinant in the ROMK channel revealed by a Bartter's disease mutation. *J. Physiol.* 544, 351-362
- Friedman, P. A.** and Gesek, F. A. (1995)  
Cellular calcium transport in renal epithelia: measurements, mechanisms, and regulation. *Physiol. Rev.* 75, 429-471
- Friedman, P. A.** (1998)  
Codependence of renal calcium and sodium transport. *Annu. Rev. Physiol.* 60, 179-197
- Frindt, G.** and Palmer, L. G. (1989)  
Low-conductance K<sup>+</sup> channels in apical membrane of rat cortical collecting tubule. *Am. J. Physiol.* 256, F143-F151
- Gallazzini, M.**, Attmane-Elakeb, A., Mount, D. B., Hebert, S. C. and Bichara, M. (2003)  
Regulation by glucocorticoids and osmolality of expression of ROMK (K<sub>r</sub>1.1), the apical K channel of thick ascending limb. *Am. J. Physiol.* 284, F977-F986
- Gamper, N.**, Fillon, S., Melzig, J., Cohen, P., Huber, S. M. and Lang, F. (2002a)  
IGF-1 up-regulates K<sup>+</sup> channels via PI3-kinase, PDK1 and SGK1. *Pflügers Arch.* 443, 625-634
- Gamper, N.**, Fillon, S., Feng, Y., Friedrich, B., Lang, P. A., Henke, G., Huber, S. M., Kobayashi, T., Cohen, P. and Lang, F. (2002b)  
K<sup>+</sup> channel activation by all three isoforms of serum and glucocorticoid dependent protein kinase SGK. *Pflügers Arch.* 445, 60-66

**Giebisch, G.** (1998)

Renal potassium transport: mechanisms and regulation. *Am. J. Physiol.* 274, F817-F833

**Gitelman, H. J.**, Graham, J. B. and Welt, L. G. (1966)

A new familial disorder characterized by hypokalemia and hypomagnesemia. *Trans. Assoc. Am. Physiol.* 79, 221-235

**Gordon, R. D.**, Stowasse M., Tunny T. J., Klemm S. A. and Rutherford J. C. (1994)

High incidence of primary aldosteronism in 199 patients referred with hypertension. *Clin. Exp. Pharmacol. Physiol.* 21, 315-318

**Goulet, C. C.**, Volk, K. A., Adams, C. M., Prince, L. S., Stokes, J. B. and Snyder, P. M. (1998)

Inhibition of the epithelial  $\text{Na}^+$  channel by interaction of Nedd4 with a PY motif deleted in Liddle's syndrome. *J. Biol. Chem.* 273, 30012-30017

**Grabner, M.** and Pastoriza-Munoz, E. (1993)

Regulation of cell pH by  $\text{K}^+/\text{H}^+$  antiport in renal epithelial cells. *Am. J. Physiol.* 265, F773-F783

**Gründer, S.**, Thiemann, A., Pusch, M. and Jentsch, T. J. (1992)

Regions involved in the opening of CIC-2 chloride channel by voltage and cell volume. *Nature* 360, 759-762

**Gurdon, J. B.**, Lane, C. D., Woodland, H. R. and Mairbax, G. (1971)

Use of frog eggs and oocytes for the study of messenger RNA and its translation in living cells. *Nature* 233, 177-182

**Hall, R. A.**, Ostedgaard, L. S., Premont, R. T., Blitzer, J. T., Rahman, N., Welsch, M. J. and Lefkowitz, R. J. (1998a)

A C-terminal motif found in the  $\beta_2$ -adrenergic receptor, P2Y<sub>1</sub> receptor and cystic fibrosis transmembrane conductance regulator determines binding to the  $\text{Na}^+/\text{H}^+$  exchanger regulatory factor family of PDZ proteins. *Proc. Natl. Acad. Sci. USA* 95, 8496-8501

**Hajdich, E.**, Alessi, D. R., Hemmings, B. A. and Hundal, H. S. (1998)

Constitutive activation of protein kinase B  $\alpha$  by membrane targeting promotes glucose and system A amino acid transport, protein synthesis, and inactivation of glycogen synthase kinase 3 in L6 muscle cells. *Diabetes* 47, 1006-1013

**Hall, R. A.**, Premont, R. T., Chow, C. W., Blitzer, J. T., Pitcher, J. A., Claing, A., Stoffel, R. H., Barak, L. S., Shenolikar, S., Weinman, E. J., Grinstein, S. and Lefkowitz, R. J. (1998b)

The  $\beta_2$ -adrenergic receptor interacts with the  $\text{Na}^+/\text{H}^+$  exchanger regulatory factor to control Na/H exchange. *Nature* 392, 626-630

- Hall, R. A.**, Spurney, R. F., Premont, R. T., Rahman, N., Blitzer, J. T., Pitcher, J. A. and Lefkowitz, R. J. (1999)  
G protein-coupled receptor kinase 6A phosphorylates the Na<sup>+</sup>/H<sup>+</sup> exchanger regulatory factor via a PDZ-domain-mediated-interaction. *J. Biol. Chem.* 274, 24328-24334
- Hamill, O. P.**, Marty, A., Neher, E., Sakmann, B. and Sigworth, F. J. (1981)  
Improved patch-clamp techniques for high-resolution current recording from cells and cell-free membrane patches. *Pflügers Arch.* 391, 85-100
- Harteneck, C.**, Plant, T. D. and Schultz, G. (2000)  
From worm to man: three subfamilies of TRP channels. *Trends Neurosci.* 23, 159-166
- Harvey, K. F.**, Dinudom, A., Komwatana, P., Jolliffe, C. N., Day, M. L., Parasivam, G., Cook, D. I. and Kumar, S. (1999)  
All three WW domains of murine Nedd4 are involved in the regulation of epithelial sodium channels by intracellular Na<sup>+</sup>. *J. Biol. Chem.* 274, 12525-12530
- Hebert, S. C.** and Andreoli, T. E. (1984)  
Control of NaCl transport in the thick ascending limb. *Am. J. Physiol.* 246, F745-F756
- Hebert, S. C.** (1998)  
Roles of Na-K-2Cl and Na-Cl cotransporters and ROMK potassium channels in urinary concentrating mechanism. *Am. J. Physiol.* 275, F325-F327
- Hebert, S. C.** (2003)  
Bartter syndrome. *Curr. Opin. Nephrol. Hypertens.* 12, 527-532
- Henke, G.**, Setiawan, I., Boehmer, C. and Lang, F. (2002)  
Activation of Na<sup>+</sup>,K<sup>+</sup>-ATPase by the serum and glucocorticoid dependent kinase isoforms. *Kidney Blood Press. Res.* 25, 370-374
- Hilgemann, D. W.** and Ball, R. (1996)  
Regulation of cardiac Na<sup>+</sup>/Ca<sup>2+</sup> exchange and KATP potassium channels by PIP2. *Science* 273, 956-959
- Ho, K.**, Nichols, C. G., Lederer, W. J., Lytton, J., Vassilev, P. M., Kanazirska, M. V. and Hebert, S. C. (1993)  
Cloning and expression of an inwardly rectifying ATP-regulated potassium channel. *Nature* 362, 31-38
- Hoenderop, J. G. J.**, van der Kemp, A. W., Hartog, A., van de Graaf, S. F., van Os, C. H., Willems, P. H. and Bindels, R. J. M. (1999a)  
Molecular identification of the apical Ca<sup>2+</sup> channel in 1, 25-dihydroxyvitamin D3-responsive epithelia. *J. Biol. Chem.* 274, 8375-8378
- Hoenderop, J. G. J.**, De Pont, J. J., Bindels, R. J. M. and Willems, P. H. (1999b)  
Hormone-stimulated Ca<sup>2+</sup> reabsorption in rabbit kidney cortical collecting system is cAMP-independent and involves a phorbol ester-insensitive PKC isotype. *Kidney Int.* 55, 225-33

- Hoenderop, J. G. J.**, van der Kemp, A. W., Hartog, A., van Os, C. H., Willems, P. H. and Bindels, R. J. M. (1999c)  
The epithelial calcium channel, ECaC1, is activated by hyperpolarization and regulated by cytosolic calcium. *Biochem. Biophys. Res. Commun.* 261, 488-492
- Hoenderop, J. G. J.**, Willems, P. H. and Bindels, R. J. M. (2000a)  
Toward a comprehensive molecular model of active calcium reabsorption. *Am. J. Physiol.* 278, F352-F360
- Hoenderop, J. G. J.**, Müller, D., Suzuki, M., van Os, C. H. and Bindels, R. J. M. (2000b)  
Epithelial calcium channel: gate-keeper of active calcium reabsorption. *Curr. Opin. Nephrol. Hypertens.* 9, 335-340
- Hoenderop, J. G. J.**, Hartog, A., Stuiver, M., Doucet, A., Willems, P. H. and Bindels, R. J. M. (2000c)  
Localization of the epithelial  $\text{Ca}^{2+}$  channel in rabbit kidney and intestine. *J. Am. Soc. Nephrol.* 11, 1171-1178
- Hoenderop, J. G. J.**, Müller, D., van der Kemp, A. W. C. M., Hartog, A., Suzuki, M., Ishibashi, K., Imai, M., Sweep, F., Willems, P. H., van Os, C. H. and Bindels, R. J. M. (2001a)  
Calcitriol controls the epithelial calcium channel in kidney. *J. Am. Soc. Nephrol.* 12, 1342-1349
- Hoenderop, J. G. J.**, Vennekens, R., Müller, D., Prenen, J., Droogmans, G., Bindels, R. J. M. and Nilius, B. (2001b)  
Function and expression of the epithelial  $\text{Ca}^{2+}$  channel family: comparison of mammalian ECaC1 and 2. *J. Physiol.* 537, 747-761
- Hoenderop, J. G. J.**, Nilius, B. and Bindels, R. J. M. (2002)  
Molecular mechanism of active  $\text{Ca}^{2+}$  reabsorption in the distal nephron. *Annu. Rev. Physiol.* 64, 529-549
- Huang, C. L.**, Feng, S. and Hilgemann, D. W. (1998)  
Direct activation of inward rectifier potassium channels by PIP2 and its stabilization by Gbetagamma. *Nature* 391, 803-806
- Hunter, M.** (2001)  
Accessory to kidney disease. *Nature* 414, 502-503
- Hunziker, W.** and Schrickel, S. (1988)  
Rat brain calbindin-D<sub>28</sub>: six domain structure and extensive amino acid homology with chicken calbindin-D<sub>28</sub>. *Mol. Endocrinol.* 2, 465-473
- International Collaborative Study Group for Bartter-like Syndromes** (1997)  
Mutations in the gene encoding the inwardly-rectifying renal potassium channel, ROMK, cause the antenatal variant of Bartter syndrome: evidence for genetic heterogeneity. *Hum. Mol. Genet.* 6, 17-26
- Jentsch, T. J.**, Steinmeyer, K. and Schwarz, G. (1990)  
Primary structure of *Torpedo marmorata* chloride channel isolated by expression cloning in *Xenopus* oocytes. *Nature* 348, 510-514

- Jentsch, T. J.**, Stein, V., Weinreich, F. and Zdebik, A. A. (2002)  
Molecular structure and physiological function of chloride channels. *Physiol. Rev.* 82, 503-568
- Jones, P. F.**, Jakubowicz, T., Pitossi, F. J., Mauer, F. and Hemmings, B. A. (1991)  
Molecular cloning and identification of a serine/threonine kinase of the second-messenger subfamily. *Proc. Natl. Acad. Sci. USA* 88, 4171-4175
- Kamynina, E.**, Tauxe, C. and Staub, O. (2001)  
Distinct characteristics of two human Nedd4 proteins with respect to epithelial Na<sup>+</sup> channel regulation. *Am. J. Physiol.* 281, F469-F477
- Kellenberger, S.**, Gautschi, I., Rossier, B. C. and Schild, L. (1998)  
Mutations causing Liddle syndrome reduce sodium-dependent down-regulation of the epithelial sodium channel in the *Xenopus* oocyte expression system. *J. Clin. Invest.* 101, 2741-2750
- Kieferle, S.**, Fong, P., Bens, M., Vandewalle, A. and Jentsch, T. J. (1994)  
Two highly homologous members of the CIC chloride channel family in both rat and human kidney. *Proc. Natl. Acad. Sci. USA* 91, 6943-6947
- Knopf, J. L.**, Lee, M. H., Sultzman, L. A., Loomis, C. R., Hewick, R. M. and Bell, R. M. (1986)  
Cloning and expression of multiple protein kinase C cDNAs. *Cell* 45, 491-502
- Köckerling, A.**, Konrad, M. and Seyberth, H. W. (1998)  
Hereditäre Tubulopathien mit Diuretika-ähnlichem Salzverlust. *Dt. Ärztebl.* 95, 1841-1846
- Kobayashi, T.**, Deak, M., Morrice, N. and Cohen, P. (1999a)  
Characterization of the structure and regulation of two novel isoforms of serum and glucocorticoid induced protein kinase. *Biochem. J.* 344, 189-197
- Kobayashi, T.** and Cohen, P. (1999b)  
Activation of serum and glucocorticoid regulated protein kinase by agonists that activate phosphatidylinositol 3-kinase is mediated by 3-phosphoinositide-dependent protein kinase 1 (PDK1) and PDK2. *Biochem. J.* 339, 319-328
- Kondo, C.**, Isomoto, S., Matsumoto, S., Yamada, M., Horio, Y., Yamashita, S., Takemura-Kameda, K., Matsuzawa, Y. and Kurachi, Y. (1996)  
Cloning and functional expression of a novel isoform of ROMK inwardly rectifying ATP-dependent K<sup>+</sup> channel, ROMK6 (K<sub>ir</sub>1.1f). *FEBS Lett.* 399, 122-126
- Konstas, A. A.**, Bielfeld-Ackermann, A. and Korbmayer, C. (2001)  
Sulfonylurea receptors inhibit the epithelial sodium channel (ENaC) by reducing surface expression. *Pflügers Arch.* 442, 752-761
- Konrad, M.**, Leonhardt, A., Hensen, P., Seyberth, H. W. and Köckerling, A. (1999)  
Prenatal and postnatal management of hyperprostaglandin E syndrome after genetic diagnosis from amniocytes. *Pediatrics* 103, 678-683
- Komwatana, P.**, Dinudom, A., Young, J. A. and Cook, D. I. (1996)  
Cytosolic Na<sup>+</sup> controls and epithelial Na<sup>+</sup> channel via the G<sub>o</sub> guanine nucleotide-binding regulatory protein. *Proc. Natl. Acad. Sci. USA* 93, 8107-8111

- Kumar, S.,** Tomooka, Y. and Noda, M. (1992)  
Identification of a set of genes with developmentally down-regulated expression in the mouse brain. *Biochem. Biophys. Res. Commun.* 185, 1155-1161
- Kumar, S.,** Harvey, K. F., Kinoshita, M., Copeland, N. G., Noda, M. and Jenkins, N. A. (1997)  
cDNA cloning, expression analysis, and mapping of the mouse *Nedd4* gene. *Genomics* 40, 435-443
- Kunzelmann, K.,** Hubner, M., Vollmer, M., Ruf, R., Hildebrandt, F., Greger, R. and Schreiber, R. (2000)  
A Bartter's syndrome mutation of ROMK1 exerts dominant negative effects on K<sup>+</sup> conductance. *Cell. Physiol. Biochem.* 10, 117-124
- Lang, F.,** Klingel, K., Wagner, C. A., Stegen, C., Wärntges, S., Friedrich, B., Lanzendörfer, M., Melzig, J., Moschen, I., Steuer, S., Waldegger, S., Sauter, M., Paulmichl, M., Gerke, V., Risler, T., Gamba, G., Capasso, G., Kandolf, R., Hebert, S. C., Massry, S. G. and Bröer, S. (2000)  
Deranged transcriptional regulation of cell volume sensitive kinase hSGK in diabetic nephropathy. *Proc. Natl. Acad. Sci. USA* 97, 8157-8162
- Lang, F.** and Cohen, P. (2001)  
Regulation and physiological roles of serum and glucocorticoid induced protein kinase isoforms. *Sci. STKE* 108, RE17
- Lee, W. S.** and Hebert, S. C. (1995)  
ROMK inwardly rectifying ATP-sensitive K<sup>+</sup> channel. I. Expression in rat distal nephron segments. *Am. J. Physiol.* 268, F1124-F1131
- Leipziger, J.,** MacGregor, G. G., Cooper, G. J., Xu, J., Hebert, S. C. and Giebisch, G. (2000)  
PKA site mutations of ROMK2 channels shift the pH dependence to more alkaline values. *Am. J. Physiol.* 279, F919-F926
- Lin, D.,** Sterling, H., Lerea, K. M., Giebisch, G. and Wang, W. H. (2002)  
Protein kinase C (PKC)-induced phosphorylation of ROMK1 is essential for the surface expression of ROMK1 channels. *J. Biol. Chem.* 277, 44278-44284
- Loffing, J.,** Loffing-Cueni, D., Valderrabano, V., Kläusli, L., Hebert, S. C., Rossier, B. C., Hoenderop, J. G. J., Bindels, R. J. M. and Kaissling, B. (2001a)  
Distribution of transcellular calcium and sodium transport pathways along mouse distal nephron. *Am. J. Physiol.* 281, F1021-F1027
- Loffing, J.,** Zecevic, M., Féraillé, E., Kaissling, B., Asher, C., Rossier, B. C., Firestone, G. L., Pearce, D. and Verrey, F. (2001b)  
Aldosterone induces rapid apical translocation of ENaC in early portion of renal collecting system: possible role of SGK. *Am. J. Physiol.* 280, F675-F682
- Loo, D. D.,** Hirsch, J. R., Sarkar, H. K. and Wright, E. M. (1996)  
Regulation of the mouse retinal taurine transporter (TAUT) by protein kinases in *Xenopus* oocytes. *FEBS Lett.* 392, 250-254



- Lu, M.**, Wang, T., Yan, Q., Yang, X., Dong, K., Knepper, M. A., Wang, W., Giebisch, G., Shull, G. E. and Hebert, S. C. (2002)  
Absence of small conductance K<sup>+</sup> channel (SK) activity in apical membranes of thick ascending limb and cortical collecting duct in ROMK (Bartter's) knockout mice. *J. Biol. Chem.* 277, 37881-37887
- Lu, P. J.**, Zhou, X. Z., Shen, M. and Lu, K. P. (1999)  
Function of WW domains as phosphoserine- or phosphothreonine-binding modules. *Science* 283, 1325-1328
- Lynch, D. K.**, Ellis, C. A., Edwards, P. A. and Hiles, I. D. (1999)  
Integrin-linked kinase regulates phosphorylation of serine 473 of protein kinase B by an indirect mechanism. *Oncogene* 18, 8024-8032
- MacGregor, G. G.**, Xu, J. Z., McNicholas, C. M., Giebisch, G. and Hebert, S. C. (1998)  
Partially active channels produced by PKA site mutation of the cloned renal K<sup>+</sup> channel, ROMK2 (k<sub>ir</sub>1.2). *Am. J. Physiol.* 275, F415-F422
- Mahon, M. J.**, Donowitz, M., Yun, C. C. and Segre, G. V. (2002)  
Na<sup>+</sup>/H<sup>+</sup> exchanger regulatory factor 2 directs parathyroid hormone 1 receptor signalling. *Nature* 417, 858-861
- Martin, R. S.**, Panese, S., Virginillo, M., Gimenez, M., Litardo, M., Arrizurieta, E. and Hayslett, J. P. (1986)  
Increased secretion of potassium in the rectum of humans with chronic renal failure. *Am. J. Kidney Dis.* 8, 105-110
- Matsumura, Y.**, Uchida, S., Kondo, Y., Miyazaki, H., Ko, S. B., Hayama, A., Morimoto, T., Liu, W., Arisawa, M., Sasaki, S. and Marumo, F. (1999)  
Overt nephrogenic diabetes insipidus in mice lacking the ClC-K1 chloride channel. *Nat. Genet.* 21, 95-98
- McNicholas, C. M.**, Wang, W., Ho, K., Hebert, S. C. and Giebisch, G. (1994)  
Regulation of ROMK1 K<sup>+</sup> channel activity involves phosphorylation processes. *Proc. Natl. Acad. Sci. USA* 91, 8077-8081
- McNicholas, C. M.**, MacGregor, G. G., Islas, L. D., Yang, Y., Hebert, S. C. and Giebisch, G. (1998)  
pH-dependent modulation of the cloned renal K<sup>+</sup> channel, ROMK. *Am. J. Physiol.* 275, F972-F981
- Mohler, P. J.**, Kreda, S. M., Boucher, R. C., Sudol, M., Stutts, M. J. and Milgram, S. L. (1999)  
Yes-associated protein 65 localizes p62 (c-Yes) to apical compartment of airway epithelia by association with EBP50. *J. Cell Biol.* 147, 879-890
- Müller, D.**, Hoenderop, J. G. J., Merks, G. F., van Os, C. H. and Bindels, R. J. M. (2000)  
Gene structure and chromosomal mapping of human epithelial calcium channel. *Biochem. Biophys. Res. Commun.* 275, 47-52

- Müller, D.**, Hoenderop, J. G. J., Vennekens, R., Eggert, P., Harangi, F., Mehes, K., Garcia-Nieto, V., Claverie-Martin, F., Os, C. H., Nilius, B. and Bindels, R. J. M. (2002)  
Epithelial  $\text{Ca}^{2+}$  channel (ECaC1) in autosomal dominant idiopathic hypercalciuria. *Nephrol. Dial. Transplant.* 17, 1614-1620
- Murthy, A.**, Gonzales-Agousti, C., Cordero, E., Pinney, D., Candia, C., Solomon, F., Gusella, J. and Ramesh, V. (1998)  
NHE-RF, a regulatory cofactor for  $\text{Na}^+/\text{H}^+$  exchange is a common interactor for merlin and ERM (MERM) proteins. *J. Biol. Chem.* 273, 1273-1276
- Náray-Fejes-Tóth, A.**, Canessa, C., Cleaveland, E. S., Aldrich, G. and Fejes-Tóth, G. (1999)  
SGK is an aldosterone-induced kinase in the renal collecting duct. Effects on epithelial  $\text{Na}^+$  channels. *J. Biol. Chem.* 274, 16973-16978
- Nichols, C. G.** and Lopatin, A. N. (1997)  
Inward rectifier potassium channels. *Annu. Rev. Physiol.* 59, 171-191
- Nieuwkoop, P. D.** (1977)  
Origin and establishment of embryonic polar axes in amphibian development. *Curr. Top. Dev. Biol.* 11, 115-132
- Nijenhuis, T.**, Hoenderop, J. G. J., Nilius, B. and Bindels, R. J. M. (2003)  
(Patho)physiological implications of the novel epithelial  $\text{Ca}^{2+}$  channels TRPV5 and TRPV6. *Pflügers Arch.* 446, 401-409
- Nilius, B.**, Vennekens, R., Prenen, J., Hoenderop, J. G. J., Droogmans, G. and Bindels, R. J. M. (2001a)  
The single pore residue Asp542 determines  $\text{Ca}^{2+}$  permeation and  $\text{Mg}^{2+}$  block of the epithelial  $\text{Ca}^{2+}$  channel. *J. Biol. Chem.* 276, 1020-1025
- Nilius, B.**, Prenen, J., Vennekens, R., Hoenderop, J. G. J., Bindels, R. J. M. and Droogmans, G. (2001b)  
Modulation of the epithelial calcium channel, ECaC, by intracellular  $\text{Ca}^{2+}$ . *Cell Calcium* 29, 417-428
- O'Neil, R. G.** (1990)  
Aldosterone regulation of sodium and potassium transport in the cortical collecting duct. *Semin. Nephrol.* 10, 365-374
- Ohlemeyer, C.** and Meyer, J. W. (1992)  
The Faraday cage and grounding arrangements, In: Kettenmann, H., Grantyn, R.: *Practical Electrophysiological Methods*; Wiley-Liss., New York, pp. 3-5
- Pak, C. Y. C.** (1992)  
Pathophysiology of calcium nephrolithiasis, In: Seldin, W., Giebisch, G.: *The Kidney*. Raven Press, New York, pp. 2461-2480
- Palmer, L. G.** (1999)  
Potassium secretion and the regulation of distal nephron K channels. *Am. J. Physiol.* 277, F821-F825

- Park, J.**, Leong, M. L., Buse, P., Maiyar, A. C., Firestone, G. L. and Hemmings, B. A. (1999)  
Serum and glucocorticoid inducible kinase (SGK) is a target of the PI3-kinase-stimulated signaling pathway. *EMBO J.* 18, 3024-3033
- Pelham, H. R.** (1991)  
Multiple targets for brefeldin A. *Cell* 67, 449-451
- Peng, J. B.**, Chen, X. Z., Berger, U. V., Vassilev, P. M., Tsukaguchi, H., Brown, E. M. and Hediger, M. A. (1999)  
Molecular cloning and characterization of a channel-like transporter mediating intestinal calcium absorption. *J. Biol. Chem.* 274, 22739-22746
- Peng, J. B.**, Chen, X. Z., Berger, U. V., Vassilev, P. M., Brown, E. M. and Hediger, M. A. (2000)  
A rat kidney-specific calcium transporter in the distal nephron. *J. Biol. Chem.* 275, 28186-28194
- Plant, P. J.**, Yeager, H., Staub, O., Howard, P. and Rotin, D. (1997)  
The C2 domain of the ubiquitin protein ligase Nedd4 mediates  $\text{Ca}^{2+}$ -dependent plasma membrane localization. *J. Biol. Chem.* 272, 32329-32336
- Ponce, A.**, Vega-Saenz de Miera, E., Kentros, C., Moreno, H., Thornhill, B. and Rudy, B. (1997)  
 $\text{K}^+$  channel subunit isoforms with divergent carboxy-terminal sequences carry distinct membrane targeting signals. *J. Membr. Biol.* 159, 149-159
- Rai, T.**, Uchida, S., Sasaki, S. and Marumo, F. (1999)  
Isolation and characterization of kidney-specific CLC-K2 chloride channel gene promoter. *Biochem. Biophys. Res. Commun.* 261, 432-438
- Reczek, D.**, Berryman, M. and Bretscher, A. (1997)  
Identification of EBP50: a PDZ-containing phosphoprotein that associates with members of the ERM family. *J. Cell Biol.* 139, 169-179
- Reczek, D.** and Bretscher, A. (1998)  
The carboxy-terminal region of EBP50 binds to a site in the amino-terminal domain of ezrin that is masked in the dormant molecule. *J. Biol. Chem.* 273, 18452-18458
- Rodriguez-Soriano, J.** (1998)  
Bartter and related syndromes: the puzzle is almost solved. *Pediatr. Nephrol.* 12, 315-327
- Sage, C. L.** and Marcus, D. C. (2001)  
Immunolocalization of CLC-K chloride channel in strial marginal cells and vestibular dark cells. *Hear. Res.* 160, 1-9
- Saito-Ohara, F.**, Uchida, S., Takeuchi, Y., Sasaki, S., Hayashi, A., Marumo, F. and Ikeuchi, T. (1996)  
Assignment of the genes encoding the human chloride channels, CLCNKA and CLCNKB, to 1p36 and of CLCN3 to 4q32-q33 by in situ hybridization. *Genomics* 36, 372-374

- Scheffner, M.**, Huibregtse, J. M., Vierstra, R. D. and Howley, P. M. (1993)  
The HPV-16 E6 and E6-AP complex functions as a ubiquitin-protein ligase in the ubiquitination of p53. *Cell* 75, 495-505
- Scheffner, M.**, Nuber, U. and Huibregtse, J. M. (1995)  
Protein ubiquitination involving an E1-E2-E3 enzyme ubiquitin thioester cascade. *Nature* 373, 81-83
- Schulte, U.**, Hahn, H., Konrad, M., Jeck, N., Derst, C., Wild, K., Weidemann, S., Ruppertsberg, J. P., Fakler, B. and Ludwig, J. (1999)  
pH gating of ROMK (K<sub>ir</sub>1.1) channels: control by an Arg-Lys-Arg triad disrupted in antenatal Bartter syndrome. *Proc. Natl. Acad. Sci. USA* 96, 15298-15303
- Schwake, M.**, Friedrich, T. and Jentsch, T. J. (2001)  
An internalization signal in CIC-5, an endosomal Cl<sup>-</sup> channel mutated in dent's disease. *J. Biol. Chem.* 276, 12049-12054
- Schwarz, W.** and Rettinger, J. (2000)  
Foundations of electrophysiology, Shaker Verlag, Aachen, pp. 52-54
- Setiawan, I.**, Henke, G., Feng, Y., Boehmer, C., Vasilets, L. A., Schwarz, W. and Lang, F. (2002)  
Stimulation of *Xenopus* oocyte Na<sup>+</sup>,K<sup>+</sup>-ATPase by the serum and glucocorticoid dependent kinase SGK1. *Pflügers Arch.* 444, 426-431
- Seyberth, H. W.**, Rascher, W., Schweer, H., Kühl, P. G., Mehls, O. and Schäfer, K. (1985)  
Congenital hypokalemia with hypercalciuria in preterm infants: a hyperprostaglandinuric tubular syndrome different from Bartter syndrome. *J. Pediatr.* 107, 694-701
- Seyberth, H. W.**, Koniger, S. J., Rascher, W., Kuhl, P. G. and Schweer, H. (1987)  
Role of prostaglandins in hyperprostaglandin E syndrome and in selected renal tubular disorders. *Pediatr. Nephrol.* 1, 491-497
- Seyberth, H. W.**, Soergel, M. and Köckerling, A. (1997)  
Hypokalemic Tubular Disorders: the hyperprostaglandin E syndrome and Gitelman-Bartter syndrome, In: Davison, A. M., Cameron, J. S., Grünfeld, J. P., Kerr, D. N. and Ritz, E. (eds.) *Oxford textbook of clinical nephrology*, 2nd Edition. Oxford University Press, Oxford, London, pp. 1045-1094
- Shenolikar, S.**, Fischer, K., Chang, L. and Weinman, E. J. (1988)  
Type II cAMP-dependent protein kinase is associated with the rabbit brush border membranes. *Sec. Mes. Phosphoprot.* 12, 95-104
- Shenolikar, S.** and Weinman, E. J. (2001)  
NHERF: targeting and trafficking membrane proteins. *Am. J. Physiol.* 280, F389-F395
- Shigaev, A.**, Asher, C., Latter, H., Garty, H. and Reuveny, E. (2000)  
Regulation of SGK by aldosterone and its effects on the epithelial Na<sup>+</sup> channel. *Am. J. Physiol.* 278, F613-F619

- Shimkets, R. A.**, Lifton, R. P. and Canessa, C. M. (1997)  
The activity of the epithelial sodium channel is regulated by clathrin-mediated endocytosis. *J. Biol. Chem.* 272, 25537-25541
- Shuck, M. E.**, Bock, J. H., Benjamin, C. W., Tsai, T. D., Lee, K. S., Slightom, J. L. and Bienkowski, M. J. (1994)  
Cloning and characterization of multiple forms of the human kidney ROMK potassium channel. *J. Biol. Chem.* 269, 24261-24270
- Simon, D. B.**, Nelson-Williams, C., Bia, M. J., Ellison, D., Karet, F. E., Molina, A. M., Vaara, I., Iwata, F., Cushner, H. M., Koolen, M., Gainza, F. J., Gitelman, H. J. and Lifton, R. P. (1996a)  
Gitelman's variant of Bartter's syndrome, inherited hypokalemic alkalosis, is caused by mutations in the thiazide-sensitive Na<sup>+</sup>-Cl<sup>-</sup> cotransporter. *Nat. Genet.* 12, 24-30
- Simon, D. B.**, Karet, F. E., Hamdan, J. M., DiPietro, A., Sanjad, S. A. and Lifton, R. P. (1996b)  
Bartter's syndrome, hypokalaemic alkalosis with hypercalciuria, is caused by mutations in the Na-K-2Cl cotransporter NKCC2. *Nat. Genet.* 13, 183-188
- Simon, D. B.**, Bindra, R. S., Mansfield, T. A., Nelson-Williams, C., Mendonca, E., Stone, R., Schurman, S., Nayir, A., Alpay, H., Bakaloglu, A., Rodriguez-Soriano, J., Morales, J. M., Sanjad, S. A., Taylor, C. M., Pilz, D., Brem, A., Trachtman, H., Griswold, W., Richard, G. A., John, E. and Lifton, R. P. (1997)  
Mutations in the chloride channel gene, CLCNKB, cause Bartter's syndrome type III. *Nat. Genet.* 17, 171-178
- Snyder, P. M.**, Olson, D. R. and Thomas, B. C. (2002)  
Serum and glucocorticoid regulated kinase modulates Nedd4-2-mediated inhibition of the epithelial Na<sup>+</sup> channel. *J. Biol. Chem.* 277, 5-8
- Stanton, B. A.** (1989)  
Renal potassium transport: morphological and functional adaptations. *Am. J. Physiol.* 257, R989-R997
- Staub, O.**, Dho, S., Henry, P., Correa, J., Ishikawa, T., McGlade, J. and Rotin, D. (1996)  
WW domains of Nedd4 bind to the proline-rich PY motifs in the epithelial Na<sup>+</sup> channel deleted in Liddle's syndrome. *EMBO J.* 15, 2371-2380
- Staub, O.**, Yeger, H., Plant, P. J., Kim, H., Ernst, S. A. and Rotin, D. (1997)  
Immunolocalization of the ubiquitin-protein ligase Nedd4 in tissues expressing the epithelial Na<sup>+</sup> channel (ENaC). *Am. J. Physiol.* 272, C1871-C1880
- Stuhmer, W.** (1992)  
Electrophysiological recording from *Xenopus* oocytes. *Methods Enzymol.* 207, 319-339
- Sudol, M.** (1996)  
Structure and function of the WW domain. *Prog. Biophys. Mol. Biol.* 65, 113-132

- Suki, W. N.** and Rose, D. (1996)  
Renal transport of calcium, magnesium and phosphate, In: Brenner, B. M.: The kidney. Saunders, Philadelphia, pp. 472-515
- Sutton, R. A.,** Wong, N. L. M. and Dirks, J. H. (1979)  
Effects of metabolic acidosis and alkalosis on sodium and calcium transport in the dog kidney. *Kidney Int.* 15, 520-533
- Swanson, R.** and Folander, K. (1992)  
*In vitro* synthesis of RNA for expression of ion channels in *Xenopus* oocytes, In: Rudy, B., Iverson, L. E.: Methods in Enzymology. Academic Press, San Diego, California, pp. 310-319
- Taglialatela, M.,** Wible, B. A., Caporaso, R. and Brown, A. M. (1994)  
Specification of pore properties by the carboxy-terminus of inwardly rectifying K<sup>+</sup> channels. *Science* 264, 844-847
- Takeda, T.,** McQuistan, T., Orlando, R. A. and Farquhar M. G. (2001)  
Loss of glomerular foot processes is associated with uncoupling of podocalyxin from the actin cytoskeleton. *J. Clin. Invest.* 108, 289-301
- Thier, S. O.** (1986)  
Potassium physiology. *Am. J. Med.* 80, 3-7
- Thomas, R. C.** (1978)  
Ion-sensitive intracellular microelectrodes, How to make and use them. Academic Press, London, pp. 1-110
- Toker, A.** and Newton, A. C. (2000)  
Akt/protein kinase B is regulated by autophosphorylation at the hypothetical PDK-2 site. *J. Biol. Chem.* 275, 8271-8274
- Tsai, K. J.,** Chen, S. K., Ma, Y. L., Hsu, W. L. and Lee, E. H. (2002)  
SGK, a primary glucocorticoid-induced gene, facilitates memory consolidation of spatial learning in rats. *Proc. Natl. Acad. Sci. USA* 99, 3990-3995
- Tsai, T. D.,** Shuck, M. E., Thompson, D. P., Bienkowski, M. J. and Lee, K. S. (1995)  
Intracellular H<sup>+</sup> inhibits a cloned rat kidney outer medulla K<sup>+</sup> channel expressed in *Xenopus* oocytes. *Am. J. Physiol.* 268, C1173-C1178
- Tzounopoulos, T.,** Maylie, J. and Adelman, J. P. (1995)  
Induction of endogenous channels by high levels of heterologous membrane proteins in *Xenopus* oocytes. *Biophys. J.* 69, 904-908
- Uchida, S.,** Sasaki, S., Furukawa, T., Hiraoka, M., Imai, T., Hirata, Y. and Marumo, F. (1993)  
Molecular cloning of a chloride channel that is regulated by dehydration and expressed predominantly in kidney medulla. *J. Biol. Chem.* 268, 3821-3824
- Uchida, S.,** Sasaki, S., Nitta, K., Uchida, K., Horita, S., Nihei, H. and Marumo, F. (1995)  
Localization and functional characterization of rat kidney-specific chloride channel, CIC-K1. *J. Clin. Invest.* 95, 104-113

- Uchida, S.**, Rai, T., Yatsushige, H., Matsumura, Y., Kawasaki, M., Sasaki, S. and Marumo, F. (1998)  
Isolation and characterization of kidney-specific ClC-K1 chloride channel gene promoter. *Am. J. Physiol.* 274, F602-F610
- Uchida, S.**, Tanaka, Y., Ito, H., Saitoh-Ohara, F., Inazawa, J., Yokoyama, K. K., Sasaki, S. and Marumo, F. (2000)  
Transcriptional regulation of the ClC-K1 promoter by myc-associated zinc finger protein and kidney-enriched Kruppel-like factor, a novel zinc finger repressor. *Mol. Cell. Biol.* 20, 7319-7331
- Van Baal, J.**, Yu, A., Hartog, A., Fransen, J. A. M., Willems, P. H. G. M., Lytton, J. and Bindels, R. J. M. (1996)  
Localization and regulation by vitamin D of calcium transport proteins in rabbit cortical collecting systems. *Am. J. Physiol.* 271, F985-F993
- Vandewalle, A.**, Cluzeaud, F., Bens, M., Kieferle, S., Steinmeyer, K. and Jentsch, T. J. (1997)  
Localization and induction by dehydration of ClC-K chloride channels in the rat kidney. *Am. J. Physiol.* 272, F678-F688
- Vasilets, L. A.** and Schwarz, W. (1992)  
Regulation of endogenous and expressed Na<sup>+</sup>/K<sup>+</sup> pumps in *Xenopus* oocytes by membrane potential and stimulation of protein kinases. *J. Membr. Biol.* 125, 119-132
- Vennekens, R.**, Hoenderop, J. G. J., Prenen, J., Stuver, M., Willems, P. H., Droogmans, G., Nilius, B. and Bindels, R. J. M. (2000)  
Permeation and gating properties of the novel epithelial Ca<sup>2+</sup> channel. *J. Biol. Chem.* 275, 3963-3969
- Vennekens, R.**, Prenen, J., Hoenderop, J. G. J., Bindels, R. J. M., Droogmans, G. and Nilius, B. (2001)  
Modulation of the epithelial Ca<sup>2+</sup> channel ECaC by extracellular pH. *Pflügers Arch.* 442, 237-242
- Wagner, C. A.**, Raber, G., Waldegger, S., Osswald, H., Biber, J., Murer, H., Busch, A. E. and Lang, F. (1996)  
Regulation of the human brush border Na<sup>+</sup>/phosphate cotransporter (NaPi-3) expressed in *Xenopus* oocytes by intracellular calcium and protein kinase C. *Cell. Physiol. Biochem.* 6, 105-111
- Wagner, C. A.**, Friedrich, B., Setiawan, I., Lang, F. and Bröer, S. (2000)  
The use of *Xenopus laevis* oocytes for the functional characterization of heterologously expressed membrane proteins. *Cell. Phys. Biochem.* 10, 1-12
- Wagner, C. A.**, Ott, M., Klingel, K., Beck, S., Melzig, J., Friedrich, B., Wild, N. K., Bröer, S., Moschen, I., Albers, A., Waldegger, S., Tümler, B., Egan, E., Geibel, J. P., Kandolf, R. and Lang, F. (2001)  
Effects of serine/threonine kinase SGK1 on the epithelial Na<sup>+</sup> channel (ENaC) and CFTR. *Cell. Physiol. Biol. Chem.* 11, 209-218

- Waldegger, S.**, Raber, G., Süssbrich, H., Ruppertsberg, J. P., Fakler, B., Murer, H., Lang, F. and Busch, A. E. (1996)  
Coexpression and stimulation of parathyroid hormone receptor positively regulates slowly activating  $I_{SK}$  channels expressed in *Xenopus* oocytes. *Kidney Int.* 49, 112-116
- Waldegger, S.**, Barth, P., Raber, G. and Lang, F. (1997)  
Cloning and characterization of a putative human serine/threonine protein kinase transcriptionally modified during anisotonic and isotonic alterations of cell volume. *Proc. Natl. Acad. Sci. USA* 94, 4440-4445
- Waldegger, S.**, Klingel, K., Barth, P., Sauter, M., Lanzendörfer, M., Kandolf, R. and Lang, F. (1999)  
hSGK serine-threonine protein kinase gene as transcriptional target of transforming growth factor beta in human intestine. *Gastroenterology* 116, 1081-1088
- Waldegger, S.** and Jentsch, T. J. (2000a)  
Functional and structural analysis of ClC-K chloride channels involved in renal disease. *J. Biol. Chem.* 275, 24527-24533
- Waldegger, S.**, Gabrysch, S., Barth, P., Fillon, S. and Lang, F. (2000b)  
h-sgk serine-threonine protein kinase as transcriptional target of p38/MAP kinase pathway in HepG2 human hepatoma cells. *Cell. Physiol. Biochem.* 10, 203-208
- Waldegger, S.**, Jeck, N., Barth, P., Peters, M., Vitzthum, H., Wolf, K., Kurtz, A., Konrad, M. and Seyberth, H. W. (2002)  
Barttin increases surface expression and changes current properties of ClC-K channels. *Pflügers Arch.* 444, 411-418
- Wang, J.**, Barbry, P., Maiyar, A. C., Rozansky, D. J., Bhargava, A., Leong, M., Firestone, G. L. and Pearce, D. (2001)  
SGK integrates insulin and mineralocorticoid regulation of epithelial sodium transport. *Am. J. Physiol.* 280, F303-F313
- Wang, W. H.**, Schwab, A. and Giebisch, G. (1990a)  
Regulation of small-conductance  $K^+$  channel in apical membrane of rat cortical collecting tubule. *Am. J. Physiol.* 259, F494-F502
- Wang, W. H.**, White, S., Geibel, J. and Giebisch, G. (1990b)  
A potassium channel in the apical membrane of rabbit thick ascending limb of Henle's loop. *Am. J. Physiol.* 258, F244-F253
- Wang, W. H.**, Sackin, H. and Giebisch, G. (1992)  
Renal potassium channels and their regulation. *Annu. Rev. Physiol.* 54, 81-96
- Wang, W. H.**, Geibel, J. and Giebisch, G. (1993)  
Mechanism of apical  $K^+$  channel modulation in principal renal tubule cells. Effect of inhibition of basolateral  $Na^+, K^+$ -ATPase. *J. Gen. Physiol.* 101, 673-694
- Wang, W. H.** (1994)  
Two types of  $K^+$  channel in thick ascending limb of rat kidney. *Am. J. Physiol.* 267, F599-F605



**Wang, W. H. (1995)**

View of K<sup>+</sup> secretion through the apical K<sup>+</sup> channel of cortical collecting duct. *Kidney Int.* 48, 1024-1030

**Wang, W. and Giebisch, G. (1991a)**

Dual effect of adenosine triphosphate on the apical small conductance K<sup>+</sup> channels of rat cortical collecting duct. *J. Gen. Physiol.* 98, 35-61

**Wang, W. and Giebisch, G. (1991b)**

Dual modulation of renal ATP-sensitive K<sup>+</sup> channel by protein kinases A and C. *Proc. Natl. Acad. Sci. USA* 88, 9722-9725

**Wang, W., Hebert, S. C. and Giebisch, G. (1997)**

Renal K<sup>+</sup> channels: structure and function. *Annu. Rev. Physiol.* 59, 413-436

**Wang, W. (1999)**

Regulation of the ROMK channel: interaction of the ROMK with associate proteins. *Am. J. Physiol.* 277, F826-F831

**Wärntges, S., Friedrich, B., Waldegger, S., Meyermann, R., Kuhl, D., Speckmann, E. J., Obermüller, N., Witzgall, R., Mack, A. F., Wagner, H. J., Bröer, S. and Lang, F. (2002)**

Cerebral localization and regulation of the cell volume sensitive serum and glucocorticoid dependent kinase SGK1. *Pflügers Arch.* 443, 617-624

**Weber, K., Erben, R. G., Rump, A. and Adamski, J. (2001)**

Gene structure and regulation of the murine epithelial calcium channels ECaC1 and 2. *Biochem. Biophys. Res. Commun.* 289, 1287-1294

**Webster, M. K., Goya, L., Ge, Y., Maiyar, A. C. and Firestone, G. L. (1993)**

Characterization of SGK, a novel member of the serine/threonine protein kinase gene family which is transcriptionally induced by glucocorticoids and serum. *Mol. Cell. Biol.* 13, 2031-2040

**Weinman, E. J., Steplock, D., Wang, Y. and Shenolikar, S. (1995)**

Characterization of a protein cofactor that mediates protein kinase A regulation of the renal brush border membrane Na<sup>+</sup>/H<sup>+</sup> exchanger. *J. Clin. Invest.* 95, 2143-2149

**Weinman, E. J., Steplock, D., Tate, K., Hall, R. A., Spurney, R. F. and Shenolikar, S. (1998)**

Structure-function of the Na<sup>+</sup>/H<sup>+</sup> exchanger regulatory factor (NHERF). *J. Clin. Invest.* 101, 2199-2206

**Welling, P. A., Olsen, O., Yoo, D., Flagg, T., Le Maout, S. and Merot, J. (2001)**

Regulating and retaining renal potassium channels by PDZ interactions. *J. Physiol.*, 535P

**Winters, C. J., Zimniak, L., Reeves, W. B. and Andreoli, T. E. (1997)**

Cl<sup>-</sup> channels in basolateral renal medullary membranes. XII. Anti-rbClC-Ka antibody blocks MTAL Cl<sup>-</sup> channels. *Am. J. Physiol.* 273, F1030-F1038

- Wissenbach, U.**, Niemeyer, B. A., Fixemer, T., Schneidewind, A., Trost, C., Cavalié, A., Reus, K., Meese, E., Bonkhoff, H. and Flockerzi, V. (2001)  
Expression of CaT-like, a novel calcium-selective channel, correlates with the malignancy of prostate cancer. *J. Biol. Chem.* 276, 19461-19468
- Wright, F. S.** and Giebisch, G. (1992)  
Regulation of potassium excretion, In: *The Kidney*, edited by Seldin DW, Giebisch, G., New York, Raven Press, pp. 2209
- Wulff, P.**, Vallon, V., Huang, D. Y., Volkl, H., Yu, F., Richter, K., Jansen, M., Schlunz, M., Klingel, K., Loffing, J., Kauselmann, G., Bosl, M. R., Lang, F. and Kuhl, D. (2002)  
Impaired renal Na<sup>+</sup> retention in the SGK1-knockout mouse. *J. Clin. Invest.* 110, 1263-1268
- Xu, J.**, Liu, D., Gill, G. and Songyang, Z. (2001)  
Regulation of cytokine-independent survival kinase (CISK) by the Phox homology domain and phosphoinositides. *J. Cell Biol.* 154, 699-705
- Xu, Z. C.**, Yang, Y. and Hebert, S. C. (1996)  
Phosphorylation of the ATP-sensitive, inwardly rectifying K<sup>+</sup> channel, ROMK, by cyclic AMP-dependent protein kinase. *J. Biol. Chem.* 271, 9313-9319
- Xu, J. Z.**, Hall, A. E., Peterson, L. N., Bienkowski, M. J., Eessalu, T. E. and Hebert, S. C. (1997)  
Localization of the ROMK protein on apical membranes of rat kidney nephron segments. *Am. J. Physiol.* 273, F739-F748
- Yano, H.**, Philipson, L. H., Kugler, J. L., Tokuyama, Y., Davis, E. M., Le Beau, M. M., Nelson, D. J., Bell, G. I. and Takeda, J. (1994)  
Alternative splicing of human inwardly rectifying K<sup>+</sup> channel ROMK1 mRNA. *Mol. Pharmacol.* 45, 854-860
- Yoo, D.**, Kim, B. Y., Campo, C., Nance, L., King, A., Maouyo, D. and Welling, P. A. (2003)  
Cell surface expression of the ROMK (K<sub>ir</sub>1.1) channel is regulated by the aldosterone-induced kinase, SGK1, and protein kinase A. *J. Biol. Chem.* 278, 23066-23075
- Yoshikawa, M.**, Uchida, S., Yamauchi, A., Miyai, A., Tanaka, Y., Sasaki, S. and Marumo, F. (1999)  
Localization of rat ClC-K2 chloride channel mRNA in the kidney. *Am. J. Physiol.* 276, F552-F558
- Yun, C. C.**, Oh, S., Zizak, M., Steplock, D., Tsao, S., Tse, C., Weinman, E. and Donowitz, M. (1997)  
cAMP-mediated inhibition of the epithelial brush border Na<sup>+</sup>/H<sup>+</sup> exchanger, NHE3, requires an associated regulatory protein. *Proc. Natl. Acad. Sci. USA* 94, 3010-3015
- Yun, C. C.**, Lamprecht, G., Forster, D. V. and Sidor, A. (1998)  
NHE3 kinase A regulatory protein E3KARP binds the epithelial brush border Na<sup>+</sup>/H<sup>+</sup> exchanger NHE3 and the cytoskeletal protein ezrin. *J. Biol. Chem.* 273, 25856-25863

- Yun, C. C.**, Chen, Y. and Lang, F. (2002a)  
Glucocorticoid activation of Na<sup>+</sup>/H<sup>+</sup> exchanger isoform 3 revisited. The roles of SGK1 and NHERF2. *J. Biol. Chem.* 277, 7676-7683
- Yun, C. C.**, Palmada, M., Embark, H. M., Fedorenko, O., Feng, Y., Henke, G., Setiawan, I., Boehmer, C., Weinman, E. J., Sandrasagra, S., Korbmacher, C., Cohen, P., Pearce, D. and Lang, F. (2002b)  
The serum and glucocorticoid inducible kinase SGK1 and the Na<sup>+</sup>/H<sup>+</sup> exchange regulating factor NHERF2 synergize to stimulate the renal outer medullary K<sup>+</sup> channel ROMK1. *J. Am. Soc. Nephrol.* 13, 2823-2830
- Yun, C. C.** (2003)  
Concerted roles of SGK1 and the Na<sup>+</sup>/H<sup>+</sup> exchanger regulatory factor 2 (NHERF2) in regulation of NHE3. *Cell. Physiol. Biochem.* 13, 29-40
- Zerangue, N.**, Schwappach, B., Jan, Y. N. and Jan, L. Y. (1999)  
A new ER trafficking signal regulates the subunit stoichiometry of plasma membrane K<sub>ATP</sub> channels. *Neuron* 22, 537-548
- Zhou, H.**, Tate, S. S. and Palmer, L. G. (1994)  
Primary structure and functional properties of an epithelial K<sup>+</sup> channel. *Am. J. Physiol.* 266, C809-C824
- Zimniak, L.**, Winters, C. J., Reeves, W. B. and Andreoli, T. E. (1996)  
Cl<sup>-</sup> channels in basolateral renal medullary vesicles XI. rbCIC-Ka cDNA encodes basolateral MTAL Cl<sup>-</sup> channels. *Am. J. Physiol.* 270, F1066-F1072

## Acknowledgments

This dissertation could not have been finished if it were not for the understanding and support of the following people.

First I would like to acknowledge and thank my supervisor Prof. Dr. Florian Lang, for giving me the opportunity to do my Ph.D work in his laboratory. Thank you for your constant and professional guidance and supervision, for lots of advice and for encouraging me. Thank you for your confidence and availability. Thank you for your intensive supervision and critical discussion during my three-years of study in Tübingen and especially throughout this dissertation writing period.

My work has also been evaluated by my co-advisor Prof. Dr. Rüdiger Gerstberger, being the second corrector, for such meticulous evaluation I would like to thank him for evaluating my work and helping to finalize my doctoral work, without which I would not have accomplished this work. Thank you for your critical reading and useful suggestions to my dissertation.

I would like to thank Dr. rer. Nat. Christoph Böhmer, with whom I have worked for 3 years, for introducing me to the fascinating world of electrophysiology, especially the application of two microelectrode voltage clamp in *Xenopus* oocyte. Thank you for your encouragements and comprehension.

Thanks to the collaborators in the lab of Prof. Dr. René J. M. Bindels in Nijmegen, The Netherlands.

Some of this work has been carried out using ion selective microelectrodes in *Xenopus* oocytes, which was established by Dr.med. Iwan Setiawan. On this occasion I also would like to thank him gratefully for his collaboration and his explanations about some projects.

The tracer flux measurements performed in this study was introduced by Dr. rer. nat. Monica Palmada and PD Dr. rer. nat. Thomas Wieder. For their kind help I am very grateful.

I would like to thank all the persons from the "oocyte lab", the electrophysiology lab, and the malaria group, the molecular biology group (the nice discussions with Dr. Stephan Huber, Dr. Monica Palmada, Dr. rer. nat. Sabine Wallisch, Dr. Amanda Wyatt (PhD) and Dr. Yuxi Feng) for their help and given me the opportunity to take part in some interesting projects.

I would like to thank all my old and current laboratory colleagues: Guido Henke, Gottlieb Maier, Roman Schniepp, Ferah Okur, Andreas Gorlow, Michael Dieter, Viktoria Wilhelm, Sabrina Wagner, Anna Bauer, Kristian Kotelac, Michael Philippin, Andreas Speil, Manzar Banoo Shojaei Fard and Ahmad Akel for the pleasant work atmosphere.

I would like to acknowledge the technical help, cooperation and friendly atmosphere from Birgitta Noll and Efi Faber.

And I don't want to forget the secretaries, especially Tanja Loch, Lejla Subasic and Marion Rabe for their kindness, patience and constant availability and endurance with all the papers and organizations.

I am indebted to Peter Dürr, Jürgen Kalke, Uwe Schüler, Charlie Schöntag, for the technical and official helps.

Thank you to all the persons working or having worked in the Institute of Physiology, with whom I had contact or communication, thank you all for the nice atmosphere.

To my wife Ghada Hamad, my daughter Reham Embark and my son Waleed Embark I am very gratefull for their patience, love and encouragement during our life distant from our family in Egypt.

To my big family in Aswan and Luxor (family Embark and family Hamad) I would like to thank for their support in my whole life.

I also would like to thank my family, especially my parents, for their full support during my three years of study. Without them, this dissertation could not have even existed.

Last but not least, I would also like to thank the Prof. Dr. Aleya Khattab - Egyptian Cultural and Educational Councillor in Germany for their support allowing me to study and do research in Germany.

---

**Curriculum Vitae**

Name : Embark  
 Sex : Male  
 Date of birth : June 15, 1971  
 Place of birth : Hagaza , Aswan, Egypt  
 Nationality : Egyptian  
 Marital Status : Married, two children  
 01/1977 – 06/1982 : Primary School in Hagaza , Aswan, Egypt  
 06/1983 – 06/1986 : Preparatory School in Hagaza, Aswan, Egypt  
 06/1987 – 05/1989 : Secondary School in Kom Ombo, Aswan, Egypt  
 08/1989 – 10/1994 : Faculty of Veterinary Medicine Cairo University in Beni-Suef, Egypt  
 06/1996 – 07/1997 : Demonstrator at the Department of Physiology, Faculty of Veterinary Medicine Mansora University in Mansora, Egypt  
 08/1997 – 02/2001 : Demonstrator at the Department of Physiology, Faculty of Veterinary Medicine South Valley University in Qena, Egypt  
 12/1999 – 03/2000 : German Language Course in Goethe Institut in Assiut, Egypt  
 02/2001 – 04/2001 : German Language Course in Goethe Institut in Freiburg, Germany  
 04/2001 – 03/2002 : Admitted as student in the Institute of Physiology, Eberhard-Karls-Universität Tübingen. Under the direction of Prof. Dr. med. F. Lang  
 04/2002 – 12/2003 : External Dr. Med. Vet. fellow in the Institut of Vet. Physiology, Faculty of Vet. Medicine, Justus-Liebig-Universität Gießen. Under the direction of Prof. Dr. Rüdiger Gerstberger  
 00/00/2004 : Dr. Med. Vet. examination

---

**List of Publications**

1. Yun, C. C., Palmada, M., **Embark, H. M.**, Fedorenko, O., Feng, Y., Henke, G., Setiawan, I., Boehmer, C., Weinman, E. J., Sandrasagra, S., Korbmacher, C., Cohen, P., Pearce, D. and Lang, F. (2002)  
The serum and glucocorticoid inducible kinase SGK1 and the Na<sup>+</sup>/H<sup>+</sup> exchange regulating factor NHERF2 synergize to stimulate the renal outer medullary K<sup>+</sup> channel ROMK1. *J. Am. Soc. Nephrol.* 13, 2823-2830
2. **Embark, H. M.**, Boehmer, C., Vallon, V., Luft, F. and Lang, F. (2003)  
Regulation of KCNE1-dependent K<sup>+</sup> current by the serum and glucocorticoid inducible kinase (SGK) isoforms. *Pflügers Arch.* 445, 601-606
3. Lang, F., Henke, G., **Embark, H. M.**, Waldegger, S., Palmada, M., Boehmer, C. and Vallon, V. (2003)  
Regulation of channels by the serum and glucocorticoid inducible kinase - implications for transport, excitability and cell proliferation. *Cell. Physiol. Biochem.* 13, 41-50
4. Palmada, M., **Embark, H. M.**, Wyatt, A. W., Boehmer, C. and Lang, F. (2003)  
Negative charge at the consensus sequence for the serum and glucocorticoid inducible kinase, SGK1, determines pH sensitivity of the renal outer medullary K<sup>+</sup> channel, ROMK1. *Biochem. Biophys. Res. Commun.* 307, 967-972
5. Palmada, M., **Embark, H. M.**, Yun, C., Boehmer, C. and Lang, F. (2003)  
Molecular requirements for the regulation of renal outer medullary K<sup>+</sup> channel ROMK1 by the serum and glucocorticoid inducible kinase SGK1. *Biochem. Biophys. Res. Commun.* 311, 629-634
6. Krikov, M., Dieter, M., Palmada, M., **Embark, H. M.**, Boehmer, C. and Lang, F. (2003)  
Regulation of sodium-coupled glucose transporter SGLT-1 by ubiquitin ligase Nedd4-2 and the serum and glucocorticoid inducible kinase SGK1. *Pflügers Arch.* 445, P 07-2
7. Speil, A., Palmada, M., Dieter, M., **Embark, H. M.**, Feng, Y. and Lang, F. (2003)  
Regulation of the intestinal phosphate transporter NaPiIIb by ubiquitin ligase Nedd4-2 and the serum and glucocorticoid inducible kinase SGK1. *Pflügers Arch.* 445, P 07-5
8. Boehmer, C., **Embark, H. M.**, Bauer, A., Palmada, M., Yun, C. H., Weinman, E. J., Endou, H., Cohen, P., Lahme, S., Bichler, K. H. and Lang, F. (2004)  
Stimulation of renal Na<sup>+</sup> dicarboxylate cotransporter 1 by Na<sup>+</sup>/H<sup>+</sup> exchanger regulating factor 2, serum and glucocorticoid inducible kinase isoforms, and protein kinase B. *Biochem. Biophys. Res. Commun.* 313, 998-1003

9. **Embark, H. M.\***, Setiawan, I.\*, Poppendieck, S., van de Graaf, S., Boehmer, C., Palmada, M., Wieder, T., Gerstberger, R., Cohen, P., Yun, C. C., Bindels, R. J. M. and Lang, F. (2003)  
Regulation of the epithelial  $\text{Ca}^{2+}$  channel TRPV5 by the NHE regulating factor NHERF2 and the serum and glucocorticoid inducible kinase isoforms SGK1 and SGK3 expressed in *Xenopus* oocytes. (Submitted to J. Biol. Chem.)
10. **Embark, H. M.**, Boehmer, C., Palmada, M., Capasso, G., Waldegger, P., Waldegger, S., Seyberth, H. W. and Lang, F. (2003)  
Regulation of ClC-Ka/barttin chloride channels by the ubiquitin ligase Nedd4-2 and the serum and glucocorticoid dependent kinases SGK1 and SGK3. (Submitted to Kidney Int.)

\* share first position



"Ich erkläre: Ich habe die vorgelegte Dissertation selbständig und ohne unerlaubte fremde Hilfe und nur mit den Hilfen angefertigt, die ich in der Dissertation angegeben habe. Alle Textstellen, die wörtlich oder sinngemäß aus veröffentlichten oder nicht veröffentlichten Schriften entnommen sind, und alle Angaben, die auf mündlichen Auskünften beruhen, sind als solche kenntlich gemacht. Bei den von mir durchgeführten und in der Dissertation erwähnten Untersuchungen habe ich die Grundsätze guter wissenschaftlicher Praxis, wie sie in der "Satzung der Justus-Liebig-Universität Gießen zur Sicherung guter wissenschaftlicher Praxis" niedergelegt sind, eingehalten."